Geoarchaeological Investigations in Southwestern Angola: macro- and micro-scale approaches to the Middle and Late Pleistocene of Leba Cave

Dissertation

der Mathematisch-Naturwissenschaftlichen Fakultät

der Eberhard Karls Universität Tübingen

zur Erlangung des Grades eines

Doktors der Naturwissenschaften

(Dr. rer. nat.)

vorgelegt von

Daniela Filipa Mirote de Matos

aus Setúbal, Portugal

Tübingen

2022

Gedruckt mit Genehmigung der Mathematisch-Naturwissenschaftlichen Fakultät der Eberhard Karls Universität Tübingen.

Tag der mündlichen Qualifikation:	10.02.2023
Dekan:	Prof. Dr. Thilo Stehle
1. Berichterstatter/-in:	Prof. Dr. Nicholas Conard
2. Berichterstatter/-in:	Prof. Dr. Christopher Miller

Dissertation declaration

I, Daniela Filipa Mirote de Matos, certify that:

This monograph was accomplished during enrollment in the doctoral degree of Archaeological Sciences and Human Evolution. The monograph does not contain material that has been submitted for the award of any other degree or diploma in my name in any other university besides the Eberhard-Karls-Universitat Tübingen, in Germany.

This dissertation does not contain any material previously published or written by another person, with the exclusion of due references made in the text.

Geographical data, photographs, and samples from the Archive of the Tropical Research Institute were used with permission from the Natural History and Science Museum of the University of Lisbon, director Marta Lourenço.

Permits for archaeological fieldwork were granted by the Instituto Nacional do Património Cultural (INPC), Ministério da Cultura de Angola. The activities were followed by the Museu Nacional de Arqueologia de Angola. Local access and permission were granted by Governo Provincial da Huíla e Administração do Município da Humpata e Chibia. Samples were collected with the authorization and presence of local leaders or representatives. Transport permits for the geological and pedological samples were granted by the Office of Ministério para o Desenvolvimento in Lubango. Artifacts are housed at the Museum of Huíla in Lubango.

The work described in the thesis was supported by the Foundation of Science and Technology Individual Doctoral Scholarships, code: SFRH/BD/117162/2016.

Fieldwork and laboratory costs were funded by the Institute for Archaeological Sciences of the University of Tübingen, the Centre of Geosciences of the University of Coimbra, Unibünd Tübingen, the Leakey Foundation “Dissertation Fieldwork” grants, and the National Geographic Society “Early Career” grant awarded to the author.

Date, Signature:

December 16th 2022 Daniela Filipa Mirote de Matos

Positionality statement

The author identifies as southern Iberian female of mixed heritage. The PaleoLeba Project stemmed from questions about human evolution and foraging populations in the southern Atlantic. Many scientific studies about Angola were initiated during the colonial period and the author recognizes the value of the literature and documentation in European institutions for this research (and further) about the Prehistory of Angola.

Since 2010 the author collaborates in the conservation and promotion of the scientific knowledge kept by the Tropical Research Institute and the Natural History and Science Museum of the University of Lisbon. The contact with the African collection of the IICT was particularly important before the dismantling of the institute in 2015. The original center created by Miguel Ramos in 1983 housed the assemblages collected by the colonial missions in Africa as well as many different other resources and documentation which inevitably inspired the research about Leba Cave.

The author and collaborators of the project do not support the prerogatives that guided the colonial research, or any illegal or unethical trading of heritage. The project has also made efforts to bridge different institutions in Europe, America, and Africa particularly those that relate to the previous colonial research structures holding collections and essential knowledge for Angola.

The project's collaborators are themselves very diverse which emphasizes an inclusive practice and integrated learning independent of gender, skin color, religion, or social background. Through the years, the field team was composed of international members of different nationalities as well as students-volunteers from the Geology Dept. of Polytechnic Institute of Huíla, and local guides led by the Soba of Leba and Tchivinguiro. All individuals directly or indirectly participating in the excavations or showcased in video or photographic outputs, did so knowingly and voluntarily at all times. All activities were directed in efforts to provide knowledge and experience in the scientific practice to students, but also engage the local population directly with their heritage. The toponymy used by the population was preferred and any new sites found by the team were named by the community with local names.

Acknowledgments

My advisors Prof. Dr. Nicholas Conard and Prof. Dr. Christopher Miller for their academic support throughout these years of my doctoral research.

To the Government of Angola, Ministério da Cultura de Angola, INPC, Governo Provincial da Huíla e Museu Regional da Huíla for permits and housing of the assemblages collected during our fieldwork. To the Universidade Mandume Ya Ndemufayo in Lubango, Magnífico Prof. Dr. Orlando da Mata and Prof. Dr. Manuel Sahando Neto, co-director of the field project in Angola. To my colleagues at the Polytechnic Institute of Huíla: José Fernandes, Aida Lussinga, Alberto Wapota. The field teams David Nora, Carlos Ariel, Adalberto, Anthony, Gabriel Handa, Mario Mata-Gonzalez, Beatriz Barros, Rui Francisco,

Colleagues at the University of Lisbon, the Natural History and Science Museum (MUHNAC), and the curation team of the African collections of the Tropical Research Institute (IICT-PRISC) in Portugal: Marta Lourenço, João Pedro Cunha-Ribeiro, Ana Cristina Martins, Ana Godinho, Inês Pinto.

Martin Pickford and Brigitte Senut for sharing valuable background information and much more about their fieldwork in Angola.

For taxonomic identification and analysis of the faunal remains: Mario Mata-Gonzalez, Julia Zastrow, and Aurore Val. Special thanks to John Mendelhson for sharing vectorized maps and much more information about the landscape of Angola and Namibia. Malte Loetz for producing the GIS maps with the data collected by the project. Dominik Goldner for help with figures.

Susan Mentzer and Patrick Schmidt for their teachings and support in microanalytical work. My colleagues in the Geoarchaeology working group: Sara Meinekat, Aris Varis, Diana Marcazzan, Abay Namen, Aspen Cooper, Ada Dinckal, Enrique Palacios, Arantzazu Jindriska, Kristen Wroth, Scotty Mclin. Special thanks to Sara Rhodes, Samantha Brown, and Aspen Cooper for proofreading and endless support.

To my family and friends in Portugal, Angola, Germany, and elsewhere.

Funding parties:

I thank the Foundation of Science and Technology Individual Ph.D. Scholarships 3+1 program (code: SFRH/BD/117162/2016) for supporting my doctoral studies in Germany. Thanks are also due to the travel support by the Institute for Archaeological Sciences of the University of Tübingen and the Centre of Geosciences of the University of Coimbra in the first two field seasons in 2018. Fieldwork in 2019 was sponsored by the Leakey Foundation “Dissertation Fieldwork” grant and the National Geographic Society “Early Career grant” awarded to the author.

Dedication

In loving memory of my friends Ivã, Gizem, and Professor João Carlos Senna-Martinez.

Abstract

Leba Cave is located in the dolomites of the Humpata district, Huíla Province in southwestern Angola. This region of escarpments and inselbergs represents the westernmost highlands of the Great Escarpment of Southern Africa, connecting a mosaic of biomes between the coastal regimes, hyper-arid Namib and Kalahari deserts and the woodlands of Central Africa. For paleoanthropological studies, understanding the cultural and environmental dynamics of this sub-tropical area is particularly challenging due to its high rates of decay, bioturbation, and erosion which often do not provide a suitable context for the preservation of organic material key for further cultural-environmental interpretation.

The area is known for a series of Plio-Pleistocene fossil-bearing infillings in caves and fissures of the highland region with abundant biostratigraphic evidence, exposed by mining activities and lime quarrying. Inside Leba Cave, a sequence of cultural remains suggested human presence at least since the Middle Stone Age (MSA), characterized by blade-point technologies and Acheulean tradition implements using local cherts and quartzites.

This study aims at building a robust contextual framework for the Stone Age of Leba Cave through the stratigraphic reassessment of the cave infillings, identification of depositional agents, anthropogenic features, and post- and syndepositional phenomena with critical comparisons of geological and historical data. The results are based on the analysis of site formation processes using contextual data from artifacts and sediments approached with geoarchaeological methods.

Fieldwork in 2018 and 2019 focused on limited excavation, cleaning, and re-evaluation of exposed sections in three different areas of the cave related to the MSA-LSA sequence previously published for the site. The targeted areas were named VOJ, JCF, and DMT.

Area VOJ (entrance trench) relates to unconsolidated sedimentary units with recent archaeological materials mixed with older ones, ranging from the colonial-industrial period to historical foraging-herding populations, including a hearth, groundstones, potsherds, and dominant Levallois lithic technology. Areas JCF (middle trench) and DMT (back wall) are located further inside the cave, behind a large cone of roof spall boulders separating the cave into two different chambers. Lithic artifacts found in both areas suggest chrono-cultural affinities with the MSA units described in past excavations, including handaxe, core tools, and flakes. Analysis of the surface exposed in area JCF showed this profile was particularly affected by post-depositional phenomena associated

with biological activity and seasonal puddling, promoting calcification and phosphatization since the excavation of 1950, which altered the base of the MSA sequence where Acheulean tradition tools were found. Area DMT is an indurated deposit in the rear of the cave that shows stratification at the micromorphological level including lithic tools and abundant mammal fauna of the Pleistocene.

Geoarchaeological investigation indicates a complex depositional history related to intense biogenic and anthropogenic activity, along with geogenic processes specific to the Leba karst and its hydrological regime. Our results propose a site formation model for the site and further avenues of research.

Zusammenfassung

Die Leba-Höhle befindet sich in den Dolomiten des Bezirks Humpata, Provinz Huila, im Südwesten Angolas. Diese Region mit ihren Steilhängen und Inselbergen ist das westlichste Hochland der Großen Randstufe im südlichen Afrika und verbindet ein Mosaik von Biomen zwischen den Küstenregionen, den hyper-trockenen Wüsten Namib und Kalahari und den Wäldern Zentralafrikas. Für paläoanthropologische Studien ist es besonders schwierig die Kultur- und Umweltdynamik dieses subtropischen Gebiets zu verstehen, da die hohen Verfalls-, Bioturbations- und Erosionsraten oft keinen geeigneten Kontext für die Erhaltung von organischem Material bieten, das für die weitere kultur- und umweltbezogene Interpretation wichtig ist.

Das Gebiet ist bekannt für eine Reihe von Fossilien aus dem Plio-Pleistozän, die in Höhlen und Klüften der Gebirgsregion zu finden sind und reichlich biostratigraphische Belege enthalten, die durch den Bergbau und die Kalksteinförderung freigelegt wurden. In der Leba-Höhle deutet eine Abfolge kultureller Überreste auf die Anwesenheit von Menschen mindestens seit der Mittelsteinzeit (MSA) hin, die sich durch hochmoderne Klingen- und Gerätetechniken der Acheulean-Tradition aus lokalen Hornsteinen und Quarziten auszeichnet.

Ziel dieser Studie ist es, durch die stratigraphische Neubewertung von Ablagerungen, die Identifizierung von Ablagerungsfaktoren, anthropogenen Merkmalen sowie post- und syndepositionalen Phänomenen und den kritischen Vergleich geologischer und historischer Daten einen robusten kontextuellen Rahmen für die Steinzeit in der Leba-Höhle zu schaffen. Die Ergebnisse beruhen auf der Analyse der Entstehungsprozesse von Fundstellen unter Verwendung von Kontextdaten aus Artefakten und Sedimenten, die mit geoarchäologischen Methoden untersucht wurden.

Die Feldarbeiten in den Jahren 2018 und 2019 konzentrierten sich auf begrenzte Ausgrabungen, Reinigung und Neubewertung von freigelegten Abschnitten in drei verschiedenen Bereichen der Höhle, die mit der zuvor veröffentlichten MSA-LSA-Sequenz für die Fundstelle in Verbindung stehen. Die Zielgebiete wurden als VOJ, JCF und DMT bezeichnet. Das VOJ-Gebiet (Graben im Eingangsbereich) bezieht sich auf unverfestigte Sedimenteinheiten mit rezentem archäologischem Material aus der Kolonialzeit bis hin zu historischen Jäger und Sammler, einschließlich einer Feuerstelle, Mahlsteinen, Topfscherben und der vorherrschenden Levallois-Steintechnik. Die Bereiche JCF (mittlerer Graben) und DMT (Rückwand) befinden sich weiter im Inneren der Höhle, hinter einem großen Kegel aus Deckenblöcken, die die Höhle in zwei verschiedene Räume unterteilen. Die in beiden Gebieten gefundenen Steinartefakte, darunter Faustkeile, Kerne und Klingen, lassen auf eine chronokulturelle Verwandtschaft mit den bei früheren Ausgrabungen beschriebenen MSA-Einheiten schließen. Die Analyse der freiliegenden Oberfläche im JCF-Areal hat gezeigt, dass dieses Profil besonders durch post-depositionelle Prozesse beeinflusst wurde, die mit biologischer Aktivität und saisonaler Grundwasserzirkulation zusammenhängen und die Entkalkung und Phosphatierung der freiliegenden Sedimente seit 1950 begünstigten. Diese Prozesse führten zu einer Veränderung der Basis der MSA-Sequenz, in welcher Acheuléen Steinwerkzeuge gefunden wurden. Das DMT-Gebiet ist eine verfestigte Ablagerung (Typ Kalksteinbrekzie) im hinteren Teil der Höhle, die eine Schichtung auf mikromorphologischer Ebene aufweist und in der Steinwerkzeuge und eine reichhaltige Säugetierfauna aus dem Pleistozän gefunden wurden.

Die geoarchäologische Forschung weist auf eine komplexe Ablagerungsgeschichte hin, die mit intensiven biogenen und anthropogenen Aktivitäten zusammenhängt, sowie mit spezifischen geogenen Prozessen der Karst-Leba und ihrem hydrologischen Regime. Unsere Ergebnisse präsentieren ein Modell für die Standortbildung und weitere Untersuchungsmöglichkeiten vor.

Sumário

A Gruta da Leba está localizada na formação dolomítica do distrito de Humpata, província de Huíla, no sudoeste de Angola. Esta região de escarpas e inselbergs representa as terras altas mais a oeste da Grande Escarpa da África Austral, ligando um mosaico de biomas entre os regimes costeiros, os desertos do Namibe e do Kalahari e as florestas da África Central. Para os estudos paleoantropológicos, a compreensão da dinâmica cultural e ambiental desta área subtropical é particularmente desafiante devido às suas elevadas taxas de decaimento, bioturbação e erosão que muitas vezes

não proporcionam um contexto adequado para a preservação de material orgânico para uma melhor interpretação cultural-ambiental.

A área é conhecida por uma série de fósseis Plio-Pleistocénico em grutas e fissuras da região montanhosa com abundantes vestígios biostratigráficos, expostos por actividades mineiras e extracção de calcário. Dentro da Gruta da Leba, a sequência cultural sugere a presença humana, pelo menos desde a Idade Média da Pedra (MSA), caracterizada por tecnologias de lâminas, pontas e utensílios de tradição Acheulense, utilizando chertes e quartzitos locais.

Este estudo visa construir um quadro contextual robusto para a Idade da Pedra da Gruta da Leba através da reavaliação estratigráfica dos preenchimentos das fissuras, identificação dos agentes deposicionais, características antropogénicas, e fenómenos pós e sindeposicionais com comparações críticas de dados geológicos e históricos. Os resultados baseiam-se na análise dos processos de formação de sítios, usando dados contextuais de artefactos e sedimentos abordados com métodos geoarqueológicos.

O trabalho de campo em 2018 e 2019 centrou-se na escavação limitada, limpeza e reavaliação de secções expostas em três áreas diferentes da gruta relacionadas com a sequência da Idade da Pedra Média e Superior (MSA-LSA) reportada para o local. As áreas visadas foram designadas como VOJ, JCF e DMT.

A área VOJ (entrada) relaciona-se com unidades sedimentares não consolidadas e materiais arqueológicos recentes, misturados com outros antigos, desde o período colonial-industrial até às populações de pastores e caçadores-recolectores, incluindo uma lareira, moventes, cerâmica e tecnologia lítica Levallois. As áreas JCF (sala-do-meio) e DMT (fundo) estão localizadas na área interior /mais profunda da gruta, atrás de um grande cone de blocos do tecto, que separam a gruta em duas salas distintas. Os artefactos líticos encontrados em ambas as áreas sugerem afinidades crono-culturais com as unidades da MSA descritas em escavações passadas, incluindo peças macrolíticas, lascas e lâminas. A análise da superfície exposta na área JCF mostrou que este perfil foi particularmente afectado por fenómenos pós-deposicionais associados à actividade biológica e circulação sazonal de águas subterrâneas, promovendo descalcificação e fosfatização dos sedimentos expostos desde 1950, o que alterou a base da sequência MSA onde foram encontrados instrumentos da tradição Acheulense. A área DMT consiste num depósito endurecido (tipo brecha calcária) na parte posterior da gruta que mostra estratificação a nível micromorfológico, onde foram encontrados utensílios líticos e numerosos vestígios de fauna de mamíferos do Pleistocénico.

A investigação geoarqueológica indica uma história deposicional complexa relacionada com uma intensa actividade biogénica e antropogénica, juntamente com processos geogénicos específicos do Carso da Leba e do seu regime hidrológico. Os nossos resultados propõem um modelo de formação do local e futuras vias de investigação.

Table of contents

Positionality statement i
Acknowledgments ii
Abstract iv
Zusammenfassung v
Sumário vi
List of figures xi
List of tables xviii
List of acronyms xix
0. Introduction: Atlantic Africa and the “West Side” of human evolution 1
Structure of the dissertation 5
1. Southwestern Angola 7
1.1. Geography and Landscape 7
1.2. Stone Age Archaeology 12
2. Site Background 23
2.1. The Humpata Karst: Local geology 23
2.2. Karst forms, infillings & fossil sites 27
2.3. The archaeological site: Leba Cave 33
3. Aims and theoretical justification 43
4. Materials and Methods 47
4.1. Field Methods 47
4.1.1. Excavation Strategy and Methods 47
4.1.2. Assemblage inventory and macroscopic observations 49
4.2. Laboratory methods 53
4.2.1. Micromorphology 53
4.2.2. Absolute dates 54
5. Field results 56
5.1. Area VOJ 56
5.1.1. Stratigraphy 56

5.1.2. Assemblages 60
5.2. Trench JCF 86
5.2.1. Stratigraphy 86
5.2.2. Assemblages 89
5.3. Trench DMT 91
5.3.1. Stratigraphy 91
5.3.2. Assemblages 95
6. Laboratorial Results 98
6.1. Micromorphology 98
6.1.1. Basic components 98
6.1.2. Sample description 105
6.2. Absolute dates 141
6.2.1. Radiocarbon ages 141
6.2.2. Other age measurements 142
7. Discussion and conclusions 144
7.1. Depositional processes 144
7.2. Post-depositional processes 146
7.3. Site formation model 148
7.4. Cultural variability and regional comparisons 155
8. Final remarks 161
Bibliography 165
Appendix 1 – Faunal analysis 193
Area VOJ 193
Area DMT 196
Appendix 2 – Lithic analysis 197

List of figures

FIG. 1 – GEOGRAPHIC REPRESENTANTION OF SOUTHWESTERN AFRICA INCLUDING THE COUNTRIES OF ANGOLA AND NAMIBIA WITH AVERAGE RAINFALL, OUTLINE OF ESCARPED REGIONS, PROVINCES AND MAIN CITIES IN RELATION TO LEBA CAVE (STAR), WITH ENGLISH AND PORTUGUESE CAPTIONS ADAPTED FROM MAP BY JOHN MENDELSOHN, ONGAVA/CIBIO (REPRODUCED WITH PERMISSION) _____ 10

FIG. 2 – DISTRIBUTION OF ARCHAEOLOGICAL SITES IN SOUTHWESTERN ANGOLA REFERENCED IN THE TEXT, BASED ON THE ARCHIVES OF THE TROPICAL RESEARCH INSTITUTE (DE MATOS ET AL., 2021B) _____ 17

FIG. 3 – A. GEOLOGY OF THE WESTERN EDGE OF THE HUÍLA PLATEAU (LOPES ET AL., 2016) AND B. LITHOLOGY OF THE CHELA GROUP (PEREIRA ET AL., 2011)_____ 24

FIG. 4 – DIGITAL ELEVATION MAP (DEM) FOR THE COASTAL ZONE WITH LOCATION OF OPEN-AIR SITES, IN THE VICINITY OF LEBA CAVE (ADAPTED FROM DE MATOS ET AL. 2021A, B) AND LOCATIONS SURVEYED BY THE PALEOLEBA PROJECT (2018-2019): 1 - PONTA NEGRA; 2 - FAZENDA AMÉLIA; 3 - GIRAÚL 8; 4 - GIRAÚL 1; 5 - GIRAÚL 9; 6 - MOÇÂMEDES 1; 7 - MOÇÂMEDES 2; 8 - VIMPONGOS; 9 - MAJOR 1; 10 - MUNHINO 20; 11 - MAONGO; 12 - MACAHAMA; 13 - PEDRA GRANDE 1; 14 - TORRES 1; 15 - CARACULO 6; 16 - MOÇÂMEDES 8; 17 - CARACULO 8; 18 - MUNHINO 3; 19 - MUNHINO 10; 20 - MUNHINO 19; 21 - ASSUNÇÃO 1; 22 - CHAMONA 1; 23 - ARRIAGA 1; 24 - CACANDA 1; 25 - MIALABE; 26 - ARRIAGA 2; 27 - BIPOPO; 28 - TECHALUNDIANGA; 29 - TUNDAVALA; 30 - MUCANCA; 31 - RIO CAPITÃO 1; 32 - BARRACÕES 1; 33 - SANTO ANTÓNIO - SÁ DA BANDEIRA; 34 - PSEUDOKARST SRA DO MONTE; 35 - ZOOTÉCNICA 2 – ESTAÇÃO; 36 - ZOOTÉCNICA 6 - 2ª BARRAGEM; 37 - ZOOTÉCNICA 5 – CASCATA; 38 - CASCATINHA DA ZOOTECNICA 1; 39 - NONDAU 1; 40 - OMPANDA 2; 41 - OMPANDA 1; 42 - MACONGE (STO ANTÓNIO); 43 - MACONGE 11; 44 - TAMPA 1; 45 - CHELA; 46 - PALANCA 1; 47 - AMURALHADO I DA HUILA; 48 - PEDREIRA/FORNO DE CAL DA TCHATICUCA I; 49 - LAPA/GRUTA DA PEDREIRA DA TCHATICUCA III; 50 - ALGAR/GRUTA DA PEDREIRA DA TCHATICUCA II; 51 - LAPA/GRUTA DA PEDREIRA DA TCHATICUCA I; 52 - GRUTA DO OMUKONGO (LAPA I E II); 53 - PEDREIRA/FORNO DE CAL DA LEBA I; 54 - ALGAR DA LEBA I; 55 - PEDREIRA DA LEBA II/PROCAL; 56 - CASCATA DA LEBA; 57 - ALGAR/GRUTA DE LEMAGOMA?; 58 - ONDIMBA DA TARTARUGA/ALGAR TCHÍUA I; 59 - GRUTA DA TCHÍUA; 60 - PEDREIRA DA TCHÍUA I; 61 - MEWÓ/TCHÍUA-UFEFUA; 62 - ALGAR/GRUTA DA MALOLA V; 63 - MACONGE 3; 64 - MACONGE 7; 65 - MACONGE 10; 66 - CAPAGOMBE - SANTO ANTÓNIO; 67 - CAPANGOMBE TERRACE; 68 - CAPANGOMBE VELHO (FORT); 69 - FORT OF CAPANGOMBE; 70 - TERRA NOVA; 71 - PROVIDÊNCIA 1; 72 - MAATIA; 73 - CHIVINGUIRO 2; 74 - BRUCO; 75 - GRUTA DA MALOLA II; 76 - LAPA/GRUTA DA MALOLA III; 77 - LAPA/GRUTA DA MALOLA IV; 78 - ALGAR/GRUTA DA MALOLA I; 79 - PEDREIRA/FORNO DE CAL DA MALOLA I; 80 - NASCENTE DO TCHIVINGUIRO; 81 - NANDIMBA 1/GRUTA DO TCHIVINGUIRO; 82 - ALGAR DO TCHIVINGUIRO VI; 83 -

ALGAR DO TCHIVINGUIRO IV; 84 - ALGAR DO TCHIVINGUIRO III; 85 - ALGAR DO TCHIVINGUIRO I - COLINA DE NANDIMBA; 86 - LAPA DA UNANDJAVA; 87 - RIO UMBUTU/UNANDJAVA; 88 - UMBUTU 1; 89 - NUATECHITE 1; 90 - HUMPATA; 91 - CATENDE 1; 92 - JAU 4; 93 - JAU 2; 94 - JAU 1; 95 - AMURALHADO DO ELÉU; 96 - CANGALONGUE; 97 - AMURALHADO DE MUELEMBA; 98 - ALGAR NKANGALONGUE/GRUTA DE CANGALONGUE; 99 - PEDREIRA DE CANGALONGUE I; 100 - CASCATA DA HUNGUÉRIA; 101 - MONGA; 102 - UMBALA 1; 103 - HUNGUÉRIA; 104 - CAVANGO - TAPAÍRA 1; 105 - CAINDE 2; 106 - CAINDE 1; 107 - LUNGO 1; 108 - AZEVEDO 1; 109 - MOÇÂMEDES 3; 110 - MOÇÂMEDES 4; 111 - MOÇÂMEDES 5; 112 - ALEXANDRE 4; 113 - ALEXANDRE 3; 114 - ARCO 1; 115 - CARVALHÃO 1; 116 - S - JOÃO 1; 117 - S - JOÃO DO SUL; 118 - ARCO; 119 - CARVALHÃO 2; 120 - OCTÁVIO 1; 121 - UNGUAIA 1; 122 - CARVALHÃO 3; 123 - ALEXANDRE 2; 124 - ALEXANDRE 1; 125 - PINDA; 126 - CONTENSIL _____ 32

FIG. 5 – PHOTOGRAPH OF LEBA CAVE IN THE 1960S (TROPICAL ARCHIVE, DO AMARAL, 1973) AND CURRENT STATE. _____ 34

FIG. 6 – SCHEMATIC STRATIGRAPHY FROM THE 1950 EXCAVATION IN LEBA CAVE PUBLISHED BY RAMOS 1982 AND CULTURAL PHASES PUBLISHED BY DE MATOS AND PEREIRA, 2020 IN RED. _____ 35

FIG. 7 – SCHEMATIC SECTION VIEW OF LEBA HILL, QUARRY AND CAVE (DASHED LINE OUTLINES TO THE UPPER LIMIT BETWEEN THE ROOF AND THE HANGING BRECCIA BLOCK) _____ 39

FIG. 8 – A: LOCATION OF THE CAVE (SQUARE) IN THE LEBA VALLEY IN WORLD VIEW (GOOGLE EARTH, IN YELLOW THE NATIONAL ROAD LUBANGO-NAMIBE); B: DETAIL OF THE SQUARE IN PICTURE 1 WITH OVERLAY OF THE CAVE OUTLINE IN RELATION TO THE QUARRY 1 (Q1) AND QUARRY 2 (Q2) (GOOGLE EARTH); C: AERIAL PHOTOGRAPH OF THE QUARRY; D: DETAIL OF FISSURE AND INFILLING WITH RED SEDIMENTS AND PLATY BEDROCK DEBRIS AT THE HILLTOP QUARRY EXPOSURE OF Q1 (2 M SCALE); E: DETAIL OF SLOPE SEDIMENTS OBLITERATED BY QUARRY. _____ 40

FIG. 9 – PLAN OF THE CAVE AND SECTION VIEWS FACING SOUTH, WITH PHOTO SECTIONS SHOWING THE HANGING BRECCIA ON THE WESTERN WALL (RIGHT SIDE OF THE PICTURES) AND THE BEDROCK WALL (LEFT SIDE). _____ 41

FIG. 10 – A: PANORAMA OF SOLUTION CHAMBER (SHADE) AND THE LIMESTONE POCKET EXPLORED BY THE QUARRY (RIGHT) INTERSTRATIFIED WITH DOLOMITES Q2; B: VIEW OF THE FISSURE (2M SCALE) AND KARST POCKETS WITH FOSSIL BRECCIA AT THE BASE; C: HYRAX MIDDEN IN SMALL CHAMBER; D: DETAIL OF THE CHAMBER COVERING THE FOSSIL BRECCIA IN F; E: DETAIL OF THE FLOWSTONES (10 CM SCALE); F: DETAIL OF BONE BRECCIA; G:DETAIL OF MAMMAL BONE (10 CM SCALE) _____ 42

FIG. 11 – SECTION VIEW OF THE CAVE WITH EXCAVATION GRID AND LOCATION OF APPROACHED AREAS AND VIRTUAL GRID USED IN THE DEM IMPLANTED WITH THE TOTAL STATION: AREA DMT – SQUARE MM; AREA JCF-SQUARE YY-ZZ; AREA VOJ: SQUARES L-M. _____ 48
FIG. 12 – SCHEMATIC REPRESENTATION OF THE SOUTH PROFILE IN AREA VOJ. ____ 58
FIG. 13 – SCHEMATIC REPRESENTATION OF THE NORTH AND EAST PROFILE IN AREA VOJ. _____ 59
FIG. 14 – POINT CLOUD FOR FINDINGS EXCAVATED IN AREA DMT PER GU WITH INDICATION OF SAMPLES FOR ^{14}C (LBC 2, 15, 18, 42). NOTE: 1) COLUMN 3 WAS LEFT UNEXCAVATED AFTER THE REMOVAL OF A LARGE BOULDER WITH ONLY ONEPOINT REFERING TO A LITHIC PIECE UNDER THE ROCK; 2) COLUMN 2 IS WHERE A PREVIOUS EXCAVATION PIT WAS LOCATED (POSSIBLY FROM THE 1974 EXCAVATION BY OLIVEIRA JORGE). _____ 60
FIG. 15 – ABUNDANCE OF BONE TISSUE TYPE IN AREA VOJ. _____ 63
FIG. 16 – BAR PLOT FOR RELATIVE FREQUENCY OF RAW MATERIALS IN THE ASSEMBLAGE. _____ 70
FIG. 17 – A-J: FLAKES IN LOCAL CHERTS AND QUARTZITES; L-P, S: PSEUDO-LEVALLOIS FLAKES; Q-R: BLADELETS; T: BLADE (KNIFE?) _____ 73
FIG. 18 – FLAKES IN MUDSTONE AND WACKESTONES FROM RIVER PEBBLES. _____ 74
FIG. 19 – FLAKES IN MILKY QUARTZ. _____ 74
FIG. 20 – “PSEUDO-LEVALLOIS” POINTS AND POINTS WITH FRAGMENTED TIPS IN MUDSTONE AND WACKESTONE (FIRST TO THIRD ROW), ORTOQUARTZITE, CHERT, WACKESTONE AND MUDSTONE (LOWER ROW) _____ 75
FIG. 21 – BOX PLOT AND DISTRIBUTION OF FLAKE, BLADE, POINT AND CORE METRICS (TOP TO BOTTOM, LENGTH, BREADTH, THICKNESS)_____ 78
FIG. 22 – SCATTER PLOT FOR LENGTH VS BREADTHS IN COMPLETE PIECES FROM AREA VOJ_____ 79
FIG. 23 – SCATTER PLOT FOR LENGTH VS THICKNESS IN COMPLETE PIECES FROM AREA VOJ _____ 79
FIG. 24 – THICK CORE ON QUARTZITE RIVER PEBBLE. _____ 83
FIG. 25 – HAMMERSTONES AND GRIND STONES ON QUARTZITE RIVER PEBBLES FROM AREA VOJ _____ 83
FIG. 26 – FRAGMENT OF BORED STONE IN PURPLE MUDSTONE FROM AREA VOJ. __ 84
FIG. 27 – DECORATED POTSHERDS FOUND IN THE COMBUSTION FEATURE OF VOJ-GU3 (A-I) AND GU 6.1. (J). _____ 85
FIG. 28 – BEAD WITH UNFINISHED DOUBLE PERFORATION. _____ 86
FIG. 29 – SCHEMATIC REPRESENTATION OF THE PROFILE OF JCF AREA. _____ 88
FIG. 30 – PROFILE EXPOSED IN AREA JCF WITH REFERENCE TO GUS._____ 88
FIG. 31 – ALMOND-SHAPED HANDAXE PRODUCED IN SILTSTONE-QUARTZITE RIVER COBBLE FROM JCF TRENCH (NOTE THE YELLOW CEMENT COATING THE TOOL) 90

FIG. 32 – MM98 BEFORE EXCAVATION (SCALE BAR DIRECTLY ON THE TESTED QUADRANTS) _____ 91
FIG. 33 – POINT CLOUD FOR FINDINGS EXCAVATED IN AREA DMT PER GU WITH INDICATION OF DOSIMETRY (LEBA2). _____ 93
FIG. 34 – PHOTOGRAPH OF THE PROFILE AND LOCATION OF THE BLOCK SAMPLES FOR MICROMORPHOLOGY (171-172), INCLUDING REFERENCE TO DOSIMETRY PLACEMENT (RED STARS); B: DETAIL OF THE SAMPLED SECTION INCLUDING REFERENCE TO LOWER PART; C: DETAIL OF A LOWER SECTION OF THE COLUMN; D: DETAIL OF THE LOWERMOST RED AND YELLOW LAMINATIONS, WHITE ROUNDED GRANULES ARE BONE FRAGMENTS. _____ 94
FIG. 35 – COPROLITE FOUND IN AREA DMT. _____ 96
FIG. 36 – ABUNDANCE OF BONE TISSUE TYPES IN AREA DMT _____ 97
FIG. 37 – THICK SCRAPER ON LEVALLOIS CORE IN QUARTZITE RIVER PEBBLE FOUND IN AREA DMT. _____ 97
FIG. 38 – TABLE OF COMPONENTS, STRUCTURES AND FEATURES OBSERVED IN THIN SECTIONS FROM LEBA CAVE (ACRONYMS: T.S. – THIN SECTION, GU- GEOLOGICAL UNIT, MU-MICROUNIT, LB – LOWER BOUNDARY, E- EROSIONAL, G-GRADATIONAL, S-SHARP) _____ 104
FIG. 39 – A) VIEW OF SHALLOW SOIL COVER OF THE HILL ABOVE THE CAVE IN Q2; B) VIEW OF SAMPLE 1X BEFORE COLLECTION (COLOUR SCLA WITH 10 CM); C) SCAN OF THIN SECTION IN PPL, D) SCAN OF THIN SECTION IN XPL (THIN SECTION WITH 60X90 MM) _____ 106
FIG. 40 – LOCATION OF THE BLOCK SAMPLES IN THE VOJ EAST PROFILE, PICTURE OF THE NEGATIVE OF THE BLOCK SAMPLES, SLAB WITH REFERENCES TO THE MICRO-UNITS DESCRIBED (3A-D) AND HIGH-RESOLUTION SCANS OF THE THIN SECTIONS (SLIDE WITH 90X60 MM) _____ 107
FIG. 41 – MICROPHOTOGRAPHS FROM SAMPLE 521. A. WELL ROUNDED AGGREGATE FROM SOIL COVER, IN PPL; B. TRAMPLED AGGREGATE NOTE THE ZIG ZAG PLANES AND VUGHS FROM SPONGY MICROSCTRUCTURE AND ROTATIONAL REARRAGMENT OF PARTICLES; C. CHARCOAL AND ASH RHOMBS IN THE HEARTH (MU3C); D. SAME IN XPL, NOTE THE AMORPHOUS MATRIX FROM THE BURNED MATERIAL AND THE ASH RHOMBS; E. SPHERULITES FROM HEATED DUNG IN A MATRIX OF AMORPHOUS ORGANIC MATERIAL AND PHOSPHATIC MINERAL AGGREGATES LIKELY LEUCOPHOSPHITE (RED ARROW); F. PLANT LEAF WITH DEFORMATION AND DRYING CRACKS IN A MATRIX OF HETEROGENOUS MATERIAL INCLUDING WIND-BLOWN SILTS, FRAGMENTS OF HEATED AND NON-HEATED BONE, SOIL AGGREGATES AND COPROLITES _____ 111
FIG. 42 – FROM LEFT TO RIGHT, A) LOW-RESOLUTION SCAN OF THIN SECTION, B) MICRO-XRF SCAN OF THE FULL THIN SECTION FOR IDENTIFICATION OF MAIN ELEMENTS (AL, SI, P, CA), NOTE THE LIGHT GREEN COMPONENTS ARE FAUNAL

REMAINS AND PINK REFER TO PHOSPHATIZED AGGREGATES; C) SCAN ONLY FOR PHOSPHOROUS. _____ 113
FIG. 43 – MICROPHOTOGRAPHS FROM SAMPLE M4. A. HEATED BONE FRAGMENT NEXT TO A RED AGGREGATE WITH PHOSPHATIC RIND, 100 µM THICK; B: SAME IN XPLNOTE THE AMORPHOUS PHOSPHATIC MATERIAL COATING ON GUANO AGGREGATE AND THE ABSENCE OF BIREFRINGENCE; C-D, E-F: CARNIVORE COPROLITES; G. ELONGATED FE NODULE (LEFT), AND LEUCOPHOSPHITE MINERAL AGGREGATE WITH SPHERULITIC SHAPE (RIGHT), A SECONDARY PHOSPHATE DERIVED FROM GUANO; H. SAME IN XPL. _____ 114
FIG. 44 – VIEW OF PROFILE OF SOUTH PROFILE OF SQUARE L2 IN AREA VOJ, CONTACT OF DRIPLINE; BLOCK SAMPLES AND THIN SECTION HIGH RESOLUTION SCAN (LEFT TO RIGHT) (THIN SECTION WITH 90X60 MM) _____ 115
FIG. 45 – THIN SECTION 251: A. CHANNEL INFILLINGS WITH WELL ROUNDED COARSE AGGREGATES AND POROUS INFILLINGS FROM BIOGENIC ACTIVITY, NOTE THE UNDULATING WALLS AND SHARP BOUNDARY OF THE AGGREGATES (RED ARROW); B. LITHOLASTS OF HANGING BRECCIA (HB) WITH SUBROUNDED SHAPES, AND INTERCONNECTED BIOGALLERIES AND CHANNEL VOIDS (V), NOTE WITH INTERGRAIN MICROAGGREGATES MICROSTRUCTURE AND ORGANIC PUNCTUATIONS (DARK PARTICLES); C. RED SANDY-CLAYEY COATING WITH INHERITED OXIC FEATURES ON COARSE BEDROCK FRAGMENT OF ALTERED CHERT (BD); D. DIFFERENT LITHOCLASTS OF HANGING BRECCIA (HB) , BEDROCK FRAGMENTS (BD) AND WELL ROUNDED AGGREGATES COM BIOGENIC ACTIVITY. THIN SECTION 250: E. ANGULAR DEBRIS OF HANGING BRECCIA WITH BEDDING AND SHOWING A SILTSTONE FRACTION (SILT), COARSE INCLUSIONS (CHERT) AND GOTHETITE RICH CLAY (C), WITH BIOGALLERY (CR); NOTE THE WELL DEFINED BOUNDARY AND SILTY-CLAYEY (RED ARROW); F) ROTATIONAL ARRANGEMENT OF ROCKFALL AND RED BRECCIA LITHOCLAST WITH BONE INCLUSIONS (RED ARROW). _____ 118
FIG. 46 – FROM LEFT TO RIGHT, SCHEMATIC PROFILE OF THE ORIGINAL EXCAVATION (BASED ON RAMOS, 1982) WITH REFERENCE TO LABELLED PROVENANCE; MUSEUM SAMPLES; CHIPS OF THE COMPLETE SAMPLE AND THIN SECTIONS ANALYSED (LEB-50-1, LEB-50-2) (THIN SECTIONS WITH 60X90 MM) _____ 120
FIG. 47 – MICROPHOTOGRAPHS FROM SAMPLE 50-2: A. BONE IN RED SANDY-CLAYEY MATRIX WITH STRONGLY DEVELOPED CALCITE NODULES, IN PPL B. VIEW OF THE SAME BONE, NOTE THE GRANULAR QUARTZ RICH GROUNDMASS IN THE TOP, AND MASSIVE MICROSTRUCTURE AT THE BOTTOM DUE TO THE CALCITE NODULE; C-D. DETAIL OF COATINGS AND CEMENTATION OF THE RED SOIL AGGREGATES OVERSHADOWING THE GROUNDMASS;; MICROPHOTOGRAPHS FROM SAMPLE 50-1: E: COARSE TO FINE CRUMBS AND ANGULAR FRAGMENTS, BONE (B) IN A GROUNDMASS OF SUPERIMPOSED SANDY CLAYEY COATINGS AND CALCITIC

CEMENT, D) SAME IN XPL, E. SECONDARY CALCITE NODULES IN A INTERGRAIN MICROAGGREGATE MICROSTRUCTURE WITH ENAULIC C/DISTRIBUTION PATTERN,, F. COARSE BONE (B) COATED WITH SILTY CLAYEY MICROAGGREGATES, NOTE THE SPARY CALCITE (RED ARROW) COATINGS IN VOIDS (V), IN XPL; G. DOLOSTONE (D) SAND AND RED SILTY-CLAYEY AGGREGATES WITH CALCITE (CA) NODULES INFILLING THE POE SPACE; H. SAME IN XPL ____ 122
FIG. 48 – SCHEMATIC REPRESENTATION OF THE PROFILE OF JCF AREA. _____ 123
FIG. 49 – LOCATION OF SAMPLE M7 IN THE SOUTH PROFILE OF JCF, DETAIL O SAMPLE, AND HIGH-RESOLUTION SCAN OF THIN SECTION (LEB-M7) (THIN SECTION WITH 90X60 MM) _____ 123
FIG. 50 – LOCATION OF SAMPLE M6 IN THE SOUTH PROFILE OF JCF, DETAIL OF SAMPLE, AND HIGH-RESOLUTION SCAN OF THIN SECTION (LEB-M6) (THIN SECTION WITH 90X60 MM) _____ 124
FIG. 51 – MICROPHOTOGRAPHS FROM THIN SECTIONS M7: A. WELL-ROUNDED SINGLE QUARTZ GRAIN FROM RIVER ALLOCHTHONOUS SOURCE IN THE RIVER VALLEY (927 µM) IN LOOSE CHANNEL INFILLINGS WITH GROUNDMASS COMPONENTS; B. DOLOSTONE FRAGMENT WITH INHERITED PYRITE AND MANGANESE CRUSTS, C. INHERITED MN NODULE WITH INTERNAL FABRIC; D. DUSTY CLAY-SILT COATINGS; MICROPHOTOGRAPHS FROM THIN SECTION M6: E. CRESCENT DUSTY AND LIMPID CLAY COATINGS; F. SAME IN XPL, NOTE THE WEAK BIREFRINGENCE (RED ARROW) OF POROSTRIATED B-FABRIC. _____ 127
FIG. 52 – SAMPLE 4 (CRUST): CHIP AND XRF SCAN OF THE CHIP (ON THE LEFT); THIN SECTION SCANS IN PPL AND XPL (ON THE RIGHT) WITH REFERENCE TO MICROUNITS IN WHITE (THIN SECTION WITH 90X60 MM). _____ 128
FIG. 53 – BLOCK SAMPLES COLLECTED IN AREA DMT WITH LOW-RESOLUTION SCAN OF CHIPS (TOP TO BOTTOM, LEB-171A, B, C, LEB-172A, B, C), THIN SECTIONS IN PPL AND XPL WITH REFERENCES TO DIFFERENT MICROUNITS (IN WHITE); AND LOW-RESOLUTION SCANS WITH MICROXRF WITH MAIN ELEMENTS AL (DARK BLUE),SI (SILICON), P (ORANGE) AND CA (LIGHT BLUE), (THIN SECTIONS WITH 90X60 MM) _____ 130
FIG. 54 – MICROPHOTOGRAPHS FROM SAMPLES 171A AND 171B; A: MU2B, RIP-UP CLASTS WITH BONE INCLUSIONS (RC), AFTER BEDROCK GRAVEL HYPERCONCENTRATED FOWS, NOTE THE EROSIONAL CONTACT (YELLOW ARROW), AND MICROLAMINATED COATING OF BEDROCK GRAVEL (RED ARROW) MU2.1A; B: SAME IN XPL; C: SAMPLE 171B, MU2.1E, COARSE BONE AGGREGATED TO FINE SILTY GREY MATERIAL; D: SAME IN XPL; E: DISSOLVED BONE (DASHED BLACK) IN A PALE YELLOW PHOSPHATIC CRUST PROBABLY FROM A COPROLITE, F: SAME IN XPL, NOTE THE UNDULATING LOWER BOUNDARY, THE VERY FINE SAND AND SILT QUARTZ GRAINS IN THE PHOSPHATIC CRUST (DASHED WHITE) AND A RIP-CLAST (RC), SUGGESTING TRANSLOCATION. _____ 135

FIG. 55 – MICROPHOTOGRAPHS FROM SAMPLES 171B AND 171C. A: MU2.1F, SUBROUNDED LITHOCLASTS FROM THE HANGING BRECCIA, WITH INTERBEDDED BEDDED SILTSTONE-CLAYSTONE, NOTE THE GOETHITE RICH YELLOW FROM FLUVIAL-KARST DEPOSIT SUGGESTING ROCKFALL AND TRANSLOCATION OF DEBRIS ERODING FROM THE ROOF; B: FRAGMENTS OF FLOWSTONE ACCOMMODATING WITH B FROM THE EROSION OF CALCITE FILMS ON THE WALLS REWORKED WITH THE HANGING BRECCIA CLASTS, AND RECEMENTED; C: CONTACT BETWEEN MU2.1F-MU2.2A UNDERLYING THE TRAINS OF CLASTS, NOTE THE RIP UP CLAST (YELLOW ARROW) OF THE CRUST SURFACE IN 2.2A; D: INHERITED MN NODULE WITH INTERNAL FABRIC (YELLOW ARROW) TYPICAL OF LATERITES OF OXISOL HORIZONS, NOTE THE ANGULAR SHAPE AND SHARP BOUNDARY; E: MU2.2B, LOOSE PACKING OF BEDROCK GRAVEL WITH MICROLAMINATED COATINGS OF SILT-CLAY AND SAND-CLAY (RED ARROW) FROM TRANSLOCATION ACROSS THE SITE, NOTE THE POE SPACE CEMENTED WITH WITH TABULAR CALCITE NODULES; F: SAME, DETAIL OF THE TABULAR CALCITE NODULES (WHITE SQUARE IN E) COATING THE MICROAGGREGATES, SEVERAL LAYERS SUGGEST SEVERAL PHASES OF SECONDARY DEPOSITION OF CALCITE _____ 136

FIG. 56 – SAMPLE 172A-C; A: COARSE AGGREGATE OF DUNG WITH COARSE BONE AND IN LOOSE MICROAGGREGATE MICROSTRUCTURE CEMENTED WITH SARY CALCITE; B: FLUVIAL-KARSTIC AGGREGATE WITH COARSE INCLUSION, NOTE THE FINE LAMINATED CLAYS AND SILTS OF THE AGGREGATE; C: WELL ROUNDED COARSE QUARTZ GRAIN WITH INHERITED FE STAINING; D: MU2.3 ROUNDED RIP-UP CLASTS (WHITE DASHED LINE) ; E: CRUS T IN MU2.2F (WHITE DASHED LINE, SUGGESTING STASIS AND PRESERVED SURFACE; F: SAME IN XPL, NOTE THE COMPACTED STRUCTURE AND ABSENCE OF SECONDARY CALCITE INFILLING PORE SPACES AS THE SURROUNDING GROUNDMASS, INTERCALATION OF FINE ENAULIC AND PORPHYRIC C/F DISTRIBUTION. _____ 140

FIG. 57 – AGE CALIBRATION OF ^{14}C DATES OBTAINED FROM COLLAGEN SAMPLES OF AREA VOJ._____ 142

FIG. 58 – SCHEMATIC SITE FORMATION MODEL REPRESENTING THE MAIN STAGES OF FORMATION AND INFILLINGS OF LEBA CAVE APPROACHED IN THIS STUDY.___ 153

FIG. 59 – SCHEMATIC REPRESENTATION OF INFILLINGS STUDIED AND CORRELATING TO FIGURE 58. _____ 154

List of tables

TABLE 1 – ABSOLUTE AGES AVAILABLE FOR LEBA CAVE DEPOSITS. 38
TABLE 2 – KEY FOR BOVID SIZE CLASSES (ADAPTED FROM BRAIN, 1974; AND CLARK AND PLUG, 2008; AND INCLUDES ADDITIONAL ANGOLAN BOVIDS AFTER HILL AND CARTER, 1941; AND AFTER HUNTLEY ET AL., 2019). 50
TABLE 3 – DESCRIPTIVE CRITERIA FOR LITHIC ASSEMBLAGES FROM LEBA CAVE 52
TABLE 4 – SUMMARY DESCRIPTION OF GEOLOGICAL UNITS OF AREA VOJ. 60
TABLE 5 – GENERAL INVENTORY OF MACROMAMMAL TAXONS IDENTIFIED IN AREA VOJ. 61
TABLE 6 – FREQUENCIES OF OBSERVED MECHANICAL AND CHEMICAL ALTERATIONS, SEDIMENT CRUSTS, GNAWING, AND ANTHROPOGENIC DAMAGE IN MACROMAMMAL SPECIMENS RECOVERED IN AREA VOJ LEBA CAVE. (*) SYMBOL INDICATES SAMPLES EXCLUDING TOOTH ELEMENTS 62
TABLE 7 – GENERAL INVENTORY OF MICROMMAMMAL TAXONS IDENTIFIED IN AREA VOJ. 65
TABLE 8 – GENERAL INVENTORY OF BIRD SIZE CLASSES IDENTIFIED IN AREA VOJ. .. 66
TABLE 9 – GENERAL INVENTORY OF LITHIC ARTIFACTS COLLECTED IN AREA VOJ. 68
TABLE 10 – FREQUENCY OF RAW MATERIALS IN THE VOJ ASSEMBLAGE. 69
TABLE 11 – FREQUENCY OF BLANKS AND CORES WITH SURFACE ALTERATIONS AND PRESENCE OF FIRE MARKS FROM AREA VOJ. 71
TABLE 12 – CORE TYPOLOGY BASED ON COMPLETE CORES CONSIDERING EXPLOITATION (EXTENSIVE, INTENSIVE, PRE-DETERMINATE); CONCEPT AND METHOD. 77
TABLE 13 – MEAN, MEDIAN AND MODE VALUES FOR METRIC ATTRIBUTES (IN CM) FOR COMPLETE FLAKES, BLADES, POINTS AND CORES OF AREA VOJ. 78
TABLE 14 – FORMAL TOOLS 81
TABLE 15 – A. POLYEDRAL CORE WITH PEBBLE CORTEX; B: PRISMATIC CORE, C: THICK SCRAPER 82
TABLE 16 – ABSOLUTE FREQUENCY OF CERAMIC FINDS AND OTHER MATERIALS FROM AREA VOJ. 84
TABLE 17 – SUMMARY DESCRIPTION OF GEOLOGICAL UNITS OF AREA JCF. 89
TABLE 18 – SUMMARY DESCRIPTION OF GEOLOGICAL UNITS OF AREA DMT. 93
TABLE 19 – GENERAL INVENTORY OF MACROMAMMALS IDENTIFIED IN AREA DMT. ... 95
TABLE 20 – FREQUENCIES OF OBSERVED MECHANICAL AND CHEMICAL ALTERATIONS, SEDIMENT CRUSTS, GNAWING, AND ANTHROPOGENIC DAMAGE IN MACROMAMMAL SPECIMENS RECOVERED IN AREA DMT, LEBA CAVE. (*) SYMBOL INDICATES SAMPLES EXCLUDING TOOTH ELEMENTS. 97
TABLE 21 – LIST OF SAMPLES FROM AREA VOJ ANALYZED WITH RADIOCARBON ^{14}C: LBC-2 VERTEBRA WITH CUTMARK (VC); LBC-42, 15, AND 18 FROM BURNED BONE (B.B) 142

List of acronyms

ESA – Early Stone Age

MSA – Middle stone Age

LSA – Late Stone Age

EIA – Early Iron Age

LIA – Late Iron Age

GU – Geological Unit

MU – Micro-unit

^{14}C – Radiocarbon

ESR – Electron Spin Ressonance

OSL – Optically Stimulated Luminescence

MIS – Marine Isotopic Stage

DNA – Deoxyribonucleic Acid

HCl – Hydrocloric acid

MAA – Missão Antropobiológica de Angola/Anthrobiological Mission of Angola

MEASA – Missão de Estudos Arqueológicos do Sudoeste de Angola/Archaeological Mission Southwest Angola

JIU – Junta das Investigações no Ultramar/Colonial Board for Missions Overseas

IICT – Instituto de Investigação Científica Tropical/Tropical Research Institute of Portugal

MNAB – Museu Nacional de Arqueologia de Benguela, Angola/National Archaeology Museum of Benguela, Angola

MUHNAC – Museu de História Natural e da Ciência de Lisboa/Natural History and Science Museum of the University of Lisbon, Portugal

0. Introduction: Atlantic Africa and the “West Side” of human evolution

What is the role of the Atlantic coast in the evolution of modern human populations? How did the western landscapes shape the development (sometimes disparity) in cultural complexity of the *Homo sapiens* population by the Atlantic coast during the Stone Age, and how do their cultures link with the sequence of other sub-continental regions in Africa? Were there landscapes and populations isolated by extreme climatic conditions over the Pleistocene? These questions connect with the idea of an “Atlantic Out of Africa” migration arguing for several *Homo sapiens* populational movements along the Atlantic coast which worked as a corridor between deserts and forests. The idea is supported by similar patterns of subsistence and fossil evidence between southern and northern Africa.

The Middle and Late Pleistocene (MP: ~781 ka – 126 ka; LP: ~126 ka -12 ka[1]) is of most interest to this discussion as it yields evidence of Middle Stone Age (MSA) innovations associated with *Homo sapiens* and relating to a diversity of culture, advanced subsistence techniques, complex technology and ritual practices. Defining the expression of the MSA in Africa as-a-whole has proven to be a considerable challenge since the different subcontinental regions show specific characteristics and sequences in the emergence of subsistence strategies and/or technological and artistic behaviors commonly perceived as advanced.

Coastal adapted behaviors associated with tool kits and symbolic art have been systematically associated with a major leap in human evolution around 130-70ka in Southern Africa (Henshilwood and Marean, 2006; Marean et al., 2007; Shipton et al., 2018; Will et al., 2013). Similar patterns are observed in Northern Africa at about the same time (Bouzouggar et al., 2007; Richter et al., 2017; Scerri, 2017). In comparison, the archaeological record of Atlantic Africa is patchy. Studies of the Stone Age in western Africa are slowly bringing forth new advances. Indirect dating of stone tools using in-situ produced cosmogenic nuclides (^{10}Be and ^{26}Al) in Gabon (Braucher et al., 2022) and Angola (Lebatard et al., 2019) point to an MIS 15-12 adaptation to tropical coastal landscapes. As the assemblages and respective dating methods are arguably accurate for the Early Stone Age, this seems to confirm the opportunistic exploitation of marine

[1] In 2020, the International Union of Geological Sciences (IUGS) replaced the term” Middle Pleistocene” with "Chibanian" currently estimated to span the time between 0.770 Ma (MIS-19 ~770 ka) and 0.126 Ma (MIS 5e ~126 ka). However, the previous terminology will be used in this study.

resources in Angola as early as 700 ka (Chazan and Horwitz, 2006; Gutierrez et al., 2001). For the Late Pleistocene

and Holocene cultures sites like the Faléme Valley in Senegal (Chevrier et al., 2020, 2016; Douze et al., 2021) or in Katanda in D.R. Congo (Cornelissen, 2016) present similar cultures and age ranges between 80-70 ka. However, these are rare exceptions on a landscape with numerous undated surface lithic assemblages and limited resolution for contexts before 50,000 BP (Clist et al., 2022). These sites are also particularly interesting as they are culturally very different from the technologies recognized as dominant in other coastal areas occupied around the same time (Porraz et al., 2018; Soriano et al., 2015).

Several potential issues have been consistently pointed out when approaching quaternary stratigraphy in tropical and sub-tropical environments, particularly in open-air contexts, and include: (1) questions of quick weathering and erosion promoted by high soil acidity; (2) intense biogenic activity by both flora (roots) and fauna (termite and other micro-organisms); (3) peculiar pedogenic phenomena such as “stone lines”; (4) aeolian processes; (5) and flash floods and other catastrophic events related to the seasonal monsoons. These challenges add to more practical research considerations in these regions from the past decades, particularly those relating to historical and social issues such as the colonial lobby, political and economic interests, poverty and warfare, and increasing disruption of climate change and extreme aridity on local communities. Crucial evidence about the habitats, and associated cultural traditions and styles of prehistoric times is still lacking for this region and can only be explained by the infrequency of research over the last few decades. A pan-African emergence of *Homo sapiens* is mostly theoretical at this point, based primarily on the contextual and fossil data gathered in Northern and Southern Africa.

Many lines of evidence demonstrated the remote origins of contemporary human groups are located in Africa within a restricted group or population (Liu et al., 2006), and suggest global demography was shaped by major bottleneck events over the course of the Late Pleistocene and early Holocene (Fagundes et al., 2007). A long history of population admixtures and regional variations is identified as a key feature in the evolution of contemporary demography (Andirkó et al., 2022; Fu et al., 2016, 2014; Hajdinjak et al., 2018; Mallick et al., 2016; Noonan et al., 2006; Prüfer et al., 2014; Slon et al., 2017), but data consistently highlights an African emergence of modern human groups sometime between ~350 ka and ~200 ka (Bergmann et al., 2022; Meneganzin et al., 2022; Schlebusch et al., 2021, 2017; Willoughby, 2020).

Recent perspectives now challenge the idea that *Homo sapiens* evolved within a single population and/or region of Africa (Scerri et al., 2018). These studies suggest a structured development resulting from a dynamic interplay of ecological drivers, demographics, and inherited traits among African prehistoric populations (Berger et al., 2017; Hublin et al., 2017; Lipson et al., 2020). This scenario seems to be consistent with the anachronic emergence of behavioral changes observed in the paleoanthropological record during the Pleistocene (Wurz, 2013a). A key trait in the evolutionary history of the *Homo sapiens* lineage is variation, not only morphological but also behavioral and cultural (Conard, 2010). Interestingly, human variation is associated with environmental variation during the Pleistocene.

Environmental research suggests that human evolution was triggered by periods of weather amelioration during the MP and LP with increased humidity allowing higher levels of biomass and demographic expansion (Basell, 2008; Ziegler et al., 2013). Climatic shifts had a significant impact on the availability of contiguous biomes of steppe, savanna, and woodland forests across sub-continental areas. During interglacials, these areas hosted vast sources of food and water. On the other hand, during periods of increased aridity and expansion of the drylands, areas with permanent water sources, mild conditions, and refuge would become hotspots for animal and human habitats. Arguably, these areas are highlighted as ecological niches, or zones for speciation due to isolation (d'Errico et al., 2017; Ziegler et al., 2013). This hypothesis connects with the Out of Africa theory on the migration of ancestral human populations. Instead of one rapid event, this hypothesis suggests several bottleneck episodes derived from successive population dispersals caused by the dynamic interplay of climate variables and landscape changes causing isolation and local adaptations (Marean, 2015). In this sense, certain African landscapes, environme,nts or landforms could work as natural boundaries or catalysts in evolutionary processes (Boaz et al., 1982).

Following this theoretical framework, the search for so-called ecological niches and their relationship to the emergence of *Homo sapiens* has focused particularly in coastal and near-coastal regions and along major river valleys where concentrations of prehistoric artifacts were identified (eg. Clark, 1971; Giresse, 2008; Nicoll, 2010; Scerri et al., 2016; Will et al., 2019; Wright et al., 2017). Fossils assigned to the *Homo* species are quite scarce in this region. Until now only one fossil at Ihu Eleru in Nigeria has been studied (Allsworth-Jones et al., 2010). This fossil corresponds to a very late upper Pleistocene (c. 12 ka) and presents archaic *Homo sapiens* features and a close morphological association to the Ngaloba LH 18 skull from Tanzania, which is roughly dated to between

490 ka and 130 ka (Harvati et al., 2011) and which has supported the idea of the tropical forest and the desert masses (Kalahari-Namib) isolating western populations.

The PaleoLeba project is motivated by the broad theoretical question of a pan-African emergence of *Homo sapiens* and the hypothesis that the Atlantic environments had a key role in human population development in the MSA. Our focus in the area of South Angola (Namibe, Kunene and Huíla) is due to this regions high concentration of Stone Age lithic artifacts associated with the ESA and MSA (de Matos et al., 2021b) and by the natural and geological conditions of the area which allow the preservation of potentially datable organic material (Berger and Libby, 1969; David and Pickford, 1999; Pickford et al., 1990). Specifically in the case of Leba Cave, paleontological remains were associated with lithic industries (Camarate-França, 1964) in a sequence of archaeological horizons relating to three archaeological levels ranging from an Acheulean traditional flake blade industry to an “undifferentiated” MSA/LSA industry (de Matos and Pereira, 2020).

Leba Cave (-15.083453°, 13.259457°) was identified by its early MSA and LSA artifacts, which include fauna, and initially interpreted as a seasonal hunting site with an MSA horizon dated to either ~80 ka or ranging between 100 ka to 50 ka. This is also the only Angolan site predictably with human occupation at the MIS 5c-MIS4 boundary or earlier. The anthropogenic features detailed by early excavators offered the opportunity to approach the MSA in Angola. Plenty of Stone Age lithic industries were identified in the region and highlighted specific regional features which can only be coarsely associated with the Southern African cultural sequence (de Matos and Pereira, 2020; Ramos, 1982) but only Leba Cave showed the preservation of bone (Gautier, 1995). This dissertation is focused on Leba Cave with the goal of establishing a site formation model informed by the interplay of depositional and post-depositional agents. Additionally, these processes are evaluated as sources of potential interpretation biases and revision of the MSA sequence is proposed for the site. This study is part of a broader project coupling geological and archaeological data to link human adaptations to the evolution of the landscape between the coastal Namibe desert and the Southern escarpment of Angola.

The geoarchaeological study of Leba Cave intends to provide a critical reappraisal of the cave infillings integrated with the material culture. Our goal is to obtain data for site-scale reconstruction in order to test whether Leba Cave was used by humans, and under what conditions, to examine how the cultural features at Leba Cave compare with local and regional sequences and demonstrate how formation theory can be applied to the

interpretation of complex archaeological sites. It is expected to discuss the so-called human occupation of the site during the Pleistocene.

At the same time, the study intends to introduce a micromorphologically informed stratigraphy for one of the caves in the Humpata plateau and define methodological approaches for continued field research in this region of southwestern Angola focused on the reconstruction of the paleolandscape.

Structure of the dissertation

The dissertation is organized in eight sections.

The first section is dedicated to the region of Southwestern Angola and divided in two sub-sections, with the first focusing on the geography, geomorphology and landscape of the region; and the second sub-section focuses on the Stone Age archaeology discussing sites, findings and cultural interpretations proposed by different authors.

The second section is about the site background and is subdivided in four sub-sections: the first dedicated to the local geology of the Humpata karst; the second is about the topography, infillings and paleontological remains previously discovered in the caves; the third is about the site Leba Cave, the context of discovery, location and background; and the fourth subsection develops on the aims of this study and what are the specific questions for the methods applied.

The third section addresses the goals of this study and the theoretical background of the geoarchaeological matrix approach guiding the field and laboratorial methods.

The fourth section describes the methodology and is divided into field and laboratory methods, describing excavation strategy, and inventory databases; the second subsection is focused on the micromorphology methods, describing the procedures and tools used in sample processing and analysis.

The fifth section is focused on the field results presented by excavation area. Three excavation areas are discussed including data from field observations, stratigraphy and assemblage analysis. Descriptive inventories of the faunal remains, lithic artifacts, pottery and other material records are presented. Technological analysis of the lithic assemblages collected is also presented.

The sixth section is focused on the laboratorial results. The first subsection presents the results of micromorphological methods applied to the samples collected at Leba focusing on main components, post-depositional features and diagenesis presented separately

per excavation area. The second subsection presents the results of radiocarbon dating applied to collagen of mammal bone of area VOJ and the discusses minimum age results using uranium/thorium-series and luminescence for materials of are DMT.

The seventh section is focused the discussion and conclusions of the study and is subdivided in three subsections: the first focuses on depositional processes observed in the cave, the second addresses the post-depositional processes, and the third proposes a site formation model, integrating data analysed in the field and laboratory results.

The eighth section provides a final synopsis of the study developed, contextualizing the geoarchaeological study of Leba Cave and final remarks about future avenues of research for the region.

1. Southwestern Angola

1.1. Geography and Landscape

The highest altitudes of the Escarpment are often referred to as a separate geomorphological unit: the Marginal Mountain Chain (Diniz, 2006; Pereira, 1977) which covers approximately 300 km of escarped relief from NE-SW, between Tchongorói, Benguela Province, in the north, and to Oncôncua, Cunene Province, in the south (Jessen, 1936; Lopes et al., 2016). The area is characterized by a series of inner plateaus with altitudes ranging from 1500 and 2650 m a.s.l., which can be sub-divided into the Highlands of Huambo, Benguela, and Huíla (Fig. 1). Locally, some of the key mountain hills are located up north, Serra da Neve in Huambo Province (2,650 m a.s.l.). In the south, the Serra da Chela in Huíla Province includes the Humpata and Bimbe plateaus. These plateaus connect the coastal and escarped regions with the extensive peneplain of interior Angola, at altitudes ranging between 1000-1500 m a.s.l., which includes 65% of the national territory (Mendelsohn, 2019). The south interior is shaped by the extensive drainage basins of the Zambezi, Cuando-Cubango (Upper Okavango), and Cunene rivers. In the southeast region, particularly, the Kalahari “sandsea” is a major geomorphological feature shaping the ecosystems of Central and Southern Africa. The evolution of the landscape in Angola is the result of the interplay between tectonics, climate, sea-level oscillations, and hydrological and sedimentary dynamics of the main river basins. Over the late Mesozoic and early Cenozoic, a series of events in the geological and paleoclimate record indicate cyclic hot-wet and cool dry episodes lasting until the Plio-Pleistocene. These pulses were followed by the expansion of deserts and contraction of forest and savanna ecosystems (Huntley, 2019), translating to an overall continental aridity trend particularly prevalent from the Late Pleistocene onwards in South Africa (Ecker et al., 2018)

The climate in the southwestern region is influenced by cumulative atmospheric, oceanic, and topographic driving forces. Global atmospheric systems have a great influence on rainfall patterns affecting Central and Southern Africa, including the low-pressure belt circling the globe near the Equator which creates strong convective activity due to the trade of winds from the North and South Hemispheres and causes thunderstorms in the inter-tropics (Huntley, 2019).This Inter-Tropical Convergence Zone (ITCZ) is a wind belt that moves southwards to Angola during the summer and returns northwards to the Equator as winter approaches. The ITCZ triggers the rainfall season which passes across northern Angola from the beginning of the summer, reaching south Angola in late summer. Sea currents, such as the Benguela Current and the Angolan Low, and trading

winds between the ITCZ and Westerlies, also play a major role in precipitation and temperature controls (Munday and Washington, 2017), as well as a shaping force of the relief and environment from the coast to the plateau (Feio, 1981, 1964). The cold winds of the Benguela Current produce a cooling effect which causes an almost permanent low-cloud and fog belt, particularly dense between Benguela and Namibe. For this reason, the winter in Angola is popularly referred to as "cacimbo" (fog season). Moisture availability and biodiversity in the coastal fringes of the Namib desert are thus mediated by this fog, even when precipitation reaches minimums close to 0 in the dry season.

The rainfall season in the Southwest of Angola occurs from October to April, reaching peaks of precipitation and monsoon between March and April. The dry season occurs from May to September, and June to July is the driest. Mean annual precipitation varies from 800-900 mm and mean annual temperatures are 17ºC to 18ºC with amplitudes of 5ºC. In the Summer, maximum temperatures may reach maximums of 35-37ºC during the day (October-January) and minimum temperatures may reach negative -2ºC or less during the night in the winter (June-August) (Barbosa, 1970; Cruz, 1940; Diniz, 2006)

However, in the interior of the Humpata Plateau, the Tchivinguiro shows a micro-climate that may be classified as temperate-warm with mean annual precipitations of 926 mm (do Amaral, 1973).

At south and west, in the plains below 500 m of altitude, the climate is classified as hot desert (BWh), following the Köppen classification (Beck et al., 2018; eg. Huntley and Ferrand, 2019). While at the plateau, the climate regime is of the Temperate Mesothermal (Cw) group, and the southwest and coastal plain the Dry Desert and Semi-desert (Bsh, Bwh) group.

In the highlands, the climate is sub-tropical warm with areas of transition from dry to humid regimes, following Thornwaite's classification based on the hydrological index. Weather regimes alternate between periods of intense rainfall and aridity.

According to the Koppen classification, the ecology varies between tropical savannas and temperate climates with dry winters (Diniz, 2006, 1991). In interior parts of the escarpment the climate at highest altitudes is characterized by Afro-alpine conditions, and sub-tropical temperate microclimates can be found, depending on the geological and topography (Diniz, 1973).

Currently, the southwest of Angola is sub-divided into a series of biomes: 1) Tropical and sub-tropical moist forests; 2) Montane grasslands and shrublands; 3) Tropical and subtropical grasslands, savannas, shrubland, and woodlands; Tropical and subtropical

dry and broadleaf forests; Deserts and xeric shrublands; Mangroves and flooded grasslands and savannas. These biomes can then be subdivided into eco-regions, i.e., “large units of land or water containing a distinct assemblage of species, habitats, and processes, and whose boundaries attempt to depict the original extent of natural communities before major land-use change” (Olson et al., 2001). The correlation between local nomenclature for vegetation types (Barbosa, 1970) and the eco-region system was summarized by Huntley (2019) and highlights the largest diversity of eco-regions within a single African country. For the southwestern region, a great deal of work is still necessary to establish a clear definition of these eco-regions, particularly in the Angolan Escarpment zone where specific patterns of biodiversity and endemism are observed (Hall, 1960; Huntley et al., 2019; Mendelsohn and Mendelsohn, 2018)(Hall, 1960; eg. Huntley et al., 2019; Mendelsohn and Mendelsohn, 2018).

The richness and taxonomic variability of flora and fauna species in the south-west zone suggests the escarpment could have provided a natural barrier between the drylands and the woodlands, creating a differentiation between coastal adapted populations and moist-forest specialists further inland. The steep gradient of the marginal mountain range would have worked as a physical barrier but also provided a refuge for moist forest specialists becoming isolated during the glacial periods (Huntley, 2019).

These would have also privileged areas during periods of extreme temperatures and wildfires. A key feature shaping the landscape and ecology of Angola are the “underground trees” (or geoxyles) and their relationship with the distribution and maintenance of savanna ecosystems. The evolution of geoxyles has been interpreted as an ecological response to high fire frequency since the late Miocene (8-6 Ma) and an increase of C4 plants over C3 dominant forests. The Savanna biome became a prominent component of tropical vegetation according to isotopic analysis of paleosols and fossil teeth (Cerling, 1984; Cerling et al., 2011, 1997; Gomes et al., 2021). Studies indicate the rapid expansion of savannas reaching their maximum extent during the Pleistocene glacial periods. Fire-maintained moist savannas predate anthropogenic fire and deforestation, extensively affecting the south of Angola today (Mendelsohn, 2019). These factors are key to understanding the diversity and complexity of environments in Angola, particularly the expansion of the southern drylands. These observations emphasize the importance of studying the region’s habitats for human evolutionary processes in southwestern Africa.

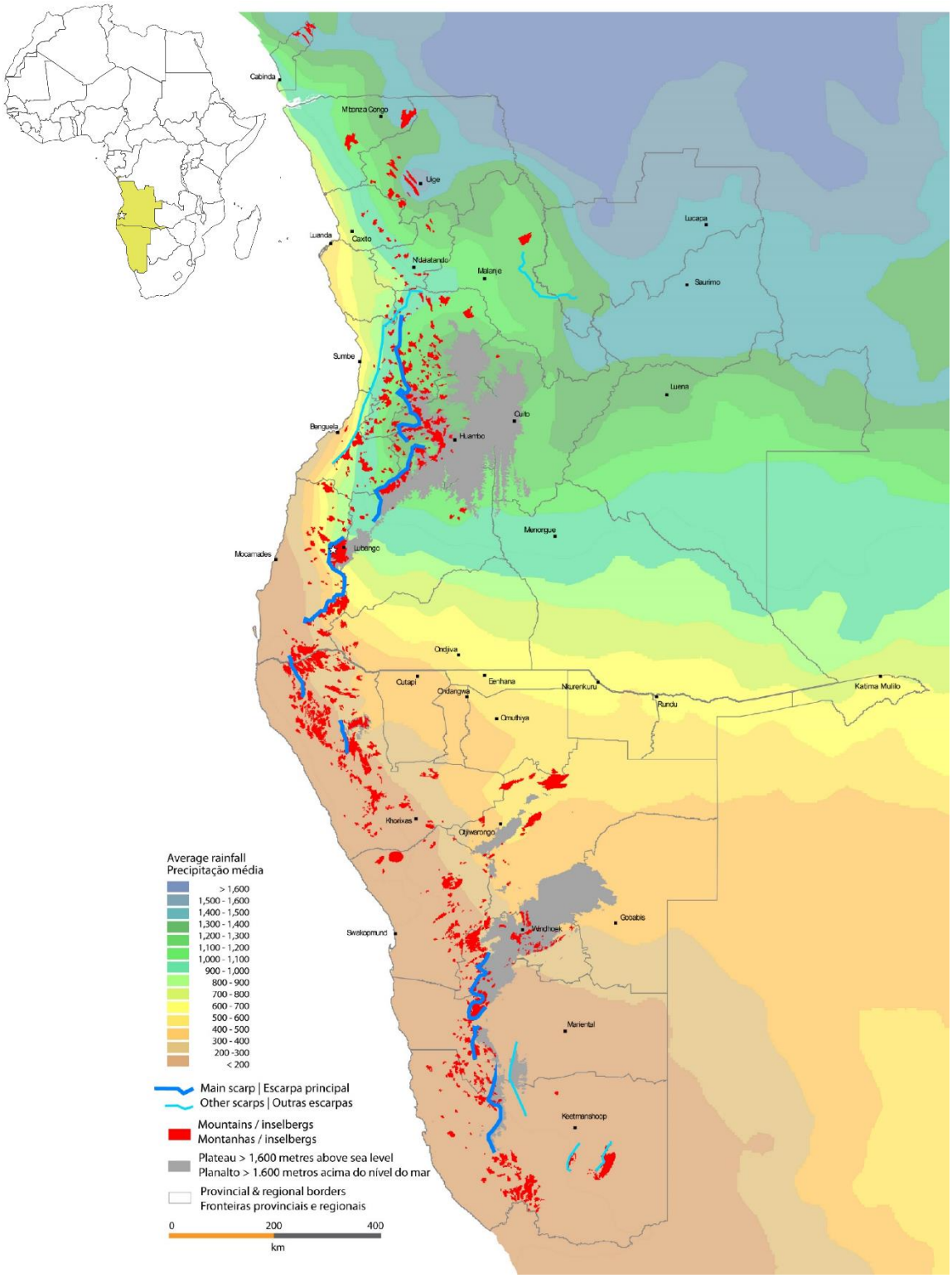

Fig. 1 – Geographic representantion of Southwestern Africa including the countries of Angola and Namibia with average rainfall, outline of escarped regions, provinces and main cities in relation to Leba Cave (star), with english and portuguese captions adapted from map by John Mendelsohn, ONGAVA/CIBIO (reproduced with permission)

Climatic records from the region are understudied and very few scenarios are yet to be available for southwestern regions, partly because there aren't specialized equipment or personnel. Climate databases for Angola mostly document the period between 1940 and 1970 (Kaspar et al., 2015; Pombo et al., 2017). Between 1975 and 2012, weather control stations were mostly deactivated across the country (with the exclusion of the main airports), and the quantity and quality of meteorological records was considerably reduced.

The recent installation of monitoring systems allowed the collection of climate and weather data, particularly at the escarpment thanks to a partnership between the Angolan government and the Southern African Science Service for Climate Change and Adaptive Land Management (SAASCAL). New data suggests the rainfall regimes in south Angola decreased to cycles of five years meaning that in each cycle, four years present a minimum rates below the previous annual rate (Carvalho et al., 2017). Long periods of drought, seasonally interrupted by flash foods, sometimes resulting in catastrophic events with high agricultural and livestock losses, as well as the destruction of wildlife habitats and extinction of native species (Cain, 2017) are common in the recent history of the landscape. Direct human impact, like bushfires and deforestation for charcoal and intensive corporative farming are cumulative influences. Increased dryness and water stress affects the majority of the population, herding and farming-dependent communities of Bantu-speakers and a minority of non-bantu groups.

The human geography of southwestern Angola was studies by several authors during the colonial period (Almeida, 1965; Estermann, 1976; Redinha, 1975). Three major Bantu ethnolinguistic groups are frequently referenced in the southwestern region: Nyaneka-Humbi, Ovambo and Herero. A minority of non-Bantu languages are frequently linked to the Khoi-San. However, several sub-groups are nonetheless recognized and distinguished among the Bantu and non-Bantu populations, and several names can apply in the different languages depending on their area of influence or which group attributed the name.

In any case, the terms used by scientists are notabily reproduced from colonialist literature and do not translate the anthropological and social complexity of Angola. For instance, the designation Nyaneka-Humbi, overarching the Nyaneka, Humbis and Handas of Huíla and Namib Province, remains far from consensual or satisfactory to its natives (Melo, 2005). Another ethnography example is the dynamics between the Bantus and non-Bantus, for instance between the Kuvale population, a sub-group of the Herero living in the Chela escarpment, and the 'Kwisi reported in ethnographical records. The

names used by most ethnographers come from Herero attributions, for instance ‘Kwisi (Cuíssi) or ‘Kwepes (Cuepes) which are depreciative to their skin tone and indumentary, although some individuals self-assigned as Twa (Vá-tuas or Mú-tuas) when enquired (Estermann, 1976). The ‘Kwisi are perceived as a lower cast even among other so-called Bushmen. Because they currently speak Kuvale it was also hypothesized an origin in pre-Bantu populations whose original language was progressively replaced by the dominant dialect (Estermann, 1976).

In more recent studies, the non-Bantu languages of Southwestern Angola were divided into three families: Kx’a, Tuu and Khoe-Kwadi (Güldemann and Fehn, 2014). Historically the Kx’a and Tuu are hunter-gatherers and interpreted as natives of the Namib desert, pre-existing before the arrival of Bantus to the southern Atlantic coast. The Khoe-Kwadi family includes both foragers and herders, and is interpreted as a later branch associated withwith an LSA migration from Eastern Africa (Barnard, 1992). Analysis of mtDNA of the different populations in the southwest currently Bantu speakers with different subsistence strategies (Kuvale, Twa, Himba, ‘Kwisi, Tjimba, Kuepes and !Xun) highlight the low homogeneity and high rate of intra- and intergroup admixture based on matriclanic lineages (Oliveira et al., 2019, 2018). In this sense, all groups of the Angolan desert share most of their genetic ancestry with other Bantu groups, but social differentiation increased since the advent of pastoralism and complex food-producing societies.

1.2. Stone Age Archaeology

Deconstructing the background of human populations in southwestern Angola is a challenging task due to the patchy paleoanthropological and ethnographic record about the communities of hunter-gatherers and foragers living there since the Pleistocene.

Stone Age studies about Angola have long recognized three eco-cultural regions of interest for paleoanthropological research, a model that was first outlined by Almeida and Breuil (Breuil and Almeida, 1964) and later developed by Clark (1966). This division of Angola into three eco-cultural zones (Congo, Zambezi, and the Southwestern zone) is the result of research that remains for the most part only superficial, relying on small assemblages from anthropological and geological surveys between the 1920s and 1960s (de Matos et al., 2021b).

The vast majority of archaeological findings known in the Southwestern zone come from surface collections at the coast (Fig. 2). Stone tool assemblages were abundantly

discovered in open-air settings in raised beach deposits across the coastal belt, from south Luanda to Moçamedes (Mascarenhas Neto 1956). The oldest toolkits were assigned to the pebble cultures of Southern Africa, occurring at elevations between 100 and 150 m, these were correlated with the Oldowan morphotypes of East and South Africa. As faunal remains or charcoal are usually absent from these contexts, comparative studies have focused on establishing the chrono-stratigraphy of the coastal platforms (Corvinus, 1983; Giresse, 2007). ESA artifacts are often very weathered, and deposited in paleo-beaches and/or river mouths. These characteristics suggest most assemblages are in secondary deposition, they might have been transported more than once over the geological scale, as part of the local sedimentation regimes associated with coastal aggradation and river capture.

One of the key locations with a high concentration of findings at the coast is Baía Farta, Benguela. Here, thirteen sites were identified in a series of terraces truncated by the seasonal floods of Dungo Creek. The dissected terraces exposed a series of Tertiary and Quaternary aged sediments. First surveys in the area identified a pebble-cobble conglomerate of Calabrian age (1.8-0.79 Ma) yielding malacological remains of *Arca senilis* at an approximate elevation of 95 m (Mascarenhas Neto, 1956; Soares de Carvalho, 1960; Feio 1960). Those fossils indicated a sea transgression in the Pliocene, forming an estuary or lagoon at the river mouth of Dungo. On top of the conglomerate, the geologists recorded assemblages of paleolithic materials, mainly handaxes and scrapers, later classified as an evolved or final Acheulean (Ervedosa, 1967).

The fieldwork by the National Archaeology Museum of Benguela has resulted in a series of discoveries in the area and suggested new questions about the behavior of the Acheulean populations in coastal Southwestern Angola. In the 1990s, the conglomerate of the north part of the paleo-lagoon referenced by Ervedosa (1980) was excavated by Manuel Gutierrez. This area was renamed Dungo III, and its excavation was soon abandoned for safety reasons. Several other areas in the Dungo valley have since then been the object of excavation by the Angolan-French collaboration team, particularly in the middle (Dungo V and V-I) and south part of the creek on the western margin (Dungo IV) and eastern margin (Dungo XII). At Dungo V, the discovery of two sub-complete whale remains associated with chopping tools was considered a remarkable finding, interpreted as an indicator of scavenging of stranded beach mammals by early hominin populations on the southwestern coast of Africa (Gutierrez et al., 2001).

Excavations of the conglomerate at Dungo IV and Dungo XII provided a rich assemblage of choppers, handaxes, bifaces, scrapers, and other tools produced mostly in milky and

hyaline quartz (Gutierrez and Benjamim, 2019). However, the information available about Dungo still presents limited value particularly when comes to the site formation processes and provenance of the lithic assemblages. Stratigraphic information about Dungo is rather vague, as very large areas have been excavated by Gutierrez and the MNAB but only one profile drawing is shown. Reconstruction of the site stratigraphy and the meaning of some of the original work is only possible through other authors (Lebatard et al., 2019). The field notes mention screes and low-range debris flows at Dungo IV and Dungo XII but the careful consideration of slope processes acting on the surface of the conglomerate, aeolian and lagoonal conditions, and how these processes may have reworked the sequence of artifacts is mostly absent from the discussion (Gutierrez and Benjamim, 2019). Nevertheless, the radiometric dates recently published offer renewed insights into the geochronology of the ESA. Four quartz tools from the lowest geological unit were dated using ^{26}Al and ^{10}Be cosmogenic nuclides, which estimated their burial date between 771 ka and 2.04 Ma (Gutierrez et al., 2018, p. 175) but no information was provided about their provenance on the profile and how erosion rates calculated with this method correlate with the observed sedimentation of the site.

Another publication by geochronology experts, Lebatard et al (2019) proposes a calibration of this radiometric dating with the calculation of the denudation rates. The statistical modeling for the sedimentation of the surface layer was calculated to be at least 614 ka ago and younger than 662 ka ago. The authors also point out that if we consider the surface deposit has been truncated, burial durations range from 585 ka to 786 ka for truncations lower than 4 m (Lebatard et al., 2019). For the authors, this study offers at least an age confirmation for the burial of the Pre-Acheulean artifacts deposited on the paleobeach. However, the method is highly controversial and most frequently used on very small assemblages with unspecific tools perceived as archaic, and often collected in terrace surfaces of incision valleys, with many satellite locations of more recent ages (eg. Braucher et al., 2022). A careful consideration of slope processes, alluvial and aeolian reworking is utterly necessary for these landscapes and can only be confirmed by multipronged approaches.

Until now, the Stone Age sequence of Angola remained mostly based on the relative sequence proposed by Clark (Ervedosa, 1980). Clark (1966) sub-divided the ESA in two phases: the Early Acheulean and the Late Acheulean, which was followed by an intermediate period (“First intermediate”) where Acheulean and “sangoan” tools co-occur with “unspecialized” MSA assemblages. This phase was perceived as contemporaneous of the “Sangoan-lower Lupemban” culture found in the Congo basin, in the Northeastern Zone of the country.

As stratigraphic information was scarce for the southwest, and some of the assemblages did not include macrolithic tools, Clark classified all the southwestern sites yielding Mode 2 and Mode 3 assemblages as MSA sites (Clark, 1966). Those assemblages included tools typically called “Stellenbosch”, “Sangoan”, or “Fauresmith”, but also other seemingly undifferentiated blade-flake industries.

The assemblages of the Namibe Province showed reduction sequences typical of technocomplexes like the Fauresmith (Munhino, Carvalhão, Ochinjau, São Nicolau, Camucuio, Maconje, and Moçamedes), while others (Caitou, Montipa) had a higher frequency of large picks and cleavers, comparable with the “Sangoan” from Southern Zimbabwe.

Between São Nicolau-Bentiaba and Moçamedes, a cluster of archaeological sites around the mouth of the Bentiaba River r (orSt. Nicolau Rive) yielded different assemblages attributed to both early and late cultural phases of the Stone Age. One of these locations called St. Nicolau- J yielded an assemblage of very crude heavily weathered sandstone chopping tools. Allchin (1964) noted this weathering may be misleading, as sandstone weathers faster than quartzite, meaning they might be of similar age as many of the tools assigned to the Acheulean or the MSA in the region, or may either be associated witha specific site use or a distinct earlier industry. It should also be considered that these materials may have been reworked by the river during flooding events and that many assemblages in the region are likely a secondary deposit because of the regional climatic regime (Ramos, 1981). Large tortoise cores produced in coarse grained quartzite and their refitting flakes were abundantly found in the area. The implements are often coarse-grained quartzite. At St. Nicolau-I, flakes are frequently circular or nearly circular in outline and interpreted as intentionally used for the production of discoidal flakes (Allchin, 1964).

Similar techniques were found at the site of Caitou, in the interior desert belt, where blade-flake cores are also present but made from comparatively small quartzite river pebbles instead of large blocks of raw material (Allchin, 1964). No type-tools like handaxes or points were found among these assemblages, but they indicate the use of similar techniques on different raw material sources, one in the plain where quartzite outcrops are to be found, and the other in the interior scarp where only quartzite river pebbles appear to have been available. Their characteristics suggest they can be placed in the upper Acheulean phase, comparable to the assemblages of Stage IV in the Vaal sequence and sites where only the flake element of the Acheulean industries is represented (Allchin, 1964). At a terrace closer to the coast, St. Nicolau-E, a handful of

almond and ovoid-shaped handaxes and well as pointed ones with step-flaking show all the attributes frequently described as the Fauresmith industry; while in another sector of the valley, about 18 km south, another small assemblage shows all the classic attributes of the Sangoan industries: handaxes, cleavers, picks, core-scrapers, and serrated scrapers, prepared cores, and flakes (Allchin, 1964). To Allchin (1964), the proximity of these two assemblages suggests that techno-typological traits refer to different purposes and not a specific ecological setting.

The Fauresmith is usually found in the open grasslands of Central Africa, while the Sangoan industries are found in terraces of river valleys in woodlands at about the same time in the upper Pleistocene. During this period, the climate became drier across the rest of Africa, and we suspect the Southwestern zone became unwelcoming to human presence. Therefore, an ecological deterministic interpretation of the use and function of these tool technologies would likely be incorrect, even though fact that these tools have been found in different environmental settings and, notably, in deserts (Cancellieri et al., 2022; Rots and Peer, 2006; Van Peer et al., 2003).

Also at the coast, near Lucira, the assemblages show prepared core technologies, including cores, flakes scrapers and small blanks with traces of use, which were likely hafted, such as chisels and adze blades (Allchin, 1964). The absence of lithic points is paradoxical and served as an argument for the existence of an “intermediate” cultural stage in southern Angola (Clark, 1966). The chief criteria therefore upon which these industries are considered to belong to the MSA are, firstly, the small size and careful preparation of the cores with prepared striking platforms. Secondly, the use marks found in small flakes with hafting indicators (Allchin, 1964). All the assemblages at which adze blades and chisel or splintered pieces occur fall into this group. Furthermore, the size and nature of the blanks used for knapping were the main criteria used in the seriation of the assemblages.

The overview of the assemblages from the Southwestern zone shows high concentrations of findings in different bays of the coastal desert and the highlands between Namibe and Huíla (de Matos et al., 2021b). Examples of re-used heavily patinated tools at St. Nicolau-L indicate that prepared core techniques occurred in different forms and during long time intervals (Allchin, 1964). Moreover, the question of the low representation of certain tool types in the Southwestern region suggests that, until further evidence is forthcoming, locations at which only certain aspects of the industries are represented were likely sites at which only certain activities took place (Allchin, 1964). The character of the surface collections in Namibe province also leads

to the conclusion both ESA and MSA sites are workshop sites from which all finished tools were removed, rather than either temporary or semi-permanent living sites (Allchin, 1964).

Fig. 2 – Distribution of archaeological sites in Southwestern Angola referenced in the text, based on the archives of the Tropical Research Institute (de Matos et al., 2021b)

The problem of the transition from the ESA to the MSA in Southwestern Angola was a major focus of Miguel Ramos and was to be addressed in his doctoral project, advised by Andre Leroi-Gourhan. Ramos started his studies in France sometime in 1965 but never completed the dissertation. As part of his dissertation fieldwork, Ramos led an expedition to southwestern Angola between 1966 and 1967. His fieldwork added 40 new sites to the archaeology database of the colonial offices, as well as thousands more artifacts exported to the colonial offices in Lisbon, which were never completely studied or published (de Matos et al., 2021b).

M. Ramos was particularly interested in assemblages with “transitional traits” as described by Allchin (1964) and explored the concept of “undifferentiated MSA” layers. Ramos plannedto revisit sites discovered by the anthropological and geological surveys and gather information for comparison with the data obtained by Clark in the Angolan Congo (Ramos, 1970). Ramos proposed the high concentration of archaeology in the area showed the drylands of Angola offered favorable conditions for human subsistence during the Pleistocene, and the diversity of tool types in the assemblages suggested that an ecological deterministic interpretation for macrolithic tools did not apply and the tool variability can be related to functional purposes other than woodworking (Ramos, 1982).

One of the key questions driving Ramos’ work focused on the significance of the complete absence or low relative percentage of handaxes from most of the sites presumed ESA; and how the handaxe technique is particularly relevant in the interpretation of the morphological entities of the African Acheulean. He believed that in certain cases these handaxe proportions may only be explained in a context of little diversity of typologies as a consequence of ecological factors that may have been unfavorable and placed restrictive conditions on the territory of Angola during this time (Ramos, 1982).

Ramos published information about two sites around the Santo António Hill: Capangombe-Santo-António (alternatively Maconge) and Capangombe-Velho. The sites are located in the river terraces of Capangombe Creek, a stream formed by the confluence of the waterfalls of Leba and Camucuio located between 400 and 600 m a.s.l. The site Capangombe-Santo-António is located in the upper valley yielding an assemblage of 1776 artifacts with 196 cleavers, among flakes and blades. The typological study of this assemblage was published in conference proceedings of the Association of Portuguese Archaeologists (AAP) in 1970. His study focused exclusively on the cleavers and described them according to the typology developed for Northern Africa (eg. Agabi, 1999; Tixier, 1956). The approach found a greater percentage of Type 2 cleavers in the assemblage, but also a relevant number of proto-cleavers (Type 0) and cleavers with a transverse flaking edge (Type 1) as well as cleavers produced using Levallois and Kombewa flakes (Type 6). Ramos considered the site to contain two assemblages: an old Acheulean tradition that would have persisted until later in southern Angola, and an evolved Acheulean or MSA (Ramos, 1970). A total of 33 pieces remained unclassified and suggested specific morphotypes in the region.

The site of Capangombe-velho was excavated by Ramos after the surface collections at Santo António, about 5 km south down the river stream. The site of Capangombe yielded

a deposit of two archaeological horizons with hearths with no bone preservation, and thousands of lithic artifacts: the uppermost horizon with 56 000 finds, and the lowermost with 47 000 pieces (Ramos, 1981). Ramos observed that the lower deposit overlaid an iron crust over the granite bedrock, probably from the Gamblian pluvial stage, and thus at least older than 30 ka. Absolute dating was not possible since the two combustion features excavated did not yield any bone or charcoal. Adding to the data from Capangombe-Santo António, Ramos suggested the existence of an "evolved Acheulean" based on the presence of tool variations that weren't found elsewhere (Ramos, 1970). The MSA at the escarpment could then be divided in two different cultural variations: the "Capangombian", classified as "MSA of Acheulean tradition", and the "Lebian", a later stage found by Camarate-França in the lower deposits of Leba Cave but analogous to the uppermost horizon of Capangombe (Ramos, 1981). In a later revision, the "evolved Acheulean" was regarded solely as an intermediate phase immediately preceding the MSA when Sangoan techniques co-occur with Acheulean or Fauresmith traditions (Ramos, 1982).

Similar lithic industries were also found in the terraces of the Lower Kunene River at the Cafema Mountains, near the border Namibia-Angola (Nicoll, 2010). A lithic assemblage of 39 pieces in quartzite, described as an extra-local fine-grained red quartzite, is very similar to the lithic materials found further north in the valleys of the Chela Mountains, for instance at Capangombe and Leba. The lithics presented a blackish-brown patina, with edgewear and evidence of abrasion, indicating long periods of exposure. The technological features described included Levallois reduction sequences with triangular flakes and points (Nicoll, 2010).

The MSA-LSA would then be subdivided into five local cultural facies: 1) Acheulean tradition; 2) Fauresmith tradition; 3) type Hope Fountain; 4) Still Bay facies; 5) coastal facies or "Bacuísso". The type Hope Fountain would refer to the sites where only the flake and core component of the Acheulean industry was observed (i.e., as the Acheulean without handaxes, cleavers, or knives) (Tryon and Potts, 2011); separate from the Still Bay facies, which is used for sites where bifacially retouched points occurred occasionally but were not considered "fossil directos".

The latter two are very loosely defined and likely represent the local LSA, sometimes also called "Still Bay-Pietesburg" or "Wilton". These assemblages are found in historical times and sometimes co-occur with ceramics (eg. Ervedosa, 1980). The Type 5) "coastal facies" would then group all other later assemblages. These coastal adaptations are observed consistently across the Angolan coast from Cabinda to Ponta das Vacas. The

coastal sites of Bentiaba appear different from the assemblages further inland, but the differences are mostly attributed to the characteristics of the local raw material sources with more frequent use of beach pebbles for cores (Allchin, 1964). Among the traces of the LSA populations, two duck-billed end scrapers were also found at St. Nicolau-D, Bentiaba, similar to the South African Smithfield tools (Allchin, 1964), and many other assemblages in the colonial record seem to relate to the LSA.

On the northern coast, at the sites of Benfica Bay and Palmeirinhas, southern Luanda, the coastal facies overlays or occurs with lanceolate points and small bifaces, morphotypes commonly associated withwith the Lupemban technocomplex. At the beach of Bom Jesus, in the Kwanza North, a horizon with very weathered artifacts, including handaxes and Tayac tools, is overlaid by a sandy layer with Still Bay points and blade-bladelet repertoires. Bellow the Kwanza River, the LSA sites often show "generic" attributes with techno-typological features more frequently associated withwith the MSA flake-blade technologies (de Matos and Pereira, 2020; Gibson and Yellen, 1978) with a general trend for the production of relatively smaller pieces using hard hammer percussion and bipolar reduction. Microlithic tools per se (<1 cm) are unfrequent, and unspecific. The absence of tool kits commonly found sub-Saharan Africa at this time, like the Lupemban or the Howiesons Poort typologies, respectively. Clark suggested that an early southwards spread of microlithic technology into the unexplored areas of Mozambique or southern Angola/ Namibia could be expected (Clark, 1971), but the hypothesis remains untested.

The coastal facies, also named Bacuísso by Ramos, carries a clear but debatable ethnocultural significance referring to the seashore tribes of the southwest of Angola, namely the 'Kuroca, 'Kwepe, and 'Kwisi, often grouped with the Bushmen (Coelho, 2015; Cruz et al., 2013). Early travelers and explorers occasionally reported encounters with nomadic fishers and hunters along the coast reported but these groups wereapproached in the early 20th century by colonial anthropologists and ethnographers, whom described the sub-group as particularly discriminated among the other so-called Bushman groups and the Bantu (Estermann, 1981, 1976). The condition of the 'Kwisi as servants of the Herero meant their activities would include herding for their patrons, although their subsistence continuously relied on fishing, hunting, and foraging fruits and tubercules, important nutrient and water sources in the desert (Estermann, 1976). Their sites would then yield hunter-gatherer technology but also materials exchanged with the farming communities With the arrival of the Europeans the foraging communities still remaining after a long period of slavery trade and colonialist claims over the land, foraging populations were segregated into the Bantu lifeways or isolated in areas along the Namib

and Kalahari deserts (Mitchell, 2017). The Khoi and San tribes of Angola have mainly been absorbed into the herder communities during the last few centuries, but a few groups still live a semi-nomadic lifeway near the Atlantic coast between Namibia and Angola, avoiding contact with all other populations. Their preferred geographic locations are the mountainous regions around the Curoca and the Cunene basins, and the hunting landscapes of the Iona Park. Remarkably, the ‘Kwisi are considered the makers of the rock art at Tchitundo-Hulo and other locations with paintings like Galangue, Caninguiri and Montenegro in the region of Huambo. They are rarely sighted in Virei and Caraculo for trading, where other rock art paintings have been found (Fernandes, 2014).

The site of Tchitundo-Hulo, one of the most famous locations with rock paintings, was approached by several authors. Surface collections by Camarate-França included a few retouched flakes and atypical points, duck-billed tools, and small polyhedral and discoidal cores (<10 cm) which were associated with a proto-Smithfield or Wilton culture (Wurz, 2013b). The excavations in another sector of the site identified another assemblage of 58 lithics and 135 glass beads (Camarate-França, 1953). The site was later re-approached by C. Ervedosa and Santos-Júnior in the 1970s who excavated a section of the rock shelter next to the painted walls and an associated open-air living area. The dwellings were reportedly attributed to the ‘Kwissi (Ervedosa, 1980).. Plenty of lithics and glass beads of European origin were collected at the surface. In the rock shelter, the excavations identified a deposit with seven archaeological horizons. Hearths and ash layers with mammal bones, beads, and microlithic stone tools were identified in the lower layers. The two upper layers showed a similar assemblage but included potsherds and an iron arrowhead. The sequence is viewed as a testimony of change in material culture, but not of the population or the culture itself. It also highlights a key factor in nomad-forager lifeways which is the repeatedd use and returns to a space or landscape. In open-air locations of the Namib desert ,for instance, terraces and workshops, co-mingling of MSA-LSA artifacts is most expected by overlapping groups equipped with these toolkits (eg. Marks and McCall, 2014).

The literature review about the southwestern Stone Age cultures shows that several names have been applied by different authors. For instance, both Macahama and Tchitundo-Hulo were classified by Clark (1966) as Brandberg/Erongo culture, something that has been argued by other authors, and replaced by Wilton (Ervedosa, 1980). Clark also classified Leba Cave as an LSA site with Erongo culture based on a small assemblage of 40 pieces observed at the SGMA in Luanda (Clark, 1966), while Ramos classified it as MSA with Acheulean tradition (de Matos and Pereira, 2020)

Curiously, Ramos' cultural model suggests alternative classifications, partially aligning with the technocomplexes of South Africa but introducing local traditions to classify the later toolkits (Ramos, 1982). The sites and lithics found in 1967 by Ramos also show a higher frequency of ESA and MSA sites at the escarpment (de Matos et al., 2021b; Ramos, 1970) than previously proposed (Breuil and Almeida, 1964).

In general, the studies available highlight the difficulties in dealing with dispersed information and comparing them with longstanding models for culture and technology in Africa. Similar issues are found in studies about the LSA and the transition from the LSA to Early Iron Age (EIA) in Southern Angola. Available radiometric dates for the Late Pleistocene and Holocene sites in Southern Africa and Central Africa (Clist et al., 2022; Clist and Lanfranchi, 1992; Russell and Steele, 2009) show a very small representation of Angolan sites with absolute ages.

The adoption of pottery and herding in the southern region is perceived as a rather late process compared with regions further north (Clark, 1963; Clist et al., 2022), or south (Sadr and Sampson, 2006). Sedentarization is usually associated withwith the migration of Bantu populations, arriving from the north and east. For instance, the coastal shell midden at Benfica Bay, South Luanda yielded pottery in a context dated to 200 AD (Ervedosa, 1980); and plenty of sites with EIA ceramic traditions retrieved radiocarbon dates to the 17th and 18th centuries (Maret et al., 1977). At the same time, the emergence of walled enclosures across the plateau escarpment is also poorly understood (Jorge, 1977) and interpretations about subsistence and ethnogenesis of foraging and herding populations in the southwestern zone of Angola remains to be explored by new researchers.

2. Site Background

2.1. The Humpata Karst: Local geology

The Humpata Karst refers to a series of caves and fissures located at the highlands of Huíla Province between parallels 14º30' S and 15º30' S, and meridians 13º15' E and 13º 45' E. Caves are found at the top of the Humpata Plateau where a combination of lithology, tectonics and climatic conditions allowed the development of karst features in dolomites, as well as the development of a pseudo-karst in quartzite-sandstone host rock found mostly in the eastern flank of the plateau between Tundavala and Senhora do Monte (de Matos et al., 2021a).

The Humpata plateau is a peneplain of polygonal shape, oriented NNW-SSE to the Atlantic coast. This sector of the Marginal Mountain range is structurally organized by systems of crossed fractures, faults, and fissures (Lopes et al., 2016) and has a maximum elevation of 2,300 m a.s.l The geomorphological evolution of the plateau is associated with the rifting of the Damara belt, affecting regions from southern Angola, Namibia, and western South Africa (Kroner and Correia, 1980). The strong ablation and dissection of the valleys during the evolution of the hydrographic network allowed the formation of deep gorges and canyons controlled by structural and tectonic forces (Mpengo et al., 2011; Pereira et al., 2011). At the edges, abrupt scarps and ravines over 1200 m (Fenda do Bimbe, Fenda da Tundavala) turn into waterfalls during torrential storms. Impressive crests of bare rock face both east and west. In locations such as Leba, Bruco, or M'basso, dendritic drainage follows the fractures of the Chela quartzites at the contact with the dolomites. Between Leba and Bruco, waterfalls can be found at the western edge reaching the Namibe. Some are only active during wet cycles like the "mulolas" (ephemeral rivers), marshes, and the interior lakes Nuantchite and Catenda, about 20 km south of Humpata village.

In the southwestern flank of the Humpata Plateau, where the dolomites are mostly concentrated, the area is crossed by numerous tectonic fractures and faults. The extensive fault of Bentiaba-Leba-Caholo-Cangalongue oriented NW-SE splits the plateau almost in half between Leba and Cangalongue villages. Another less extensive fault follows an NNW-SSE axis from Molo-Muange-Nuinge-Numbalo, which is partially filled by norite sills of post-Permian Age intrusive to the Chela sequence. These two main faults are structurally connected by other EEN-WSW smaller fractures and fissures at different locations: Leba, Bruco, Tchivinguiro, Bata-Bata, and Cangalongue. This important movement of blocks shaping the basin is key to understanding the development of the karst.

Local geology at the plateau is dominated by the Pre-Cambrian rocks. The Chela Group is a general term for a volcano-sedimentary sequence described by Correia (1976), previously called Chela Formation by Mouta (1954) and Beetz (1933). Correia divided the lithostratigraphy of the Chela Group into four different formations, from the lowest: Tundavala, Humpata, Bruco, and Cangalongue (Fig. 3). These formations comprise a complete tectonic-sedimentary cycle, separated from the upper carbonated member, the Leba-Tchamalindi Formation (or simply Leba Formation, sensu Pereira et al. 2011).

Several studies correlated the Leba Formation with Abenab Sudgroup of the Otavi Group – Nosib Formation of the Damara belt outcropping in Northern Namibia (Carvalho, 1983; Jones et al., 1992; Kroner and Correia, 1980) confirming orogenic events and environmental conditions homologous to other areas south of Angola, commonly known as the Damara-Kaoko belt (Kröner and Stern, 2005).

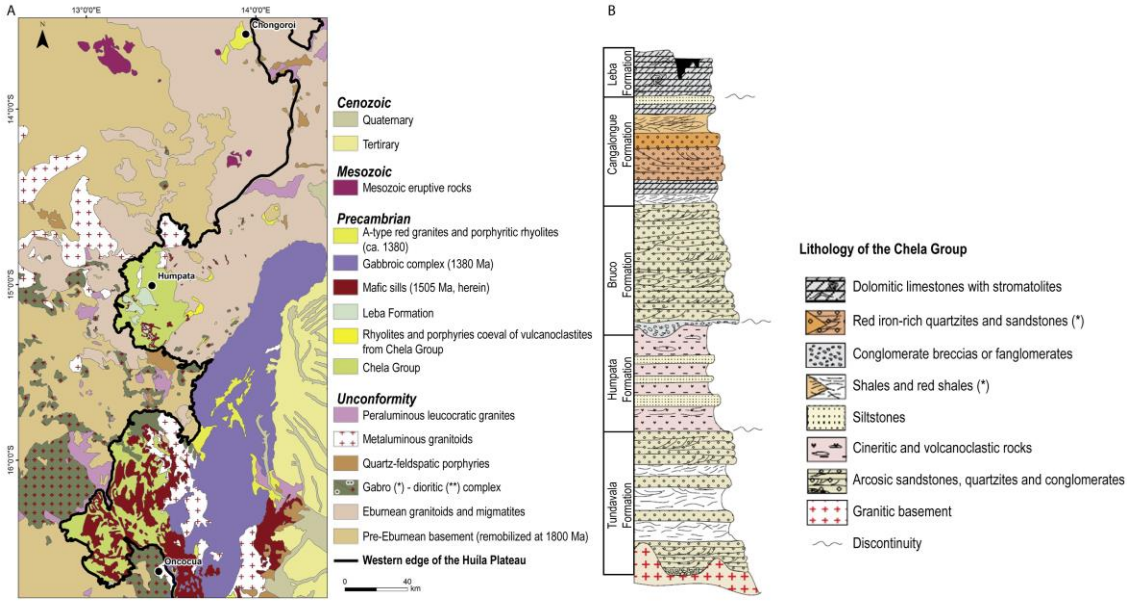

Fig. 3 – A. Geology of the western edge of the Huíla Plateau (Lopes et al., 2016) and B. Lithology of the Chela Group (Pereira et al., 2011)

The Leba Formation is composed of layers of dark greyish-blue dolomitic limestone scattered with stromatolites, chert, and argillites (lightly metamorphosed mudstone and siltstones). The diversity of dolostones and silicified structures is related to a younger graben-controlled sedimentary cycle (Correia, 1976; Kroner and Correia, 1980).. The underlying stratum, the Cangalongue Formation, is composed of interbedded red sandstones, red shales, quartzites, and siltstones (Pereira et al., 2011).

In the northern (Leba) and southern (Cangalongue) flanks of the dolomite massif, fracture zones associated with the intrusion of post-Permian dolerite and norite dykes and sills can be observed between the Leba and Cangalongue Formation (Pereira et al.,

2011). These intrusions had some effect on the formation of cave systems within the dolomites, presumably because the ancient water table was perched.

The Leba formation has been interpreted as a member of carbonate rocks formed in conditions of shallow water either in marine coastal conditions or lacustrine of very high salinity related to a paleoshore during the pre-Cambrian (Correia, 1976). Stromatolite structures are observed nearly everywhere across the Formation, consisting of several meters thick of layered biochemical accretionary structures derived from microbial mats of Pre-Cambrian cyanobacteria. Towards the top of the formation, flaggy chert layers are common and interbedded with the stromatolite laminations (Correia, 1976; Tavares et al., 2015). The thin lamination of algal origin is correlated to "mode P" stromatolites classified by Aitken (1967). The "mode P" or planar lamination is characteristic of the green-blue algae which develops in colonies of unicellular organisms (connected by a jelly-like substance) or colonies of filaments forming algal mats. At the genesis, the consistency and nature of the algal mat enhance adherence allowing the fixation of micrite in water suspension. This process happened successively allowing the lamination morphology and mineralogical segregation, with alternating fine beds of carbonate and chert. The presence of anhydrite in the bedrock was interpreted as an indicator of the primary evaporitic origin of the dolomite and the syngenetic chert bands associated with seasonal variations in the depositional milieu (Kroner and Correia, 1980). These characteristics make up a highly heterogenous karst bedrock which is expressed in a variety of dissolution shapes and forms.

The thickness of the Leba Formation is variable across the Humpata Plateau. In the area between Leba and Tchivinguiro, the maximum thickness is 60 m. In some areas like in the villages of Bata Bata and Cangalongue the bed does not exceed 30 m of thickness. At the surface, the dolomitic pavement presents numerous corrosion shapes and flat incised surfaces following reticulated drainage associated with the fault-fracture network.

The physical and mineral properties of the bedrock allowed the formation of a network of underground water drainage favorable to cave formation, sinkholes, and springs, which can be classified as semi-arid paleokarst (Veress, 2020). Due to underground water flow, soil cover in the highlands is usually thin, except in poljes and valleys, where ephemeral rivers often emerge during the rainfall season due to the water saturation of the bedrock. In general, the soils on the Humpata Plateau consist mainly of leptosols and ferralsols which tend to be shallow and have low fertility (Mendelsohn, 2019).

Studies about the soils of the Huíla province were developed by Pedological Missions of the colonial agency for the soil mapping of Angola and are partially available in the online

resources of the IICT about the soil collections, including photographs and summary descriptions [2]. Information from locations studied in Tchivinguiro and Humpata, in the vicinity of Leba, indicate the occurrence of orange and red ferralitic or weakly ferralitic soil types associated with sedimentary and quarzitic rocks (Mendelsohn, 2019; Ricardo et al., 1980). In the World soil taxonomy terminology these soils are included in the order of Oxisols (Blum et al., 2018), and this terminology was adopted in this study.

[2] Webpage https://actd.iict.pt/collection/actd:SOLPC001 for online resources for the soil collection of the Tropical Research Institute, University of Lisbon

2.2. Karst forms, infillings & fossil sites

Karst features are not exclusive of the dolomites and dolostones of the Leba Formation and have been observed in the non-carbonated host rocks of the Chela series. These solution features can be described as pseudo-karst and occur in quartzites and sandstones in the northern and eastern flanks of the Humpata plateau.

In the eastern flank of the plateau, facing Lubango city, there are small "fendas" (fissures) in the quartzitic crests, for instance, Fenda da Mapunda. At the top of the crest, many forms of a pseudo-karst can be observed at the surface. Small circular depressions, undulation marks, narrow chimneys, and fissures give access to underground galleries with traces of intense anthropogenic and biogenic use. These forms are associated with the spring of Senhora do Monte, located about 1 km NW of the chapel, which supplies part of the city of Lubango. Galleries with vertical development have maximum drops of 60 m and entry requires specialized equipment (de Matos et al., 2021a). The fissures are occupied by communities of horseshoe bats (*Rhinolophus* sp.*)* and plenty of other animals, like reptiles and rodents. Pseudo-karst features can also be observed at Fendas da Tundavala, Bimbe, and Zootécnica, where deep valleys and gorges develop between impressive crests of quartzite of Chela Group.

In the southwestern flank of the Humpata Plateau where the dolomite outcrops are located, the same structural controls can be observed as the area is crossed by numerous fractures and faults, but instead of "fendas", a larger variety of different karst morphologies and infillings can be observed.

The extensive fault of Bentiaba-Leba-Caholo-Cangalongue oriented NW-SE, which splits the plateau almost in half between Leba and Cangalongue villages, has many karstic forms associated like tubules, tunnels, and fissures with breccias. Another less extensive fault follows an NNW-SSE axis from Molo-Muange-Nuinge-Numbalo and is partially filled by norite sills of post-Permian Age intrusive to the Chela sequence. These two main faults are structurally connected by other EEN-WSW smaller fractures and fissures at different locations: Leba, Bruco, Tchivinguiro, Bata-Bata, and Cangalongue. This important movement of blocks shaping the basin is key to understanding the corrosive drainage networks developing the karst and the concentration of springs and lagoons, as well as important caves with vertical development.

In locations such as Leba, Bruco, or M'basso, dendritic drainage facing east follows the fractures of the Chela quartzites at the contact with the dolomites. Between Leba and Bruco, waterfalls can be found at the western edge reaching the Namibe. Some are only active during wet cycles, sourced by reactivated mulolas (ephemeral rivers).

The landscape is characterized by mounds or cupula-shaped hills, some highly dissected, along wide valleys. Some of these cupula-shaped hills or poljes are already isolated by high denudation rates and are frequently soil-covered. A geographer, Ilídio do Amaral (1973) described the speleogenesis of the Leba karst in two phases: a hypogenetic phase relating to the exposure of the carbonates; followed by an epigenetic phase associated with the exhumation, lowering of the water table and fossilization of the karst. Slope retreat and bedrock incisions by intense rainfall later contribute to diverse subterranean forms and structures, and progressive infilling starting sometime in the Neogene (Pickford et al., 1994)

A general model of cave formation and infilling has been outlined in the literature (do Amaral, 1973). First, there is the opening and development of a solution chamber or a cave below the water table. Second, the water table is progressively reduced, exposing the chamber and likely other solution galleries or tubes in the system. Once the main chamber is exposed, joints and fissures in the bedrock serve as conduits for rainwater percolation and chemical dissolution of the cave. This results in secondary precipitation of carbonates and other residues, forming speleothems and travertines. Thirdly, the widening of the joints and cracks progressively places the cave at a sub-surface level with more direct contact with earth surface processes and allows, during an infilling phase, not only the percolation of rainwater and minerals in solution but also colluvial and aeolian laminations intercalated with the cave debris. Finally, depending on the speed of fracturing and widening of the joints, allochthonous sediments start to accumulate, frequently including biogenic and anthropogenic material and occasionally concealing anterior residual material of the cave dissolution. Similar patterns have been observed in sub-tropical karst in dolomites of South Africa and Northern Namibia (Brain, 1981; Pickford and Senut, 2010).

Most of the known caves at Humpata are located at the old foothills, usually between 6-15 m of elevation above the talwegs. The hills usually have labyrinths of chimneys and tubules connecting with the main chamber and adjacent solution chambers. Breccias and tufa deposits infill these fissures. Most of the cave entrances became available during the Quaternary by the erosional retreat of the slopes, for instance at Leba or Malola. Others, for instance, the solution chambers of Tchaticuca or Cangalongue, were connected to the surface through chimneys and were exposed only after a horizontal entrance was created by the quarry. Columns and pinnacles are evident from a distance but are covered by dense shrubs. Species of the genera Brachistegia, Jubernalia, Ficus, Aloe, and Euphorbia common to the Miombo Woodlands of the Angolan and Zambezian

plateau environments (Types 49 and 50, Burgess et al., 2004) are some of the most frequent vegetation types observed on the cliffs and between fissures.

In the upper stream of the Cudeje River (Bruco), located in the Malola-Ufefua area, the dolomite hills are mostly residual and have been heavily explored for hydraulic lime up until today. Nonetheless, the important development of the endokarst has been observed here. For instance, Malola II cave is located in a blind valley and has a cave mouth of about 4m wide. A vertical entrance with a talus cone of guano and silts leads to a large chamber with the floor covered by boulders of roof spall and guano. A few stalagmites are visible, and boulders possibly cover more. The walls have travertines and speleothem drapes, but the environment is dry and dusty. The chamber connects with a labyrinth of other galleries upward where eccentric flowstones and dripstones cover the walls. These structures are correlated with heavy biological activity associated with a large community of bats roosting inside the solution chambers. The cave also has abundant Iron Age/historical material at the surface, including pottery, baskets, faunal remains, and human burials. Older infillings are likely concealed under the roof spall.

Similar patterns are observed elsewhere in the dolomite formation. Tchivinguiro-Nandimba is a cave-spring with an underground network extending for more than 1 km on a cupula-shaped hill. Numerous chimneys connect the spring to the surface, but some are completely choked with red sand and coarse rubble. The "dry" part of the cave is accessible without the use of caving gear through a gate built in the 1960s.

Impressive speleothem formations like stalagmites and columns are observed at the entrance and further inside, where the floors are covered with large boulders of roof spall of rectangular shapes. Outside, the spring forms a natural pool of approximately 8 m^2 next to the entrance of the cave. The water is channeled by the local population for crop fields. Intense agricultural activity has raised the demand on the storm waters of the plateau and dissected most of the main lagoons (Nuantechite and Otite). At Nandimba, fossiliferous pink breccia deposits have been observed in the walls of small cavities above the spring and plenty of archaeological material reportedly from the MSA has been recorded in the area

Many fossil sites are in the Leba Formation. The dynamics of local tectonics and climatic regimes (microclimates) across the Plateau influenced the timing and sequences observed in different cave sites. Studies of the fossiliferous deposits in these caves provide some clues about the chronostratigraphy and paleoecology of the area during phases of infilling. The earliest discoveries occurred at Tchíua quarry, sometimes

referenced as Leba 1 in literature (Delson et al., 2000; Gilbert et al., 2009), creating confusion between this site and Leba Cave.

Tchíua refers to a quarry site with a series of fissures and collapsed galleries with breccia infillings and yielding vertebrae fauna of different species and ages. Sometime in the 1940s, eight post-cranial fragments of primates were discovered during the quarry opening and were initially identified as *Dinopithecus ingens* (Dart, 1950). Later on, it was proposed that at least three different Cercopithecoidea were present in the collection, including *Dinopithecus, Parapapio* and the colobine *Cercopithecoides*. The findings of fossil papionines extinct since the Middle Pleistocene, and often co-occurring with such hominin species like the Australopithecine, stimulated the idea that Humpata may be a "cradle" as other karstic regions in the Transvaal, an idea that has been since then set aside (eg. Klein, 1994).

In the early 1990s, Pickford and Senut developed fieldwork in the region to explore the fossil fissures and the variety of endemic vertebrae fauna. The work by Pickford and Senut resulted in a vast record of fossil sites, introducing the discoveries at Ufefua, Malola, and Cangalongue. The faunal assemblages offered an interesting overlook of sedimentary deposits and their contents, with new taxons proposed for this region of southwestern Africa (Pickford et al., 1990, 1992)

Several types of infillings were described in the reports, including red breccias, pink breccias, white breccias, and grey breccias. New ages were proposed based on the biostratigraphy, particularly of rodents and primates. The morphometric analysis of specimens from Angola collected by Pickford and Senut argues there are only one species of Theropithecus present across the new assemblages from Tchíua, Malola, and Cangalongue (Jablonski, 1994). This idea is contrary to that of Delson and others whom proposed the presence of *Papio* (Dinopithecus) *quadratirostris* (Delson et al., 2000). Since the assigned taxa for these specimens continue to be a source of debate, the post-depositional features of the materials have been republished using solely family and sub-family classifications, but noting that many of the recovered specimens are, in fact, subadult individuals and therefore of significantly smaller body mass (Gilbert et al., 2009). The only consensus seems to be about the chronology of the fossils as Plio-Pleistocene based on morphological comparisons with other specimens found elsewhere in Africa. In fact, the only radiocarbon dates that were calculated from travertines collected in these caves suggest a much later age. Materials from the collection of J.D. Clark (Table 1) identified as “Cangalongue 3”, a travertine interbedded with red-brown breccia containing much fauna of Upper Pleistocene age was dated to

>34 ka years (Berger and Libby, 1969). However, Pickford et al (1994) estimated an age between 1.3 and 1.8 Ma for the breccia he encountered at Cangalongue 2 and 3, (among the three existing in the area). The idea is supported by the occurrence of extinct rodent: three specimens of *Metridiochoerus andrewsi* stage II from Cangalongue (quarries 2 and 3) occurring in the Pliocene of East Africa.

Moreover, Pickford considered that all the paleontological sites at the Leba dolomites are of late Pliocene to early Pleistocene age. This idea is supported by the occurrence of extinct rodent species, three specimens of *Metridiochoerus andrewsi stage II* at Cangalongue (quarries 2 and 3) which correlate with specimens from the time period 1.8 to 1.3 Ma in East Africa. The occurrence of primates like *Dinopithecus* and *Cercopithecoides* at Tchíua along with the presence of *Gigantohyrax* at Malola are interpreted as corroborating indicators for karst infilling between the Upper Pliocene and Middle Pleistocene (Pickford et al., 1990). As noted by Pickford, the pink breccias with fauna found at the fossil sites of Malola, Tchíua and Ufefua are the result of near surface genesis, frequently coarse and composed mostly of bedrock rubble. It seems that cementation and induration (breccia formation) happened much later as demonstrated by the dating obtained from travertines pointing to a Late Pleistocene age.

During periods of infill, accumulations of nocturnal rodents in the fissures likely derived from bird prey (Pickford et al., 1990). Furthermore, taphonomical indicators suggested that raptor predation by the crowned eagle (*Stephanaoetus coronatus*) is also a possible explanation for the primate fossil accumulations at Tchíua and an "underappreciated selective force" in African primate evolution (Gilbert et al., 2009). This interpretation is also a source of debate and is considered unlikely since the "grey breccia" deposit has been described as an indurated bat guano accumulation deep inside the cave (Pickford et al., 1994; Sen and Pickford, 2022).

According to the authors (Pickford et al., 1994; eg. Sen and Pickford, 2022), four types of infillings can be found at Humpata: 1) speleothems (sometimes referred to as travertines), 2) coarse angular dolomite blocks cemented by speleothems (cavern roof and wall collapse breccias, 3) red sandy breccia, and 4) grey calcified guano. The vast majority of the fossils collected by Pickford are prevenient from red and grey breccias discarded by the miners. The geochemical taphonomic processes were investigated using FTIR (David and Pickford, 1999), comparing bones from fossil and current *Theropitecus* sp. and *Bos* sp. identified the mineral phases and found proteins in the bone material, indicating promising preservation of material for proteomic studies among the Pleistocene remains of the region.

The literature available about the caves of Leba shows a rich biostratigraphy but no clear sequence has been established for the sites as plenty of the remains were collected from the quarry debris. Further work is thus necessary across the karst, to characterize the stratigraphy, establish the different depositional and erosional sequences across the sites and further integrate the paleontological and archaeological data.

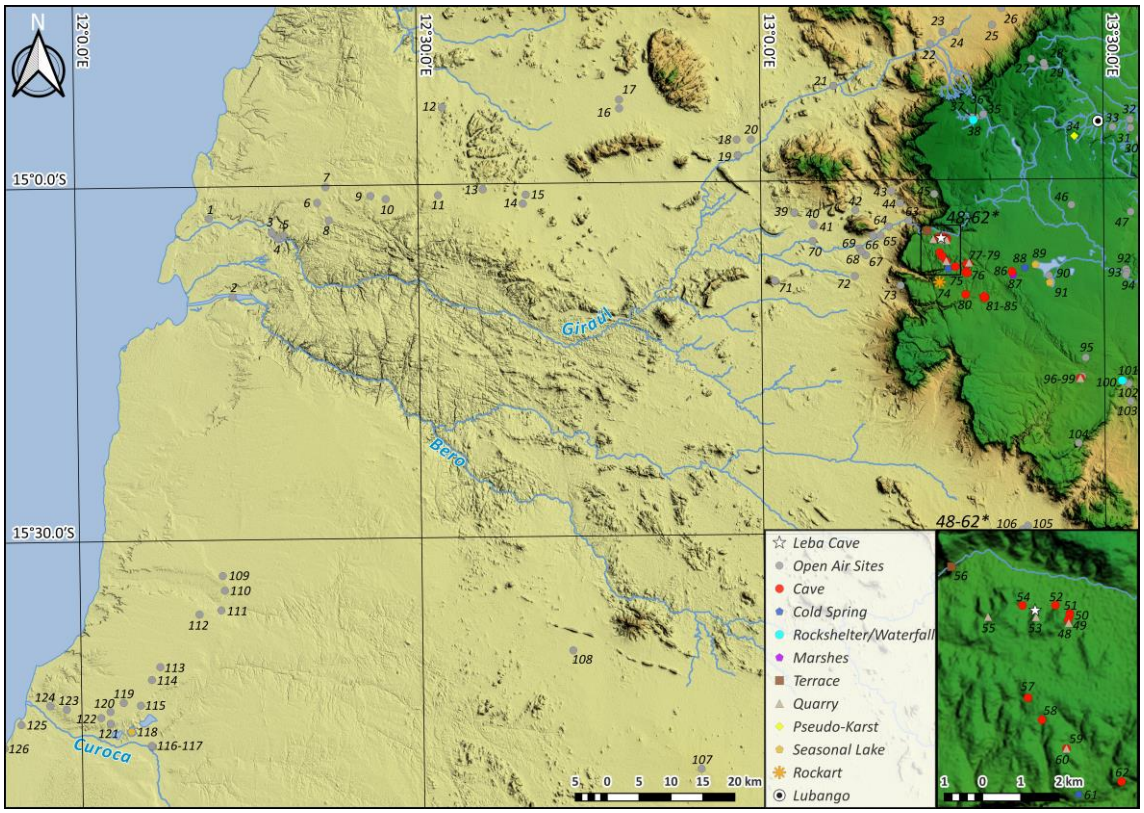

Fig. 4 – Digital elevation map (DEM) for the coastal zone with location of open-air sites, in the vicinity of Leba Cave (adapted from de Matos et al. 2021a, b) and locations surveyed by the PaleoLeba Project (2018-2019): 1 - Ponta Negra; 2 - Fazenda Amélia; 3 - Giraúl 8; 4 - Giraúl 1; 5 - Giraúl 9; 6 - Moçâmedes 1; 7 - Moçâmedes 2; 8 - Vimpongos; 9 - Major 1; 10 - Munhino 20; 11 - Maongo; 12 - Macahama; 13 - Pedra Grande 1; 14 - Torres 1; 15 - Caraculo 6; 16 - Moçâmedes 8; 17 - Caraculo 8; 18 - Munhino 3; 19 - Munhino 10; 20 - Munhino 19; 21 - Assunção 1; 22 - Chamona 1; 23 - Arriaga 1; 24 - Cacanda 1; 25 - Mialabe; 26 - Arriaga 2; 27 - Bipopo; 28 - Techalundianga; 29 - Tundavala; 30 - Mucanca; 31 - Rio Capitão 1; 32 - Barracões 1; 33 - Santo António - Sá da Bandeira; 34 - Pseudokarst Sra do Monte; 35 - Zootécnica 2 – estação; 36 - Zootécnica 6 - 2ª Barragem; 37 - Zootécnica 5 – Cascata; 38 - Cascatinha da Zootecnica 1; 39 - Nondau 1; 40 - Ompanda 2; 41 - Ompanda 1; 42 - Maconge (Sto António); 43 - Maconge 11; 44 - Tampa 1; 45 - Chela; 46 - Palanca 1; 47 - Amuralhado I da Huila; 48 - Pedreira/Forno de Cal da Tchaticuca I; 49 - Lapa/Gruta da Pedreira da Tchaticuca III; 50 - Algar/Gruta da Pedreira da Tchaticuca II; 51 - Lapa/Gruta da Pedreira da Tchaticuca I; 52 - Gruta do Omukongo (Lapa I e II); 53 - Pedreira/Forno de Cal da Leba I; 54 - Algar da Leba I; 55 - Pedreira da Leba II/PROCAL; 56 - Cascata da Leba; 57 - Algar/Gruta de Lemagoma?; 58 - Ondimba da Tartaruga/Algar Tchíua I; 59 - Gruta da Tchíua; 60 - Pedreira da Tchíua I; 61 - Mewó/Tchíua-Ufefua; 62 - Algar/Gruta da Malola V; 63 - Maconge 3; 64 - Maconge 7; 65 - Maconge 10; 66 - Capagombe - Santo António; 67 - Capangombe terrace; 68 - Capangombe Velho (Fort); 69 - Fort of Capangombe; 70 - Terra Nova; 71 - Providência 1; 72 - Maatia; 73 - Chivinguiro 2; 74 - Bruco; 75 - Gruta da Malola II; 76 - Lapa/Gruta da Malola III; 77 - Lapa/Gruta da Malola IV; 78 - Algar/Gruta da Malola I; 79 - Pedreira/Forno de Cal da Malola I; 80 - Nascente do Tchivinguiro; 81 - Nandimba 1/Gruta do Tchivinguiro; 82 - Algar do Tchivinguiro VI; 83 - Algar do Tchivinguiro IV; 84 - Algar do Tchivinguiro III; 85 - Algar do Tchivinguiro I - Colina de Nandimba; 86 - Lapa da Unandjava; 87 - Rio Umbutu/Unandjava; 88 - Umbutu 1; 89 - Nuatechite 1; 90 - Humpata; 91 - Catende 1; 92 - Jau 4; 93 - Jau 2; 94 - Jau 1; 95 - Amuralhado do Eléu; 96 - Cangalongue; 97 - Amuralhado de Muelemba; 98 - Algar Nkangalongue/Gruta de Cangalongue; 99 - Pedreira de Cangalongue I; 100 - Cascata da Hunguéria; 101 - Monga; 102 - Umbala 1; 103 - Hunguéria; 104 - Cavango - Tapaíra 1; 105 - Cainde 2; 106 - Cainde 1; 107 - Lungo 1; 108 - Azevedo 1; 109 - Moçâmedes 3; 110 - Moçâmedes 4; 111

- Moçâmedes 5; 112 - Alexandre 4; 113 - Alexandre 3; 114 - Arco 1; 115 - Carvalhão 1; 116 - S - João 1; 117 - S - João do Sul; 118 - Arco; 119 - Carvalhão 2; 120 - Octávio 1; 121 - Unguaia 1; 122 - Carvalhão 3; 123 - Alexandre 2; 124 - Alexandre 1; 125 - Pinda; 126 - Contensil

2.3. The archaeological site: Leba Cave

Leba Cave (-15.083453°, 13.259457°) refers to a 50 m phreatic tube and adjacent solution chambers located at c. 1.757 m a.s.l., in the vicinity of the Humpata village, 25 km west from Lubango city, Huíla Province (Fig. 5 - 8).

The cave entrance is located about 1 km south of the Leba River, at an elevation of about 12 m above the stream. In front of the cave entrance, two kilns and the ruins of a lime factory built in 1950 are found. The farm/complex has many buildings at road mark 45, National Road EN128, direction Lubango-Moçamedes, Namibe. Infrastructures related to the colonial company are visible, mostly in ruins, including barns, housing, warehouses, and a chapel.

Around these ruins, the village of Leba is home to Nyaneka-Humbi speakers, mainly Mumúilas, although many families migrated from the north during the war and integrated into the community in the 1990s. The dwellings are built with sun-dried mudbricks and daga. Some modern buildings include a water pump, a health center, and a school. The community of Leba remains fairly traditional, with an economy relying mostly on cattle and farming activities. The river is mainly channeled for irrigation and its margins are covered by crop fields. At the cliff, about 2,5 km west of the cave, the river turns into a waterfall forming stepped pools across a 1,200 m drop until it reaches the foothill of Santo António-Capangombe as a shallow creek. Alluvial beds (gravel) accumulate close to the waterfall including lithic assemblages.

The discovery of the archaeological site occured during the construction of the two kilns adjacent to the cliff, as they were built in front of the cave entrance using the natural slope as a master wall. The construction started in 1947, a period when the "Calcários da Leba", a company operating there since the 1930s, expanded the area of exploration from Tchivinguiro to the northern (Leba valley) and southern (Cangalongue) flanks of the massif. Several quarries and kilns were active at the same time across the dolomites. The abundance of fissures and crevices offered natural conditions for the exploration of calcite sinter.

The first archaeological excavations at the site occurred during the Anthropological Mission of Angola in the 1950s, a large expedition by the Portuguese colonial Board of Scientific Missions (JIU) dedicated to understanding the distribution and history of the indigenous populations of Angola. Following the discovery of Cercophitecide crania at

Tchíua (or Leba 1 in old records), which sparked the interest of local and international peers in the Pan-African conference meetings (Arambourg and Mouta, 1952; Borges and Mouta, 1926; Dart, 1950; Mouta, 1953), excavations at Leba Cave were directed by geologist José Camarate-França (JCF). No field diaries were found but some field results were published as part of a JIU volume in his honor (Almeida, 1964). Hence, the only existing report about this excavation is not a real original paper by the author but an interpretation of his field notes attached to the artifacts. This small report indicates the excavation lasted only a couple of days before it was suddenly interrupted, in the year 1950 (Camarate-França, 1964). It is unclear what reasons caused the interruption of the excavation work, but most likely these were related to the quarry activities involving dynamite. Considering the volume of the assemblage currently kept in Lisbon, it is unlikely the site was excavated only once. There is no direct evidence of a second excavation at the cave, but some authors suggested Camarate-França returned to the site sometime between 1951 and 1953 (Jorge, 1974; Ramos, 1982).

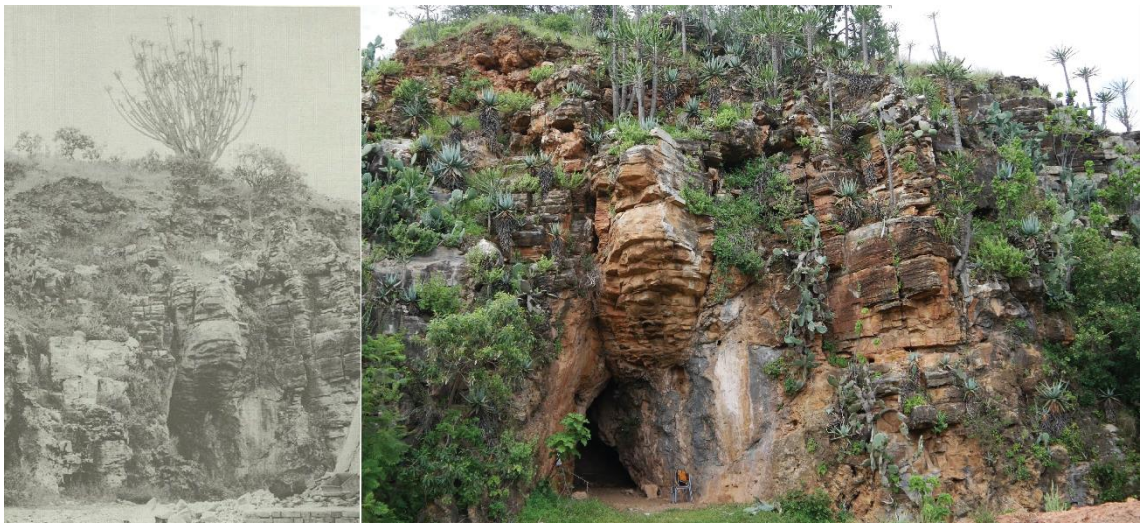

Fig. 5 – Photograph of Leba Cave in the 1960s (Tropical Archive, do Amaral, 1973) and current state.

The complete collection from Leba Cave is composed of 1409 lithic artifacts and more than 5000 pieces of associated faunal remains including birds, fish, rodents, ungulates, carnivores and papionines. Many bone fragments (shafts) and blanks are preserved in indurated blocks (breccia like), unlike teeth and tools which appear to have been cleaned with acid. For these reasons, it is more possible the Camarate-França returned to the site and collected bulks of sediment for further processing in the laboratory.

The complete collection from Leba Cave is composed of 1409 lithic artifacts and more than 5000 pieces of associated faunal remains including birds, fish, rodents, ungulates, carnivores, and papionines. Many bone fragments (shafts) and blanks are preserved in indurated blocks (breccia-like), unlike teeth and tools which appear to have been cleaned

with acid. For these reasons, it is more possible that Camarate-França returned to the site and collected bulks of sediment for further processing in the laboratory.

The author provided the following stratigraphic information, reproduced in de Matos and Pereira (2020):

I. Unit with modern debris fragments of pottery, bricks, and charcoal mixed with stone tools (20-30 cm);
II. Unit of loose, dark-grey sands with a high percentage of organic matter, including pieces of metals, pottery, and lithics, but possibly reworked (30 cm);
III. Unit of dark-brown silt-clayey sediments rich in organic matter with lenses of charcoal and ash, vertebrate fauna, and stone tools; at the base of the horizon concentrations of charcoal and bones were observed and interpreted as combustion features;
IV. Unit of reddish marl with concretions, rich in vertebrate fauna and lithic industries;
V. Unit of reddish marl, sterile;
VI. Unit of reddish marl with large flakes and bifacial core tools similar to the “Sangoan” or “Kalinian” handaxes

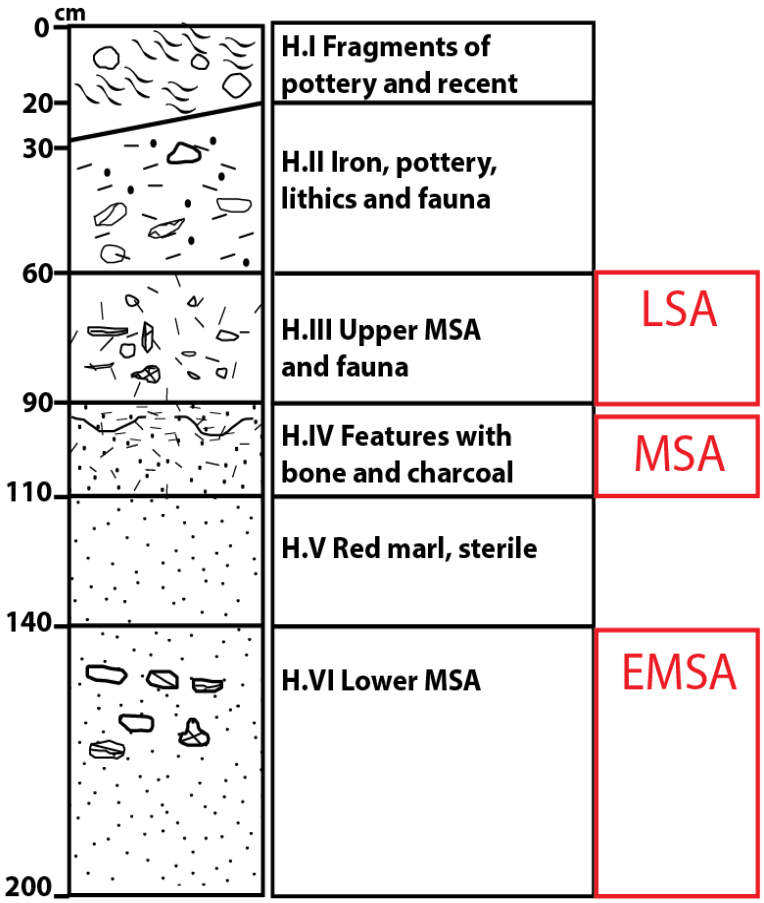

Fig. 6 – Schematic stratigraphy from the 1950 excavation in Leba Cave published by Ramos 1982 and cultural phases published by de Matos and Pereira, 2020 in red.

The assemblages from this excavation were taken to Lisbon and remained unstudied for a long time. The site was referenced in Clark's synthesis of the prehistoric record of Angola (Clark, 1966) but not the materials excavated by Camarate-França. The assemblage of 28 artifacts described by Clark was deposited at the SGMA offices in Luanda and was probably collected in 1947 by F. Mouta of the Geological Survey Brigade. From this small assemblage, Clark describes an Erongo culture, leading to the conclusion the site should be LSA or "Neolithic" (Clark, 1966). He did not report, however, on the radiocarbon dates later published by the UCLA laboratory (Berger and Libby, 1969) which indicate infinite dates for fossil breccias prevenient from the cave (Table 1).

In March 1974, a second excavation was directed by archaeologists Vítor and Susana Oliveira Jorge focused on excavating a 1 m^2 test pit at the entrance of the cave with the aid of the students and volunteers from Sá da Bandeira (Lubango) over five days (Sá Pinto, pers. comm.). The assemblages collected were deposited in Lubango. Due to the 25th April 1974 revolution in Portugal happening shortly thereafter interrupting all colonial agency, the lithic assemblages were never studied and remained at the School of Educational Sciences (ISCED). After Jorge's return to Portugal, little data was made available by the author as it seems pictures taken during fieldwork were also lost (Jorge, 1975). The author described a Wilton culture with two archaeological horizons, suggesting the excavations reached the bedrock at 0.80 m of depth (Jorge 1974). Volunteers in the excavations mentioned the discovery of human remains inside the cave, in a more interior area of the channel. Personal consultation of the collection housed at the ISCED in Lubango in 2018, was not successful in finding those osteological remains and no written references have been found either. The assemblages from 1974 include mostly patinated lithic materials, pottery fragments, bored stones, and groundstones.

In the 1980s, M. Ramos, who was developing his doctoral thesis about the Early and Middle Stone Age of Southwest Angola, re-addressed the possible relationship between Leba Cave and Capangombe with the samples available in Portugal (Ramos, 1981). The faunal assemblages collected by Camarate-França in 1950 were sent to paleontologist Achilles Gautier at the University of Gent sometime in the late 1980s. The unexpected passing of Ramos in 1991 left the co-authorship with Gautier incomplete and a short report about the fauna was published and signed only by Gautier (1995).

In this report, the stratigraphic information presented differs from the original published by Camarate-França (1964). Gautier (1995) described a series of assemblages from five

sedimentary units, considering two interfaces (horizons III/IV) following indications from Ramos. Gautier attributed the faunal assemblages to at least three taphonomic agents: human hunting activities, predators, and their necrophages. Ichnofossils such as carnivore coprolites and bone shafts with gastric dissolution damage were observed (Gautier, 1995). The author concluded that carnivores were important depositional and reworking agents at Leba before the cementation of the deposit (Gautier, 1995). The author also interpreted the fragments of Papio as leopard prey, although considering that these specimens may correlate to the baboons currently known in Angola such as the *Papio cynophalus* (Hill and Carter, 1949), natural death conditions cannot be disregarded.

In 2011, a study of the lithic assemblages was undertaken focused the techno-typology of horizons III-VI from the 1950 assemblage stored at the IICT in Lisbon (Matos, 2013). The goal was to develop an updated descriptive sheet for the lithic collection of Angola in the IICT starting with Leba Cave, describe the sequence of techno-typological attributes, and test possible correlations between these assemblages and Southern African cultures. This study proposed the existence of three cultural phases, being the lowest (VI) an early MSA of Acheulean tradition including cleavers (or evolved Acheulean in Ramos, 1982); (IV) a classic MSA blade-point industries in chert and quartzite; and the upper unit (III) an LSA cultural phase of quartz predominant bipolar strategies. The absence of fossil directors such as the bifacial points or geometrics did not allow any direct correlation with the techno-complexes of the South African repertoires (de Matos and Pereira, 2020).

A tentative dating of the faunal assemblages from horizon IV was also pursued during the master studies in collaboration with Curtis Mckinney at Miami Dade University. Bone and enamel from a Hippotragus equinus tooth were analyzed using the Uranium-Thorium series. The results shown are only preliminary (Table 1) because of McKinney's sudden passing in 2015. Neverthless, these results offered a preliminary age for the faunal accumulations of the MSA.

In Q2, the quarry section showed the negatives of dynamite explosions to access a much larger chamber. Pockets with similar vertical connections to the surface are observed and plenty of succulents have developed their roots into the fractures, some of them showing sheets of travertine. The section of the chamber shows how the quarry targeted the calcite contained in the solution chambers forming near surface (5-6m) interstratified limestone-dolostone beds as it has been observed in the hills about 1 km

east of Leba (Tchaticuca complex) and in most of the cave sites surveyed around the Leba Formation (eg. de Matos et al., 2021a).

Site/Name	Lab ID	Type	Analyses	Age	Notes
Leba 2 Cave	UCLA-708A	travertine	^{14}C	>34,000 BP	following Berger and Libby 1966: Coll. by J. D. Clark.
Leba 2 Cave	UCLA-708B	travertine	^{14}C	30,800 BP ± 1700 (28,850 BC)	following Berger and Libby 1966: travertine sheet sealing red breccia believed to be of Upper Pleistocene age. Coll, by J. D. Clark.
Leba 3 Cave	UCLA-708C	travertine	^{14}C	29800 ± 1650 (27,850 BC)	following Berger and Libby 1966 Leba 3 Fissure; travertine and grey/cream breccia incorporating fossil bone. Grey/cream breccia was believed to be of lower Pleistocene age on the identification of fossil fauna but is also Upper Pleistocene. It is important to confirm this for this site. Coll. by J. D. Clark.
Leba Cave (Horizon IV/III)	#65-376 (4-2013)	Dentine (*Hippotragus equinus*)	U/Th series	80,000±5000	2.3 ppm Uranium, U234/U238 =2.3, Age Ratio Th230/U234 = .59 + or – 6% = 80,000 + or – 5000
Leba Cave (Horizon IV/III)	#66-376Bone1 (4-2013)	Bone (*Hippotragus equinus*)	U/Th series	100,000±50,000/40,000	2.7 ppm Uranium, U234/U238 =2.3, Age Ratio Th230/U234 = .68 + or – 20% = 110,000 + 50,000 or – 40,000

Table 1 – Absolute ages available for Leba Cave deposits.

Small pockets of about 0,50-0,80 m in height with shallow horizontal development are infilled with hyrax middens. Dripstone and speleothems cover the wall and an older infill at the base of the chamber is composed of grey breccia with mammal bone fragments. Similar bone fragments were observed in the blocks discarded by the quarry located

about 2 m north, towards the slope. Relics of breccias with angular inclusions of dolostone and reddish cement are found associated with limestone walls.

Inside the cave, a peculiar "hanging breccia" can be observed along the western wall and part of the roof, as well as in boulders packed at the center of the cave channel and dividing the space into two rooms. The connection between rooms is made through a path under the blocks or through a narrow passage between the eastern wall and the blocks.

The "hanging breccia" is particularly evident in the inner area of the cave. A large block of "hanging breccia" is tilted and cemented to the western wall, forming a narrow dripline. This breccia is composed of chert and dolostone angular debris, yellow sands, and white calcite cementum, effervescent under 10% HCl tests. As part of the breccia is coated by dripstone which would also react with the HCl further confirmation is necessary using other methods. Hanging breccias have been observed in other cave sites with paleolithic occupation but are rather poorly documented. The breccia is a relict of an earlier infill and erosion of the cave likely relating to a collapse associated with a fracture or fault. The origins and relationship of the breccias found in the cave wall and the quarry are not clear but the composition and textures observed seem to differ, being the "hanging breccia" the likely earliest stage of infill of the cave.

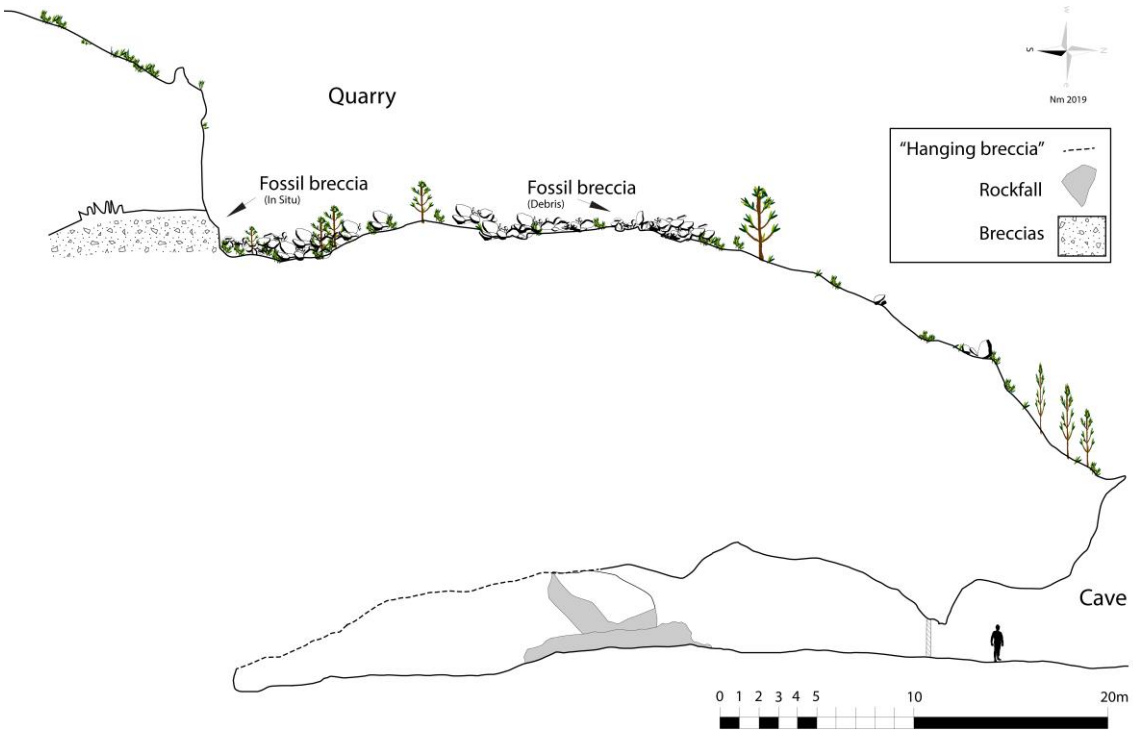

Fig. 7 – Schematic section view of Leba hill, quarry and cave (dashed line outlines to the upper limit between the roof and the hanging breccia block)

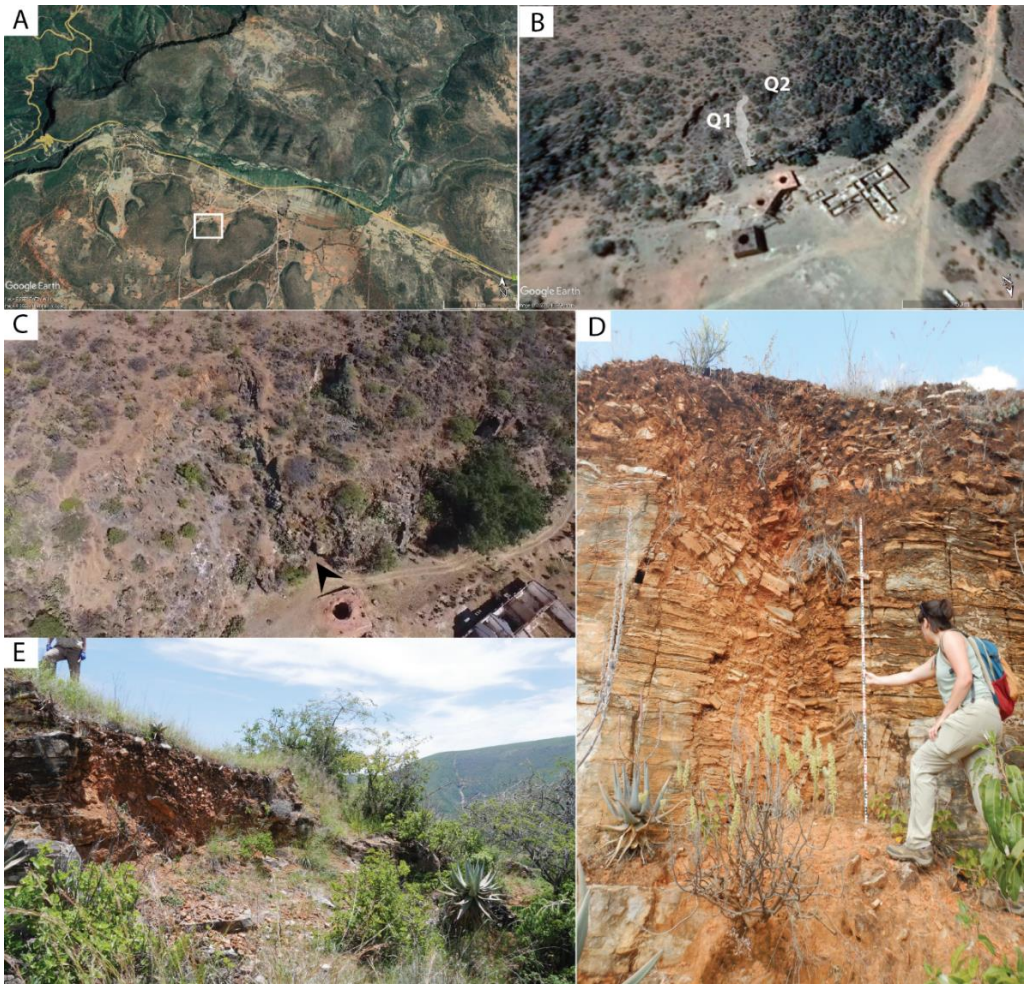

Fig. 8 – A: Location of the cave (square) in the Leba Valley in world view (Google Earth, in yellow the National Road Lubango-Namibe); B: Detail of the square in picture 1 with overlay of the cave outline in relation to the Quarry 1 (Q1) and Quarry 2 (Q2) (Google Earth); C: Aerial photograph of the quarry; D: Detail of fissure and infilling with red sediments and platy bedrock debris at the hilltop quarry exposure of Q1 (2 m scale); E: Detail of slope sediments obliterated by quarry.

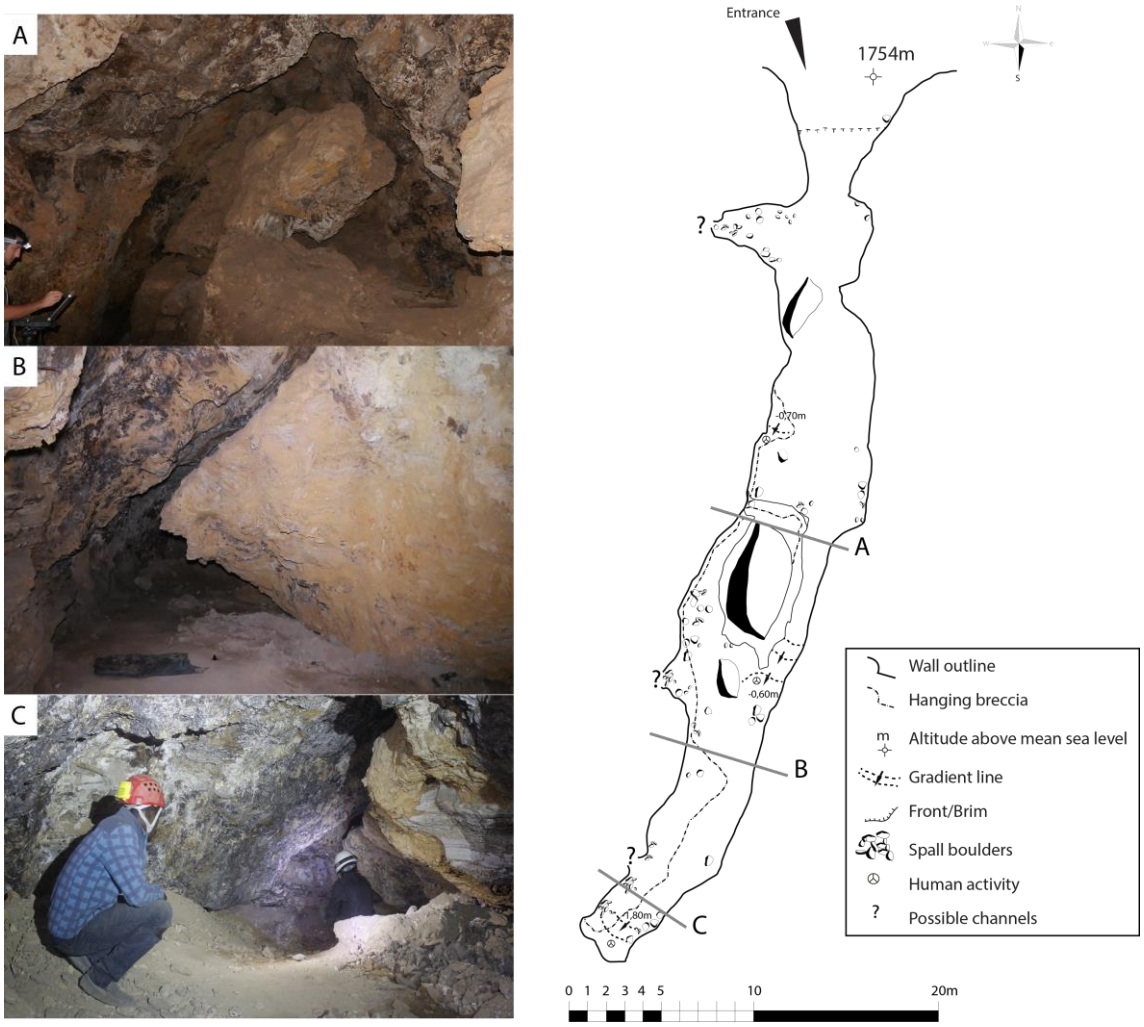

Fig. 9 – Plan of the cave and section views facing south, with photo sections showing the hanging breccia on the western wall (right side of the pictures) and the bedrock wall (left side).

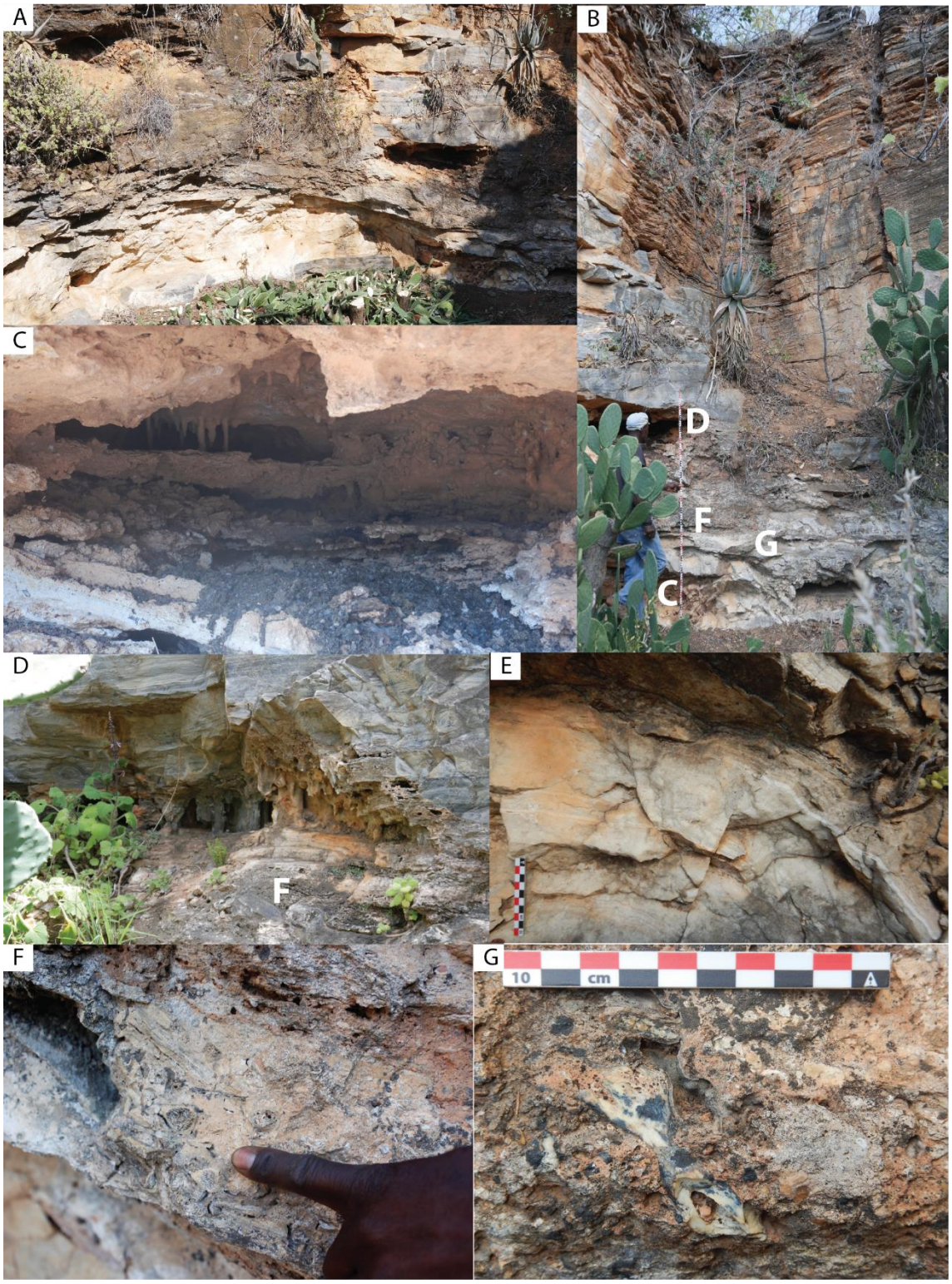

Fig. 10 – A: Panorama of solution chamber (shade) and the limestone pocket explored by the quarry (right) interstratified with dolomites Q2; B: View of the fissure (2m scale) and karst pockets with fossil breccia at the base; C: Hyrax midden in small chamber; D: Detail of the chamber covering the fossil breccia in F; E: Detail of the flowstones (10 cm scale); F: Detail of bone breccia; G:Detail of mammal bone (10 cm scale)

3. Aims and theoretical justification

The goal of this study is to reconstruct the depositional history of Leba Cave to provide better insight into the timing and context of human occupation which produced archaeological signatures at Leba Cave. In this study, I employ a site formation approach by identifying and describing the depositional and post-depositional processes, to contextualize human occupation events since the Pleistocene.

The analysis of archaeological materials and features help us understand how the site changed through time. This inherently includes all the transformations that occurred during and after the deposition of the material culture, how these are influenced by the environmental context, and its taphonomical implications (Butzer, 1982; Goldberg and Sherwood, 2006; Karkanas and Goldberg, 2018a). Site use is analyzed by combining macroscopic and microscopic analysis of the archaeological accumulations found at Leba Cave.

Archaeological sites can be defined as the result of the accumulating byproducts of processes of geogenic, biogenic, or anthropogenic origins within a specific place. The interaction of these multiple agents is the basic postulate for the formation of archaeological accumulations at a given location. Depending on several intrinsic and extrinsic factors, archaeological accumulations are part of complex depositional environments which are finally approached by the archaeologist (Karkanas and Goldberg, 2018a; Mallol and Mentzer, 2015; Miller, 2011; Patania et al., 2022; Shahack-Gross, 2017; Stiner et al., 2001).

Formation theory is the discipline that confronts the complicated nature of the formation of the archaeological record (or archaeological accumulations) and the dynamics of depositional environments in anthropogenically modified locations, habitats, or landscapes i.e., site formation processes. Among the archaeological sciences, geoarchaeology, (and the micromorphologist toolkit) has proven most useful to the methodological and practical development of formation theory. The dynamics between systems, either natural or non-natural, were widely documented by Schiffer (1987).

In the early days of the discipline, site formation processes were broadly subdivided into natural processes vs. cultural processes. The first relates to any physical and/or chemical processes naturally occurring at a site, influencing the stratigraphic units, features, or loci. The latter includes all non-natural processes, associated with features or remains of human activities, which are extremely variable and often integrate both geogenic and biogenic elements derived from anthropogenic activity. On the other hand, natural processes are recognized as being regulated by the same laws of geological sciences.

Thus, the dynamic of the formation agents can be characterized, compared, and (to a certain degree) predicted by the same morphological and chemical signatures (Shahack-Gross, 2017).

The archaeological sciences, and particularly geoarchaeology, has the potential to characterize human behavior by relying on the theory and practice of the natural sciences, and also the social sciences, particularly anthropology, and ethnography (Stein, 2001). Geoarchaeology analyses different relationships (between components, features, structures, and sites) to understand the formation of the archaeological record. Currently, the discipline has moved forward from the binary interpretation of cultural vs. natural processes of Schiffer to a more integrative approach to the geoarchaeological matrix based on observation, description, experimentation, and ethnoarchaeological work (Brain, 1981; Goldberg and Macphail, 2006; Karkanas et al., 2021; Karkanas and Goldberg, 2018a; Macphail, 2020).

In the case of Leba Cave, it is essential to reassess the degree of disturbance, not only related to bioturbation but also recent anthropogenic alterations and how these impact our interpretation of the assemblages collected at the site (eg. Binford, 1983). Leba cave system is recognized by a continuum of paleontological remains since the Plio-Pleistocene and a Stone Age sequence with at least three phases: 1) late ESA/early MSA with macrolithic tools; 2) “generic” MSA with blade-point technology, and 3) late MSA/LSA with quartz tools analogous to other toolkits in Namibia and South Africa. The minimum age of 75 ka obtained for phase 2 pushed back the initial dating strategy for the region (Berger and Libby, 1969) (Band is the only absolute dating obtained for MSA deposits in Angola, south of the Congo basin (Clark, 1968, 1966; Ervedosa, 1980). A fourth phase may also be identified in the Holocene deposits of the cave related to historical hunter-gatherers and contact with Bantu populations and European colonialists (Jorge, 1975, 1974).

Karstic formations, either caves, fissures, or rock shelters, are usually efficient and peculiar sediment traps while also playing host to the accumulation of anthropogenically derived material, either by use of the space itself or its surroundings. In caves, materials undergo various syndepositional and postdepositional processes related to specific phenomena occurring in these enclosed environments which can produce dramatic alteration in the nature and content of the sediment and its contextual relationship with artifacts (Goldberg and Sherwood, 2006; Karkanas et al., 2021). On the other hand, caves and rockshelters are recognized as excellent locations for preservation of prehistoric sequences in southern Africa (Clark, 2001).

Karstic regions are scarce in Africa, and open-air sites are more abundant but often exhibit conditions with high rates of erosion and decay of organic matter, intense biogenic activity, or high acidity soil cover derived from the oxidation of the granite bedrocks (McBrearty, 1990; Morley and Goldberg, 2017). Any carbonated sedimentary matrix has the potential to preserve organic remains like bone and plant tissues that allow the unraveling of a wide range of behavioral traits and material relationships. They are prime locations for the preservation of skeletal material which offer the opportunity to explore different datasets about environmental change, human dietary preferences, territoriality, technology, and symbolic behaviors. Cave sediments and their conditions of deposition and erosion are often representative of the environmental conditions and habitats inside or around them.

High-resolution studies have established or refined important chronostratigraphic sequences in many other regions of Africa (Backwell et al., 2008; Chazan et al., 2020; Goldberg, 2000; Inglis et al., 2018; Karkanas et al., 2021, 2015; Miller et al., 2016; Rhodes et al., 2022; Thompson et al., 2021; Tribolo et al., 2016), as well as bring further understanding of the behavioral complexity of human populations in the region. By using the geoarchaeological matrix approach, it will be possible to control for different biases in the sequence. It can also help track the fine sequence of depositional horizons, anthropogenic and biogenic inputs, and paleoenvironmental signatures that may have affected the landscape and contributed to the different phases of infilling. It will also help understand the cementation of sedimentary units or questions of preservation of artifacts. For instance, differential preservation of bone is related to the strong weathering of slopes outside of the cave and the rise of the water table, contributing to specific alternating diagenetic and syngenetic regimes, or rather by intertwined physical-chemical phenomena derived from bio-anthropogenic activity.

The Humpata plateau (and the Leba Dolomites) is a particularly special area due to the reported occurrence of early Quaternary fauna in karstic infillings (Camarate-França, 1964; de Matos et al., 2021b; Pickford et al., 1990).

Clark's observations about the Humpata Plateau indicated that cultural conditions were highly independent of environmental conditions as environmental change was never significant enough to bring about the dissolution of the carbonated features (Clark, 1966). This argument was based on the abundance of fossil-bearing sites in the remaining karstic formations (David and Pickford, 1999; Pickford et al., 1994; Sen and Pickford, 2022). His observations across Central and Southern Africa suggest that weather conditions alternated seasonally, and in this regime, both animal and human populations

would have been most mobile and dispersed during the monsoons and most concentrated during the dry season (Clark, 1971). In this sense, the area of Humpata with its springs and lakes would have been a permanently attractive location for many species

The sequence of mammal fauna studied by Gautier (1995) was interpreted as the result of both carnivore accumulations and human consumption, suggesting that human occupation until the LSA was probably short-termed and seasonal (Gautier, 1995), possibly during cycles of high humidity and intense summer rainfalll (eg. Clark, 1963).

Previous studies highlighted specific phenomena such as surface alterations of the lithic artifacts and bones, carbonate crusts, and other features. These features were described in the 2m sequence of archaeological horizons collected in the middle of the cave chamber. Geologically, previous studies suggest an active and dynamic environment where physical-chemical processes had an impact on the state of preservation of the archaeological remains. It is also known how complex interactions of biogenic and anthropogenic agents generate peculiar sedimentological patterns in organization and composition at archaeological sites. As these conditions may suggest a bias in the archaeological record, particularly for the application of absolute dating methods and future paleoenvironmental reconstructions, it is necessary to readdress the sequence and reconstruct the formation history of Leba Cave from a micromorphological perspective.

The reassessment of the Leba Cave and its sedimentary sequence intends to answer the following key questions:

- what is the sequence of formation of geogenic, biogenic, and anthropogenic deposits in the cave infill?
- what is the relationship between depositional and post-depositional processes?
- may this sequence be correlated to microenvironmental (cave) and macroenvironmental (surrounding landscape) changes? Or rather anthropogenic change?
- how cave formation processes (sedimentation and post-depositional phenomena) affect the integrity of the archaeological record in this region of southwestern Africa.

This study aims to zoom in on the sequence of Leba Cave and propose a site formation model that will help scrutinize the different interpretations of the site and understand the cultural sequence used to further integrate the absolute dating methods.

4. Materials and Methods

4.1. Field Methods

4.1.1. Excavation Strategy and Methods

Since 2018, three field seasons were developed at Leba Cave. Before the first visit to the site, the season was planned to address specifically the MSA sedimentary sequence excavated in 1950 (Camarate-França, 1964; de Matos and Pereira, 2020) and collect micromorphology samples from those profiles.

The first field season occurred in February 2018. From the first assessment, it became clear there were two areas with indications of previous trenches at the archaeological site: a first one, close to the entrance of the cave, and a second one, approximately 35 m inside, after a narrow passage through the middle of the phreatic tube. A third area, at the very end of the cave, also showed evidence of mechanical excavation (likely with an electric hammer), leaving the debris in place. The local population informed the team that they searched for a water spring at the end of the cave sometime between 2010 and 2016.

The geographical system for the cave was established by horizontally dividing the space with a grid of 1x1 m^2 squares, which are divided into quadrants of 0.5 m. Because the initial strategy was to follow the literal information provided by the report of 1964, the first excavations focused on the area close to the entrance, which seemed to correlate to the "first chamber" described by França. As the work progressed, and despite the abundant material culture it became clear the sedimentary sequence did not match the original description and it was likely the area excavated by V. Oliveira Jorge, hence the acronym VOJ.

For this reason, during the second field season in October 2018, excavations focused on the exposed profile at the end of the cave (DMT) showing faunal remains, mainly bone shatter and mammal teeth, and a few lithic tools that could be generally assigned to the MSA. Moreover, the deposit was similar to the sediment samples collected by França, although it was not the actual provenance of the MSA assemblages. Conditions for excavation were not ideal due to the narrow space available to host one excavator and one gunner adding to the hardness of the units which made it extremely difficult to excavate manually. Because the excavated deposit yielded very few lithics, the excavations the next field season in 2019 focused again on area VOJ. The JCF trench was clean and prepared at the end of the field season of 2019 for a future field season.

.

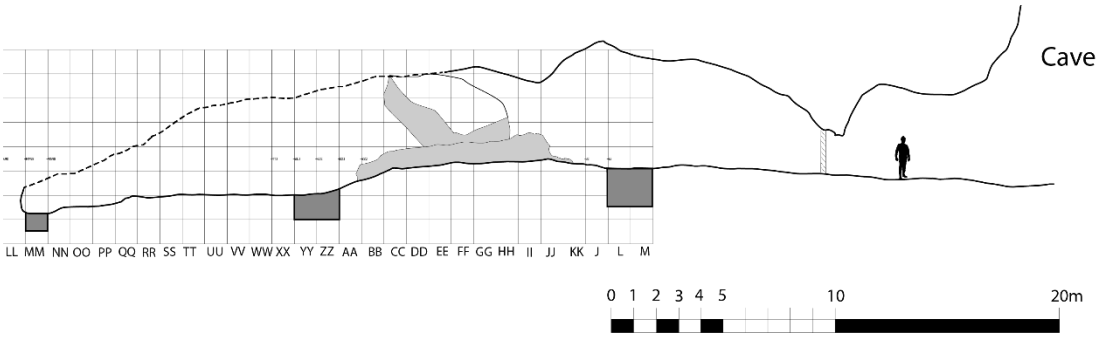

Fig. 11 – Section view of the cave with excavation grid and location of approached areas and virtual grid used in the DEM implanted with the total station: Area DMT – square MM; Area JCF-square YY-ZZ; Area VOJ: squares L-M.

Excavation followed the natural stratigraphy. The term geological unit (GU) was applied to any sedimentary unit macroscopically observed showing differences in fine and clastic components from the overlying sediment, also considering biogenic or anthropogenic materials and features.

A new GU was defined every time discontinuities in sediment patterns (texture, compactness, color, features) were found. Every GU was described by the excavators on site using a descriptive sheet of basic components and features.

Excavation protocols were adapted from the “Tübinger” excavation system which has been applied in archaeological sites of Germany and South Africa (eg. Conard et al., 2022), and similar to the “bucket system” frequently used in other paleolithic sites in Europe and Africa (McPherron and Dibble, 2002). Buckets of sediment form the basic unit of analysis when excavating archaeological deposits and can vary in volume, with a full bucket usually representing around 10 liters of sediment with any possible variation. The “Abtrag” refers to the series of buckets that translate the volume of sediment running parallel to the slope and shaping a GU.

Record of GUs, bucket, and piece-plotting of finds are combined with dry sieving and water screening as appropriate. Adaptations to the method are justified by the logistical constraints, namely, the water and energy supply. For these reasons, dry sieving with a 5 mm mesh was applied on site. This was true for all the abtrage excavated in VOJ, while in JCF and DMT, where the stratigraphy is far more indurated and harder to excavate manually, plotted finds sometimes refer to aggregates including several bone shafts.

Piece-plotting was used for archaeological finds with the following measurements: all lithic artifacts > 1 cm (including classes of blanks, cores, and tools); bones, teeth, and other faunal material > 3 cm or identifiable (including concentrations of microfauna when possible); rounded cobbles > 3 cm (including burned clasts). Any charcoal, mineral (such

as ochre), or other unidentified materials were piece-plotted. The same strategy was used for decorated pottery and metals.

4.1.2. Assemblage inventory and macroscopic observations

The inventory of collected finds occurred during the field seasons and visits to Angola. The collection from Leba Cave is housed at the Regional Museum of Huíla, in Lubango (Huíla, Angola).

Finds were labeled with the codes used in the excavation. During the screening of the material, the assemblages were subdivided into sub-samples: lithics, fauna, pottery, wood charcoal, metals, and others. Sediment samples for micromorphology and faunal material for absolute dating were transported to the laboratories of the University of Tübingen for analysis.

The faunal assemblage was subdivided into four groups: macromammal fauna, micromammal fauna, birds, and arthropods. Taxonomic identification was made by the members of the PaleoLeba project. This task was often challenging (particularly with the micromammal sample) and possible through comparisons with the Zooarchaeology reference collections of Tübingen, photography references from the Leba Cave assemblage in Lisbon published by Gautier (1995), and collaboration with other peers in the Angola-Namibia biodiversity research group (Huntley et al., 2019).

For macromammals, a key for bovid size classes (Table 2) was adapted from other studies of southern African fauna (Brain, 1974; Clark and Plug, 2008), considering the Angolan bovids first described by Hill and Carter (1949) and summarized by Beja et al (2019). For this study, absolute frequencies and other taphonomical observations including processes such as burning, calcination, weathering by movement/water, patination, and precipitation of carbonates and other chemical crusts or diagenetic traces were retained following standard literature (Fisher, 1995; Lyman, 1994; Stiner et al., 1995). Gnawing damage was also recorded following Saladié et al. (2013) and recent literature (eg. Pineda and Saladié, 2022). The mammal reference collection at the University of Tübingen was also key for the taxonomic identification (M. Mata-Gonzalez, pers. comm).

For micromammals, the reference collection from Durban Natural History Museum was key for taxonomic identification (J. Zastrow, pers. comm) in combination with literature about the rodents of sub-Saharan Africa (Monadjem et al., 2015).

For bird taxa, the reference collection housed at the University of Tübingen in Germany was used (A. Val, pers. comm), along with literature about modern avifauna occurring in Angola (Mills and Melo, 2013).

Size class	**Live weight (Kg)**	**Species (list not inclusive)**
Bovid I	< 23	Klipspringer – small antelope (*Oreotragus oreotragus*) Common duiker (*Sylvicapra grimmia*) Oribi (*Ourebia* sp.) Steenbok (*Raphicerus* sp.)
Bovid II	23 – 84	Reedbuck (Redunca arendinum) Springbuck (Antidorcas marsupialis)
Bovid III	85 – 300	Greater Kudu (*Tragelaphus* cf. *Strepsiceros*) Roan Antelope (*Hippotragus equinus*) Hartebeest/ African antelope (*Alcelaphus* sp.) Common tsessebe or sassaby (*Damaliscus* sp.*)*
Bovid IV	295 – 950	African/ Cape buffalo (*Syncerus caffer*) African wild cattle (*Syncerus antiquus*)*
*Although it is widely cited as *Pelorovis antiquus*, Klein (1994) suggested that taxon should be removed from the genus *Pelorovis* and reassigned to *Syncerus*, as *S. antiquus.*		

Table 2 – Key for bovid size classes (adapted from Brain, 1974; and Clark and Plug, 2008; and includes additional Angolan bovids after Hill and Carter, 1941; and after Huntley et al., 2019).

Other materials were also recorded and subdivided into classes. Pottery fragments were particularly present in area VOJ and were described whenever possible. The rest of the assemblages were subdivided into metals, ochre, and other clay construction materials such as “daga” (also called dakha in other regions of Africa).

For lithic analysis, terminology and descriptive criteria used in this study were adapted from the methodology previously used for Leba Cave (de Matos and Pereira, 2020). Since cultural artifacts were not allowed to leave the country, the analysis of the lithic artifacts occurred during the fieldwork and, thus the data collection was reduced to essential entries allowing to overcome the time challenges of the field season but still providing an overview of techno-typological attributes and metric patterns of the assemblage at this stage of the research project (Table 3). The adaptations were necessary to deal with time and logistical contingencies but still provide comparable data for chrono-cultural aspects of the assemblages prevenient from Leba Cave. More attention was drawn to the physical condition of the artifacts (both modified and non-

modified clasts) as it could yield important indicators for site formation processes such as burning, calcination, weathering by movement and/or water, or concretions particularly precipitation of carbonates.

More than 90% of the lithics collected during the field seasons were prevenient from the entrance hall of the cave excavation (area VOJ) which yielded recent Late Holocene units. Only modified material was considered in the analysis. Further comparison and integration

As for the other excavation areas, since only a few pieces were found, these were individually described.

General Attributes	
Type of raw material	Chert; Wackestone, Mudstone, Claystone; Siltstone; Jasper; Chalcedony; Sandstone; Quartzite; Milky Quartz; Hyaline Quartz; Silicified dolostone; Dolerite
Cortex %	0-25; 25-50, 50-75, 75-100%
Cortex type	Thick powdered, water worn, altered-rolled
Find class	Core, Blank
Presence of cortex	Yes / No
Surface alterations	Patinated, concreted, water-worn, mixed
Fire Marks	Yes/No
Completeness	Complete / Fragment
Dimensions	Length, Width, Thickness (mm)
For cores:	
Platf. Nr	Number of striking platforms
Blank products	Flakes, Blades, Bladelets, Mixed
Exploitation	Extensive (few large flakes >100 mm); Intensive (multiple small flakes <100 mm), Pre-determinate, Indeterminate
Concept	*For extensive core*s: not organized, organized, pre-configurated; *For intensive and predeterminate cores*: Not organized, organized, chopper, Radial, Levallois, Prismatic, Quina, Polyhedral, Pucheuil, Kombewa, Bipolar, Fragment
Method	*For not organized cores*: disconnected; *For all cores except radial and Levallois*: Unipolar, Two poles, Two opposed poles, Two alternate poles, Crossed, Three Poles, Multipolar; *For radial*

	cores: convergent, centripetal, discoidal; *For Levallois cores*: Recurrent, Preferential,
Retouch	Yes/No
For blanks:	
Type	Flake, Blade, Bladelet, Burin Blow, Debordant flake, Core front, Core flank, Crest, Cornice, Bifacial thinning flake, Chip, Nodule/Chunk, River cobble/pebble, Crystal rock, Ind Fragment
Fraction	Proximal, mesial, distal, siret
Butt type	Cortical, Flat, Dihedral, Faceted, Micro-faceted, Retouched, Smashed, Punctiform, Indeterminate
Butt - Dimensions	Length, Width, Thickness (mm)
Butt - alterations	Lateral notches, chipping, small retouches
Section	Triangular, Trapezoidal, Irregular, other
Profile	Straight, Arched, Twisted, Other
Edges	Parallel, Biconvex, Convergent, Divergent, Irregular, circular, Convex-concave, other
Dorsal Pattern	Cortical, Unidirectional-Indeterminate, Unidirectional parallel, Unidirectional Convergent, Opposed parallel, Opposed Convergent, Alternate, Unidirectional parallel fracture, Unidirectional opposed fracture, Multidirectional, Crossed, Radial/Centripetal, Bulb (Kombewa), Indeterminate, None (dorsal surface caused by a fracture)
Termination	Thick, Feathered, Stepped, Overpassed, Burinated, Retouched, Pointed, Fractured, Cleavage
Retouch	Yes/No
Tool typology	following Bordes, Sonneville-Bordes and others mentioned occasionally

Table 3 – Descriptive criteria for lithic assemblages from Leba Cave

4.2. Laboratory methods

4.2.1. Micromorphology

Standard processes for thin section preparation of micromorphology samples followed the work of Courty et al. (1989) Blocks of sediment were collected from the three different areas inside and outside. These were encased in plaster or aluminum boxes kubiena-like, designed and produced at the University of Tübingen.

In area VOJ, the sampling strategy focused on the unit boundaries of the East and South walls. The collection was difficult because of the low compactness of the strata.

In area JCF, two samples were collected, one from the West profile and another from the South profile.

In area DMT a full column was collected from quadrant B in square MM98 and was divided into two block samples. The sediment blocks were transported to the Geoarchaeology working group laboratory of the Department of Geosciences at the University of Tübingen for processing and analysis.

Sediment monoliths were firstly air dried and stayed for several days in a heating muffle at 60o Celsius before impregnation with a mix of polyester resin diluted with styrene at a ratio of seven parts resin to three parts styrene, with methyl ethyl ketone peroxide (MEKP) added as a catalyst at about 7 mL MEKP to 1 L resin/styrene mixture. The resin was distributed through the sides of each sample and let to infiltrate slowly into the sediment, and then allowed to cure over several weeks. After hardening, the hardened monoliths (or slabs) were sliced into chips (single or multiple) using a diamond rock saw. These chips were then glued to 60x90x10 mm glass slides and ground to a thickness of 30µm. Thin sections were processed at the Laboratory of the Geoarchaeology working group of the University of Tübingen, with the exclusion of three samples which were polished and finished by Terrascope Laboratory, in France. External processing followed the same methods, but the glass is 5 mm thicker. A total of 16 thin sections were obtained for this study.

Thin sections were observed at a macroscale to identify the main sub-units visible in natural light. High-resolution scans of the thin sections were made using a Nikon digital film scanner (Nikon COOLSCAN 8000 ED). All thin sections were observed using a Zeiss polarizing petrographic microscope coupled with an Axio camera for microphotography available at the laboratory of the Geoarchaeology working group. Identification, description, and abundance estimations of individual components and aggregates were

made under plane-polarized light (PPL) and crossed-polarized light (XPL) using different magnifications (2 ×, 5 ×, 10 ×, 25 ×)

Micromorphological analysis was conducted for detailed observations and description of areas/features/inclusions using petrographic microscopy. Individual components, fabrics, and microstructures were identified, and described using the standard terminology in the discipline (Bullock, 1985; Courty et al., 1989; Cristiano. Nicosia and Stoops, 2017; Stoops, 2020, 2003; Stoops et al., 2018). Qualitative analysis of site formation processes, post-depositional patterns, and anthropogenic features was made considering the bibliography on the subject (Aldeias et al., 2014; Cañaveras et al., 2021; Goldberg, 2000; Goldberg and Sherwood, 2006; Karkanas and Goldberg, 2018a; Mallol and Mentzer, 2015; Mentzer, 2014; Morley and Goldberg, 2017; Nicoll and Zerboni, 2019; Cristiano Nicosia and Stoops, 2017; Sessa et al., 2019) and the comparative resources available at the reference collection of the Geoarchaeology working group of the University of Tübingen.

In addition to standard petrographic analysis, µ-Xray fluorescence (XRF) was used for qualitative assessment of elemental proprieties in the thin sections analyzed. Results were interpreted using the Bruker AXS software package Diffracplus Eva 10 (2003) for element identification and mapping, further integrated with the micromorphological analysis and interpretation.

4.2.2. Absolute dates

Sampling and dating protocols were applied to geological materials and sediments inside and outside of the cave. During excavation, bulk samples were collected every time the excavation of a new GU was initiated typically in quadrant C, except in squares where this is not possible. These loose samples have approximately 300gr and were collected using a trowel and spoon, avoiding contamination. Sediment samples from the excavation area were piece-plotted as single finds. The same was applied to block samples for micromorphology collected after the excavation and cleaning of profiles at the end of each season. Depending on the compactness of the targeted GUs or features collection was made using different tools. In sector 1 samples were mainly collected using knife, spatula, and plaster bandages, although, on a few occasions, a metal box (Kubiena box) was preferred for unconsolidated loose sediment. In sector, specifically in MM98, the collection of a column separated into two samples was made using a disc because it was the only way to efficiently overcome the hardness of the sediment. All other samples mainly targeted the contacts between stratigraphic units and/or features.

Block samples and geological references collected outside of the cave were mapped with GIS, photographed, and described individually. All sediment samples were always collected to document the site and excavation as part of the geoarchaeological approach or with prospects of absolute dating.

A three-pronged dating strategy relying on luminescence, uranium-thorium series, and radiocarbon was planned for the absolute dating of the cave infillings. The development of absolute dating methods such as luminescence, particularly Optically Stimulated Luminescence (OSL), and Uranium/Thorium series (U/Th-series) have strongly benefited fields of research on MSA sequences that fall beyond the limit of the radiocarbon (^{14}C) but some of these still show problems and are prone to error under the varying conditions of archaeological contexts and inherent limitations of each technique (Tribolo et al., 2013, 2005). For most of them, the successful application requires accurate reconstruction of sedimentary and diagenetic processes, temperature history, and groundwater action, which can only be obtained with high-resolution geoarchaeological approaches such as micromorphology. In this sense, samples for Optically stimulated luminescence (OSL) preferentially but not exclusively targeted the points of collection of block samples for micromorphology.

The IRAMAT-CRP2A laboratory in Bordeaux is fully equipped for performing TL and OSL dating on burnt lithics and quartz or feldspar grains extracted from sediments. Besides a dark room for sample preparation, it holds four Risoe single-grain luminescence readers, two Smart Lexsyg readers, and two Research Lexsyg readers for the determination of the equivalent doses. All are equipped with a 90 Sr-90Y beta source and there is a separate alpha (241Am) source. For the determination of the dose rate, the laboratory has three high-resolution gamma spectrometers to analyze dosimetry. Dosimetry was implanted in cave profiles 1 (L5-L4, south wall; MM98, east wall) in collaboration with Chantal Tribolo from the IRAMAT-CRP2A laboratory. Due to the pandemic, the collection of the dosimetry essential for the conclusion of the analysis is delayed and results from OSL on sediments and Electron spin resonance (ESR) on mammal teeth are not included in this dissertation.

For radiocarbon, samples with anthropogenic use (cut marks or burning) were selected among the faunal assemblage. Collagen screening was made at the Isotope laboratory of the University of Tübingen in collaboration with Dorothée Drucker and Hervé Bocherens. Four dry-sieved samples were sent to an external service at the University of Zurich, Switzerland. Results were calibrated and plotted with OxCal4.

5. Field results

5.1. Area VOJ

5.1.1. Stratigraphy

Area VOJ is located 8 m from the gate entrance to the cave. Access is horizontal and the environment inside is dry and dusty. Guano covers the walls and boulders of roof spall blocks are observed across the floors. Large monoliths are accumulated at the center of the channel and next to the western wall. Most of these boulders derive from a "hanging breccia", granular yellow muddy sediment when scrapped, while others are fragments of grey-blue dolomite.

The negative of a previous excavation was located next to the western wall of the cave having an approximate area of 1x1 m^2, and a depth of 0,7 m. The area showed recent disturbances, related to human and animal trampling. The excavation grid was established to intercross the old test-pit and refresh the profile, hence the y-axis of square L2 was established around 10 cm south of the pit. The first field season focused on squares L2 to L5 to obtain a section of the infill from the central axis of the cave to the western wall. In the 2019 fields season, the excavation was extended north focusing on the squares with a higher concentration of anthropogenic material but soon showed all the strata excavated in the area correlate to modern infills over large rockfall monoliths.

Squares L4 and L5 showed a higher frequency of archaeological material and at least two anthropogenic units, namely the mudbrick floor (GU2), overlying a "black layer" related to a combustion feature and rack-out spreading across the two squares. Plenty of lithics, plant remains, charcoal, heated bone shafts, and pottery were found to be likely related to a cooking area.

The interface between the Basal area of the combustion feature and the sediment was named GU4, which corresponds to a rubified region, overlaying a gravelly lense of angular bedrock debris (sub-unit 4.1) which seems to spread from the center of the cave (direction S-N) but can also relate to anthropogenic preparation of the surface for the hearths. Another sub-unit 4.2, was outlined to describe the rockfall and unsorted coarse-grained material, which may be coeval to GU5 but shows more mixture of coarse components derived from the "hanging breccia". This was interpreted as likely deriving

from a debris flow from the center of the cave and walls. These units are nonetheless obliterated by the excavation pit, causing some slumping of GU5 in square M4.

The sedimentary units excavated in Area VOJ were organized as follows:

GU1: Fine-grained crumby structure of grey sands and silts, organic-rich, poorly sorted, continuous with sharp wavy lower boundary. Few well-rounded aggregates of reddish, white, and yellow sands (>1 mm) can be observed by the naked eye. Fresh droplets of horseshoe bats inhabiting the cave, and arthropod exoskeletons are also observed on the floor. Dry sheep and cattle dung were observed;

GU2: Coarse-grained, crumby structure, orange-red sandy-clayey aggregates of construction debris, mixed with gravels and organic material, poorly sorted, parallel, discontinuous, non-compacted with erosional lower boundary. Components are mostly polyhedral sundried mudbrick, but also subrounded heated construction debris, mixed with coarse angular bedrock debris (dolostones, limestones, likely from the quarry and kiln construction), weakly imbricated and horizontally oriented, covering the area between squares L-M. Organic materials such as plant remains and charcoal were observed in low frequency (<10%);

GU3: Organic rich, lenticular structure, dark grey to black, silty-sandy, discontinuous, parallel, lightly compacted with clear lower boundary, associated with a hearth of ellipsoidal shape partially excavated. Poorly sorted, well-rounded red sandy aggregates can be observed by the naked eye, and appear heated. Abundant artifacts including charcoal, plant tissues, dung, burned bone, potsherds, and lithics were found with traces of heating across rows 4-5 and gradually decreasing towards the cave wall (rows 2-3);

GU4: Fine-grained, crumby structure, reddish brown to light brown, sandy-silty, continuous, inclined, with rubified regions, corresponding to the basal area of the hearth zone, gradual lower boundary. A sub-unit, 4.1, corresponds to a gravel lense mostly observed in square L5, with angular bedrock debris. Lithics, fauna, and plant remains were found randomly distributed and oriented. Pockets with rodent remains were observed suggesting burrowing. Sub-unit 4.2 presents the same characteristics but increased inclusion of coarser components and large boulders deriving from roof and wall, paraconformable contact with GU5. Clasts include angular debris of bedrock but also yellow and white silty-sandy aggregates deriving from the weathering of the

"hanging breccia". Ecofacts are less frequent towards the dripping line of the western wall;

GU5: Undulating stratum, crumby structure, grey, silty-sandy, moderately aggregated, poorly sorted, continuous, with black and white specks, gradual lower boundary. Coarse particles include mostly angular debris from cave roof spall, and anthropogenic materials (like lithics, potsherds, and charcoal) randomly distributed and oriented;

GU6: Undulating, weakly compacted unit covering the rockfall composed of light brown-grey fine sandy-silty, with occasional black and white staining. Coarse material includes unsorted angular cave debris, with few river pebbles, lithics, and potsherds. A sub-unit, 6.1., refers to burrow features, as it seems there is a network connecting with the surface, a higher concentration of smaller ecofacts, like plant fibers and fine charcoal, and pockets of microfauna including juvenile and adult rodent bones. Sub-unit 6.2 refers to the infill closer to the wall;

GU7: Rockfall unit, unsorted, inclined, discontinuous, sandy-silty yellow-white rounded aggregates from the weathering of the large blocks infill the voids between simple packing of monoliths and boulders of roof wall. Sub-unit 7.1 relates to the infill closer to the wall under the dripline, although there.

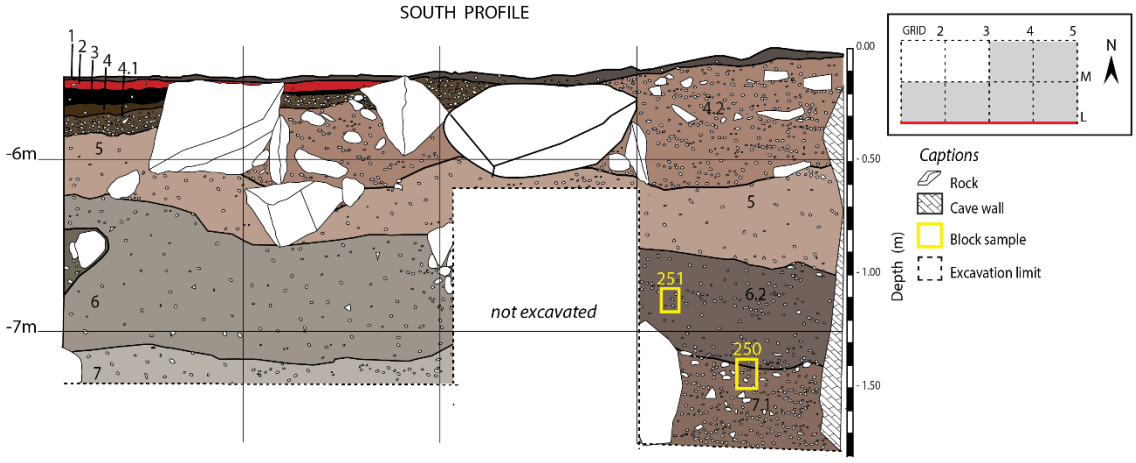

Fig. 12 – Schematic representation of the South profile in area VOJ.

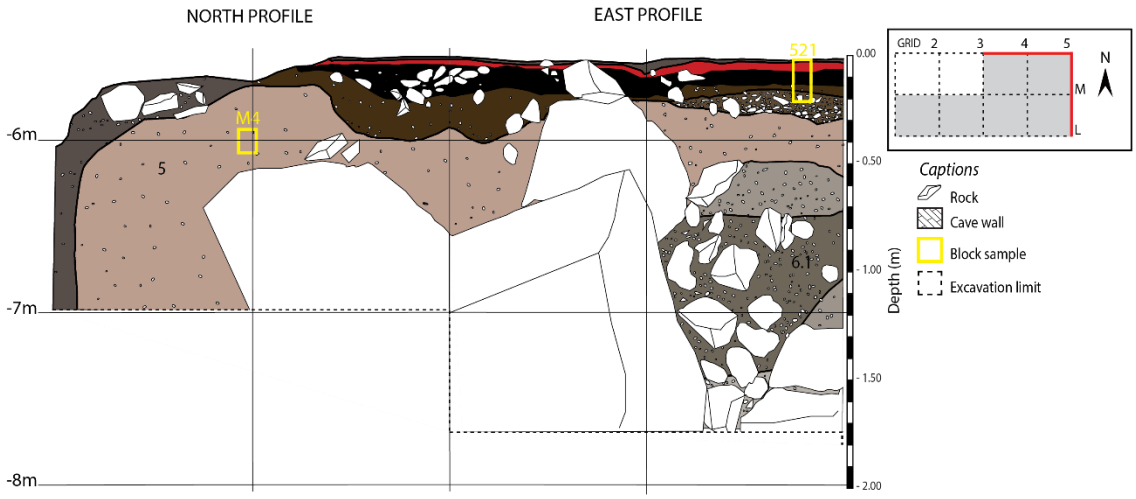

Fig. 13 – Schematic representation of the North and East profile in area VOJ.

GU	Thickness (cm)	Colour	Munsell	Description
1	1-2.5	Reddish grey	10R, 5/1	Fine-grained, loose, silty-sandy, humic with dung, clear wavy lower boundary
2	2-5	Red	10R, 5/8	Coarse-grained (gravels and red-orange sandy-clayey aggregates from construction debris) and few dung concentrated along the central axis of the cave (M/L5), moderately aggregated, abrupt lower boundary
3	5-10	Dark reddish grey	10R, 3/1	Fine-grained, organic, ash and charcoal rich unit associated with a hearth, abundant river-pebbles, lithic artifacts and burned bone, clear lower boundary
4	15-30	Very pale brown	10YR, 7/4	Coarse-grained, moderately aggregated, gradual lower boundary Sub-unit 4.1: gravel-sandy lense increasing thickness towards the wall, the unit is mostly concentrated along the southern profile of squares L5 and L4. Sub-unit 4.2:
5		Very pale brown	10YR, 7/3	Gravel-sandy-silty sediment, weakly aggregated, gradual lower boundary

6		Very pale brown	10YR, 8/2	Coarse-grained with few silts, moderately aggregated, gradual wavy lower boundary Sub-unit 6.1: sub-unit concentrations of microfauna, with organic fibers Sub-unit 6.2: gravel-sand with few organic components, under the dripline; lateral infill related to
7	>50	Light grey	10YR, 7/1	Rockfall monoliths and boulders Sub-unit 7.1: white-yellow laminations from hanging breccia and angular debris

Table 4 – Summary description of geological units of area VOJ.

5.1.2. Assemblages

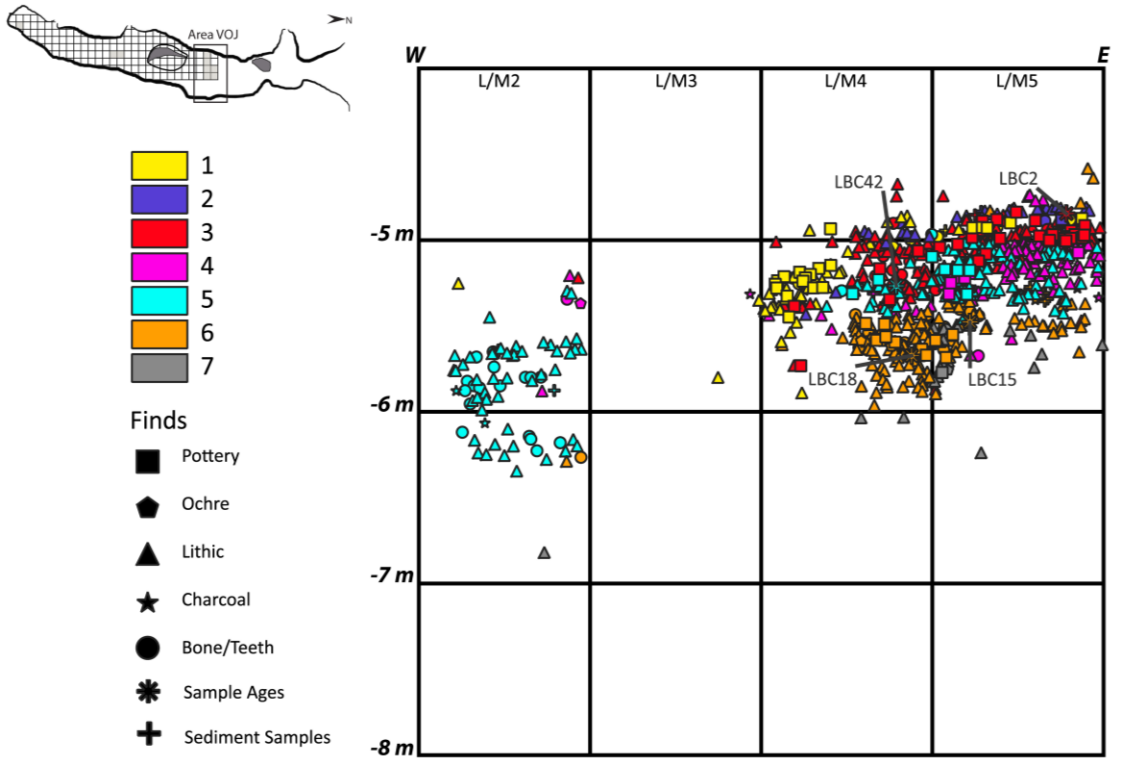

Fig. 14 – Point cloud for findings excavated in area DMT per GU with indication of samples for ^{14}C (LBC 2, 15, 18, 42). Note: 1) column 3 was left unexcavated after the removal of a large boulder with only onepoint refering to a lithic piece under the rock; 2) column 2 is where a previous excavation pit was located (possibly from the 1974 excavation by Oliveira Jorge).

4.1.2.1. Fauna

The faunal assemblages include skeletal remains from different biological groups: macromammals, micromammals, birds, arthropods, and gastropods. Detailed taxonomic lists can be found in Appendix 1.

Macromammals

The assemblage is mostly composed of bone shatter >5 cm found throughout the sequence decreasing frequency with depth. A total of 146 specimens were collected during the excavation. The vast majority are small bone fragments or flakes. Long bone shafts, teeth, and phalanges, are rare compared with other friable elements.

Taxon	NISP	%
Bovids		
Bov I/ II	2	1.4
Bov II	12	8.2
Springbuck (*Antidorcas marsupialis*)	3	2.1
Bov II/ III	15	10.3
Bov III	5	3.4
Bov III/IV	6	4.1
Bov IV	1	0.7
Indet. Bov.	13	8.9
Other ungulates		
Zebra (*Equus* cf. *quagga*)	2	1.4
Pig/ warthog (Cf. *Phacochoerus*/*Potamochoerus*)	1	0.7
Rodents		
Porcupine (*Hystrix africaeaustralis*)	4	2.7
Indet. Mammals		
Indet. Medium mammals	75	51.4
Indet. Small/ medium mammals	4	2.7
Indet. Small mammals	1	0.7
Total	**146**	**100**

Table 5 – General Inventory of macromammal taxons identified in area VOJ.

The fragmentary state of the assemblage contributes to a high percentage of unidentified taxa. In most cases, only size ranges or tribes were proposed. The highest frequency of elements is observed for medium-sized mammals (NISP= 51.4%).

The class of bovids represents 39% NISP of the assemblage and includes specimens of all size ranges. The elements are mostly concentrated in the combustion feature and GH4. The identification of three specimens of springbok (*Antidorcas marsupialis*) was only possible because of the presence of teeth elements. Other ungulates include an equid species, zebra (*Equus* cf. *quagga*), and suids, pig/warthog (*Phacochoerus*/ *Potamochoerus*). The porcupine (*Hystrix africaeaustralis*) is represented by four specimens in GU1 and GU6.

The species identified in VOJ assemblage are common in this region of southern Angola comparable with assemblages from the site previously described (Gautier, 1995).

Although populations in this area of the plateau are very depleted nowadays, wild game can still be found in areas with less human density and game reserves of Huíla province. The accumulations seem to relate almost exclusively to human activity.

Type of alterations	**NISP**	**%**
Alterations		
Fine cracks, some “open”	1	0.7
Chemical weathering	4	2.7
Staining	64	43.8
Abrasion	4	2.7
Bone covered or partially crusted with sediment	18	12.3
Total NISP	146	100
Gnawing		
Carnivore damage	8	9.8
Possibly carnivore damage	7	8.5
Rodent	8	9.8
	-	-
Total NISP*	82	100.0
Anthropogenic damage		
Burning damage	5	6.1
Possibly burning damage	1	1.2
Cut marks	2	2.4
Possibly cut marks	4	4.9
Scraping	-	-
Total NISP*	82	100

Table 6 – Frequencies of observed mechanical and chemical alterations, sediment crusts, gnawing, and anthropogenic damage in macromammal specimens recovered in area VOJ Leba Cave. (*) symbol indicates samples excluding tooth elements

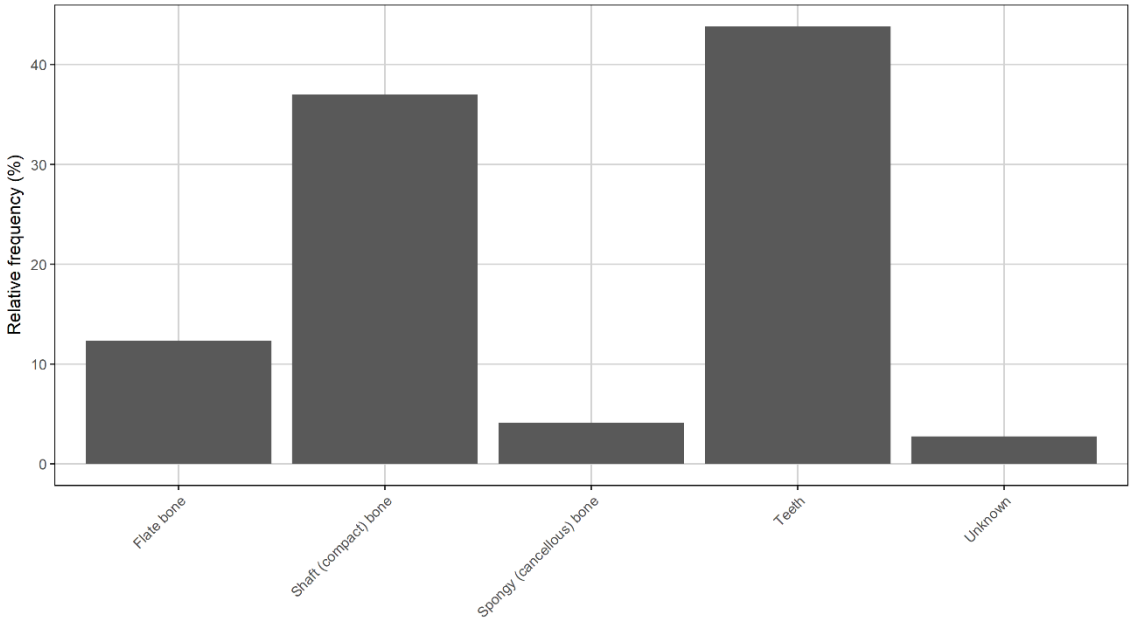

Fig. 15 – Abundance of bone tissue type in area VOJ.

Micromammals

Micromammal specimens are frequent in area VOJ where a total of 1301 specimens were identified and a minimal number of individuals (MNI) of 274 (Table 7). Taxonomic identification was possible for many of the finds (Appendix 1) provided by the frequency of diagnostic remains like maxilla and dental elements.

A total of 19 micromammal species were identified. Rodent species represent the vast majority of the micromammal assemblage (75.3%). The Muridae family yielded many of the fragments with a total of 152 specimens (MNI=42, 15.3%), and the Murinae subfamily with 194 specimens (MNI=46, 16.8%).

Shrews (14.6%) and gerbils (9.2%) are also importantly represented groups represented. They are more frequent in the upper units but they occur throughout the sequence of VOJ. Lagomorphs (*Pronolagus* sp.) are represented by a single specimen at the surface.

Taphonomic analysis was not extensively pursued but indicators of digestion were found in a few samples which may relate to predation of the barn owl, frequent interpretation for the southern African mammal record in cave sites, or by carnivores. Nevertheless, it can be assumed that these were mostly natural deaths and likely these species were living in the surroundings. The stratigraphy also showed important bioturbation agents burrowing inside the cave and adjacent fissures. For further prediction of the accumulation a detailed taphonomic study of the material is required.

The micromammal species observed can have restricted distributions in Angola depending on their favored habitat. Transitional conditions related to local factors like variability in altitude, climate, and vegetation impact the patchy distribution of certain endemic groups in the highlands. This is the case for the Cape Short-eared Gerbil (*Desmodillus auricularis*), Hairy-footed Gerbil (*Gerbillurus. paeba*), Black-tailed Tree Rat (*Thallomys nigricauda*), and the Striped Mouse (*Rhabdomys* sp.), whose dispersion is restricted to the southwest Angola.

In general, the identified taxa correlate with the current semi-arid biome prevalent in the plateau. All the species identified are associated with desert, arid or semi-arid habitats. Other recognized species as the Namaqua rock mouse (*Aethomys namaquensis*) or the Vlei rat (*Otomys* sp.) are naturally found in rocky areas and at higher altitudes. In general, it can be assumed, that all species were living at the site or its immediate vicinity.

The seasonal increase of moisture in the escarpment would transform some of the usually dry areas into an evergreen forest-woodland mosaic. The riverine conditions provided by the Leba valley and the permanent springs of Humpata would be favorable to the vlei rat (*Otomys* sp.), Tullberg's soft-furred mouse (*Praomys tullbergi*), and the greater dwarf shrew (*Suncus lixus*). Also, where of springs, marshes, and lakes of the plateau, habitats would be more suitable for species typically favoring locations with wetlands like the African marsh rat (*Dasymus incomtus*)

AREA VOJ – Taxon	**NISP**	**MNI**	**%**
Rodentia			
Muridae	152	42	15.3
Murinae	194	46	16.8
Aethomys namaquensis	23	5	1.8
Aethomys sp.	49	10	3.6
Cryptomys sp.	5	2	0.7
Dasymys incomtus	5	1	0.4
Hylomyscus sp.	9	2	0.7
Lemniscomys sp.	14	4	1.5
Mastomys natalensis	12	3	1.1
Mastomys sp.	32	10	3.6
Mus sp.	142	18	6.6
Oeonomys hypoxantos	3	1	0.4
Otomys sp.	252	40	14.6
Otomys cuanzensis	5	1	0.4

Praomys tullbergi	3	1	0.4
Praomys sp.	10	3	1.1
Rhabdomys pumilio	15	4	1.5
Saccostomus camprestris	11	3	1.1
Steatomys sp.	4	1	0.4
Thallomys nigricauda	18	4	1.5
Thallomys sp.	5	3	1.1
Zelotomys sp.	4	2	0.7
Gerbillidae	19	4	1.5
Gerbilliscus sp.	38	9	3.3
Desmodillus auricularis	14	4	1.5
Desmodillus sp.	2	2	0.7
Gerbillurus paeba	5	2	0.7
Tatera leucogaster	19	3	1.1
Tatera sp	7	1	0.4
Insectivora			
Macroscilidae	1	1	0.4
Atelerix sp.	1	1	0.4
Crocidura sp.	62	8	2.9
Elephantulus sp.	108	22	8
Suncus lixus	39	7	2.5
Sylvisorex megalura	9	1	0.4
Lagomorpha			
Leporidae	1	1	0.4
Sciuridae			
Heliosciurus gambianus	9	2	0.7
Grand total	1301	274	100

Table 7 – General Inventory of micrommammal taxons identified in area VOJ.

Birds

The bird specimens account for a total of 206 finds, including 168 identifiable elements. Birds were found throughout the sequence but decreased in frequency with depth (Appendix 1)

A total of 64% of the identifiable remains belong to the class of small and medium passerines. (NISP = 119; MNI = 13). The others were not possible to identify taxonomically but they are all small bird species considering the size of the quail/flufftail. The diversity of passerines and their similar morphology makes it impossible to attribute

the skeletal remains to one or several species in particular. The dimensions of the bones, however, illustrate the presence of at least two small and two medium passerine species. Other, non-passerine taxa include a small dove (number of bones = 9, representing at least two birds), one or several Piciformes of the barbet (*Lybiidae* sp.) and/or honeyguide (*Indicatoridae* sp.) families (NISP = 13; MNI = 5) and a small owlet (*Glaucidium/Otus* sp.; number of bones = 6 belonging to at least one bird).

No surface alterations were noted, as bones appear fresh and generally unfragmented. The bones do not show clear evidence of predator gnawing or acid etching. In the passerine assemblage, 82 remains (63%) are complete elements. The remaining bones preserve at least 75% of their original length, which confirms the low fragmentation rate.

Birds	**NISP**	**%**
Small passerines	75	36.4
Medium passerines	53	25.7
Non passerines (small)	15	7.3
Non passerines (medium)	20	9.7
Non passerines (large)	1	0.5
Non-identifiable material	37	18.0
Total	**206**	100.0

Table 8 – General inventory of bird size classes identified in area VOJ.

In the non-passerine sample (NISP = 37; MNI = 7), most bones (70%) are also complete or almost complete (30% with >75% of the bone preserved). In the bird assemblage, only two remains belong to juvenile individuals, and there is no element with medullary bone, which would indicate the presence of females inside the cave during the egg-laying phase.

No articulated elements were observed but there are several sets of antimeric bone (pairs of bones belonging to the same individual). Long bones dominate the birds' sample and elements from the wing (humeri, ulnae, and radii) and the leg (femora, tibiotarsi, and tarso-metatarsi) are equally represented. Cranial elements (beaks, skull fragments, quadrate bones, and dentary bone) are relatively well-represented (12% of the birds' sample). The combination of these skeletal and taphonomical features suggests the bone assemblage was accumulated naturally and there was limited movement of the bones in the sedimentary unit. Overall, the bird remains from Leba Cave belong to small passerines and other small bird species that likely occupied the cave and/or the cave entrance for roosting.

Other taxa

Gastropods were also recorded namely one specimen of *Achatina* sp. Arthropod remains include amblypygia and dung beetle exoskeletons (*Heliocopris* sp.), although rare and surficial findings.

4.1.2.2. Plant remains & others

Plant macro remains were collected during the excavation of area VOJ including materials such as leaves, tree wood, and bark. Wood charcoal was also collected from GU3. Many of these plant remains were found in aggregates of dry cattle dung (caprid and bovid). In the lower units, cells and other plant remains are found concentrated in channels burrowed by micromammals. Phytoliths were extracted from the bulk samples but are not part of this study.

4.1.2.3. Lithic Analysis

General Inventory

A total of 1776 lithic finds were collected. Cores represent only a small fraction of the assemblage with 75 pieces, 4.2%. Blanks represent the vast majority of the lithic assemblage. Main technological classes like flakes, blades, points, and bladelets represent the highest represented groups, accounting for a total of 992 finds.

Preparation and maintenance products include several elements associated with core rejuvenation and knapping platforms. These pieces include many core flanks (N=48) and fronts (N=21), bifacial thinning flakes (N=11), Debordant flakes (N=2), crest (N=7) and tablettes (N=3). Residual products like chips and other waste were observed in a total of 65 finds, less than 4% of the assemblage.

Formal tools were classified separately. Abundant lithic materials were found in VOJ mostly concentrated around the combustion feature, decreasing in frequency with depth. The high frequency of elements transported to the cave such as river pebbles and cobbles, many of which do not present any anthropogenic transformation or use-wear, were also accounted for. Of a total of 113 pieces, 6.4% of the assemblage are indeterminate fragments, consisting of natural debris.

Chunks and nodules account for 317 specimens in total, representing 17.7% of the assemblage, and include all blocks of raw material that showed less than three detachments and were not river pebbles or cobbles brought to the cave. Another class of manuports is the quartz crystals which could be used for tools or beads; artifacts that are frequently used by the modern population.

Class of artifact	N	%
Core	75	4.20%
Flake	920	51.80%
Blade	38	2.10%
Bladelet	3	0.20%
Point	31	1.70%
Burin Blow	2	0.10%
Bifacial thinning flake	11	0.60%
Debórdant	2	0.10%
Cornice	1	0.10%
Crest	7	0.40%
Tablette	3	0.20%
Flank	48	2.70%
Front	21	1.20%
Chip	18	1.00%
Waste	47	2.60%
River cobble	22	1.20%
River Pebble	77	4.30%
Crystal rock	22	1.20%
Chunk/nodule	315	17.70%
Indet. Fragment	113	6.40%
Total	**1776**	**100.00%**

Table 9 – General Inventory of lithic artifacts collected in area VOJ.

Raw materials

Raw materials were recorded in geological classes. Chert is the most frequent in the assemblage (50.1%, n=889), and frequency in all stratigraphic units shows an overriding preference for this type of raw material (Table 10, Fig. 16), followed by mudstone, quartzite, and milky quartz.

Cherts are naturally present in the Leba bedrock interbedded with dolomites and dolostones (Correia, 1976). In some areas of the Leba Valley, and likely also in the southern flank of the formation, the siliceous beds are overriding the carbonated features typically associated with karstic environments. Chert beds can be observed in surficial forms of the karst landscape like in pinnacles interstratified with stromatolites. In hand specimens, these cherts have colors ranging from dark-bluish grey to light grey, sometimes laminated and showing reddish striations. Knapped materials from these primary sources may have faces with a white thick cortex easily recognized by the typical bedrock cortex but also by their internal characteristics. The primary cherts observed frequently show impurities like mineral inclusions, voids, and fractures which may cause knapping accidents.

Raw material type	N	%
Chalcedony	2	0.1
Chert	889	50.1
Claystone	58	3.3
Dolerite	3	0.2
Granite	1	0.1
Hyaline quartz	23	1.3
Milky quartz	162	9.1
Mudstone	354	19.9
Non ident	2	0.1
Orthoquartzite	22	1.2
Quartzite	186	10.5
Sandstone	13	0.7
Shale	1	0.1
Wackestone	60	3.4
Total	**1776**	**100**

Table 10 – Frequency of raw materials in the VOJ assemblage.

Cherts can also be found in the form of water-worn cobles and pebbles on the Leba river banks. The terraces and river banks of rounded pebbles and cobbles provided naturally sorted blanks for the lithic technology. During torrential storms, these may be redistributed across the floodplains of the plateau but considering the elevation and distance of the cave mouth from the river valley it is clear that river clasts identified in VOJ were transported to the cave intentionally.

Quartzites and all other rocks identified in the assemblage like quartz, siltstone, mudstone, wackestone, and sandstone can be found in these deposits. In hand specimens, the quartzites can appear similar to the cherts in terms of color range but can be distinguished by their coarser particle size and lightly gritty surfaces when fractured. Orthoquartzites were also explored from river pebbles and cobbles for blanks and can be found in colors ranging from pale pink and grey. The remainder of the fine-grained siliceous rocks like the siltstones and mudstones present strong red and purple colors in hand specimens. These raw materials have been previously classified as silcrete (de Matos and Pereira, 2020), a raw material that might be found on the western plateau scarp, at about 1000 m of altitude, but rather infrequently observed in cobble beaches. A closer look into the compositional variability of the so-called Chela "volcano-clastic" rocks is beyond the scope of this macroscopic analysis but could improve the understanding of local raw material types and sources. Plenty of pieces classified as "chert" due to their conchoidal fracture may well be very fine-grained quartzites or silicified argillites, mudstones, and wackestones.

Milky quartz can be found as water-worn pebbles likely from colluvium deposits of the slopes and weathering of the conglomerate units intercalating with the quartzites outcropping on the northern margin of the river valley. In the assemblage, there are quartz blanks showing one or more water-worn faces, as well as hammerstones and non-modified river pebbles transported to the cave. Quartz veins can be observed in different areas of the plateau. Hyaline quartz can be found in primary sources on the scarp about 2,5 km northwest of the cave close to the Bimbe hills. It can also be found outcropping as veins in the Cangalongue and Humpata Members of the Chela Group, underlying the dolomites. Non-formatted crystal rocks have been identified in the assemblage.

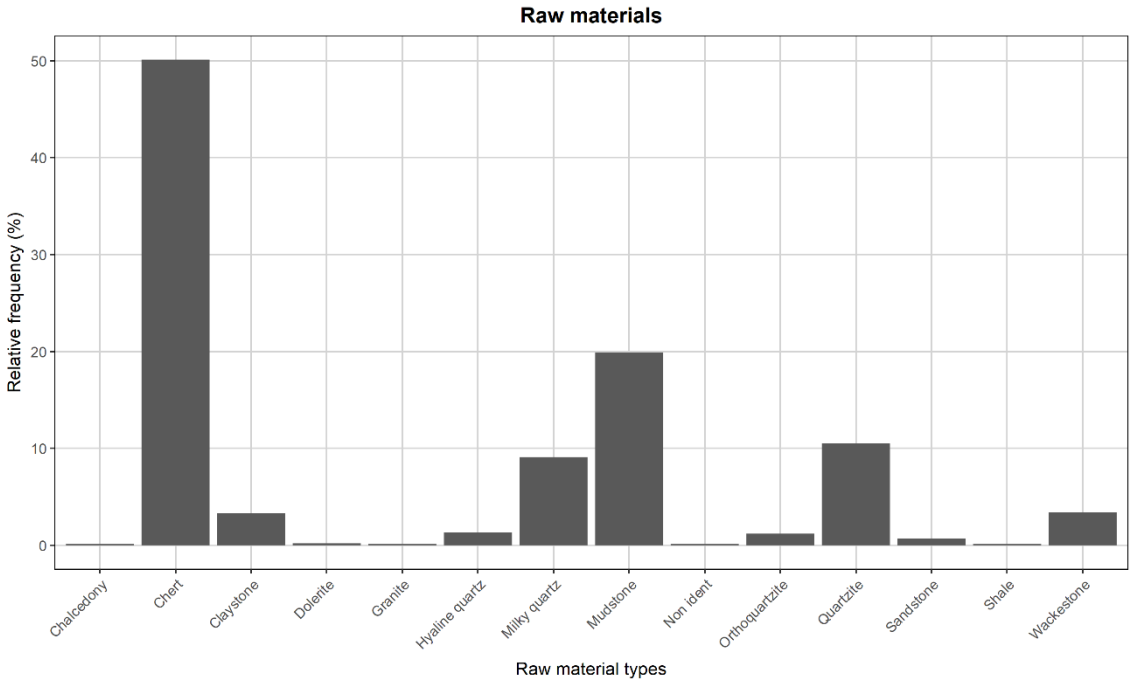

Fig. 16 – Bar plot for relative frequency of raw materials in the assemblage.

Dolerite is also available in the plateau and occasionally found in the river banks or colluvial deposits at the hillslopes. Dolerite sills are intrusive to the Chela Group and outcrops can be found less than 1 km west of the cave. This raw material has a residual representation in the assemblage.

Surface alterations

Geogenic and anthropogenic alterations observed in the surfaces of the lithic artifacts were recorded for each lithic find. The majority of the lithic finds appeared fresh and didn't show particular alterations of the surfaces in 61.7% % of the pieces analyzed Plenty of materials showed carbonate cements and or crystal concretions independently of find class. A total of 12% of the assemblage showed mixed features, like carbonates and burning (Table 11). Materials with fire marks usually showed more than one glossy face

and were concentrated around the hearths. About 1% of the blanks seemed like they were heated at high temperatures showing dull surfaces, and complete alteration of the mineral structure. Only 21.7% of the blanks showed fire marks among 1702 pieces and very few cores showed the same alterations.

Alterations	**Blank**	**%**	**Core**	**%**	**Total**	**%**
Heating	16	0.9			16	0.9
Concretions	215	12.1	8	0.5	223	12.6
Mixed	213	12			213	12
Patina	209	11.8	8	0.5	217	12.2
Rolled	11	0.6	1	0.1	12	0.7
None	1038	58.4	57	3.2	1095	61.7
Total	**1702**	**95.8**	**74**	**4.2**	**1776**	**100**
Fire marks	**Blank**	%	**Core**	%	**Total**	%
Yes	386	21.7	9	0.5	395	22.2
No	1316	74.1	65	3.7	1381	77.8
Total	**1702**	**95.8**	**74**	**4.2**	**1776**	**100**

Table 11 – Frequency of blanks and cores with surface alterations and presence of fire marks from area VOJ.

Technological classes

Detailed analysis of morphological attributes and metric analysis of flakes, points, blades, and bladelets is presented in Appendix 2.

Flakes account for the vast majority of knapping products with a total of 920 pieces 92.7% of the assemblage. About half of the flakes are complete. Pieces with broken tips represent 6% of the assemblage. Proximal fragments preserve only the platforms 9.2% of the assemblage. Distal fractions preserving the tips are a total of 101 pieces, 10.2%. Mesial fragments are a total of 106 pieces which represent 10.7% of the class of flakes. The presence of cortex is not frequent, when it occurs it is more often water worn, occurring in a total of 111 pieces, 11.2% of the flakes. A thick powdery cortex is present in 73 pieces corresponding to 7.4% of the assemblage. More often cortex is present in less than 25% of the find.

Cortical platforms were observed in 91 pieces, corresponding to 9.2% of the assemblage. Flat platforms were the most frequently observed with 412 specimens representing 41.5% of the assemblage. Dihedral platforms were observed in 60 pieces which represent 6% of the finds. Punctiform, smashed, and removed platforms were also observed in similar frequencies. Burinated platforms were observed in 6 pieces, 0.6%. Other preparation features of flake butts were occasionally observed, in about 17% of

the pieces. These included lateral notches, frontal retouches, and chipping, frequently with associated abrasion marks.

Morphological features like sections and profiles were also recorded. Triangular and trapezoidal are the most frequent, with 27.4% (N=272) and 28.2%(N=280) respectively. Other shapes were found in 2.7% of the pieces. Flake profile is more frequently straight with 46.4% (N=460) in 6.6% (N=65) of cases the profile is arched and in 2.2% (N=22) of the pieces profile is twisted. Among the flakes showing preserved length for edge identification, the majority showed divergent edges with 13.5%(N=134) of the assemblage irregular edges with 8.2% (N=81). Biconvex and convergent edges or observed in similar frequencies at 5.3% and 4.8%, respectively. Convex-concave edges were also observed in 2.6% of 26 pieces and circular edges in 1.8% of the assemblage. Description of the flake tips shows the most frequent pattern is thick with 183 pieces representing 18.4% of the assemblage. A feathered tip pattern was observed in 122 pieces representing 12.3% of the assemblage. Fractured pointed tips were observed in similar frequencies with 7.6%(N=75) and 7.1%(N=70). A retouched tip was observed in 10 flakes.

Although about half of the flake assemblage was not complete to allow reconstruction of its morphology, a total of 205 pieces, representing 20.7% of the knapping products showed radial/centripetal dorsal patterns. Unidirectional detachment patterns were observed in 17% of the cases, mostly unidirectional-convergent patterns (N= 61, 6.1%), but also unidirectional-parallel (N=54, 5.4%) and a few pieces with unidirectional-opposed-fracture (N=4, 0.4%). In about 5% of the pieces, a unidirectional-indeterminate pattern was observed (N=50).

Blades account for a total of 38 pieces, representing 3.8% of the assemblage. Most blades are not fragmented (N=20). They also do not present cortex in most cases (N=35). Blade platforms are more frequently flat (N=14) there are also a few dihedrals, cortical, smashed, and punctiform types in the assemblage. Preparation with chipping of the basal region was only observed in one blade.

Fig. 17 – A-J: Flakes in local cherts and quartzites; L-P, S: pseudo-Levallois flakes; Q-R: bladelets; T: blade (knife?)

Fig. 18 – Flakes in mudstone and wackestones from river pebbles.

Fig. 19 – Flakes in milky quartz.

Fig. 20 – "Pseudo-Levallois" points and points with fragmented tips in mudstone and wackestone (first to third row), ortoquartzite, chert, wackestone and mudstone (lower row)

The blade sections are more frequently trapezoidal (N=22, 2.2%) and occasionally triangular (N=8). Profiles are mostly straight (N=25) and only in a few cases arched (N=5). The blade edges are generally parallel (N=21) but convex-concave, irregular, and divergent edges were observed in a few pieces. The tip pattern was more often thick, but fractured or pointed tips were also observed. Dorsal patterns observed are mostly unidirectional-parallel in 1.7% of the pieces (N=17). A radial/centripetal pattern was observed in a few cases (N=4, 0.4%).

The class of points occurs in a similar frequency as the blades. A total of 31 pieces were identified, from which 23 are complete, consisting of 2.3% of the knapping products. A few pieces are almost complete (N=3, 0.3%) show the tip or part of the butt fractured, or

were fractured in the middle, and consist of proximal (N=4) and distal (N=1) fragments. Platforms observed were mostly flat, consisting of 1.7% of the products (N=17), but also faceted (N=7, 0.7%) and dihedral (N=3, 0.3%). Frontal retouches were observed in one of the points. Only one piece presented cortical butt, and in the other two cases, this was smashed and removed. The sections observed were generally triangular and occasionally trapezoidal. Profiles are straight (N=18, 1.8%), and in a few cases twisted (N=2, 0.2%). By definition, points have convergent edges, but in rare cases, circular and convex-concave edges were also observed. Dorsal patterns are more frequently unidirectional-convergent (N=19, 1.9%) and radial/centripetal (N=6, 0.6%).

Bladelets are residual elements in the assemblage since only three pieces were recognized in hyaline quartz and chert. Only one piece was complete, and the two striking platforms observed showed a flat and a dihedral shape. The complete piece showed parallel edges and a pointed tip.

Cores represent only 4.2% of the assemblage, with 75 specimens. From these pieces a total of 52 were complete. The cores identified were mainly chert, wackestone, mudstone, and siltstone. Cortex was identified in more than 50% of the cores, as 26.9% showed a thick cortex and in 25% of the pieces a water-worn cortex associated with the knapping of the river pebble-cobbles.

The vast majority of the complete cores showed predetermined knapping strategies, corresponding to 75% of the cores. Prismatic cores were observed more frequently, representing 21.2% of the cores. Levallois and polyhedral cores were observed in similar frequencies with 9 pieces respectively, 17.3% of the core assemblage. Levallois preferential cores are more abundant (N=6) compared with Levallois recurrent methods (N=3). Radial knapping concepts were observed with centripetal, convergent, and discoidal methods applied in a few flakes.

Analysis of morphological attributes of the several technological classes emphasizes the use of prepared cores for the debitage of different products. Reduction aimed at obtaining mainly triangular and square flakes, but also just the goal of obtaining a pointed edge. Many elements corresponding to the "pseudo-Levallois" morphology are associated with discoid knapping methods. Direct percussion using a hard hammer is the norm. For bipolar knapping, a hard surface or groundstone would have been used to stabilize the core and control the flaking of small quartz and chert cores.

Core typology	N	%
Intensive	***11***	***21.20%***
Not organized	9	17.30%
Disconnected	8	15.40%
Two opposed poles	1	1.90%
Organized	**2**	3.80%
Three poles	1	1.90%
Two alternate poles	1	1.90%
Predetermined	***39***	***75.00%***
Bipolar	5	9.60%
Multipolar	1	1.90%
Two opposed poles	4	7.70%
Levallois	9	17.30%
Preferential	6	11.50%
Recurrent	3	5.80%
Polyhedral	9	17.30%
Multipolar	8	15.40%
Two opposed poles	1	1.90%
Prismatic	11	21.20%
Multipolar	1	1.90%
Two opposed poles	3	5.80%
Unipolar	6	11.50%
Two poles	1	1.90%
Radial	5	9.60%
Centripetal	2	3.80%
Convergent	2	3.80%
Discoidal	1	1.90%
Extensive	*2*	***3.80%***
Not organized	2	3.80%
Multipolar	2	3.80%
Total	**52**	***100.00%***

Table 12 – Core typology based on complete cores considering Exploitation (Extensive, Intensive, Pre-determinate); Concept and Method.

Metric analysis

asic metric variables for technological classes (flakes, points, blades, and cores) are presented in Table 13 and Fig. 21-Fig. 23. Measurements collected show that the different technological classes have similar distributions. Length mean values range from 45 to 55 mm. Length mode values from flakes, blades, and cores show very similar values and some degree of regularity in the assemblage. As already hinted by the core types, reduction sequences are mainly focused on intensive strategies producing implements smaller than 100 cm.

Nonetheless, the distributions show a few outliers in each technological class (Fig. 21).

Attr/Class	FLAKES		BLADES		POINTS		CORES	
Length	Mean	45	Mean	50	Mean	52	Mean	55
	Median	42	Median	47	Median	54	Median	52
	Mode	40	Mode	47	Mode	66	Mode	40
Breadth	Mean	36	Mean	28	Mean	34	Mean	44
	Median	34	Median	28	Median	33	Median	41
	Mode	29	Mode	39	Mode	32	Mode	31
Thickness	Mean	13	Mean	12	Mean	10	Mean	30
	Median	11	Median	10	Median	10	Median	27
	Mode	10	Mode	10	Mode	8	Mode	23

Table 13 – Mean, Median and Mode values for metric attributes (in cm) for complete flakes, blades, points and cores of area VOJ.

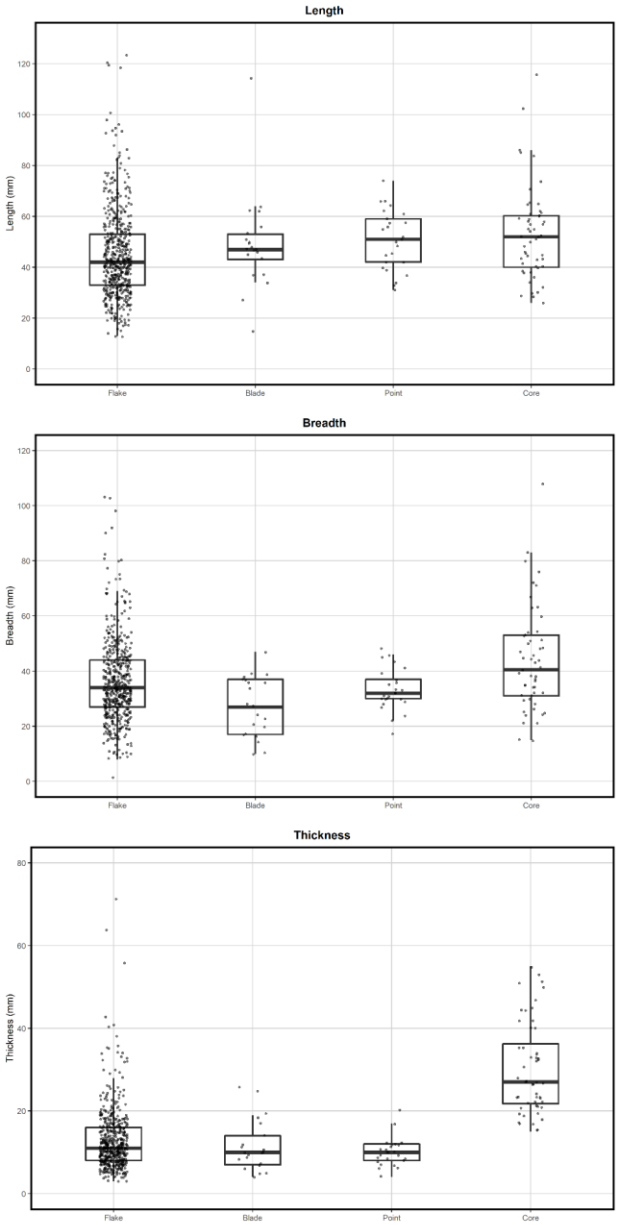

Fig. 21 – Box plot and distribution of flake, blade, point and core metrics (top to bottom, length, breadth, thickness)

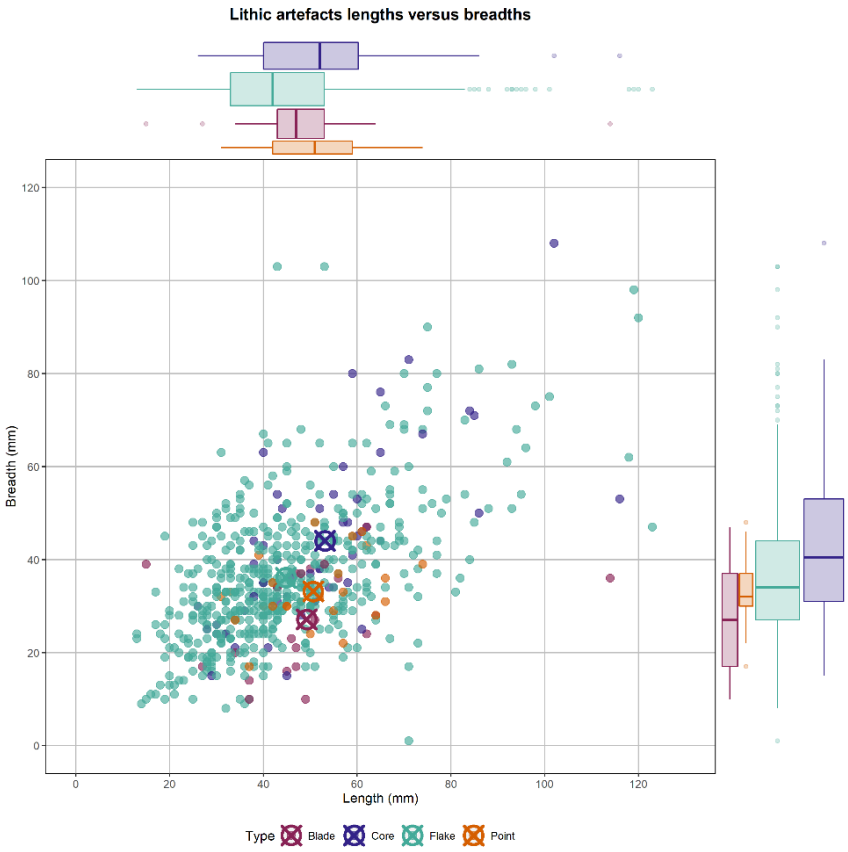

Fig. 22 – Scatter plot for length vs breadths in complete pieces from area VOJ

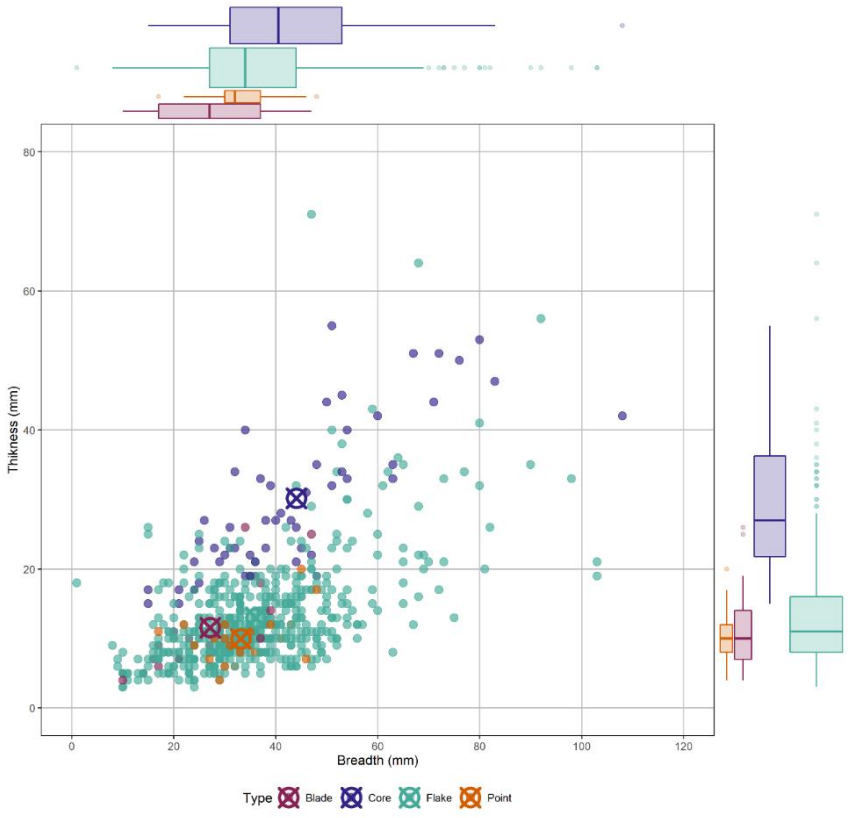

Fig. 23 – Scatter plot for length vs thickness in complete pieces from area VOJ

Formal tools

Typological categories were ascribed to retouched pieces or elements with macro use wear and indications of anthropogenic activity. Retouched pieces are generally rare in the lithic assemblage from area VOJ. A total of 21.4% are manuports, mostly river pebbles and cobbles transported inside the cave. Pieces with macro-use wear (Fig. 25) are also river clasts which were used mostly as hammerstones, and occasionally as polishers. Large cobbles of quartzite and sandstone were also observed with traces of use as grinding stones and groundstones. A fragment of a rounded bored stone in a quartzite pebble was also identified (Fig. 26).

Large cutting tools from extensive knapping reduction strategies were identified in very low frequencies. Two picks were identified as well as fragments of possible cleavers and handaxes. The volumes used for the large cutting tools were river cobbles of quartzite and mudstones. For handaxes and cleavers, in two cases two flakes extracted from these cobbles were used to shape the final core tool, but showing water-worn faces.

Debitage with retouched edges was observed presenting marginal retouches. Retouched flakes represent 19.9% (N=67) and blades 10.7% (N=37). Retouched points consist of 1.8% of the tools and show similar patterns. The vast majority of the retouched flakes and points were Levallois products.

Scrapers are about 11% of tool assemblage with several types represented. Classification derives from the working edge position and morphologies observed in retouch. Sidescrapers were more frequently observed showing retouches along one edge of the flake. Thick endscrapers are thick flakes showing a retouched tip. Retouch can also partially cover the dorsal surface; these consist of 3.7% (N=10). Other types were only occasionally observed such as transverse scraper (N=2, 0.7%), endscraper (N=2, 0.7%), circular scraper (N=1, 0.4%); and ventral scraper (N=1, 0.4%)

Splintered pieces correspond to 13.6% of the tools. The vast majority of these pieces were in quartz, mostly milky or vein quartz collected in tablets, but also a crystal of hyaline quartz. A few of these splintered pieces were also identified in chert (N=3) and mudstone (N=2) chunks/nodules.

Notches were also frequently observed representing 6.6% (N=18) of the formal tools. Burins were also detected. These are mostly dihedral burins but there are also transverse types in the assemblage. Other tools such as denticulates and mixed pieces like the flake cores or the burin-scraper were also recorded in the assemblage. Two duck-billed tools were also identified.

Tool	N	%
Retouched flake	67	19.90%
Retouched blade	36	10.70%
Retouched point	7	2.10%
Knife	3	0.90%
Borer-scraper	1	0.30%
Dihedral burin	16	4.80%
Burin-notch	1	0.30%
Denticulate	3	0.90%
Notch	18	5.40%
Flake-core	3	0.90%
Geometric (Crescent)?	1	0.30%
Borer	3	0.90%
Sidescraper	30	8.90%
Endscraper	2	0.60%
Circular scraper	1	0.30%
Transverse scraper	2	0.60%
Ventral Scraper	1	0.30%
Splintered piece	37	11.00%
Duck billed tool	2	0.60%
Pick	2	0.60%
Handaxe	2	0.60%
Cleaver?	1	0.30%
Cleaver	1	0.30%
Groundstone	8	2.40%
Grinding stone	1	0.30%
Hammerstone/Polisher	1	0.30%
Hammerstone	8	2.40%
Bored Stone	1	0.30%
Manuport/Fire stone	5	1.50%
Manuport	72	21.40%
Total	**336**	**100.00%**

Table 14 – Formal tools

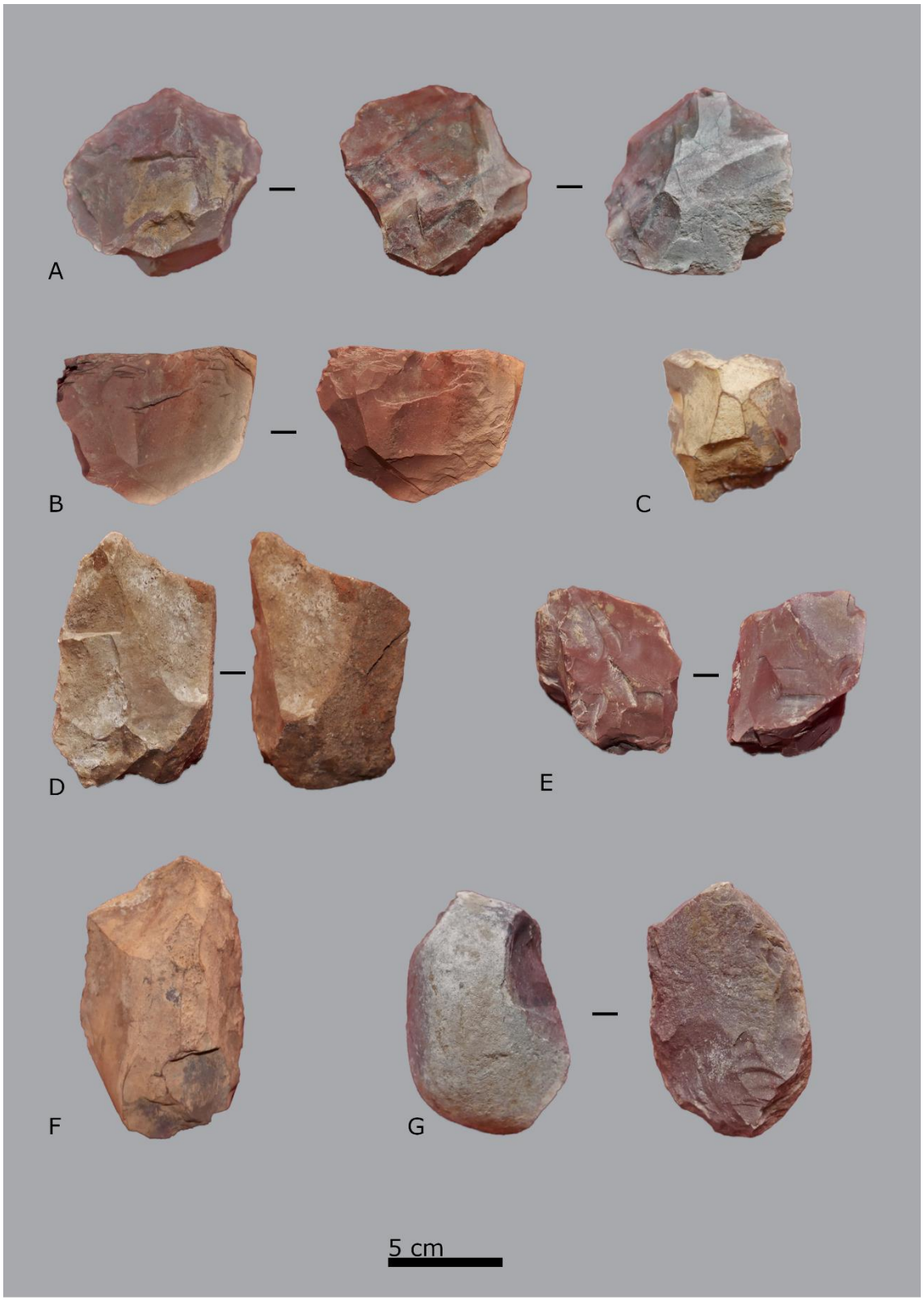

Table 15 – A. polyedral core with pebble cortex; B: prismatic core, C: thick scraper

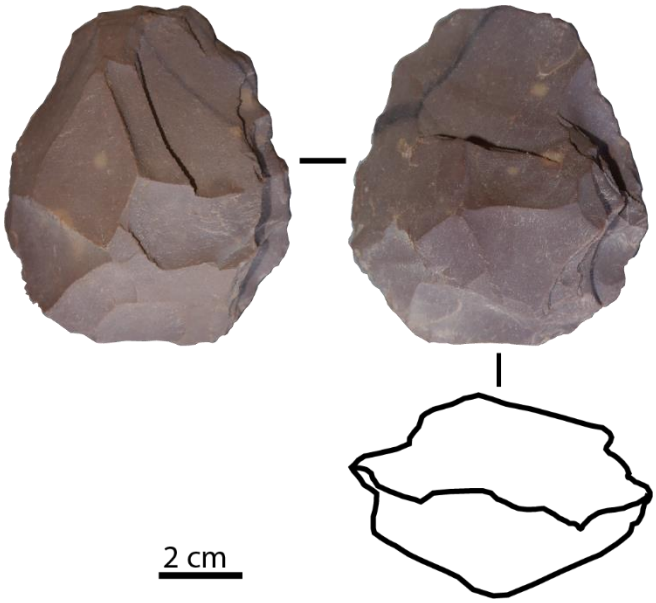

Fig. 24 – Thick core on quartzite river pebble.

Fig. 25 – Hammerstones and grind stones on quartzite river pebbles from area VOJ

.

Fig. 26 – Fragment of bored stone in purple mudstone from area VOJ.

4.1.2.4. Pottery & others

Type	Total
Construction material/red earth brick	104
Potsherds	272
Decorated/rim fragments	10
Bead preform	1
Metals (iron)	3

Table 16 – Absolute frequency of ceramic finds and other materials from area VOJ.

Ceramic materials found at Leba Cave include fragments of pottery vessels, angular mudbrick fragments, and sandy-clayey construction aggregates like "daga" used in traditional housing.

A total of 282 potsherds were collected in area VOJ (Table 16). The vast majority were undecorated potsherds, too small to allow reconstruction of their morphology. The pottery fragments observed were manufactured using fine red-brown fraction and quartzite tamper. Non-plastic composition is characterized by crushed coarse sands and granules. Potsherds were collected from all geological units but their frequency decreased with depth. Decorated and rim fragments account for about 3% of the potsherd assemblage and were mostly concentrated around the hearth likely relate to a few vessels used for cooking.

The decorated pottery shows incised geometric designs likely triangles with variations. Many of the incisions are likely bands of herringbone (Fig. 27, A-H), elements typically classified as Class 1 in African ceramic studies (Denbow, 2013). The characteristics of this series of potsherds relate to decorations and types found in the EIA assemblages of Angola, for instance, site Cabolombo, Benfica Bay, south of Luanda (Ervedosa, 1980). The potsherds showing superimposed cross-hatching (Fig. 27, C, F-G) are typically observed in the Kay Ladio Group of the Lower Congo Basin (Clist, person. Comm).

Other cultural remains found at the site include a few metal objects, mostly indeterminate, and a bead preform (Fig. 28).

Oxides chunks, hematite, or possible ochre aggregates, were also collected during excavation but it is unclear whether they are by-products of anthropogenic processes or rather geogenic components.

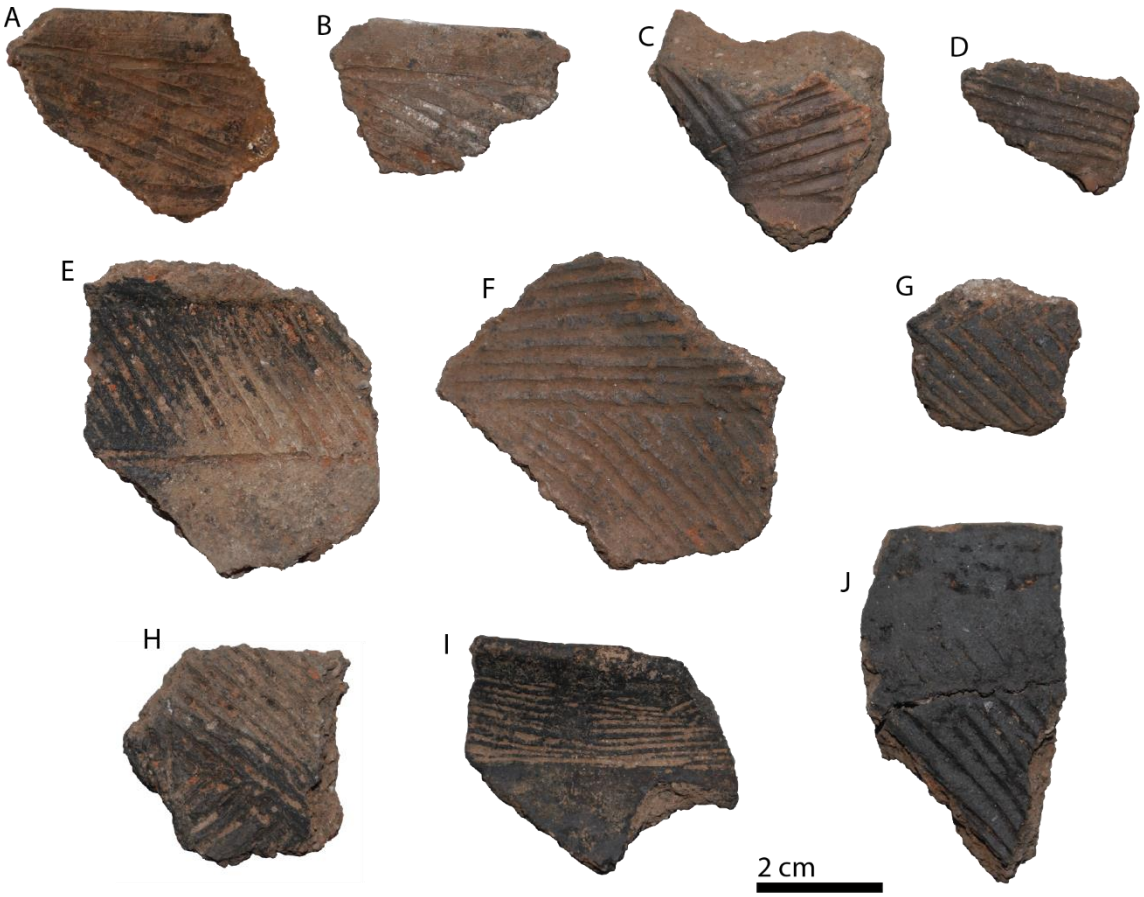

Fig. 27 – Decorated potsherds found in the combustion feature of VOJ-GU3 (A-I) and GU 6.1. (J).

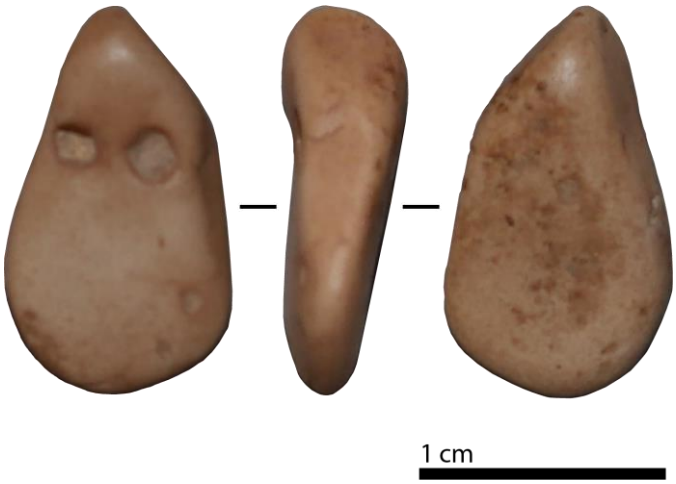

Fig. 28 – Bead with unfinished double perforation.

5.2. Trench JCF

5.2.1. Stratigraphy

Area JCF is located in the middle of the phreatic tube approximately 25 m from the entrance after the narrow channel (0.5 m width) between the eastern wall of the cave and the cluster of boulders form breccia and roof spall at the center of the cave channel. The debris creates a very narrow passage between the entrance gallery and the back of the cave, impeding any sunlight from reaching the southern part of the cave.

Bat roosting was most frequent in this particular area, where the irregularities of wall and ceiling, as well as the "bell holes" provide a safe place for horseshoe bats during daytime. Organic materials like wood bark and charcoal, porcupine quails, and dung were found scattered across the cave floor suggesting recent trampling and use of the cave. Throughout several visits to the site, it was noticed that the area became puddled during the rainy season.

A negative of a previous excavation was located right after the narrow passage, in the middle of the chamber. A square with approximately 1,20 m^2 and 0.6 cm of depth was filled with recent debris. Many rounded river clasts were found at the surface of the pit with burning traces. The team proceeded with a profile-cleaning intervention by the end of the 2019 field season. The goal was to clean the modern debris in the old pit, and at the same time assess and prepare the area for the following field season.

The profile observed showed the surficial dark-brown sediment with guano overlayed a sedimentary unit of light grey to white sands with red sandy-clayey laminations,

increasingly thicker and dipping towards the north. The sediment appeared leached due to the dripping/puddling but was also disturbed by the recent activity, with a more granular structure and weakly aggregated. HCl tests with sediment samples did not show any chemical reaction, hence no calcium appeared to be present. The upper boundary is sharp slightly diffuse towards the north, and following the morphology of the old test pit which seems to indicate increased diagenesis since the exposure.

The units below were considerably more compacted with a sub-angular blocky structure, showing a gradual change from yellow to red. In the south profile (Fig. 29-Fig. 30) a fissure was observed crossing the profile which can be promoted by dissolution processes occurring below. Pedofeatures are visible to the naked eye, with mottled regions and concentrations of iron oxides, indicating hydromorphic conditions causing lateral and downward variations in color.

At the base of the unit, a gravel lense composed of pebble-sized angular bedrock debris is horizontally distributed and encased in red mud. A sharp erosional boundary separates the red mud from a highly compacted lower yellow sandy-silty unit. The intervention was interrupted at that point for drawing and collection of sediment samples.

Seven geological units were outlined and described in the profile (Table 16 – Summary description of geological units of area JCF.Table 16 – Summary description of geological units of area JCF.Table 16):

GU1: Fine-grained, silty, grey, undulating, parallel with granular structure; the surface unit covers the chamber and infills the excavation trench of Camarate-França. River pebbles were found at the bottom of the test pit with burning marks, possibly indicating recent use of the pit for a hearth, but organic material is rare, but organic material was not present.

GU2: Disturbed/Altered region, fine sandy grey-white laminae with red zones (bleached zone?), inclined, undulating, erosional lower boundary. The area represented in the profile shows lateral recent hydromorphic disturbance (Fig. 29) related to the exposure.

GU3: Sandy-clayey, yellow-red, mottled region (white to orange), lateral and downward variation color, highly aggregated, moderately indurated. Oxide nodules, sharp lower boundary;

GU4: Sandy-clayey, light red, gradual lower boundary;

GU5: Clast-supported sandy-clayey matrix, red, undulating, parallel, imbricated, very compacted, sedimentary breccia composed of moderately sorted angular bedrock debris, imbricated, randomly oriented, and parallel distributed, sharp lower boundary;

GU6: Fine-grained, sandy-clayey, angular blocky structure, very compacted, with smooth-walled round channels (<1 cm diameter)) with oxide nodules, erosional lower boundary;

GU7: Silty-sandy, yellow, granular structure, compacted, few angular bedrock clasts.

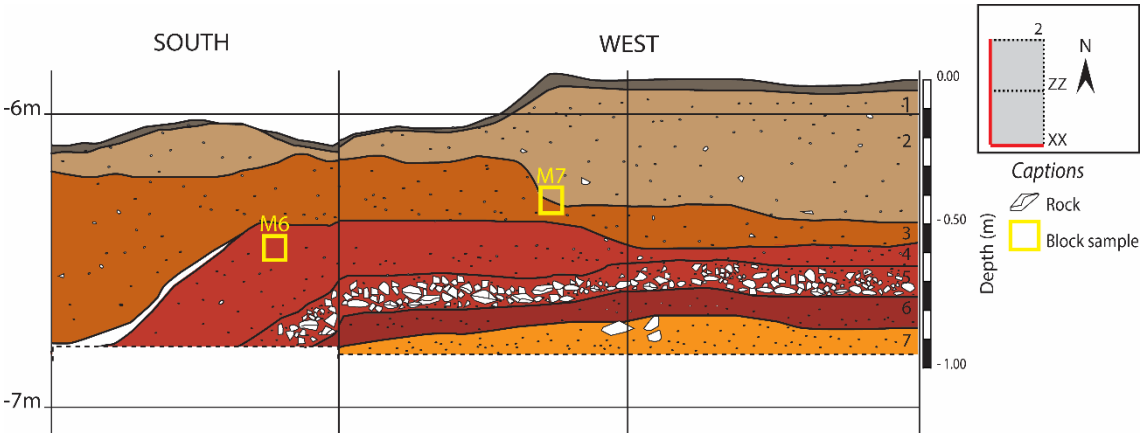

Fig. 29 – Schematic representation of the profile of JCF area.

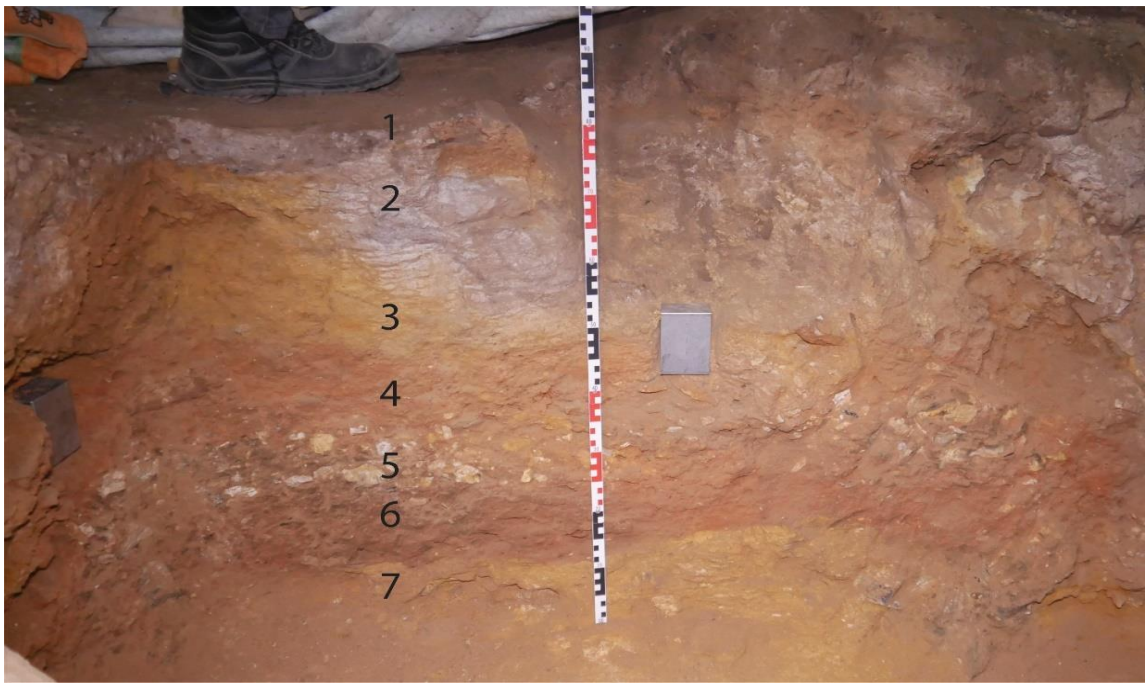

Fig. 30 – Profile exposed in area JCF with reference to GUs.

GU	Thickness (cm)	Colour	Munsell	Description
1	5-20	Reddish grey	10R, 5/1	Fine-grained, loose, silty-sandy with guano, clear wavy lower boundary
2	10-40	Light grey-red	10R, 7/1	Coarse-grained, granular, with sandy-clayey lenses and abundant sub-angular bedrock clasts, weak to moderately aggregated, gradual lower boundary with moderate mottling
3	10-30	Yellow red	5YR, 5/8	Matrix-supported, fine-grained, sandy-clayey, blocky texture, with angular cave debris, lateral and downward color variation, highly aggregated, difuse lower boundary
4	6	Red	10R, 5/8	Matrix-supported, fine-grained, sandy-clayey, blocky texture, clear lower boundary
5	10	Dark red	10R, 3/6	Clast-supported, sandy-clayey, granular texture, with Fe/Mn crusts in coarse grains, clear lower boundary
6	10	Dark red	10R, 3/6-3-/4	Matrix-supported, fine-grained, sandy-clayey, blocky texture, sharp lower boundary
7	7	Yellow	7.5YR, 7/8	Silty-sandy, granular texture, compacted

Table 17 – Summary description of geological units of area JCF.

5.2.2. Assemblages

4.3.3.1. Lithics

The lithics found in the modern infill (post-1950 AD) of the JCF trench were only a few and showed traces of heating and in some cases macro-use wear as a hammer- or grinding stones. A total of 23 cobbles were recorded at the surface during the cleaning of the pit. GU2 yielded two cortical flakes in chert and a small polyhedral core in milky quartz. GU3 to 6 did not yield any artifacts.

At the base of the JCF trench, at the top of GU7, an almond-shaped handaxe with rounded basal shaping was found with the tip dipping obliquely oriented. The handaxe was crusted by silty-sandy yellow sediment difficult to clean.

The handaxe was manufactured using a river cobble and shows the typical water-worn surface in the basal area (Fig. 31). The raw material is a red mudstone with grey-blue laminations of quartzite likely prevenient from a local source, since these are widely present across the the river valley. The blank was shaped using a soft hammer and indirect percussion, finalized with continuous marginal retouches to form a rounded cutting edge. In Bordes (1961) classification scheme, the tool classified as lanceolate biface. The morphology is frequently associated to later Acheulean tool kits or ealy Middle Paleolithic/Middle Stone Age cultural stages (eg. Barham and Mitchell, 2002; Debénath and Dibble, 1994) .

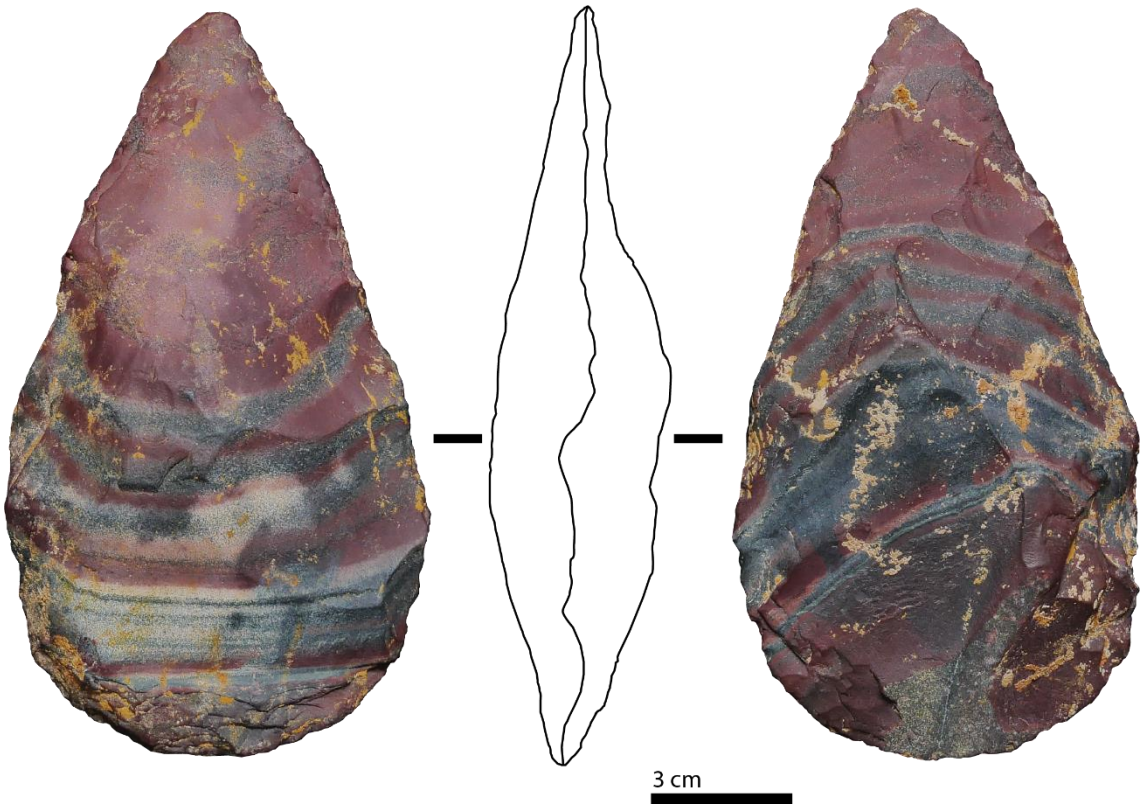

Fig. 31 – Almond-shaped handaxe produced in siltstone-quartzite river cobble from JCF trench (note the yellow cement coating the tool)

5.3. Trench DMT

5.3.1. Stratigraphy

Area DMT corresponds to the last 5 m of the cave channel. In 2018, the fieldwork focused on two quadrants (A-C) in square MM98 to refresh an existing profile that exposed about 1.3 m of sediment cemented to the wall.

Evidence of a past intervention using a mechanical hammer was clear and was later found that this excavation occurred sometime after 2015 in an attempt to find a water spring which is told by the elders in the village to have existed there (person. Comm. Soba da Leba, Rui Francisco). The debris from this intervention remains inside the cave, next to the pit. The blocks showed a porous reddish-yellow sandy deposit with abundant and poorly sorted angular debris from walls and ceilings mixed with bone shatter and cemented with white spheroidal calcitic crystal intergrowths (>5 mm). In general terms, the deposit is similar to the pink and yellow breccias described by Pickford(Pickford et al., 1992; Sen and Pickford, 2022). (Pickford et al., 1992; Sen and Pickford, 2022). At the same time, it seemed to directly correlate to the description of J. Camarate França about peculiar "Mousterian-like" artifacts as inclusions in a hard cemented surface at the end of the cave.

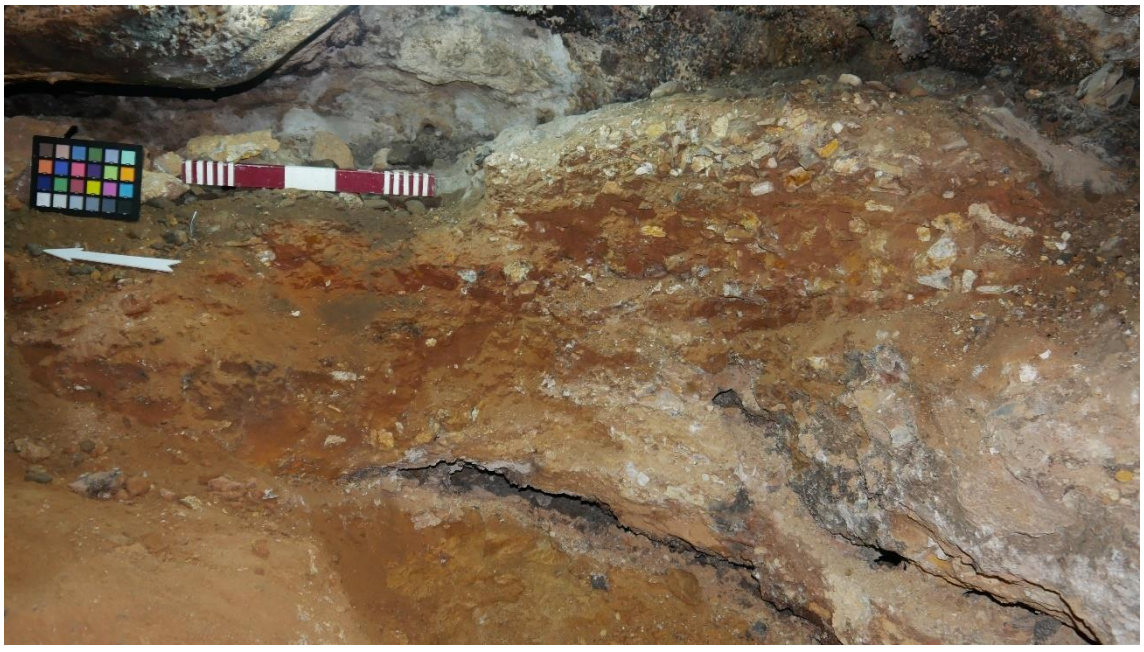

Fig. 32 – MM98 before excavation (Scale bar directly on the tested quadrants)

The excavation was particularly slow with the use of a pick and hammer. The space between the roof and the surface was very low and irregular, as a result, excavations could only host one technician on the total station and one excavator at a time. Conditions for excavation were the most humid inside the cave, with active drippings

from the cave wall and the left overhang over square MM98. Moisture remains fairly stable across the year. During excavation, a dark-brown crust was identified following the dripping line (Fig. 32-Fig. 34).

In the preliminary assessment of the section left by the previous excavators, and the materials left piled next to it, it was clear there were abundant faunal remains. Plenty of bovid teeth could be observed as well as two flakes which suggested there might be a relationship between this backfill and the anthropogenic occupation. Gravel-sandy lenses cemented with botryoidal and ellipsoidal white crystals intergrowths (popcorn-like dripstone), but also grey sheets of flowstone across planar voids can be observed by the naked eye.

A very thin layer of loose dark-brown silts with guano (GU1) covers a continuous undulating crust over the deposit (GU2). Aggregates have abundant biogenic inclusions, mostly bone shafts but also mammal teeth. Yellow and red sandy laminations intercalating with "trains" of angular clasts showing inverse grading have a parallel distribution with a higher concentration of the larger clasts closer to the surface which can be due to the wall effect. Although most of the angular debris is from the bedrock, a few flakes and water-worn quartzite pebbles were also observed in the profile.

Excavation in the area started in square MM98, with quadrants A-C. Due to the observed difficulties in excavation and predictably for collection of a micromorphology sample, part of quadrant C was left to collect a column.

GU1: Fine-grained, loose, grey silts with occasional coarse rounded pink and white sandy aggregates, discontinuous, wavy sharp lower boundary. Guano and microfauna elements;

GU2: Gravel-sandy laminations (2-3 cm) crusted and calcite cemented. The geological unit excavated had about 0,80 m of thickness, and the excavation reached a horizontal fissure. The deposit develops in sub-horizontal beds of gravel-sandy lenses showing parallel-distributed trains of clasts close accommodating. The clasts include several lithologies observed in the system. Coarse sandy aggregates of yellow and red granules can be observed by the naked eye coating the coarser grains. Biogenic inclusions were abundant including bone shafts, teeth, and a coprolite. Secondary carbonates are visible throughout the profile infilling the pore spaces and cementing the deposit. Coarse crystal intergrowths are more frequently botryoidal or spherical white minerals but some domains develop in grey sheets;

Three sub-horizontal units were defined during the excavation (sub-unit 2.1, 2.2, 2.3), but later understood these are composed of 17 cm thick gravel-sand laminations described individually in the micromorphological analysis.

GU	Thickness (cm)	Colour	Munsell	Description
1	1-3	Reddish grey	10R, 5/1	Fine-grained, loose, silty-sandy, clear wavy lower boundary
2	70-85	Pale pink-yellow	-	Carbonate crust capping cm thick gravel-mud laminations, moderately porous, massive texture, intercalations of sub-rounded pebble-sized angular cave debris, fossil breccia aggregates concreted by grey irregular flowstone sheets, and “popcorn” crystals

Table 18 – Summary description of geological units of area DMT.

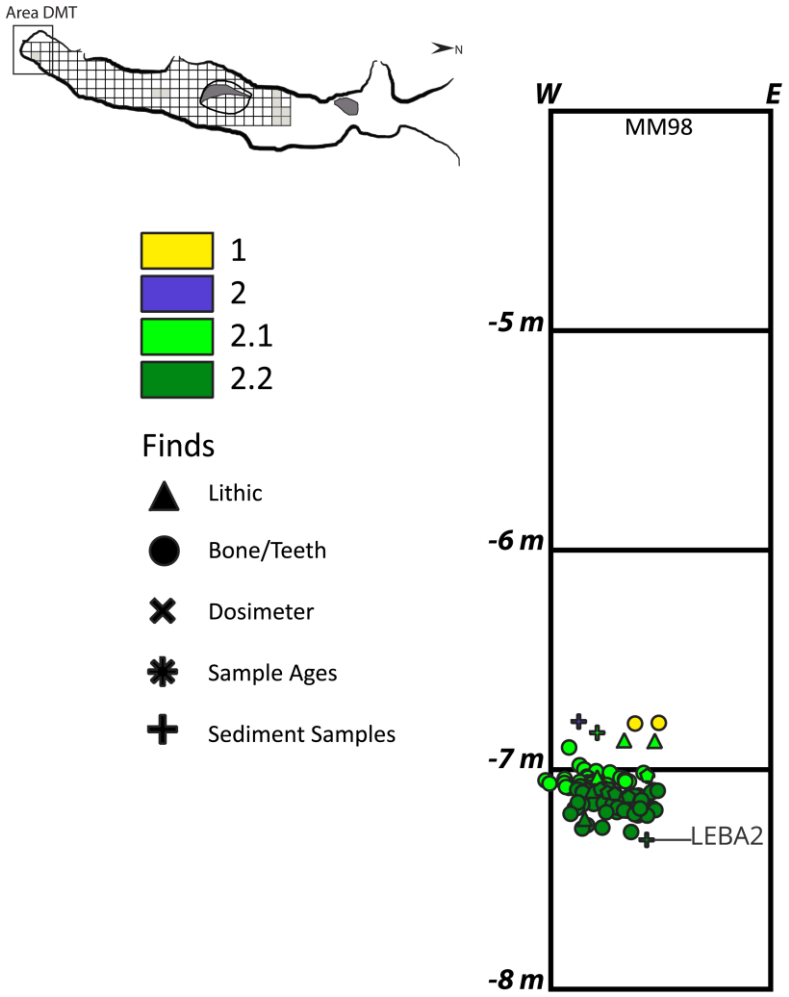

Fig. 33 – Point cloud for findings excavated in area DMT per GU with indication of dosimetry (LEBA2).

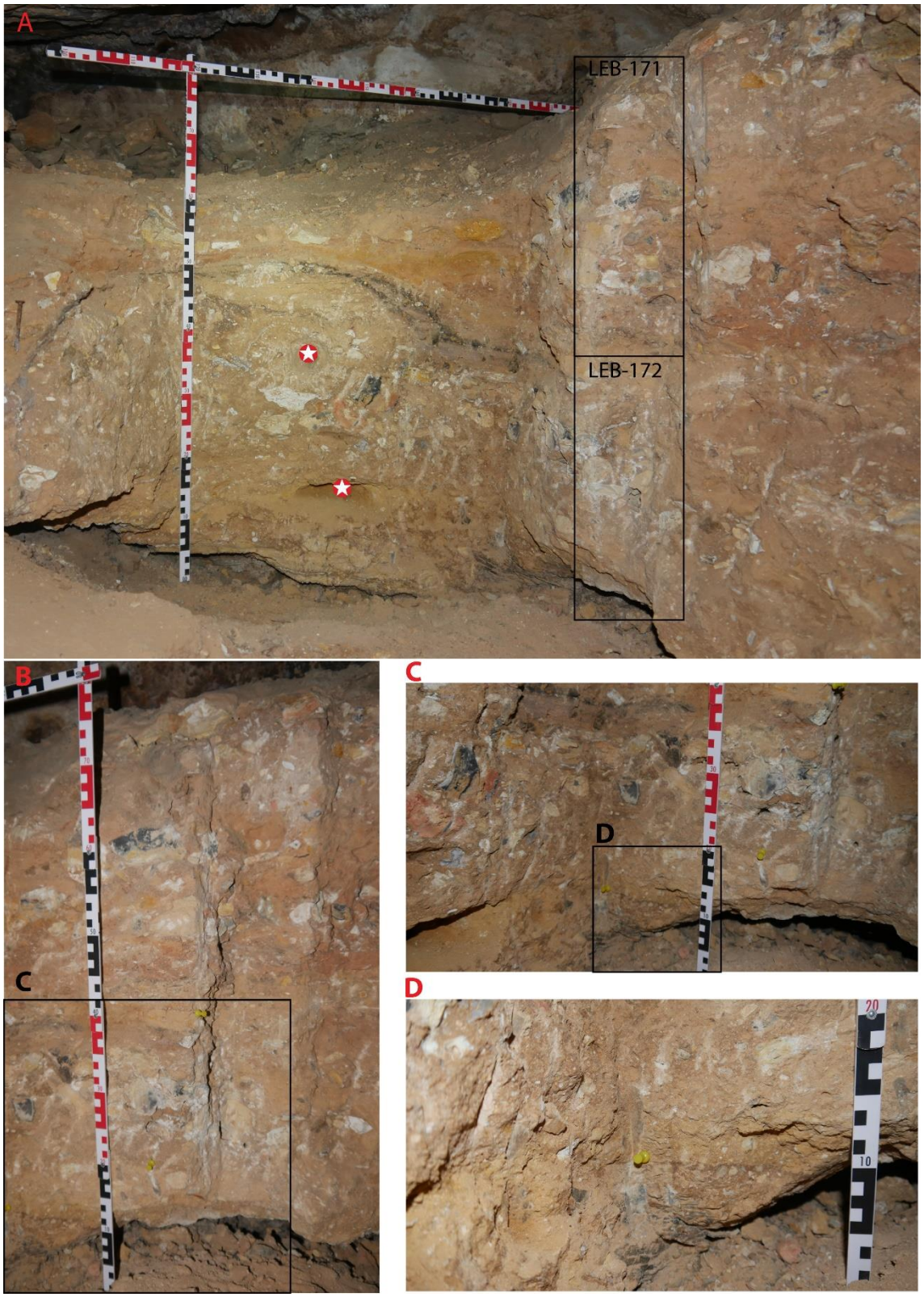

Fig. 34 – Photograph of the profile and location of the block samples for micromorphology (171-172), including reference to dosimetry placement (red stars); B: Detail of the sampled section including reference to lower part; C: Detail of a lower section of the column; D: Detail of the lowermost red and yellow laminations, white rounded granules are bone fragments.

5.3.2. Assemblages

4.2.3.1. Fauna

Macromammals

The faunal remains collected in the DMT trench account for a total of 141 specimens (Appendix 1). Skeletal material is very fragmented and concreted making it difficult for taxonomic identification and morphological description.

Area DMT	**NISP**	**%**
Bovids		
Bov I	1	0.7
Klipspringer (*Oreotragus oreotragus*)	1	0.7
Bov I/ II	3	2.1
Bov II	15	10.6
Bov II/ III	10	7.1
Bov III	9	6.4
Bov III/IV	3	2.1
Bov IV		
Indet. Bov.	18	12.8
Other ungulates		
Zebra (*Equus* cf. *quagga*)	1	0.7
Pig/ warthog (Cf. *Phacochoerus*/ *Potamochoerus*)	7	5.0
Carnivores		
Indet. Small carnivore	1	0.7
Rodents		
Porcupine (*Hystrix africaeaustralis*)	1	0.7
Indeterminate		
Indet. Medium mammals	71	50.4
Grand total	141	100

Table 19 – General Inventory of macromammals identified in area DMT.

Bone and teeth fragments are found in unequal frequencies. During excavation N=33 bones were collected, compared with N=64 for tooth elements. For part of the assemblage, it was not possible to identify the species or tribe. Indeterminate medium and small-sized mammals account for 50.4% of the assemblage. Bovids represent the most frequent group with NISP=42.6% including all size ranges. Among these medium-sized (Bovid II) are the most frequent group. A small antelope, the klipspringer

(Oreotragus oreotragus), was identified by the presence of well-preserved teeth elements.

Other ungulates include the zebra (*Equus* cf. *quagga*/*burchelli*?) represented by one tooth; the pig/warthog represented by 7 specimens.

Carnivore activity is indicated by a coprolite and occasional taphonomical observations relating to carnivore damage and gnawing (Table 20), which present similar patterns and agents observed in area VOJ.

Fig. 35 – Coprolite found in area DMT.

Despite the morpho-analytical difficulties deriving from the fragmentary and fossilized state of the assemblage, it seems likely the assemblage is derived from anthropogenic activity, although the presence of one ichnofossil suggests carnivore activity in the inner area of the cave, as previously documented by Gautier (1995)

Alterations	**NISP**	**%**
Fine cracks, some “open”	-	-
Chemical weathering	-	-
Staining	92	65.2
Abrasion	0	0.0
Bone covered or partially crusted with sediment	105	74.5
Total NISP	141	100
Gnawing		
Carnivore damage	1	2.1
Possibly carnivore damage	1	2.1
Rodent	-	-
Possible rodent	1	2.1
Total NISP*	47	100
Anthropogenic damage		
Burning damage	1	2.1
Possibly burning damage	2	4.3
Cut marks	-	-
Possibly cut marks	1	2.1
Scraping	1	2.1
Total NISP*	47	100

Table 20 – Frequencies of observed mechanical and chemical alterations, sediment crusts, gnawing, and anthropogenic damage in macromammal specimens recovered in area DMT, Leba Cave. (*) symbol indicates samples excluding tooth elements.

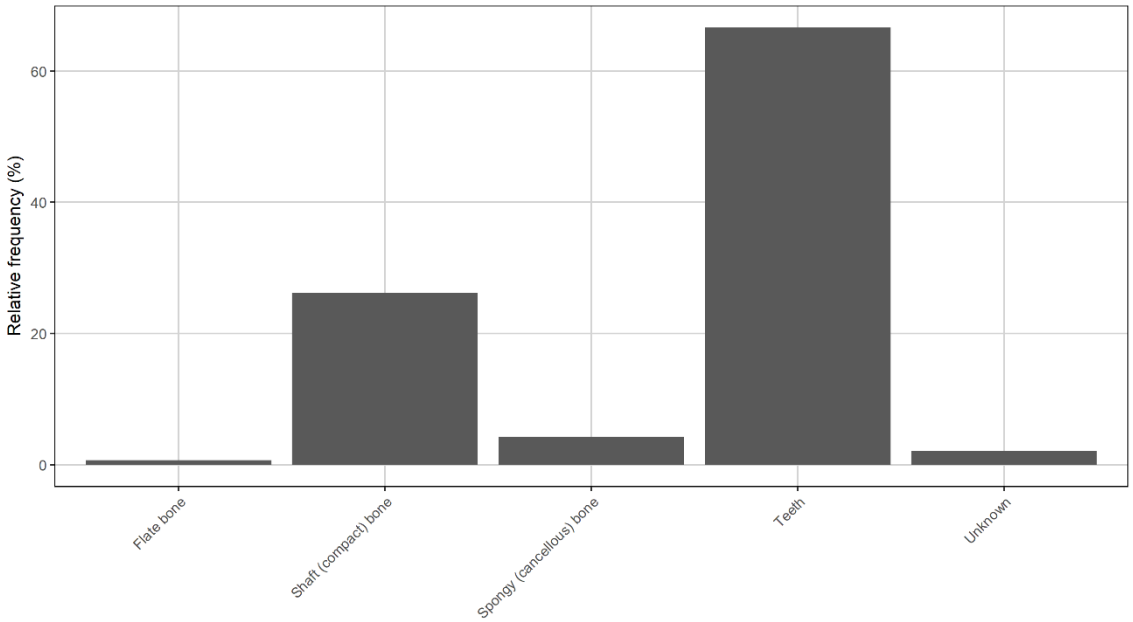

Fig. 36 – Abundance of bone tissue types in area DMT

4.2.3.2. Lithics

Knapped materials were rare findings in the excavated quadrants. Two lithic artifacts were collected at the surface of the deposit but covered by the crust (GU2), included in the gravel laminations observed in the profile. Raw materials are pink quartzites from the river sources showing water-worn surfaces. One of the river pebbles is anthropogenically modified. This find is a core tool produced by Levallois preferential method, showing a retouched distal edge as an active surface. Typologically, it can be classified as a thick scraper (Fig. 37).

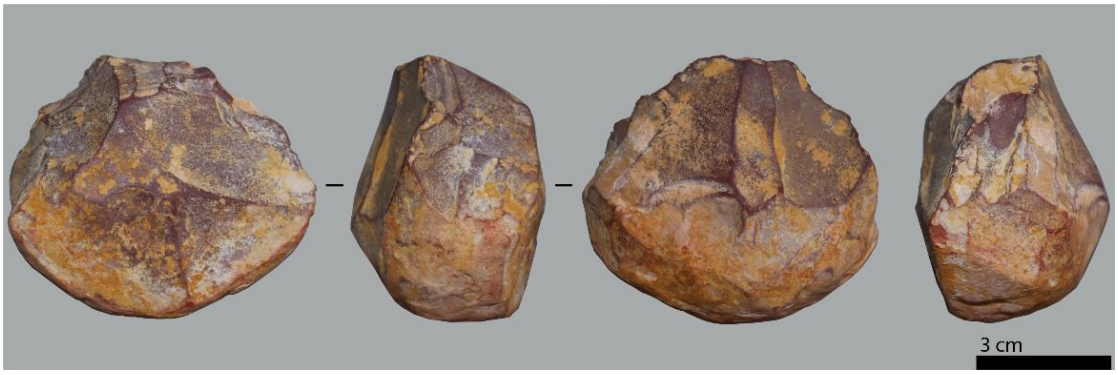

Fig. 37 – Thick scraper on Levallois core in quartzite river pebble found in area DMT.

6. Laboratorial Results

6.1. Micromorphology

6.1.1. Basic components

Bedrock fragments

The most frequent component observed in Leba Cave deposits and most karst sediments in the Humpata system is bedrock debris from the disaggregation of cave roofs and walls. In studies about limestone caves, these are commonly known as *éboulis* (Miller, 2015).

In the case of the Leba Formation, and specifically of Leba Cave, the characteristics of the host rock are not those of pure limestone or dolomite. The Leba Formation has been described as a dolomitic limestone with stromatolites, and bands of cherts and mudstones (argillites) of Pre-Cambrian age (Kroner and Correia, 1980). Observations of the outcrop in the Leba valley and cave system suggest this area is dominated by a siliceous dolostone with occasional limestone beds which were explored by the quarry.

Field tests with 10% HCl proved that CACO3 is not consistently present throughout the quarry exposures or in the cave walls. Inside the cave, carbonate was only confirmed on the eastern wall following joints between chert bands, while the western wall is completely covered with clastic sediments forming a "hanging breccia", and obscuring the bedrock wall.

The bedrock debris observed in the thin section consists of dolostones, chert, and mudstone, sometimes interbedded. The cherts are composed of cryptocrystalline silica and are distinctive by their blueish-grey to light-grey color in the field. Mudstones are grey to reddish brown and frequently display more abundant silt content. Some bedrock fragments have very distinctive intercalations of ferromanganese minerals, and a preferential columnar or circular orientation of bands, depending on the sections, and relate to observations of the stromatolites.

Cherts and mudstone banded versions will include mica and oriented clays when observed in the petrographic thin section. In some fragments of mudstones, mica grains can be fine and medium sand-sized, distributed in thick laminations resembling a sericitic shale.

Other types of weathering products from the wall and roof are fragments of flowstone, calcite films, or dripstone. Ornaments with spherulitic or botryoidal shapes (sometimes called "coralloids" or "cave popcorn" in speleological terminology) are also present. These are formed by percolating water through the host rock and seeping into the cave

through the walls and roofs (Onac and Forti, 2011). These components were observed more frequently in the rear of the cave where they are visible on the wall, but they were also found in thin sections of the front where flowstones are no longer observable.

Former infills

Many of the clasts observed in the coarse fraction of the cave are lithified sediment aggregates (or lithoclasts) derived from former infills of the Leba cave system. The vast majority of lithoclasts observed inside the cave are fragments of the hanging breccia observed cemented to the western wall and roof of the cave and relate to former fluvial-karstic conditions. They can be found in a large range of grain sizes, from large rockfall boulders to granules.

In the thin sections from the rear of the cave, gravel, and sand-sized debris are easily recognized by yellow iron-rich matrix. These lithoclasts have bimodal distributions (poorly sorted fine quartz, well-sorted medium sand-sized grains) associated with stream flow. Other lithoclasts with similar color and texture have intercalated white siltstone-yellow claystone lithologies, and suggest grain settling and secondary iron deposition, some of the fragments show coarse inclusions of chert and biogalleries.

Another class of lithoclasts recognized in the cave sediments and prevenient from former infills of the cave system are the pink breccias, although their color can range from pink to red, depending on the degree of secondary calcite. Under the high-resolution microscope, they are composed of moderately sorted quartz sand and silt with dusty iron-rich clays, red in PPL and dark maroon in XPL, frequently with inherited Fe/Mn nodules, cemented by micritic calcite. These components are easily identified by these characteristics, with the occurrence of organic inclusions, like micro-bone and micro-charcoal.

Coarse Sands

Coarse sand-sized grains are abundant across the thin sections analysed. Quartz is the dominant mineral as either well rounded single grains or embedded in granules deriving from the outside of the cave.

Coarse sand-sized grains are abundant across the thin sections analyzed. Quartz is the dominant mineral as either well-rounded single grains or embedded in granules deriving from the outside of the cave.

Quartz single grains with staining and Fe-Mn Nodules with internal fabric are inherited from the outside sediments and soil horizons in the river valley. Inherited coarse sand-sized iron-manganese nodules with sharp boundaries and internal fabric were observed

in thin sections from area JCF and DMT. These features are frequently associated with lateritic and oxisol horizons of tropical and sub-tropical regions (Gasparatos et al., 2019, 2005; Marcelino et al., 2018) and are present in the surroundings (Ricardo et al., 1980). In the Leba valley, and particularly around the Leba Cave, there are no indications of pedogenesis and soil cover is incredibly shallow, which leads to the conclusion that these consist mainly of relicts and were likely redistributed.

Sandstones composed of well-rounded coarse grains have been observed in the upper Leba River valley during the survey, and are widely present in the plateau. These grains are deposited in river banks, streams, and floodplains, showing the bimodal distribution of quartz poorly sorted silt-fine sand, and well-sorted coarse sand grains. They are also components of soil aggregates and regoliths found covering the karst formation. These allochthonous coarse grains were systematically observed across the site stratigraphy.

Fragments of claystone with strong birefringence were also observed in the sediments of area VOJ and DMT. While in area VOJ these are likely derived from anthropogenic action since the raw material was used for knapping and plenty of water-worn pebbles and lithic artifacts were found in the occupational levels of the cave.

Anthropogenic components

Components derived from the anthropogenic activity are abundant throughout the cave sediments and are present in all areas approached.

The most common anthropogenic component is burned bone which was observed in samples from areas VOJ and JCF. The particle size of burned bone is variable and ranges from centimeter-sized fragments to fine-sand-sized grains. These are more frequently subrounded.

Wood charcoal is the most frequent plant-derived component in the cave stratigraphy, and can be found in all sizes. While it is clear in area VOJ that these components are associated with hearths, it is not clear if in the rear of the cave if the micro-charcoal and other amorphous punctuations derive from anthropogenic activity or consist of natural inclusions from the tree cover of the cave hill.

Other plant-derived components like leaves, stems and plant tissues ranging from coarse to fine sand-sized particles are more frequently heated and are exclusive to the front of the cave.

Herbivore dung was also observed in the upper part of the sequence closer to the entrance of the cave in VOJ, relating to cattle. Bovid dung can be easily identified as thinly packed plant material, sometimes forming laminations, with granular inclusions,

prevenient from soil or sediment aggregated to the ingested plants or trampled by the animals, and coated with fine phosphates. Calcite spherulites are easily observed in XPL, and in GU3 these form fumier laminations derived from the burning of the dung. Some of the most rounded coarse aggregates of dung may relate to caprid agents.

Some of the subrounded and altered rocks from these lithologies are naturally derived from colluvial processes infilling the cave fissure with relicts of soils and regoliths from the river valley which were at the surface.

Pottery and construction debris were found during excavation exclusively at the front of the cave, in the top horizons of area VOJ. In the thin section, the construction debris was observed mostly as red earth aggregates with polyhedral and subrounded shapes ranging from pebble to medium sand-sized compound mineral grains. Sun-dried brick is composed of quartz bimodal sands and iron-rich fine material, with occasional organic punctuations and iron nodules. These characteristics are consistent with a local source in the river valley and slopes. Sun-dried brick and daga are widely used by the local population for house construction and maintenance and are still produced by the population using the alluvial sediments of the Leba Valley.

Biological components

Bone and teeth are found across the several areas approached in the cave. Plenty of small fragments (sand-sized particles) but also coarser shafts and complete bones were found in all areas of the excavation. For instance, rodent skeletons some of them complete were abundantly found during the excavation area VOJ. Some of the fresh micro-bone (<1 mm) observed in thin section may derive from the natural deaths of these burrowing agents. Bones present different types of alterations, such as dissolution, heating, fossilization, manganese crusts, and staining. In areas VOJ and JCF, bone is more frequently heated and dissolved. In area DMT, bone is highly fragmented and remineralized. It is not clear whether these elements derive from human refuse or carnivore activity. Since the bones found in area DMT do not present notable traces of heating, it is assumed these derive from carnivore activity, although it cannot be excluded that these bones originally derived from anthropic action and were further reworked by carnivores inside the cave.

During excavation, plenty of complete bovid teeth and fragments were collected in the rear of the cave. A complete carnivore coprolite was also collected in the sequence approached in area DMT. In the thin section, carnivore excrements were observed not only as ichnofossils in the samples from the rear of the cave (DMT) but also frequently in the front of the cave (VOJ). These are usually yellow and pale brown dense rounded

and subrounded particles in PPL with vesicles and granular inclusions, and occasional organic components like micro-bone and phytoliths. Omnivore excrements were also detected in one thin section from area VOJ. Other fine-rounded excrements are slightly denser but with similar composition as the herbivore dung likely deriving from the micromammals.

Fragments of chitin from insects were occasionally observed in thin sections from area VOJ. Dung beetle exoskeletons were collected during excavation, and are some of the likely bioturbation agents. However, these were also observed as bat prey during the field season.

Phosphates

Phosphatic minerals are present in samples from the different areas of the cave and derive from organic matter decay. Biological components like excrement, urine, and bone are the most likely sources but future microanalytical work is necessary to determine the chemical composition and source of the fine phosphates detected in the different areas.

Fine fraction

Fine sand and silt-sized grains

The dominant component in the site stratigraphy is quartz very fine sand and silt (<125µm). Angular very fine sands and silts were observed in all thin sections, and also in some of the bedrock fragments which show a siltstone-fine sandstone matrix, sometimes interbedded with chert and mudstone. As the cave is located in the valley where a contact of the Leba Formation (dolomite-dolostones) with the quartzite-sandstone beds of the Chela Group series, these particles derive from the disaggregation of the walls and roofs, including the erosion of former infills. These are also components in the allochthonous aggregates and seem to be widely present in the valley.

Fine and silt-sized mica and alkali feldspars (particularly microcline with tartan-twining) were observed more frequently in the sediments of area VOJ, closer to the entrance of the cave. Along with quartz, these stable minerals were moving on the landscape through dust flux or remobilized colluvial-alluvial transport from the erosion of the Chela Group rocks. In any case, it should be noted that some fragments of the bedrock with interbedded chert-mudstone sometimes present mica and can relate to an intracave source.

Clay

Clay is found in many of the samples collected at Leba Cave but its nature and history are highly variable. Coarse components with the clayey matrix are varied and relate to different sources of material introduced into the cave.

The vast majority of loose sand- or silt-clay aggregates are allochthonous. These components derive from the soil cover of the hill which would have been introduced through the entrance, chimneys, and cracks in the roof. Other clays may derive from karst-fluvial conditions or stream and floodplain deposits in the valley mostly already eroded today.

Other pure clay brown aggregates with undulating edges found in the front of the cave are likely aeolian, but can also be trampled by biological agents.

Karst residual clay circulating in joint fissures was also deposited by dripping water through the walls and roof, particularly in areas JCF and DMT. In the rear deposit excavated in area DMT, thin clay laminae with occasional silt-sized quartz grains were deposited by shallow water.

Sample				Coarse Fraction																				Microstructure					c/f related distribution pattern										Void pattern						Secondary features									
T.S.	GU	MU	Lb	Bedrock	Alloct rock	Hanging breccia	Red breccia	Soil aggr./Oxisol relicts	Quartz, coarse well rounded single grains	Mica	K-feldspar	Flowstone/Ca film	Red earth brick	Pottery	Burned bone	Mammal bone/ teeth	Herbivore dung	Omnivore excrements	carnivore excrements	Wood charcoal	Plant tissues/cells	Guano/Leucophosphite nodule	Ash	Massive	Intergrain microaggregate	Crumb	Granular	Lenticular	Close Fine enaulic	Single space Fine enaulic	Double space Fine enaulic	Single spaced equal enaulic	Double spaced equal enaulic	Coarse enaulic	Close Porphyric	Single spaced Porphyric	Double spaced Porphyric	Open Porphyric	Spongy	Compound packing	Complex packing	Biogalleries	Vughs	Planes	Coatings	Microlaminated coatings	Crescent coatings	Phosphatic rims	Fe/Mn staining	Fire-heating	Pyrite	Calcite nodules	Rip-up clasts	Illuviation
521A	2	-	E	x	x				x				x	x		x				x							x		x											x		x						x	x					
	3	3a	S	x	x			x	x		x			x	x	x	x		x	x	x		x			x																x	x		x			x	x					
		3b	S	x				x	x								x			x	x							x	x													x	x	x	x				x	x				
		3c	S	x				x	x					x			x			x	x							x	x													x		x	x					x				
		3d	S	x				x	x								x			x								x	x													x			x					x				
	4	4a	G	x				x	x					x			x		?	x						x									x				x			x		x	x					x				
		4b	G	x				x	x								x	?	?	x						x									x				x			x		x	x					x				
		4.1a	S	x				x	x											x	x						x								x				x			x			x									
		4.1b	G	x	x			x	x											x	x						x							x					x			x			x									
M4	5	-	-	x	x	x		x	x	x	x	x		x	x	x	x	x	x	x	x	x	?	x		x								x					x			x			x			x						
251	6		-					x	x							x				x						x					x										x	x	x		x				x					
250	6		-	x	x	x	x	x	x	x	x				x	x				x						x			x												x	x	x		x				x					
50-2	III	-	x					x								x								x	x													x		x					x				x			x		
50-1	III/IV	-		x				x	x	x						x											x							x							x				x				x			x		
M7	2	E						x	x																		x					x								x		x	x	x	x				x					
	3	-			x			x	x						?	x											x					x								x		x			x		x							x
M6		-	x					x	x	x						x										x						x								x		x	x		x		x	x	x					x
4	2	2a	E	x		x		x	x			x				x	x			?		?		x	x									x							x	x	x									x		
		2b	S	x		x		x	x							x	x								x					x													x	x	x							x		
		2.1a	E	x					x							x	?								x						x							x			x		x		x							x		
171A		2a	E	x																?		?					x																x		x							x		
		2b	E	x		x		x	x			x				x	?								x	x					x										x	x			x							x	x	
		2.1a	S	x				x	x							x															x										x	x			x	x			x			x		
		2.1b	E	x					x																x							x						x			x	x			x							x		
		2.1c	E	x	x	x		x	x							x	x										x													x		x			x	x			x			x		
171B		2.1d	E	x		x																			x				x								x				x	x			x				x			x		
		2.1e	E	x				x	x							x											x													x		x			x				x			x	x	
		2.1f	E	x		x		x				x				x						?			x		x							x							x				x	x						x		
171C		2.2a	E	x												x													x												x				x						x	x	x	
		2.2b	E	x				x								x									x									x							x				x	x						x		
		2.2c	E	x				x	x							x									x									x							x				x						x	x		
172A		2.2d	E	x				x								x									x						x										x				x				x			x		
172B		2.2e	S	x	x	x		x	x							x									x									x				x			x				x	x						x	?	
		2.2f	E	x		x										x									x		x			x											x				x				x		x	x		
		2.2g	E	x		x		x	x							x				?					x	x								x							x				x				x			x	x	
172C		2.2h	E	x				x	x							x	x								x				x												x				x				x		x	x	x	
		2.3	E	x				x	x							x									x									x							x				x				x		x	x	x	

Fig. 38 – Table of components, structures and features observed in thin sections from Leba Cave (acronyms: T.S. – thin section, GU- geological unit, MU-microunit, Lb – lower boundary, E- erosional, G-gradational, S-sharp)

6.1.2. Sample description

Cave Hill

Sample 1x (outside)

One control sample was collected above the cave entrance in 2018, about 3 m from the edge of the brim towards the quarry, in a section created for a wagon path, currently covered with grasses. The sample was obtained at -43 cm depth (Fig. 39). At the meso-scale, the sample shows two bedrock fragments with the typical roll-up structures of stromatolites (Bosak et al., 2013). The bedrock fragments are perpendicular oriented to the surface plane and derive from the erosion of the bedrock. They are generally platy, but with irregular boundaries.

Under the microscope, the bedrock components show intercalation of dolostone, chert, and mudstone, with very fine angular quartz grains embedded. The bedrock fragments are siliceous and have subangular shapes and rough edges. Irregular alteration pattern seems related to the dissolution of Ca minerals since exposure and fracturing of the bedrock. Other coarse components include rounded and subrounded coarse and medium sand-sized quartz grains and inherited iron-bearing rounded nodules (0.5-4 mm).

The gravel is coated with red sandy-clayey rounded microaggregates, more or less welded together but disrupted by biological activity. Biogalleries have undulating walls coated with limpid red clay. The microstructure is crumby with a double-spaced fine enaulic distribution pattern. Quartz bimodal sands (80% well-sorted silt, 20% poorly sorted sands). One of the coarse red aggregates has weakly expressed bedding and sorting which suggest shallow water lain deposition. The micromass is dominated by limpid red and dusty dark-brown clay with undifferentiated b-fabric, locally dotted. Secondary features observed relate to bioturbation and local oxic conditions, with strongly developed Fe-Mn staining of components.

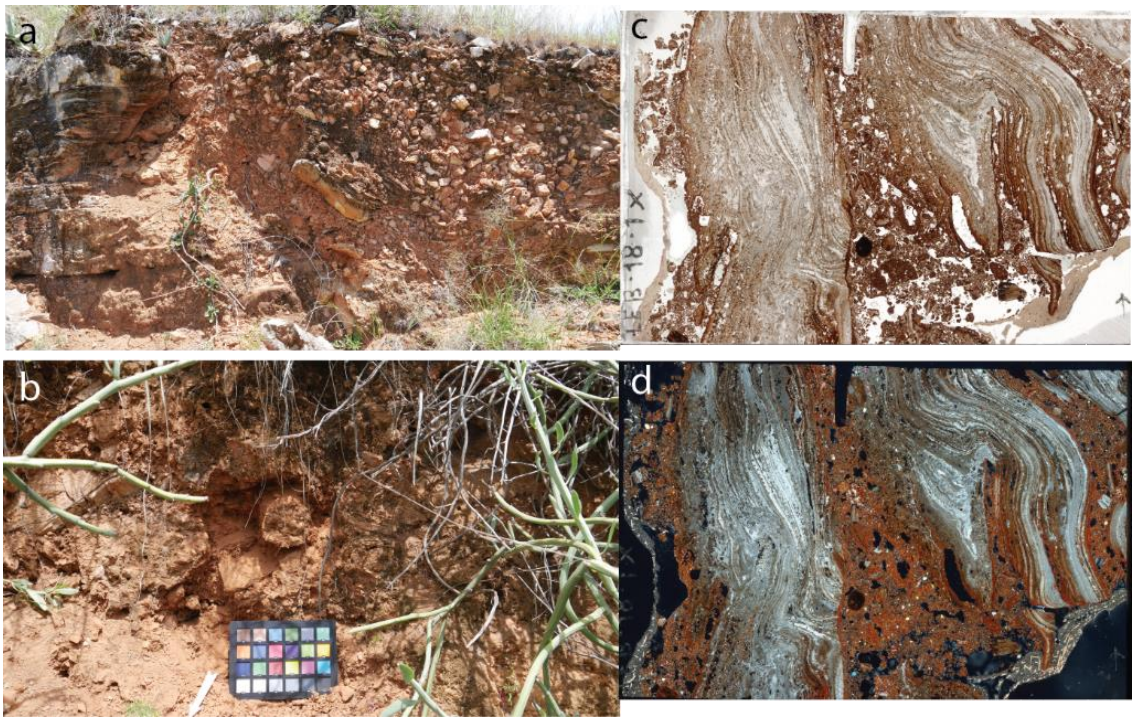

Fig. 39 – a) View of shallow soil cover of the hill above the cave in Q2; b) view of sample 1x before collection (colour scla with 10 cm); c) scan of thin section in PPL, d) scan of thin section in XPL (thin section with 60x90 mm)

VOJ

Four samples were collected in area VOJ, and five thin sections were produced. Sample 521 was collected in square L5 in 2018 documenting the anthropogenic laminations including the "black layer" which would relate to the hearth later partially excavated in 2019. The block sample was collected from the East wall of square L5. Two thin sections were produced from this block sample, from top to bottom: 521A and 521B. Other samples were tentatively collected in this profile but were not successful for thin sections. Two other samples were collected in the southern profile, LEB-250 and 251 documenting the infill in L2 which could relate to the excavation of Oliveira Jorge in 1975. In 2019, sample M4 was collected from square M4 documenting the sediments below the hearth, with no visible rubefication, and which covers all the large roof spall boulders.

North-East profile

Sample 521

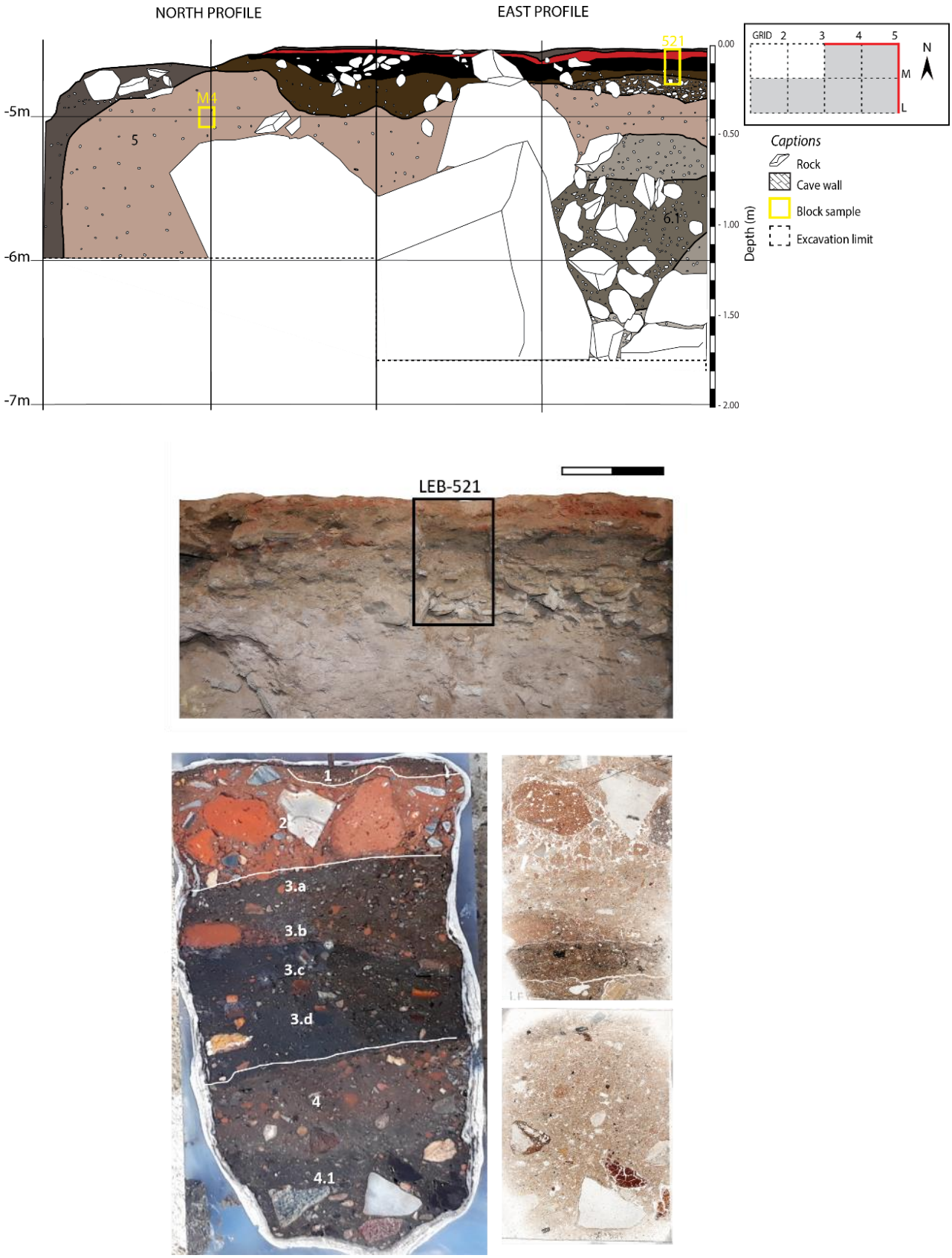

Fig. 40 – Location of the block samples in the VOJ East profile, picture of the negative of the block samples, slab with references to the micro-units described (3a-d) and high-resolution scans of the thin sections (slide with 90x60 mm)

The micromorphological analysis of sample 521A-B in area VOJ shows mostly components derived from anthropogenic activity as clear horizontal lenses (Fig. 40). GU 2 is almost exclusively composed of coarse polyhedral aggregates of red-earth sundried brick mixed with angular rock fragments of bedrock showing accommodating edges and parallel distributed. The aggregates are sandy-clayey and moderately porous (20%), with rounded to sub-rounded shapes and sharp edges, ranging from very coarse to fine sand-sized clods, mixed with angular rock fragments. The coarse components are randomly oriented and parallel distributed across the surface of the chamber sealing the underlying deposits. The sands are bimodal which suggests a source nearby in the river valley for the manufacture of mudbrick.

The rock fragments are represented by angular debris of chert and siltstone but also dolomite was observed. Rare medium-sand-sized calcitic single grains were observed with angular shapes and are likely part of the colluvial sands present in the cave system or from the quarry and used for construction work.

The rock fragments are represented by angular debris of chert and siltstone but also dolomite was observed. Rare medium-sand-sized calcitic single grains were observed with angular shapes and are likely part of the colluvial sands present in the cave system or from the quarry and used for construction work.

The lower boundary with GU3 is sharp in the field due to the color change and decrease in grain size. In the thin section, the boundary is clear by the differences in composition and microstructure from crumby to lenticular.

GU3 was informally called the "black layer" in the field as it extended across most of the excavated area. The top of the "black layer", MU3a, (Fig. 40) also shows abundant red sandy-clayey aggregates similar to a fabric similar to the red-earth aggregates observed in GU2 but decreasing in size. Differentiation between red earth brick and soil aggregates which could have been trampled from the outside is difficult. Traditional mudbrick (sun-dried) uses alluvial sands observed in the river valley and are difficult to distinguish from natural/trampled aggregates in bulk samples. When compared with the control sample collected from the red sands above the cave entrance (control sample 1x), the sandy aggregates from the outside typically show a maroon-brown color in PPL. This would suggest that the vast majority of rounded red aggregates observed in sample 521 derive from GU2. In any case, it is possible they were naturally reworked in the cave before the construction material was deposited and oxidation would be related to the combustion event in GU3.

The "black layer" has the highest concentration of organic materials with laminations of ash, plant tissues, and wood charcoal, as well as heated bone fragments, suggesting a preserved hearth. Microunits 3a-d include lenses of burned material and 4a-b correlate with the basal area of the hearth including a rubified region at the top.

The contact between GU2 and GU3 is clear. Mu3a has a crumby microstructure. The analysis shows a mixture of different coarse materials deriving from the top unit but also components that covered the hearth before the deposition of GU2. The fine fraction is composed of quartz silts, with occasional mica and feldspar. Micro-charcoal and ash are found scattered across the groundmass, some very weathered and rounded. The basic components have a parallel arrangement and parallel-oblique orientation with some indications of rotational movement, which is likely associated with the stepping and traffic.

The boundary with the lower unit (MU3b) and undulating. Micro-charcoal increases in frequency along with a few coarser components, and other anthropogenic components like coarse pottery fragments. Heat-induced voids like interconnected zig zags and planes suggest this is the top lens of a burning zone. The lower lens (MU3c) is composed almost exclusively of wood charcoal and other plant material of different shapes and sizes, including phytoliths thinly packed. Herbivore excrements composed of cell fragments and amorphous organic material, with visible spherulites are observed in thin section 521-A, at the lower boundary of micro-unit 3b. Domains of dung were observed at the macro-scale during excavation.

Calcium carbonate pseudomorphs and druses deriving from leaves and plant remains (Brochier and Thinon, 2003) were observed in MU3b and 3c. Ash rhombs and weakly developed fumier from burned herbivore dung were also observed which indicated the use of the space by domestic animals. Although it is known that dung may be used to ignite and maintain fires there is no direct evidence for such purpose. Other organic materials include burnt bone fragments

A sharp lower boundary between MU3d and GU4 is marked by the interconnected planar and horizontal arrangement of the charcoal particles. The GU4 observed in thin section 521 B, corresponds to the basal part of the hearth. The microstructure is crumby and its composition is similar to MU3a, but aggregates are randomly oriented and distributed. GU4 was subdivided into two micro units, showing rubefication from heating typical of combustion features. Coarse components are dominated by well-rounded coarse single grains, coarse red earth aggregates, and biogenic material. Wood charcoal is abundant

mostly as fine <100 µm particles and few coarse fragments are dispersed. Dung, omnivore, and carnivore excrements were also observed to be frequently altered.

Burnt dung spherulites and ash pseudomorphs are observed in the fine fraction from the coating of the coarse rock fragments in GU4 and 4.1.

In GU4.1, coarse bedrock fragments and organic material are fresh non-burned faunal fragments sometimes coarse (>500 µm) are also visible and may be exclusively deposited by biological elements. Micromammal activity is a likely explanation as plenty of rodent species were identified during the excavation.

Fine phosphatic aggregates, spheroidal and rounded particles, ranging from very fine to coarse sand-sized particles are frequent in thin sections 521B and M4. Phosphatic aggregates grey in PPL and golden in XPL likely relate to excrements. While some particles seem to be fragments of fecal pellets scattered in the groundmass, others are coalesced, sometimes showing irregular edges. The phosphatic aggregates have sandy inclusions.

Bats also eliminate parts of the animals they consume. Elements of chitin are rarely found in the sample. Dung beetle exoskeletons were collected during excavation, and are some of the likely bioturbation agents, but they were also observed as bat prey. Cattle dung is found mostly scattered and not in specific structures which would be expected in a pen where dung beetles find interesting meals. Possibly, these were located elsewhere in the cave near the entrance.

The depositional processes observed in sample 521 are for the most part associated with anthropogenic activity. Two different anthropogenic events occurred in this specific area of the cave: a hearth and an intentional floor created by the factory. Between these two events, windblown material and other aggregates were reworked by biogenic traffic into the chamber and partially obliterated when the construction material was dumped in the hall to create the floor. Components derived from anthropic action are abundant in the underlying sediments. A parallel arrangement of coarse components and bio-anthropogenic material may indicate the area was prepared before the fire was started, although rotational rearrangement and generalized parallel arrangement of particles and bedding occur due to human-animal traffic (Miller et al., 2008). These were important agents of deposition of organic content but also low-range reworking of sediments. Exclusively geogenic phenomena are related to dust circulation and weathering of the roof and walls. During periods of non-occupation material derived from anthropogenic action was still being accumulated in the cave chamber.

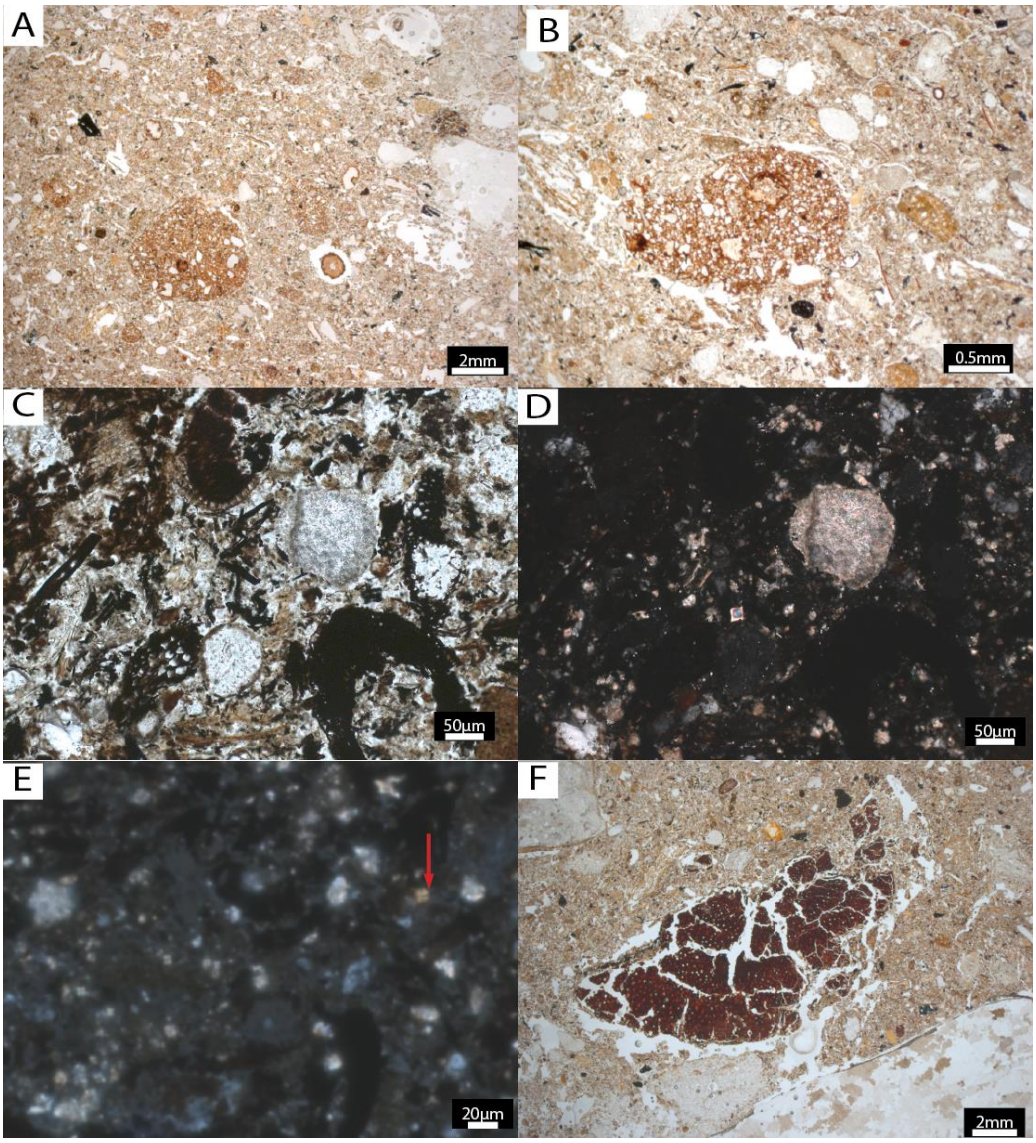

Fig. 41 – Microphotographs from sample 521. A. Well rounded aggregate from soil cover, in PPL; B. trampled aggregate note the zig zag planes and vughs from spongy microsctructure and rotational rearragment of particles; C. Charcoal and ash rhombs in the hearth (MU3c); D. Same in XPL, note the amorphous matrix from the burned material and the ash rhombs; E. Spherulites from heated dung in a matrix of amorphous organic material and phosphatic mineral aggregates likely leucophosphite (red arrow); F. Plant leaf with deformation and drying cracks in a matrix of heterogenous material including wind-blown silts, fragments of heated and non-heated bone, soil aggregates and coprolites

Sample M4

The sample was very difficult to collect using plaster because the sediment was loose and fine but with abundant gravel from cave debris. The sample was collected using a metal box (kubiena type).

At the meso-scale, coarse gravels of bedrock randomly float on a matrix of unsorted sorted sands and silts, with a crumby microstructure. Under the microscope, the microstructure of the sample is spongy.

Coarse components are heterogenous and particularly abundant (40-60%), including gravel, granules, and sand-sized rock fragments from intra-cave system but also

allochthonous rocks, pottery fragments, and numerous biological components from human and animal waste.

The bedrock fragments are present from coarse to fine particles which seem to indicate a frequent input of material from the weathering of roofs and walls in the cave. Pebble and coarse sand-sized, chert and laminated chert-mudstone are randomly distributed, showing subrounded shapes. In thin section, they present a fine textural coating suggesting some translocation and movement. The rock fragments often show inherited oxidative features and alteration. Alteration patterns are generally irregular and linear but also some pellicular features can be observed in a few fragments, suggesting dissolution of minerals.

The vast majority of particles identified of then the thin section are excrements from herbivores, carnivores, and omnivores. Abundant phosphatic grains of different sizes and morphologies, composition, and degrees of alteration are scattered throughout the sample with no particular structure or preferred orientation.

The vast majority of the dung aggregates present a more homogeneous sandy composition similar to the groundmass, frequently with fine quartz and occasional mica embedded in a fine isotropic mass with vesicles forming well-rounded grains. Some of them are very altered, disintegrating into fine sand grains.

Some of the aggregates are very distinctive coarse well-rounded and include plant material and coated with fine phosphatic material, which can be associated with human and biogenic trampling. Red sandy-clayey are well-rounded to sub-rounded shape, with undulating edges; chert and quartz fine grains coated with fine red hematitic silt-clay, deriving from sediments in the river margin and floodplain. Coarse medium sand-sized single quartz grains are also frequent and present iron staining.

The fine fraction is composed of dusty quartz silts and mica with abundant fine phosphate and organic punctuations. There is no specific structure or bedding of the phosphate aggregates. Porosity is about 15% with complex packing voids, a few vughs, and channels.

Anthropogenic components consist of burned bone and charcoal fragments. A few coarse bone and tooth fragments were observed with no specific distribution or orientation pattern. Bone material was observed both fresh and heated with the typical orange gloss. Finer particles (<250 µm) are more frequently very weathered with undulating shapes, rugose edges. Coarse pottery fragments were also observed in low frequency.

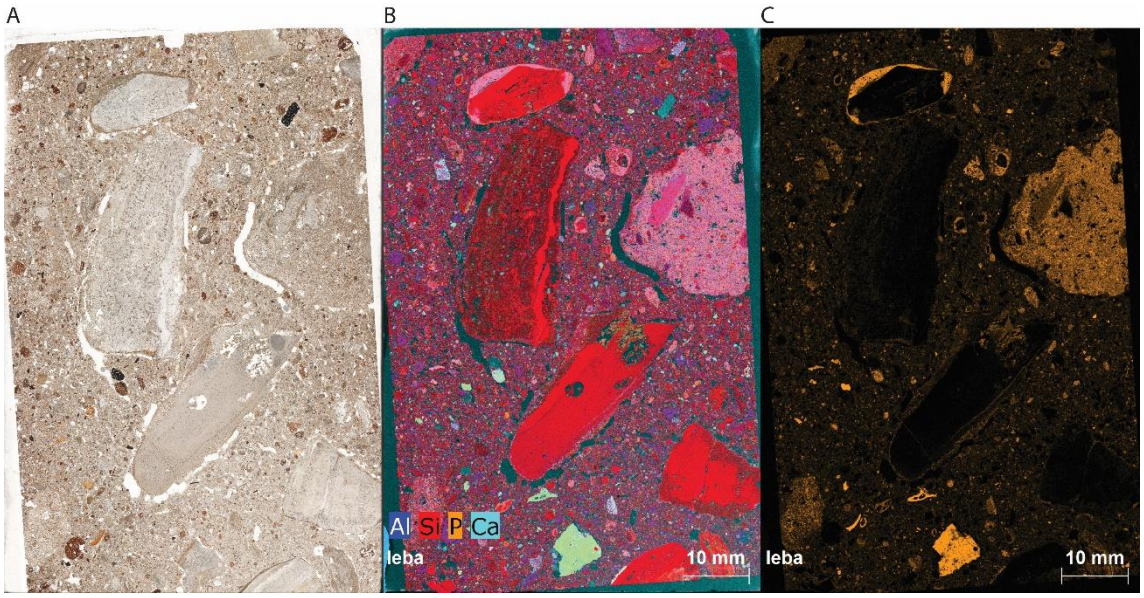

Fig. 42 – From left to right, A) Low-resolution scan of thin section, B) micro-XRF scan of the full thin section for identification of main elements (Al, Si, P, Ca), note the light green components are faunal remains and pink refer to phosphatized aggregates; C) scan only for phosphorous.

Overall, GU5 is a very loose sedimentary unit with different types of components deriving from anthropogenic action were likely middening in this area of the cave, correlating to previous occupations in the surrounding area. Considering the field observaions, reworking of material by burrowing agents like rodents occurred and affected most of the stratigraphy. They also produce rounded excrements with abundant plant material which can also be the case in some of the rounded aggregates and altered phosphatic grains.

Phosphatization was observed in sandy coarse and fine aggregates, as observed in Fig. 42. A phosphatic rind (100 µm thick) on well rounded red clayey aggregate with coarse bedrock clast and hematitic clays; with layered coatings.

Leucophosphite mineral aggregates with a spherulitic shape were also observed. Several authors have pointed out that the the combination of leucophosphite and amorphous silica is one possible diagenetic outcome of the exposure of wood ashes to phosphatic solutions, such as those derived from weathered bat or bird guano (Karkanas et al., 2000; Karkanas and Goldberg, 2018b; Wurz et al., 2022).

Iron and manganese dendritic staining and typic nodules in coarse rock fragments and occasionally sediment aggregates wss observed.

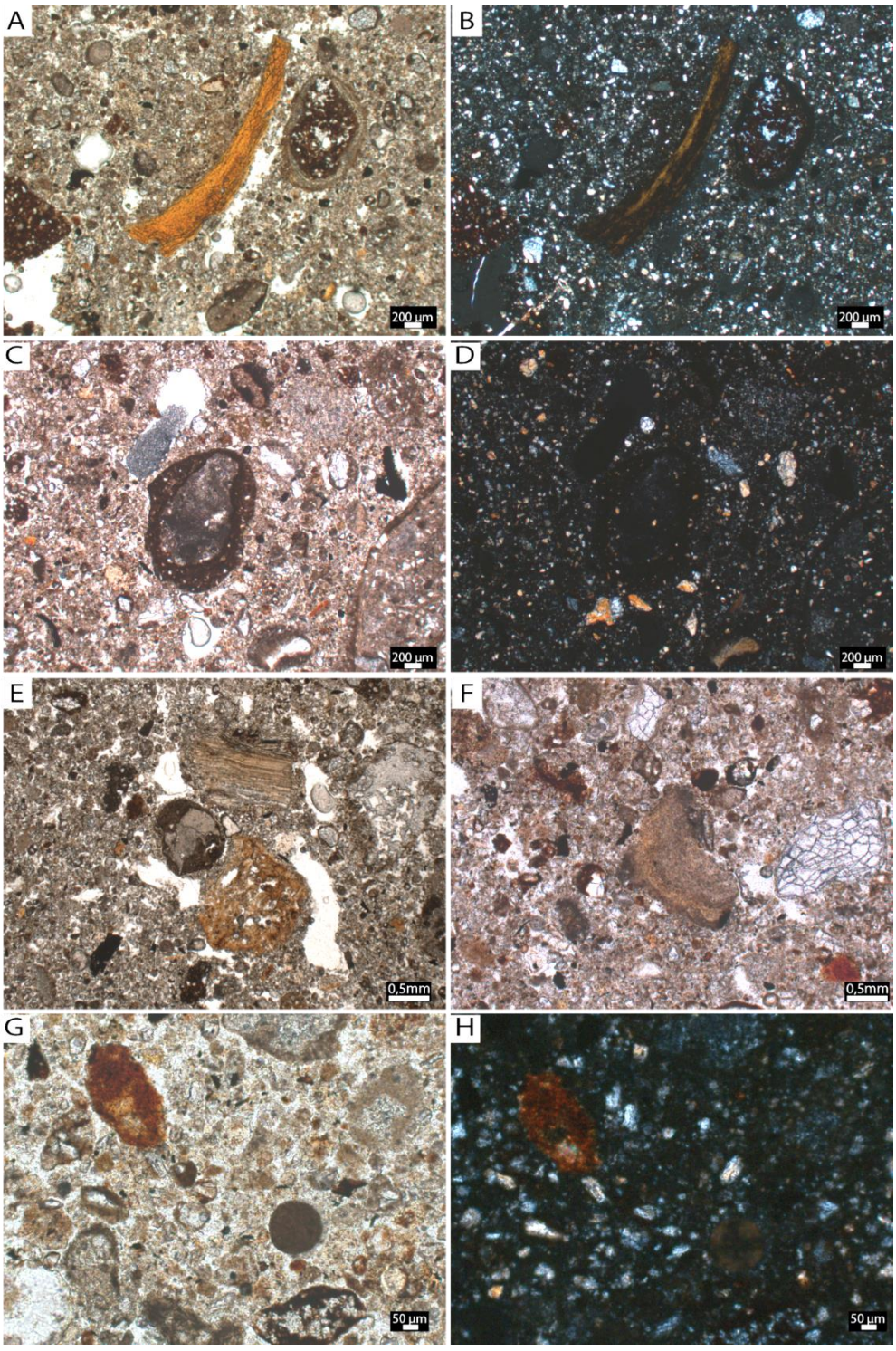

Fig. 43 – Microphotographs from sample M4. A. Heated bone fragment next to a red aggregate with phosphatic rind, 100 µm thick; B: same in XPLnote the amorphous phosphatic material coating on guano aggregate and the absence of birefringence; C-D, E-F: carnivore coprolites; G. Elongated Fe nodule (left), and leucophosphite mineral aggregate with spherulitic shape (right), a secondary phosphate derived from guano; H. same in XPL.

South profile

The samples collected in L2 targeted the lower infills bellow the test pit negative, which to relate with the units observed at the centre of the cave (squares L and M).

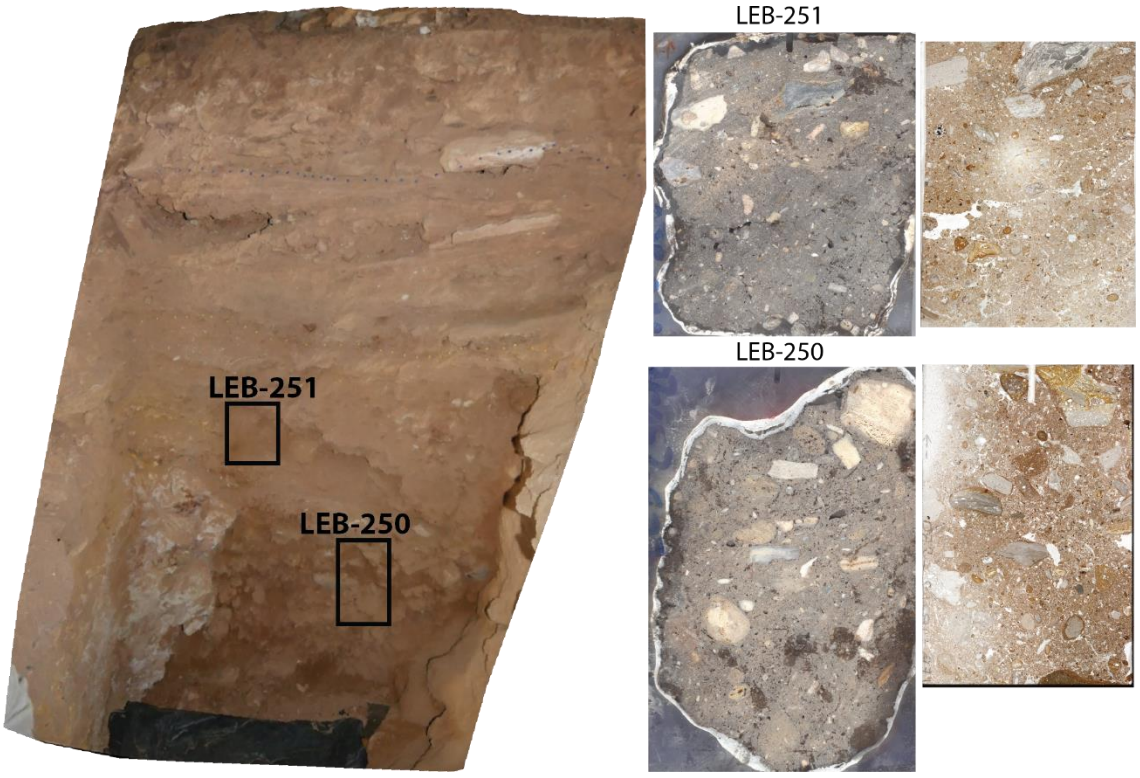

Fig. 44 – View of profile of south profile of square L2 in area VOJ, contact of dripline; block samples and thin section high resolution scan (left to right) (thin section with 90x60 mm)

Sample 251

The micromorphological analysis suggests the deposit is a mixture of material from the disaggregation of wall and roof, with a fine fraction of windblown material and components of anthropogenic origin which were reworked in its current position. The general subrounded shapes are related to a low-range transport inside the cave. The coarse gravels have an elliptical arrangement, with accommodating edges and random orientations, but clustering suggests rotational rearrangement (Fig. 45-F). Rock fragments are subrounded, and consist of chert, dolostone (with pyrite inherited nodules), and mudstone fragments. Other rock fragments with subrounded edges are beige wackestones and packstones derived from an allochthonous source, from local outcrops in the Leba River. Well-rounded single quartz grains are also frequent. Other coarse components are dominated by subrounded and rounded sandy aggregates ranging from granules to fine particles. Yellow sandy goethite-rich aggregates derive from the erosion of hanging breccia are subrounded.

Bio-anthropogenic material is not abundant consisting mostly of micro-bone particles (5%). These are heavily altered, and almost dissolved, and were difficult to identify. A low-resolution micro-XRF scan of the complete thin section highlights different particles containing apatite scattered across the thin section, mostly horizontally arranged or slightly oblique. Amorphous organic material is randomly distributed across the thin section as very fine particles. Excrements, dense grey in PPL, isotropic in XPL, with fine sandy inclusions are rare and heavily altered.

The sample has a crumb microstructure with a double-spaced fine enaulic c/f related distribution. The fine fraction is dominated by quartz silts with occasional muscovite which were windblown as dust. A pore pattern with zig-zag planes, and few fissures suggest post-depositional hydromorphic activity which can be related to the wall moisture.

Pedofeatures mostly relate to bioturbation, identified by the channels with smooth undulating edges that are infilled with groundmass. Some of the groundmass infillings are well-rounded coarse aggregates with sharp edges suggesting intense bioturbation agents, such as burrowing animals (Fig. 45).

Iron and manganese crusts and moderately developed dendritic staining were also observed in bone fragments, aggregates, and grains, which are associated with overall organic matter decay and oxidative environmental conditions.

Sample 250

The sample was collected from the lowermost unit in square L2 (Fig. 44) which was particularly coarse with abundant bedrock gravels and yellow granules. In the thin section, the nature of the coarse components is very heterogeneous. Subrounded clasts of debris from the wall and roof are particularly abundant and generally randomly distributed. In the middle of the thin section, pebbles and granules of different lithologies and aggregates with organic inclusions are clustered with accommodating edges, suggesting rotational movement, and indicating the reworking of sediments into the current position. Orientations are random but the deposit is slightly inclined towards the wall showing the direction of the infill suggesting a debris or grain flow including different types of clasts from different sources.

Rock fragments include fragments from the host rock disaggregation of the host rock. The general shape of the coarse material is rounded to subrounded. Rock fragments present inherited pedofeatures like concentric iron nodules, and black or dark-maroon impregnations They also present alteration with a dotted pattern, suggesting mineral dissolution.

Other clasts with similar distribution and transport are the bedrock fragments of hanging breccia which is typically white-yellow, composed of very fine quartz sands and goethitic clays, mostly undifferentiated b-fabrics and locally stippled.

A very coarse fragment of the hanging breccia (Fig. 45-E) shows a layered white-yellow fabric with a complex microstructure. The fragment has coarse inclusions of chert, channels, and crumbs coated by a yellow silty-clayey micromass with fissures. Finer subrounded yellowish or white aggregates ranging from medium to fine sand-size, are frequent and randomly distributed in the thin section and appear to derive from the same source.

Other sediment aggregates with coarse rock fragments can be observed sometimes with inherited iron nodules or micro-charcoal derive from another source. For instance, a coarse red silty-clayey aggregate with micro-bone inclusions (500-350 µm) presents sub-rounded edges and fine laminations, Fe-rich clay and inherited iron nodules, and secondary calcite cementation. The aggregate has a small fissure crack, from mechanical weathering. This would suggest the reworking of sediments from other areas or previous infills in the cave. Under high resolution, the aggregate shows fine laminations of silt-clay and sand which may suggest shallow water or low-level hydromorphic conditions. These are prevenient from other galleries in the karst system or can derive from eroded infillings inside the cave.

It seems the gravels observed in the thin section are a mixture of elements from the erosion of different parts of the cave like the wall and roof, but also past infills which were obliterated probably by anthropogenic action. The poor sorting of sediments and the rotational arrangement of the gravel observed in the thin section relates these sediments with colluvial reworking. As there is also plenty of micro-charcoal as well as micro-bone, some heated and heavily altered, mixed with the sands.

Organic components are mostly bone fragments scattered throughout the thin section showing a parallel orientation. Micro-bone elements are most frequent (<1 mm) and consist of rounded particles frequently burned. Other elongated particles and coarse bone shafts are observed showing different shapes and degrees of weathering. Bone material presenting inherited pyrite and Fe-Mn nodules were also observed.

Amorphous organic material is observed through the thin section. Few dark brown tissue residues and organic punctuations can be observed scattered in the groundmass. Only a few coarser fragments of wood charcoal were observed and one plant tissue showed articulated cells.

Pedofeatures are mostly related to bioturbation. Fine material consists of quartz silt and occasional muscovite and k-feldspar grains, from aeolian source. A coarse enaulic c/f-related distribution pattern can be observed in both thin sections from square L2. Biogalleries can also be observed. Rough edge coarse channels infilled with loose fabric elements randomly distributed and oriented relating to burrowing agents reworking of the groundmass.

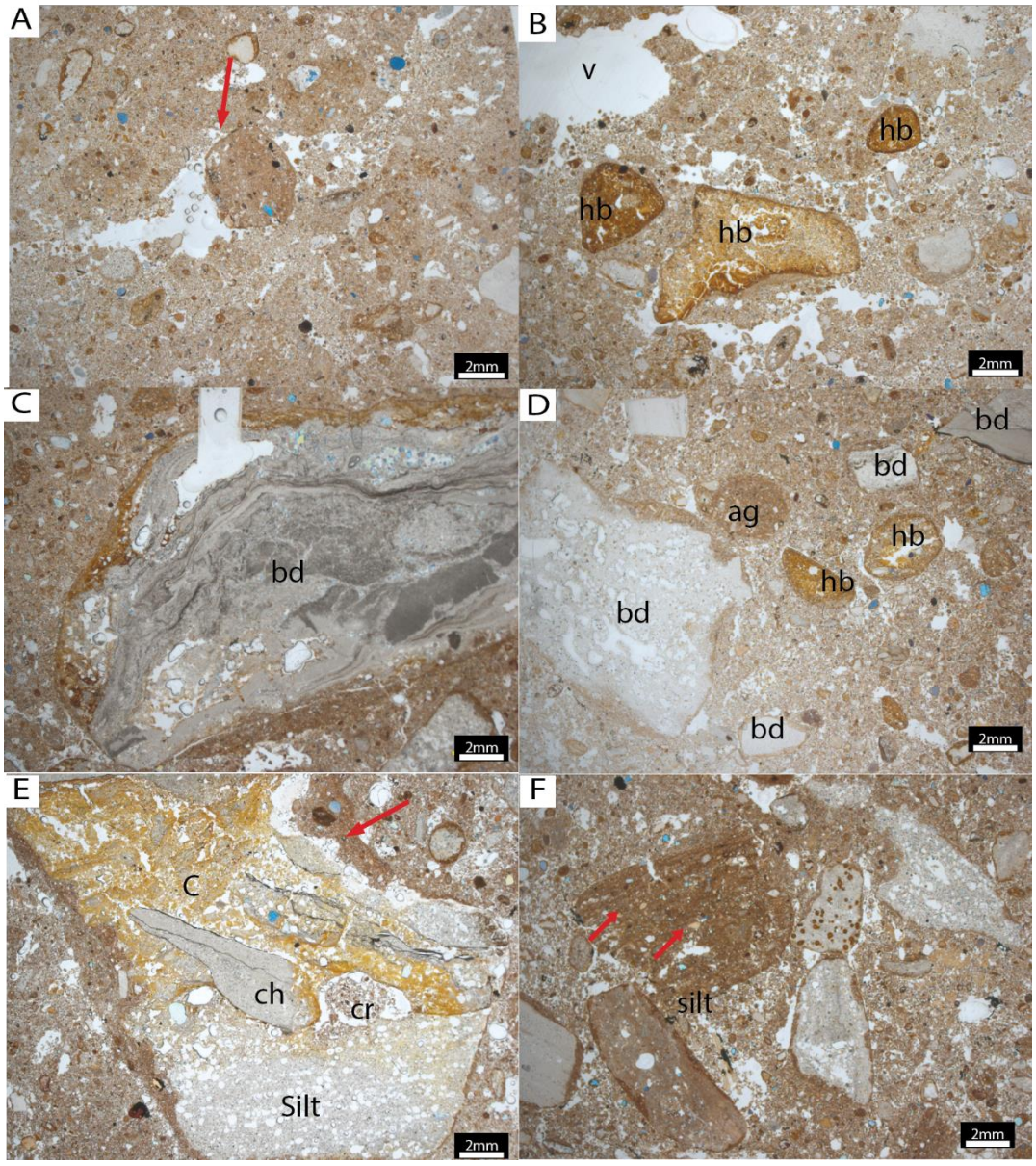

Fig. 45 – Thin section 251: A. channel infillings with well rounded coarse aggregates and porous infillings from biogenic activity, note the undulating walls and sharp boundary of the aggregates (red arrow); B. litholasts of hanging breccia (hb) with subrounded shapes, and interconnected biogalleries and channel voids (v), note with intergrain microaggregates microstructure and organic punctuations (dark particles); C. red sandy-clayey coating with inherited oxic features on coarse bedrock fragment of altered chert (bd); D. Different lithoclasts of hanging breccia (hb) , bedrock fragments (bd) and well rounded aggregates com biogenic activity. Thin section 250: E. angular debris of hanging breccia with bedding and showing a siltstone fraction (Silt), coarse inclusions (chert) and gothetite rich clay (C), with biogallery (cr); note the well defined boundary and silty-clayey (red arrow); F) rotational arrangement of rockfall and red breccia lithoclast with bone inclusions (red arrow).

Phosphatic aggregates can also be observed, some with quartz fine grain inclusions are likely excrements although structures are not highly diagnostic and are mostly fragmented and altered.

Coarse aggregates and quartz grains are coated with sandy clayey material but are inherited. Amorphous organic punctuations and inherited orthic nodules can be observed in these aggregates. These textural features relate to the rotational movement of the particles, which corroborates the weathering of other surfaces pre-existing in the karst system. and are common in reworked colluvial sediments (refs)

Bioturbation features are observed across the thin sections as biogalleries and channel infillings with groundmass particles. Other secondary features are the iron-manganese features, mostly dendritic staining but also crusts.

JCF

The micromorphological analysis of the samples from area JCF focused on the comparative assessment between the samples from horizons excavated in 1950 in the IICT museum collection and samples collected in 2019 after cleaning the excavation trench as preparation for future work. The goal was to provide information about the diagenesis of the deposit since the exposure.

Museum samples

Samples 50-1/2

Two thin sections were produced from the block samples housed at the University of Lisbon collected by Camarate-França in 1950. These samples were labeled with stratigraphic reference, namely one from the interface unit III/IV (sample 50-1) and from unit III (sample 50-2), predictably corresponding to the MSA-LSA boundary in the cultural assemblages (de Matos and Pereira, 2020). The block samples did not have a reference to orientation and the choice was arbitrary as presentedin Fig. 46.

In hand specimens, the samples were similar in composition, showing an indurated red sandy aggregate with rock fragments and bone inclusions. Sample 50-2 was notably more cemented and indurated. At the mesoscale, the red sands have a light pink color and are mostly overshadowed by subrounded carbonate nodules, and very coarse bone fragments are observed.

Fig. 46 – From left to right, schematic profile of the original excavation (based on Ramos, 1982) with reference to labelled provenance; museum samples; chips of the complete sample and thin sections analysed (LEB-50-1, LEB-50-2) (thin sections with 60x90 mm)

Although it is not possible to fully reconstruct the sedimentary deposits excavated by authors in the past, and the samples analyzed did not have orientation, these provide

some clues about the composition and nature of the deposit from which the MSA lithics were excavated in 1950 (de Matos and Pereira, 2020).

The analysis of the thin sections shows a similar microstructure and composition of the blocks but different degrees of cementation by carbonate.

The coarse components identified are rock fragments derived from the bedrock. The main lithology observed is chert but also fragments of banded chert-mudstone and dolostone are present. The size of bedrock fragments ranges from very coarse to fine sand-sized grains with angular to sub-rounded shapes, with sharp edges. These features are consistent with the disaggregation of the walls and roof. Alteration of the rock fragments can be observed in some instances as patchy or minute residues.

The rock fragments are coated by more or less rounded sandy-clayey aggregates with a bimodal distribution and are iron-rich. The micromass of the aggregates is dusty and rich in hematite and has inherited Fe-Mn secondary features. Inherited iron and manganese features observed in the aggregates and fragments indicate general oxic conditions. The loose packing of the sediments, only compacted and indurated by the secondary deposition of calcite, seems to translate some reworking of the sediments which link to the red sediment from oxisol and laterites from the surface or sub-surface, trapped in fissures.

Coarse bone shafts and teeth fragments are abundant in these samples. They are dominant in sample 50-2. In sample 50-2, a very coarse bone shaft is highly fossilized and surrounded by poorly sorted angular cave debris and red sands completely coated by calcite micrite. In sample 50-1, coarse bone fragments and micro-bone are also remineralized and easily discerned as single particles. Fine plant residues were rarely observed in thin section 50-1.

Secondary formation of carbonate nodules is evident in both samples and particularly dominant in sample 50-2 covering almost the entire sample. Microscopically, micritic calcite can be observed coating aggregates and individual grains.

Iron staining was also observed. Microscopically these features are commonly dark maroon and are associated with single grains, rock fragments, aggregates, or small bone fragments. Weak to moderately developed mamillated and dendritic Mn nodules can also be observed in low frequency associated with bone material.

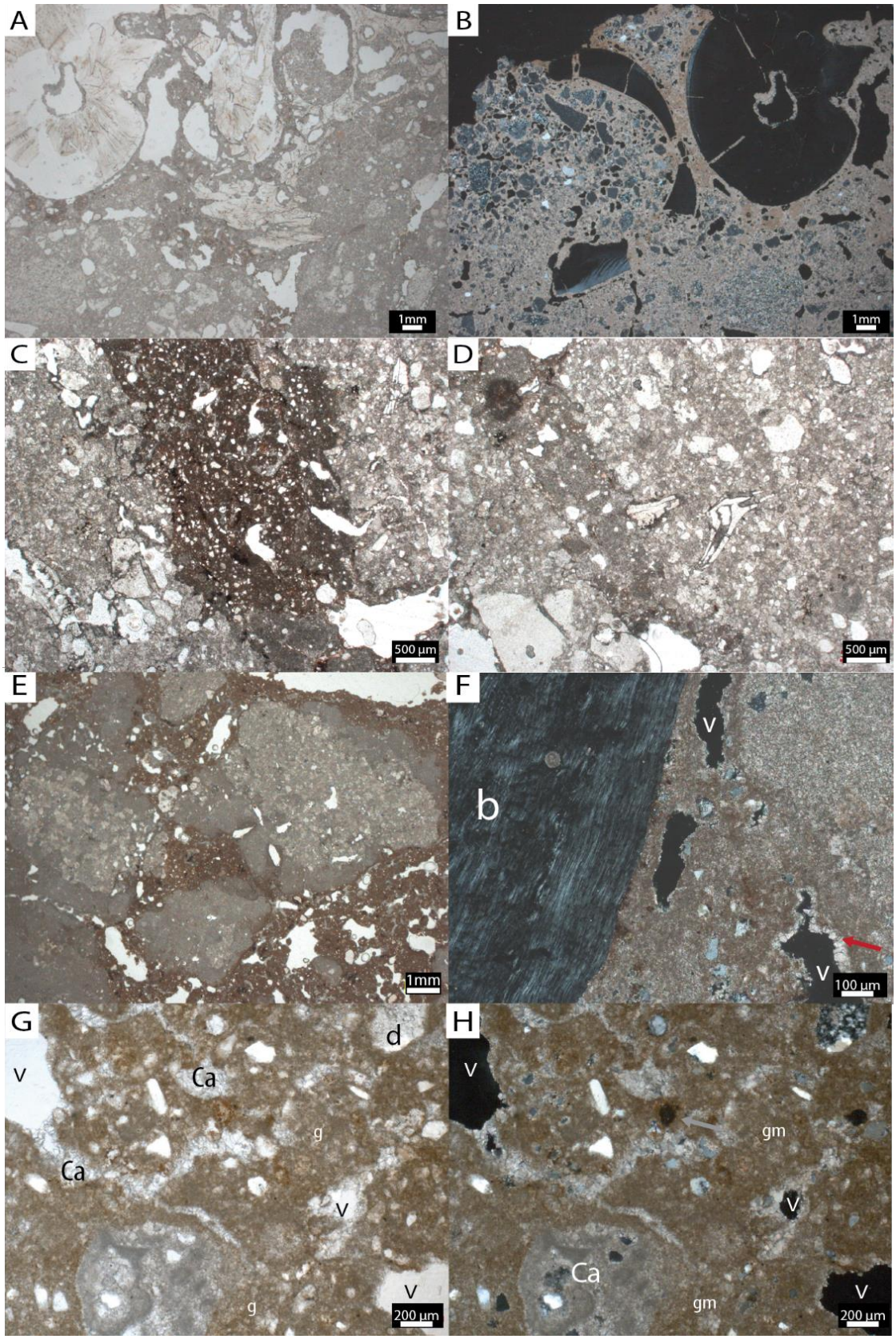

Fig. 47 – Microphotographs from sample 50-2: A. Bone in red sandy-clayey matrix with strongly developed calcite nodules, in PPL B. view of the same bone, note the granular quartz rich groundmass in the top, and massive microstructure at the bottom due to the calcite nodule; C-D. detail of coatings and cementation of the red soil aggregates overshadowing the groundmass;; Microphotographs from Sample 50-1: E: Coarse to fine crumbs and angular fragments, bone (b) in a groundmass of superimposed sandy clayey coatings

and calcitic cement, D) same in XPL, E. Secondary calcite nodules in a intergrain microaggregate microstructure with enaulic c/distribution pattern,, F. coarse bone (b) coated with silty clayey microaggregates, note the spary calcite (red arrow) coatings in voids (v), in XPL; G. Dolostone (d) sand and red silty-clayey aggregates with calcite (Ca) nodules infilling the poe space; H. same in XPL

South-West profile

Samples collected from the profile in the JCF trench focused on the lateral variation of the sediments exposed, and the lower horizons were left for analysis in the following season.

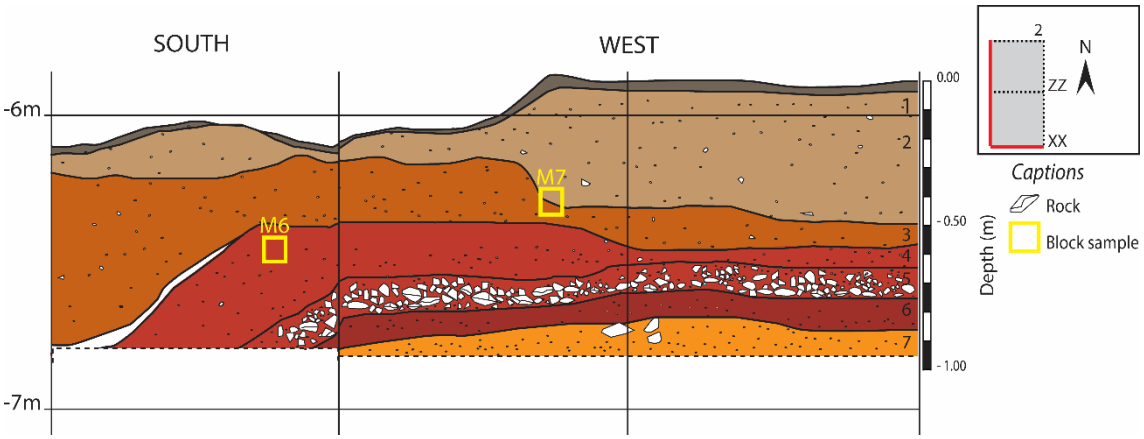

Fig. 48 – Schematic representation of the profile of JCF area.

Fig. 49 – Location of sample M7 in the South profile of JCF, detail o sample, and high-resolution scan of thin section (LEB-M7) (thin section with 90x60 mm)

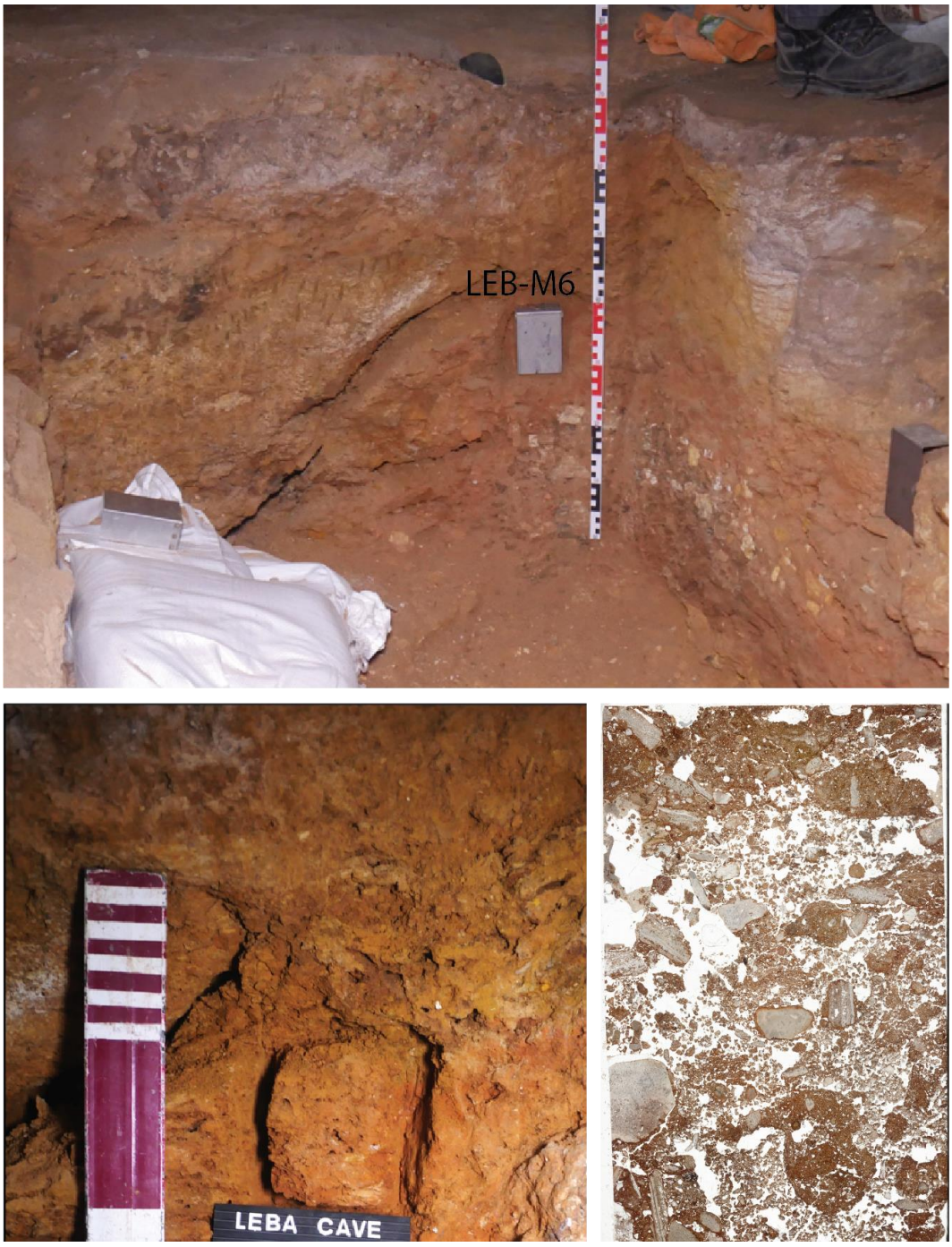

Fig. 50 – Location of sample M6 in the South profile of JCF, detail of sample, and high-resolution scan of thin section (LEB-M6) (thin section with 90x60 mm)

Sample M7

Sample M7 (Fig. 49) was collected from the contact between GU2 and GU3, which was clear in the field by a color gradation of white-yellow-red. Two micro units can be observed at the mesoscale, a light grey sandy lens, and the red-orange unit regions, from top to bottom. An erosional contact is clear at the microscale by the differences in void pattern, micromass, and pedofeatures. The groundmass does not change

significantly across the thin section, and the color gradation seems to be mostly associated with changes in the micromass caused by the water, dispersing iron oxides. Hematite and goethite are aerobic natural weathering products of iron-bearing minerals and are naturally present in the sediments of the river valley and soil covering slopes in the plateau.

In the top portion of sample M7, the grey domains consist of moderately sorted quartz sands and silts with a typical crystallitic b-fabric. Very coarse rock fragments are very few consisting of subrounded bedrock clasts, randomly distributed. The fragments frequently show pellicular alteration. The matrix is dominated by sand-sized grains which are bimodal, being the fine material composed of very fine and fine angular quartz grains (80%) and coarse rounded quartz the coarse material (20%). The microstructure is granular with a close porphyric to gefuric-related distribution pattern. Clay-rich dark brown and yellow fluffy aggregates occur as coarse and fine components, with subrounded shapes and undulating, lightly deformed, or broken down. The fine fraction is mostly composed of quartz silts with occasional mica.

The lower half of the thin section, GU3, has a peculiar pattern almost drappy/flocculated due to the interconnected zig-zag planes, channels and vesicles with coatings. Coarse components are randomly distributed and consist of chert and mudstone rounded and subrounded very coarse to fine sand-sized grains, and quartz grains of variable shape. The quartz sands are bimodal, being the fine material composed of very fine and fine angular quartz grains (80%), and coarse rounded quartz grains, being the coarse material (20%). In the lower right corner of the thin section, a coarse (2.5 mm) iron nodule with a sharp boundary and internal fabric indicates an allochthonous source, from the soil cover outside the cave where pedogenic processes form these pedofeatures. The nodule is subrounded with undulating edges and appears to be a fragment of a larger particle. Iron nodules are frequent in oxisols, lateritic ad bauxitic deposits. These are present in the plateau and the occurrence in thin section indicates these are being reworked into the cave system from the outside and did not occur in situ.

The pedofeatures observed in GU3 relate mostly to bioturbation and hydromorphic conditions related to wet-dry processes. Silt and dusty clay coatings in voids, particularly the planes. Discontinuous capping and link cappings, and crescent clay coatings with grano- and porostriated b-fabrics indicate these features are associated with water. These commonly occur in shrink-swell stress due to wet-dry phenomena (Stoops et al., 2010) and are associated with localized dripping water.

Coarser grains are coated with finer material, mostly dusty silt clay. Some of these features are compound juxtaposed yellow and red coatings which are consistent with alternating water-lain deposition. Compound silt and dusty clay coatings around voids are typical of periodically flooded sediment (Karkanas and Goldberg, 2018a). In caves, dripping water with suspended silt and clay can result in the illuviation of the grains beneath the substrate where the drops fall (Karkanas and Goldberg, 2018a).

Fine phosphates were also observed but are not clear in PPL. Secondary phosphates are extremely varied and can be associated with chemical reactions in the presence of water, organic material, and under variable oxidation states. Bone and guano are common sources of phosphates but biological elements were not identified in these thin sections. Bone was remarkably rare in the unit as only one micro-bone particle was observed, rounded, and altered. This could suggest the phosphates present in the micromass derive from pre-existing bone material, but the hypothesis remains to be tested.

Sample M6

Sample M6 (Fig. 50) was collected from the south profile at a similar depth to M7 but targeted a region of very compacted yellow-red sands which would relate to the same unit GU3. The microstructure is granular, with an open porphyric distribution pattern with domains of close porphyric to gefuric pattern. Coarse components are randomly distributed in the thin section consisting of subrounded fragments of bedrock and sand-sized aggregates rich in iron oxides. The sands are bimodal with similar c/f relation in quartz grains observed in sample M7.

Two coarse (1.2-2 mm) iron nodules with internal fabric were observed as coarse components, easily identified at the meso-scale. Microscopically, they have a sharp boundary with undulating edges and are subrounded. In one of the nodules the internal fabric is very clear and is composed of poorly sorted angular quartz grains coated with opaque fine material, mostly isotropic but with few red streaks. A low-resolution scan of the thin section using micro-XRF indicated these are Fe-Mn nodules. These are features frequently observed in lateritic saprolites and which are still understudied (Stoops and Marcelino, 2018), but their occurrence in the stratigraphy suggests an allochthonous source in the soil cover of the plateau being reworked by either aeolian or fluvial processes, and further infilling the cave as colluvium.

The fine fraction is composed of quartz silts, occasional mica, and a micromass rich in iron oxides. Red and yellow silts and coarse clays indicate hematitic and goethitic pigments coating the coarse grains.

The porosity is high (30%) and the pattern is peculiar with complex packing voids. Wide (1 cm) channels and interconnected undulating planar voids and fissures relate to bioturbation and wet-dry phenomena.

Organic components were very few. Only two bone fragments were identified with a size >200 µm. The fragments appear heated presenting an orange gloss typical of burnt bone but are heavily weathered. In any case, these are only anthropogenic components observed in the thin section.

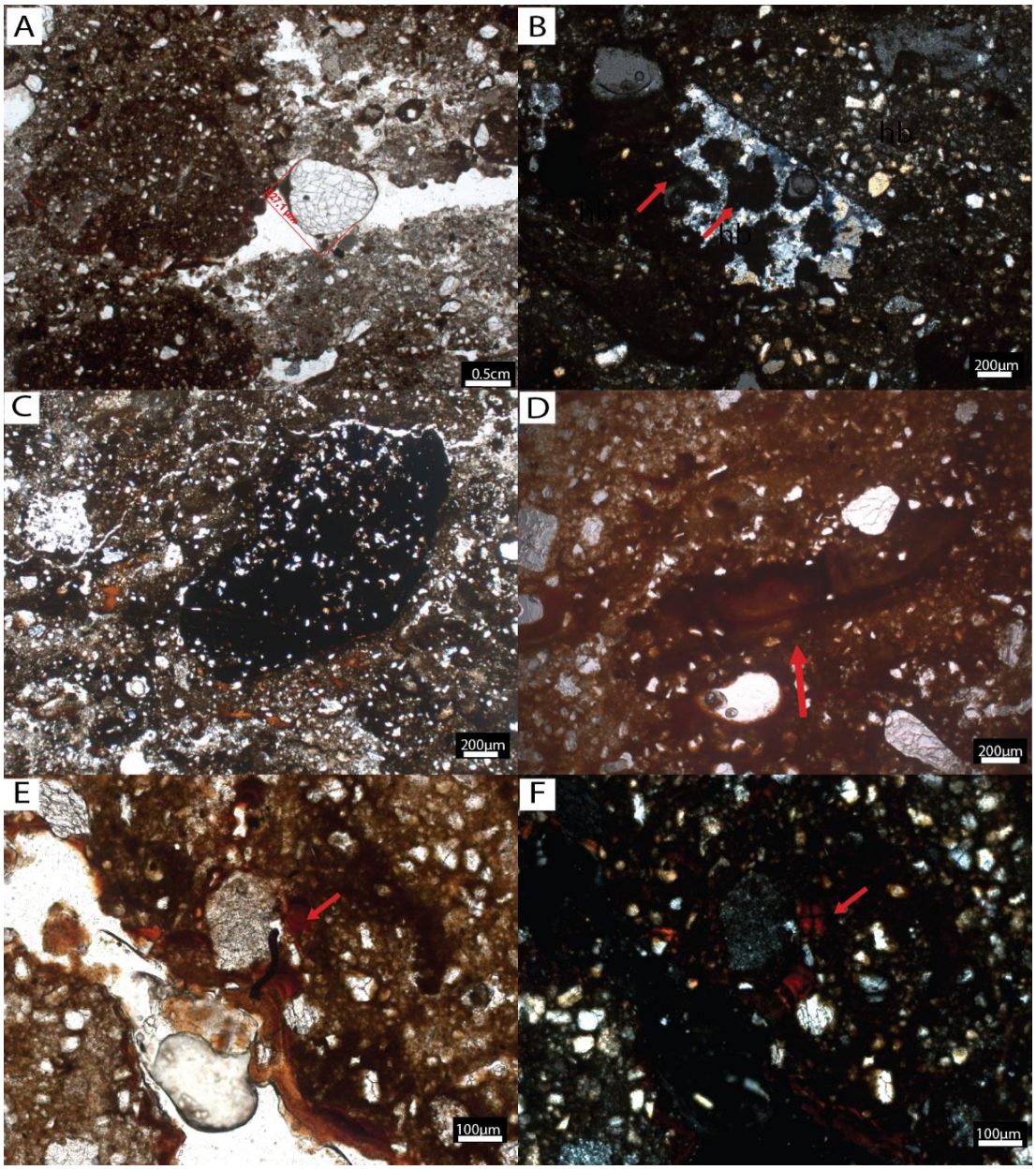

Fig. 51 – Microphotographs from thin sections M7: A. Well-rounded single quartz grain from river allochthonous source in the river valley (927 µm) in loose channel infillings with groundmass components; B. Dolostone fragment with inherited pyrite and manganese crusts, C. Inherited Mn nodule with internal fabric; D. Dusty clay-silt coatings; Microphotographs from thin section M6: E. Crescent dusty and limpid clay coatings; F. same in XPL, note the weak birefringence (red arrow) of porostriated b-fabric.

The whole central part of the sample is heavily altered. Secondary features associated with bioturbation and hydromorphic action contribute to the peculiar void pattern. Water dripping from the walls and roof, and movement on the profile seem to have caused some mineral depletion following the voids, biogalleries, and channels from microorganisms

Other secondary features are dendritic and mamillated weakly developed Mn staining, and phosphatization, affecting particularly the lower right side of the thin section. Fine orthic nodules are also present (5%). The pedofeatures can be complex, and fine phosphatic material seems to overlap the clay coatings, forming superimposed microlaminated coatings of dusty red clay and yellow-brown silt-clay, occasionally granostriated and porostriated b-fabrics.

DMT

Sample 4 (Crust)

Sample 4 (Fig. 52) was collected at the start of the excavation from the crust sealing the deposit and further sliced. At the microscale the crust was very indurated with a micritic calcite cement and appeared massive with quartz grains as dominant components, and subrounded sandy-clayey aggregates cemented with secondary calcite. The crust was subdivided in two microunits (MU2a, MU2b). A fine yellow silty-clayey sediment (not cemented) was called MU2.1. At the mesoscale, vughs and channels are visible, with a sharp boundary between MU2b and 2.1.

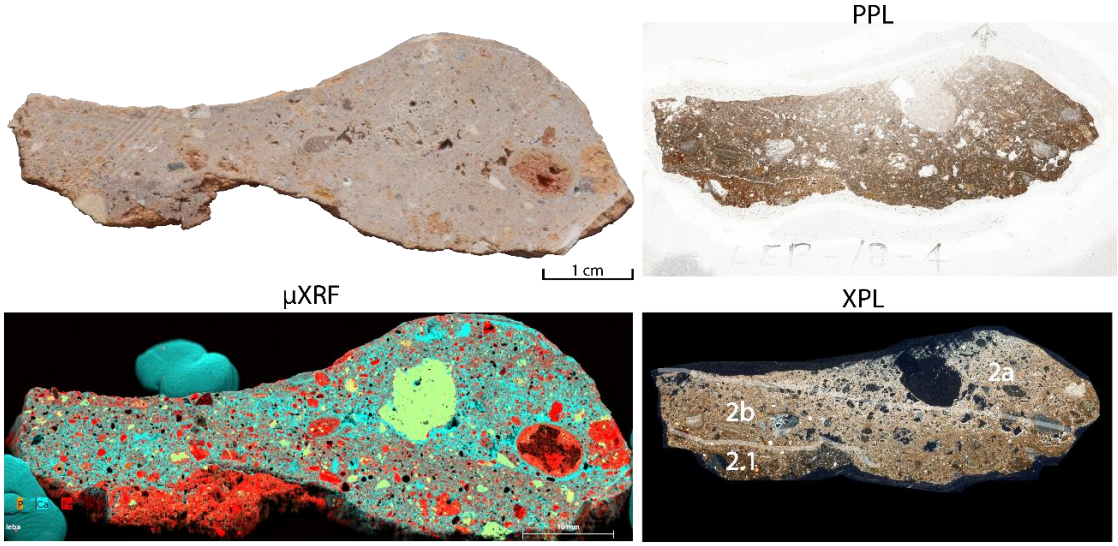

Fig. 52 – Sample 4 (crust): chip and XRF scan of the chip (on the left); thin section scans in PPL and XPL (on the right) with reference to microunits in white (thin section with 90x60 mm).

The coarse components are parallel arranged with oblique orientations. Reddish-brown silty-clay aggregates and sandy-clayey aggregates and biological elements such as teeth are visible to the naked eye. Fine sand-sized fragments of bone are frequent and

scattered with a generally parallel arrangement. Bedrock fragments such as chert are frequent as subrounded sand grains. Sand-sized grains are dominated by quartz, but also calcite grains derived from flowstone. Yellow medium sand-sized silty-sandy lithocasts are also present deriving from the hanging breccia.

Medium sand-sized grains from erosion and disaggregation of the calcite films and dripstone in the wall directly above the excavation area were also observed. They have sharp boundaries and rounded edges and are reworked. These have been associated with the weakly bound structure of the calcite-forming minerals to the underlying rock wall which is easily loosened by the action of microorganisms or percolating solutions rich in organic matter, or even by the alternating cycles of wetting and drying which may also favor the formation of a new layer on the floor containing dissolved calcified fragments (Courty et al., 1989, p. 200). They are different from the micritic and secondary calcite infilling the void space between packing voids.

The biogenic coarse components are also rounded. It is not clear whether the bone material is derived from anthropic action or carnivore activity. Because a few stone tools were identified in the stratigraphy could be a case of an anthropogenic-derived midden in the rear of the cave. The bones do not present signs of heating but are remineralized by secondary precipitation of carbonate.

Secondary features observed are mainly associated with water dripping from the walls and roof. The phenomena caused the formation of calcite nodules which infill the void space between aggregates and laminations, forming a seal of the deposit and is a good indicator of preservation of the original depositional structures. Calcite nodules completely infill the pore space as micritic coatings of microaggregates bridging them and creating locally chito-gefuric distribution patterns.

The question about the timing of the formation of crusts is difficult to address and not consensual among authors. Usually mean the deposit would have been exposed to seeping water or runoff over a long time, possibly several hundreds of years. In the case of the rear of Leba Cave, water dripping from the wall was observed almost year-round and is more intense during the rainfall season.

Samples 171/172

These samples refer to the column collected in area DMT. Because of the induration of the deposit, it was easier to collect a full column at the corner of quadrant C. Conventional procedure using manual methods was impossible to control and for this reason, it was necessary to resort to an electric disk which allowed to clean cut the sides of the column and finally remove it with a spatula. Due to difficulties during collection, the column was

divided in two block samples called 171 and 172, from top to bottom. Sampling relicts are visible in the thin sections, particularly in the thin sections from sample 172 (Fig. 53). Six thin sections were produced in total, three thin sections from each block sample.

Analysis of the chips showed the entire deposit was made up of cm-thick laminations of red and yellow sands, intercalated with trains of subrounded clasts. The clasts included bedrock debris, hanging breccia, red and yellow sandy clayey granules, and organic components of biological origin.

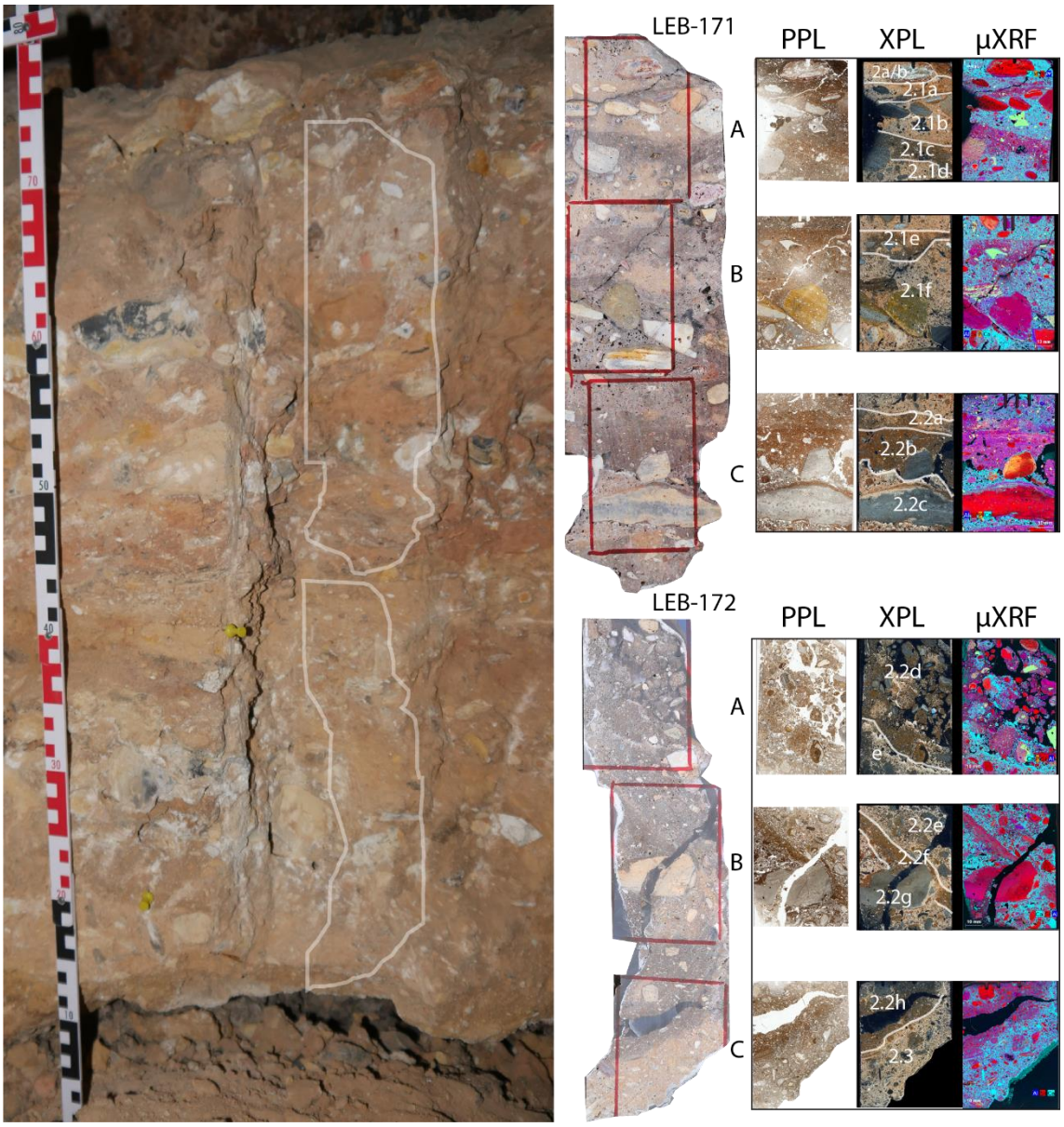

Fig. 53 – Block samples collected in area DMT with low-resolution scan of chips (top to bottom, LEB-171A, B, C, LEB-172A, B, C), thin sections in PPL and XPL with references to different microunits (in white); and low-resolution scans with microXRF with main elements Al (dark blue),Si (Silicon), P (orange) and Ca (light blue), (thin sections with 90x60 mm)

A total of 16 contacts were detected through the column and 17 microunits were described individually. The boundaries are particularly evident in XPL and low-resolution

µ-XRF scans by the occurrence and degree of secondary carbonate development in each lamination (Fig. 53).

This type of collection allowed us to obtain a clean section which was not possible during excavation due to the induration of the deposit. Observation of the field section it became apparent that the deposit which seemed like a diamicton had microstratification.

Analysis of the chips suggested the entire deposit was made up of cm-thick laminations of red and yellow sands, intercalated with trains of subrounded clasts. The clasts included bedrock debris, fragments of the hanging breccia, red sandy clayey granules, and organic components of biogenic origin.

The top of the column has two microunits, analogous to sample 2 (crust) collected at the start of the excavation.

Only a small portion of MU2a is visible in the thin section, on the upper right corner, and corresponds to a dark brown clayey aggregate with few quartz silt grains and abundant organic amorphous material forming thinly packed laminae. The aggregate is completely coated with micritic calcite showing a weak birefringence and is probably associated with guano.

The seal covers MU2b, a thick lamina (1 cm) with an intergrain microaggregate microstructure. At the top, a subrounded bedrock clast (4 cm) shows pellicular alteration. The clast is coated with different laminations of yellow silt-clay and red sand-clay of about 100 µm forming complex coatings. Rip-up clasts (Fig. 54) composed of thinly bedded fine sands with micro-bone fragments and fine undulating planar voids infilled with calcite show the same groundmass as the lower unit, suggesting an erosional phase. These features suggest the translocation of the gravel across different surfaces until reaching the current position indicate the gravel was deposited after. Rip-up clasts are typical of hyper concentrated flows (Karkanas and Goldberg, 2018a)

Across the profile, microlaminated coatings are present on the gravels. The unit is poorly sorted with abundant Subrounded coarse and medium sand-sized rounded grains of chert-dolostone, occasional well-rounded single quartz grains among microaggregates of different sizes, rounded.

The aggregates are composed of fine quartz sand, coated with silt and dusty clay. Bone fragments have different sizes and shapes, but range mostly from 200-600 µm, with few coarse elements up to 1.5 mm.

At the microscale, MU2b has a double-spaced fine enaulic c/f related distribution pattern and shows complex packing voids between grains and aggregates. Porosity is high (25%) but the voids are coated with secondary carbonate, at times completely infilling the space and bridging aggregates. Secondary calcite was observed in micritic and sparitic calcite coatings following the void space, reaching a maximum thickness of 120 µm. The lower boundary is sharp and outlined by a fine planar void cemented by the calcite. Characteristics of the boundary and the rip clasts suggest the underlying micro-unit was already cemented before the deposition of this gravel lense.

MU2.1a (Fig. 54) is a more compact unit with 1 cm of thickness, showing a similar microstructure as above but with a fine enaulic c/f related distribution pattern, few channels, and vughs (5%). Bedrock fragments of chert are present as well-rounded subangular fragments. Yellow silty-sandy aggregates deriving from the hanging breccia and red-brown bimodal sands are also present and well-rounded, showing inherited oxic features. Inherited and well-rounded iron nodules with quartz fine inclusions are also present. Sand-sized bone fragments are frequent (5-10%), ranging from very fine well rounded prolate and oblate particles to elongated angular medium sand-sized grains. More than half of the fragments detected appear burned, with the typical orange gloss. The unit is cemented by micritic calcite and the bone fragments are remineralized by secondary carbonate. Pedofeatures observed in the unit include mamilate and digitate manganese staining and iron nodules. Dusty coatings, hypocoatings, and quasicoatings of coarse grains are common in both internal and external features. The matrix was further cemented with micritic calcite with tabular habit following the void space. The lower boundary is sharp and undulating.

MU2.1b is 3 cm thick and is characterized by a gravel lense with parallel arranged and accommodating well-rounded aggregates with coarse bedrock fragments. In thin section, these components have a sandy clayey thick coating suggesting translocation of the grains. A mammal tooth (1 cm) is located under the coarse bedrock gravel and is parallel-oriented in relation to the gravel lense. Fine bone components, soil aggregates, and sand-sized grains show complex packing voids, with an intergrain microaggregates microstructure with single-spaced to equal enaulic c/f related distribution pattern. The lower boundary is sharp, and planar but inclined with a soft gradient of 9o south, towards the rear wall of the cave. The unit is heavily cemented by sparitic calcite with a tabular habit, infilling the void space. In regions where microaggregates are more separated and pores are larger, the calcite forms spherical crystals.

MU2.1c is a unit with a thickness of 1.5 cm and an open porphyric distribution pattern, composed of poorly sorted granules and sand size aggregates randomly distributed and by micritic calcite. Coarse components are generally rounded, with sharp and smooth edges. Rock fragments of chert and dolostone fragments are occasionally angular and frequently coated with red and brown dusty clays. A coarse well-rounded siltstone on the left shows a silty-sandy coating similar to the groundmass. Angular medium sand-sized grains of claystone were also observed but are rare. Well-rounded quartz single grains, frequently coated with brown and red dusty clays are frequent, just like the soil aggregates with inherited Fe-Mn pedofeatures, which are associated with allochthonous sources.

Subrounded rounded silty clayey yellow aggregates composed of angular silt-sized quartz grains were also observed, ranging from fine sand-sized grains to granules. The fine fraction is dominated by quartz silt and occasional mica. Organic components are almost exclusively bone, ranging from 200 µm to pebble-sized bone shafts (15-25%). These particles are rounded and remineralized. A Mammal tooth is visible in the center of the thin section with 7mm. A coprolite with granular inclusions is also visible in the near vicinity of the tooth. Fragments of red clay pedofeatures with undifferentiated b-fabric are also identified. Indeed, pedofeatures like coatings and quasicoatings observed appear inherited. In-situ mamillated and dendritic Fe-Mn nodules are moderate to highly developed, and associated with geogenic grains and organic components. Cementation by secondary carbonate was observed as micritic calcite coatings of grains and pores. The lower boundary is undulating and diffuse.

MU2.1d is 3.6 cm thick and more porous, showing a close fine enaulic c/f related distribution pattern, although in some instances may appear chito-gefuric due to secondary features coating and bridging aggregates. Coarse components are the same type of siliceous aggregates described above but more variable in size and shape. Subrounded red sandy-clayey aggregates with smooth edges and subangular yellow silty sandy aggregates with rugose edges show random distributions and orientations that dominate this unit. Bone fragments are frequently embedded in these sediment aggregates but are also observed as single particles, ranging from very fine sands to granules. Occasional fragments of carnivore coprolites are also visible. Mamillated and dendritic Mn nodules are moderately developed while cementation with micritic and sparitic calcite is strongly developed. The lower boundary is sharp and appears linear in low-resolution, but undulated at the microscopic scale suggesting erosional contact.

MU2.1e is 1.6 cm thick and has a double-spaced porphyric c/f related distribution pattern. A coarse bone is aggregated in a fine grey dusty material and surrounded by reddish sandy-clayey aggregates. Bedrock fragments of chert and dolostone are coarse to fine sand-sized grains randomly distributed and parallel oriented. An inherited coarse Mn nodule with internal fabric visible was cut by the sampling. Fine anorthic fe nodules are also observed across the matrix. Mamillated and dendritic Mn staining features are weakly developed, and associated with bone material.

MU2.1f (Fig. 54 - Fig. 55) is about 7 cm thick, and only part of the top is represented in thin section 171B. The microstructure is characterized by a coarse enaulic c/f related distribution pattern. The unit is dominated by angular to well-rounded gravel-sized components deriving from the Hanging breccia observed on the roof of the cave. This is evident by the inherited yellow coatings with drying cracks, sandstone, and siltstone fractions, which have been observed in other thin sections. The coarse well-rounded lithoclast in the middle of the thin section is bimodal and lightly bedded indicating a fluvial-karst origin. The clasts are parallel-oriented and closely accommodated. Inherited Fe-Mn nodules with internal fabric of silt sand-sized quartz grains with sharp boundaries are also present in this unit, and visible at the top of thin section 171C. A coarse fragment of flowstone is part of the gravel lense, showing a secondary formation of calcite.

MU2.2a (Fig. 55) has about 1.5 cm thickness and is characterized by accommodating rip-up clasts with a fine enaulic c/f distribution. The lower boundary is erosional and clear at the mesoscale by interconnected undulating planar voids. Coarse components are bedrock fragments and bone, generally randomly distributed, but lighter particles show oblique orientations, with inclinations translating the direction of flow towards the south wall of the cave.

MU2.2b is a compact unit with a maximum thickness of 2 cm. Few fissures and channel voids with undulating walls are observed. Coarse components are subrounded and parallel oriented in relation to the surface, which appears crusted by a silty-clayey sediment of about 0.7 cm. Bone fragments are frequent. Secondary carbonate is weakly developed and features are dominated by micritic calcite coatings. Contact with the lower unit is sharp and undulating and is coated with sparry tabular calcite.

MU2.2c is a gravel lens with 3 cm thickness, composed of bedrock subrounded grains and coarse red sandy clayey granules with inherited pedofeatures and bone sand (250 µm), with a coarse enaulic c/f related distribution pattern. Coarse well rounded single quartz grains and iron-rich sandy-clayey aggregates indicate an allochthonous source in

the river valley. The gravel components have microlaminated coatings (Fig. 55), indicating translocation, similar to what is observed in the coarse components of MU2a.

Cementation is evident by well-developed carbonate secondary features with sparry calcite, in some instances forming large nodules. In the field, these crystals were spherical and botryoidal; at the microscopic scale they appear tabular and in areas where void space is wider, they have four microlayers intercalating tabular-acicular forms, suggesting several phases of generation (Fig. 55).

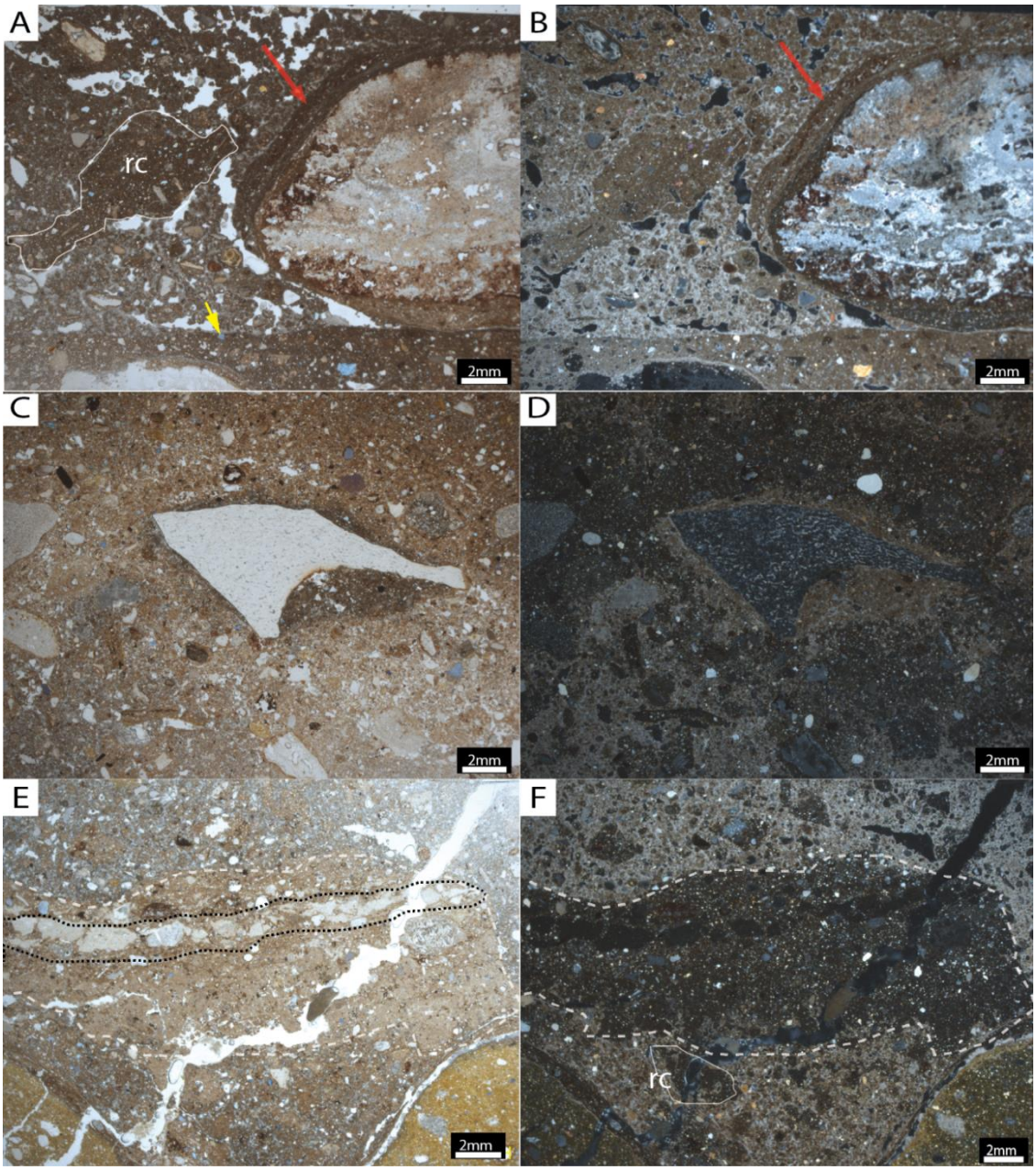

Fig. 54 – Microphotographs from samples 171A and 171B; A: MU2b, Rip-up clasts with bone inclusions (rc), after bedrock gravel hyperconcentrated fows, note the erosional contact (yellow arrow), and microlaminated coating of bedrock gravel (Red arrow) MU2.1a; B: Same in XPL; C: Sample 171B, MU2.1e, coarse bone aggregated to fine silty grey material; D: same in XPL; E: dissolved bone (dashed black) in a pale yellow phosphatic crust probably from a coprolite, F: same in XPL, note the undulating

lower boundary, the very fine sand and silt quartz grains in the phosphatic crust (dashed white) and a rip-clast (rc), suggesting translocation.

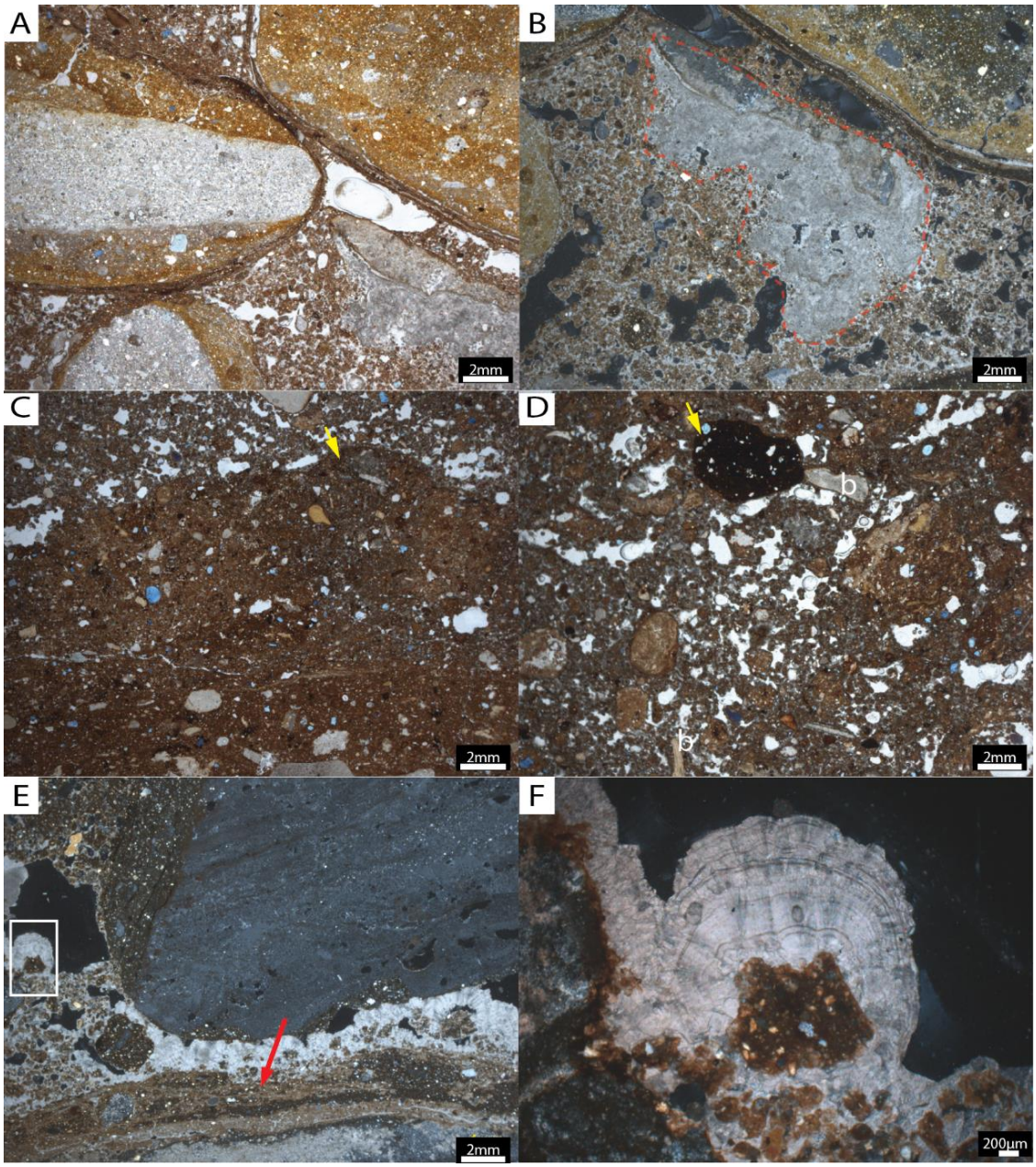

Fig. 55 – Microphotographs from samples 171B and 171C. A: MU2.1f, subrounded lithoclasts from the hanging breccia, with interbedded bedded siltstone-claystone, note the goethite rich yellow from fluvial-karst deposit suggesting rockfall and translocation of debris eroding from the roof; B: fragments of flowstone accommodating with B from the erosion of calcite films on the walls reworked with the hanging breccia clasts, and recemented; C: Contact between MU2.1f-MU2.2a underlying the trains of clasts, note the rip up clast (yellow arrow) of the crust surface in 2.2a; D: inherited Mn nodule with internal fabric (yellow arrow) typical of laterites of oxisol horizons, note the angular shape and sharp boundary; E: MU2.2b, loose packing of bedrock gravel with microlaminated coatings of silt-clay and sand-clay (red arrow) from translocation across the site, note the poe space cemented with with tabular calcite nodules; F: Same, detail of the tabular calcite nodules (white square in E) coating the microaggregates, several layers suggest several phases of secondary deposition of calcite

The lower boundary is sharp and linear to the naked eye, but undulating and erosional. The contact has several rip-up clasts with undulating and rugose edges. These clasts are composed of quartz silt and silt, coarse bedrock grains, and many bone fragments

ranging from coarse to fine sand-sized grains. Medium-sand-sized claystone angular fragments were also observed. The unit is further represented in the sample below.

Sample 172 has several sampling relicts visible through the three thin sections produced, and these seem to follow planes of weakness or less cemented microunits.

In thin section 172A, the top of the sample is partially broken by the sampling, however, it is clear the laminations are inclined and dipping towards the back of the cave.

MU2.2d is composed of very coarse rounded aggregates with poorly sorted sands and quartz silt, fragments of bone, and teeth, coated with micritic and sparitic calcite. Bedrock fragments are gravel to medium-sand-sized grains of chert and dolostone. Coarse bone and teeth are abundant in these coarse aggregates showing a single-spaced enaulic c/f related distribution pattern. Subangular to well-rounded medium and fine yellow grains with quartz silt and goethite micromass also occur deriving from the hanging breccia. Fe-Mn inherited nodules were also observed. Secondary features observed consist of Mn dendritic staining, weakly developed in groundmass but strongly developed in bone aggregates. Secondary carbonate features are strongly developed along the surfaces of grains and in intra-aggregate void space. are mostly related to the cementation of the deposit. The unit appears bioturbated before sparry calcite-coated grains and infilled pore spaces. In some domains, calcite infills wide pores (>3 mm) forming circular and eccentric forms shapes. The contact is sharp, inclined, and undulating.

MU 2.2e has about 6 cm thickness and is characterized by a coarse enaulic c/f related distribution pattern. Granules of fluvio-karstic origin with clear well sorted and laminated silt-clay with bedrock inclusions show undulating and rugose edges deriving from waterlain units in the system were observed. Coarse sand-sized aggregates with bedrock fragments are rounded or subrounded and are randomly oriented. Angular dolostone and banded chert-mudstone debris are frequent but aggregated, sometimes showing microlaminated sandy-silt and silt clay coatings suggesting translocation of the grains. Pure clay red clay aggregates with undifferentiated b-fabric and inherited Fe-Mn nodules are also present, deriving from an allochthonous source. Well-rounded coarse quartz grains are embedded in the aggregates. Bone fragments are frequent and range from very coarse to fine grains. Coarser elements have sharp undulating edges, while finer elements appear more sub-rounded. Secondary cementation of the unit is characterized by sparitic calcite with tabular habit. These features follow the pore space and surfaces of grains, with domains filled reaching 3 mm of thickness and bridging the microaggregates and coarse grains.

MU2.2f is a thin lamination 0.6 mm thickness with a massive microstructure with an open porphyric c/f related distribution pattern. Coarse components are dominated by medium sand-sized chert and dolostone subrounded fragments and a few well-rounded coarse and medium-sand-sized quartz grains, embedded in a matrix of quartz silt and reddish-brown clay. Yellow silt-clay goethite-rich aggregates are rare, and may include coarser inclusions of the bedrock likely derive from the hanging breccia. Bone material is also rare (<2%), as only a few well-rounded grains smooth with an orange gloss were detected, no larger than 250 µm. Inherited Fe-Mn pedofeatures are visible in aggregates. In situ, pedofeatures are dendritic Mn staining weakly developed. The lower boundary is sharp and undulating, and rip-up clasts indicate an erosional contact. It seems MU2.2f acted as a crust, but micritic calcite is only visible at the base.

MU2.2g has a maximum thickness of 3 cm and is inclined with a dip of 40 degrees. The unit is very loose with a coarse enaulic c/f related distribution pattern. Coarse components include gravel and granule-sized fragments of bedrock (chert, dolostone, and siltstone grains) with subangular to rounded shapes, and smooth edges. Dolostone fragments show coarse cubic pyrite crystals. Cherts and siltstones show inherited oxic features but are frequently altered. Reddish brown aggregates range from subrounded coarse sand-sized particles to very fine microaggregates, with undulating and rugose edges. These aggregates are composed of angular quartz silt and poorly sorted bedrock grains. Fragments of claystone from allochthonous sources were also observed with inherited clay pedofeatures. Bone material is frequent, and also poorly sorted. The fragments are remineralized. Carbonate secondary features are strongly developed, and characterized by tabular calcite-sparitic coatings of pores and grain surfaces. Dendritic and mammilated Fe-Mn staining is strongly developed, but in some instances appears inherited.

MU2.2h has a maximum thickness of 6 cm, although only the lower portion is represented in thin section 172C. The unit has an intergrain microaggregate microstructure with complex packing voids and a double-spaced fine enaulic distribution pattern. Coarse components are randomly distributed and poorly sorted, and include pebbles, granules, and coarse sand-sized aggregates including fragments of bedrock with subangular to rounded shapes. Chert-dolostone and dolostone grains show pyrite crystals, and silt-clay goethite-rich coatings, related to inherited oxic features. The matrix is brown with abundant silt-sized angular quartz grains coated with brown clay. Coarse to fine yellow silty-clayey well-rounded grains deriving intra-cave infills are present and distinctive by the goethite micromass. Organic components are represented by bone fragments. Coarse and medium sand-sized bone fragments are subangular with sharp

undulating and rugose edges. Few well-rounded fine bone particles are also present. Dendritic Mn staining is weakly to moderately developed. Secondary carbonate formation is weakly developed with sparse micritic coatings. The lower boundary is sharp and undulating, and a coarse elongated rip-up clast suggests an erosional contact

MU2.3 has a maximum thickness of 4 cm and shows an intergrain microaggregate microstructure with complex packing voids with a single-spaced fine enaulic distribution pattern. Coarse components are poorly sorted and include pebbles, granules, and coarse sand-sized aggregates with coarse inclusions, either bedrock debris with a subangular shape or well-rounded chert-dolostone grains. The matrix is reddish brown with abundant silt-sized angular quartz grains coated with brown clay. Coarse to fine yellow silty-clayey well-rounded grains deriving from the hanging breccia are present and distinctive by the goethite micromass. Fine red and yellow clayey rounded aggregates also occur (2%) as well as inherited Fe nodules in the same size fraction. Quartz well-rounded grains from allochthonous sources are embedded in sandy-clayey aggregates, frequently including bone. Biological elements are exclusively represented by bone. Elongated coarse shafts (>3 mm) were observed, but sand-sized bones are more frequent, ranging from coarse subangular to rounded fine particles. Dendritic Mn staining is weakly to moderately developed. frequently associated with bone and bedrock fragments. Secondary carbonate formation is strongly developed and characterized by micritic and sparitic calcite infilling the pore space and crusting coarse components. The lower boundary is crusted with sparitic tabular and acicular calcite secondary carbonate, forming a calcitic crust of 1 mm.

Overall, the micromorphological analysis of the column reveals a history of different erosional phases of intra-cave rockfall and aggregates from allochthonous sources and cementation. This is evident by the intercalation of simple and complex microstructures, and alternating enaulic and porphyric c/f distributions. Coarse gravels intercalate with sandy laminations of loosely packed aggregates composed of heterogeneous elements, including debris from the bedrock (siliceous and carbonated). Elongated and subrounded fragments deriving from rockfall and disaggregation of the walls and roofs include former infills like the hanging breccia, intercalate with allochthonous aggregates from the outside of the cave. Adding to the presence of rip-up clasts in the gravelly laminations it seems fair to assume these materials relate to hyper-concentrated flows described by Karkanas and Goldberg (2018a).

Mammal bone is abundant across these microunits, but poorly sorted and more frequently as inclusions in rounded silty and sandy aggregates which suggest some

degree of translocation. Several teeth were observed in the thin sections. The bone material is fossilized and is possible to observe the secondary carbonates crusting even the smallest particles.

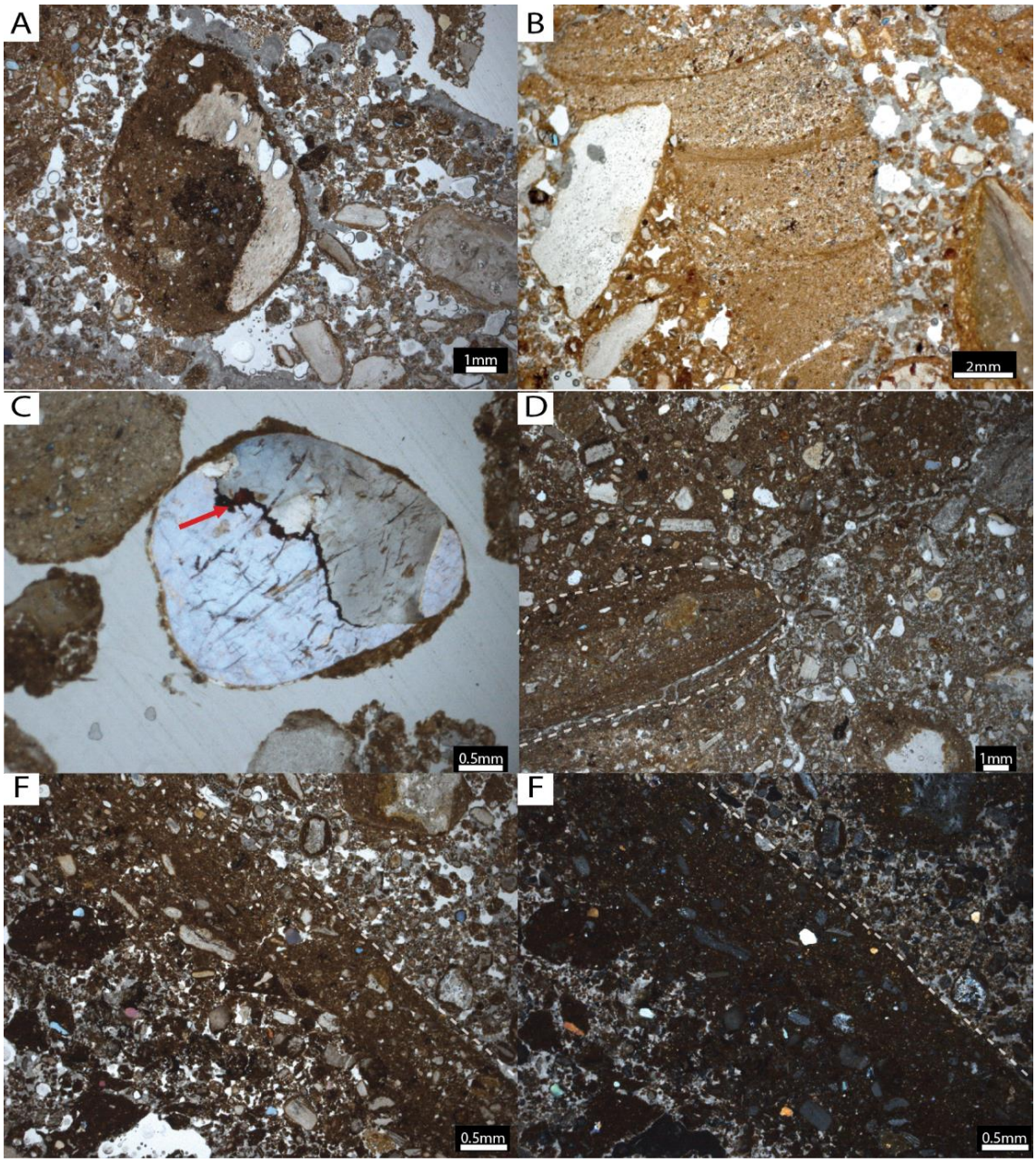

Fig. 56 – Sample 172A-C; A: coarse aggregate of dung with coarse bone and in loose microaggregate microstructure cemented with sary calcite; B: fluvial-karstic aggregate with coarse inclusion, note the fine laminated clays and silts of the aggregate; C: Well rounded coarse quartz grain with inherited Fe staining; D: MU2.3 rounded rip-up clasts (white dashed line) ; E: Crus t in MU2.2f (white dashed line, suggesting stasis and preserved surface; F: same in xpl, note the compacted structure and absence of secondary calcite infilling pore spaces as the surrounding groundmass, intercalation of fine enaulic and porphyric c/f distribution.

6.2. Absolute dates

6.2.1. Radiocarbon ages

Absolute dating of the assemblages focused on collagen from mammal bone with anthropogenic modifications either burning or cut marks. Preliminary FTIR analysis of the bone fragments suggested collagen preservation was generally low across the site.

Collagen preservation was first assessed through the nitrogen content of the untreated bone. This measurement compares the ratio of nitrogen mass to the sample mass which is measured through an elemental analyzer. The technique is commonly known as %N. The minimum threshold of 0.7% N is generally accepted as sufficient protein content for radiocarbon dating to be carried out (Brock et al., 2012). From a total of 22 samples screened for collagen content, only four reached this minimum threshold of 0.7% N (Table 21).

^{14}C age results were calibrated using OxCal (v4.4, Bronk Ramsey 2021). When plotted against the calibration curve, all samples returned an age younger than 1000 AD. Interestingly, sample LBC-42 returns an older date (909 cal BP, 95,4%) than the stratigraphically deeper samples LBC 15 (854 cal BP) and 18 (836 cal BP) which seems to indicate post-depositional movement of the samples. Interlayer bioturbation was initially identified in the field of stratigraphy and micromorphology analysis. Although there is little micromorphological representation of GU 5 to 7 in squares M/L-5, field observation of burrows in these horizons suggests some degree of mixing. This seems particularly true for the infillings deposited before the occupation related to the combustion feature. A curve plot of the radiometric dates shows how these samples concentrate at ages younger than 1000 AD (Fig. 57).

The ^{14}C data was obtained from a vertebra with cut marks and ochre traces found in GU3 sediments associated with the combustion feature located in the last occupation before the colonial warehouse (GU2) at 1694 years AD (326 cal BP).

These dates were crucial to propose an age range for the deposits infilling the first chamber of Leba Cave. They are not surprising since pottery fragments and polished tools are found in these horizons.

Sample	Code	GU	Depth	Notes	C14 age BP	±1σ	2σ range cal BP Lower	Upper
LBC-2	ETH-104484	3	-0.845	v. c.	326	21	461	309
LBC-42	ETH-112947	5	-1.243	b.b.	909	22	1043	1213
LBC-15	ETH-112946	6	-1.477	b.b.	854	22	1160	1259
LBC-18	ETH-104485	6.1	-1.673	b.b.	836	23	786	696

Table 21 – List of samples from area VOJ analyzed with radiocarbon ^{14}C: LBC-2 vertebra with cutmark (vc); LBC-42, 15, and 18 from burned bone (b.b)

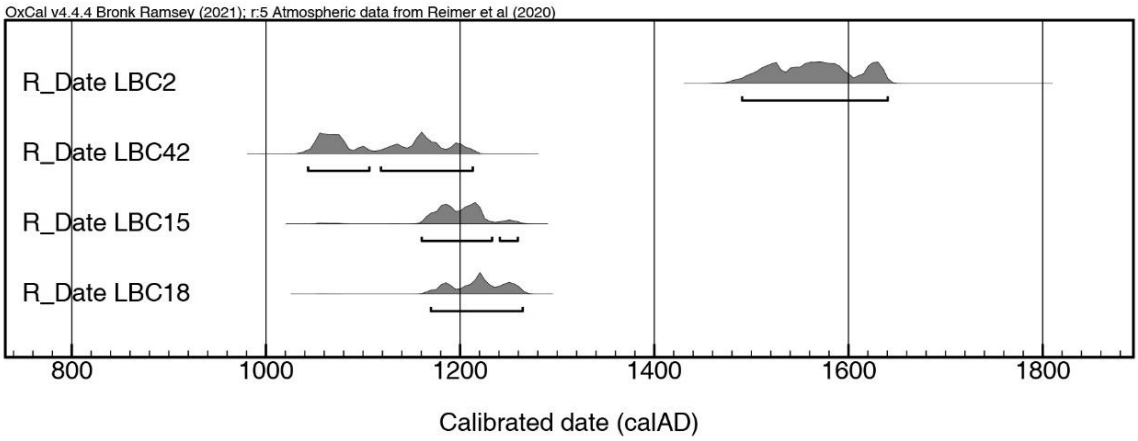

Fig. 57 – Age calibration of ^{14}C dates obtained from collagen samples of area VOJ.

6.2.2. Other age measurements

Quaternary dating methods like Optical stimulated Luminescence (OSL) and Uranium series combined with Electron spin resonance (combined US-ESR) are being used to date sediments and fossil material, respectively. Combined US-ESR are being employed to date the tooth enamel mineral hydroxyapatite, which will provide a direct dating of anthropogenic occupations beyond the limits of ^{14}C.

On burial, hydroxyapatite minerals or sedimentary minerals undergo exposure to energy emissions released by natural radioactivity present in sedimentary beds through hundreds or thousands of years. Within their crystal structure, these minerals store a small proportion of the energy delivered by environmental radiation (a rechargeable battery provides a useful analogy). The energy stored by the material is the equivalent dose or De (expressed in Gray—Gy) and is measured in the laboratory. The equivalent dose is divided by the amount of energy that the sample receives from its surroundings each year, called the annual dose or Da (expressed in Gy.ka-1 or µGy.a-1). From this, it is possible to calculate the duration of time that the sample has been receiving energy and therefore, an age.

Combined US-ESR age estimates are the result of a rigorous analytical process that combines fieldwork and laboratory activities: 1) sampling and in situ measurements; 2)

sample preparation; 3) determination of the equivalent dose; 4) determination of the annual dose and 5) age calculation.

For Leba Cave, steps 1,2, and 3 are completed. The team awaits ICP data (Uranium and Thorium contents + ratio) to finalize steps 4 and 5 (E. Ben Arous, pers. comm.).

For OSL dating, the principle is the same as for ESR, except that OSL is applied to sedimentary quartz and feldspar grains, and dates the last time these grains have been exposed to (a sufficient amount of) light.

Two sediment samples have been taken under subdued orange light at "the back trench". 100-140 µm quartz and feldspar grains have been extracted through mechanical and chemical processes. Quartz has been preferred however for the subsequent measurements because it bleaches more rapidly than the feldspar grains (i.e. it might have fewer issues with zeroing of the signal at the time of deposition). Preliminary measurements for sample LEBA2 show that 80% of pre-selected grains are saturated (the dose recorded is too high for being determined with the standard single-grain protocol). The remaining 20% have a mean De close to 260 Gy, but this must be confirmed with more measurements and a consolidated protocol and the performances of the current one suggest it is likely a minimum De. Most of the measurements have also been performed for the determination of the dose rate, which is close to 1.8Gy/ka. Consequently, a preliminary age of 150 ka is calculated for sample LEBA2, but this must be considered as a minimum age for the sediments (C. Tribolo, pers. comm.).

7. Discussion and conclusions

7.1. Depositional processes

The micromorphological study combined with field observations of sedimentary units and dynamics of the cave system, provide new insights into the infilling of the cave. Several erosional phases and a long history of biological activity resulted in a complex depositional environment. Part of the sedimentation and erosional phases may be hard to reconstruct but the infillings currently observed inside the cave offer clues about the sequence in which these occurred.

The depositional processes observed in the front of the cave are recent, and it's clear the chamber was at least partially eroded, likely more than once. The base of the stratigraphic sequence recorded in area VOJ was dated to the historical period, post-1000 AD. Components deriving from anthropogenic activity are frequent throughout the sequence which suggests human occupation was occurring at the site. Excluding the colonial floor and the combustion feature, these deposits are chaotic and structureless with a matrix dominated by quartz and mica silts from aeolian sources. Numerous clasts from bedrock and others deriving from the hanging breccia or previous infills are mixed with components of biogenic and anthropogenic waste covering the large roof spall boulders at the base. These accumulations were the result of anthropogenic reworking (by dumping) which served to prepare the space or even the floor before the last occupation when the fire-pit was opened. In any case, before mining operations in the 1950, the phreatic tube was definitely longer and the entrance was located several meters further north than today.

Rockfall debris deriving from breakdown of the host rock across the cave suggests a permanent source of geogenic material inside the phreatic tube. The products of bedrock breakdown are a heterogenous group of sediments including different sizes and lithologies. Greyish-blue chert, siltstone and mudstones are observed across the site, frequently interbedded with dolostone, and consisting of intra-cave fragments deriving from the roof and walls. Calcite films, flowstones and dripstone fragments are some of Ca-rich coarse components, although consisting of secondary features on the dolostone bedrock.

The same mechanical breakdown of the cave bedrock seems to apply to the hanging breccia fragments which are found across the the several areas either as angular or subrounded clasts, from boulders to granules.

Sediments observed across the cave are loose and poorly sorted, and generally fall in the concept of karst colluvial processes. However, discrete micromorphological structures and features found in these colluvial sediments suggest different sources and types of deposition in the cave system involving geogenic, biogenic and anthropogenic agents. This is particularly true for the discussion of the depositional processes in area JCF and DMT.

For instance, the fragments of the hanging breccia, angular and pebble-sized, preserve bedding and offer further insights into the depositional processes in the cave before the lithification and erosion of the deposit. In these clasts, there is evidence for bioturbation and oxidation with the deposition of secondary iron (goethite) relating to fluvio-karstic conditions. They are indicative of deposition of fine goethitic clay further dried out forming cracks, bioturbated and covered with quartz silt which suggest alternating depositional regimes. It is not clear what is the timing of deposition of this material but definitely anterior to any of the excavated and sampled horizons.

Currently the original deposit is only partially aggregated to the western wall, but plenty of blocks at the center of the cave can also be a source for colluvial material. Dry flow and gravitational forces are most evident, as few waterlain sediments have been found within the studied profiles. When we do encounter evidence for water-lain deposition, like for instance in area JCF-GH3 or DMT-MU 2.2a it is associated with localized shallow water flow, likely deriving from small seeps or dripping water. In any case, different lithoclasts and aggregates from former infills, like the yellow and red bimodal aggregates which provide evidence for chambers that were infilled with material associated with former river floodplains or terraces when the river was at an elevation closer to the cave, not visible at the present day due to the slope retreat and quarrying activities.

Neverthless the comparative assessement of the samples from the inside of the cave and the control sample collected outside, on top of the hill, are consistent with a general sedimentation of the cave by collapse and mass wasting of materials from the surface or trapped in cracks and fissures, which is evident by the presence of numerous inherited pedofeatures of oxisols.

Reworked soil fragments have been found in karstic contexts, as components of heterogeneous infillings of sinkholes and karst pockets (Patania et al., 2019; Stoops et al., 2018). They can derive from colluvial reworking of surface regoliths, wind-blown dust particles, or biological transport. These particles are indicative of former environmental conditions and the existence of landscape surfaces being dismantled by erosion and further infilling the cave. Considering that all lithologies are found in the karst system,

and fine fractions are similar to the slope regoliths identified it seems fair to assume that the geogenic materials derive from cumulative processes associated with the local environmental regime with a strong seasonal variation in day-night temperature (termoclasty) during the winter and heavy rainfall (flash floods, run off) during the summer. These processes are particularly important for joint widening, cracking and fissuring of the bedrock, and control the amount, size and frequency of sediments introduced in the cave.

Unsorted and poorly sorted highly porous sediments with heterogenous elements are common structural characteristics of dry grain flows (Karkanas and Goldberg, 2018a). In the back of the cave the fine laminations, erosional contacts, and rip-up clasts are consistent with hyperconcentrated flows and phases of stasis promoting cementation and crusting. Biological input is evident and carnivore activity is the likely explanation for the high frequency of bone fragments. However, only a few coprolites were observed in the thin section, and plenty of rounded micro-bones which appear heated, showing orange gloss or lustre, suggest there is an anthropogenic origin at least for some of the bones.

7.2. Post-depositional processes

The micromorphological analysis of pedofeatures in thin section is also indicative of different post-depositional processes occurring across the site.

In area VOJ, secondary features are mostly associated with human activity and bioturbation, including a wide range of phenomena. Rubification of sediments in VOJ-GU4 is indicative of *in-situ* fire and a preserved combustion feature. Plenty of artifacts are present in the stratigraphic sequence of VOJ, but the hearth offers undisputable evidence for human occupation in the chamber and post-depositional alteration of the sediments by anthropogenic agents. The micromorphological characteristics observed in sample 521A-B suggest this was a single event around 200 years ago, judging by the radiocarbon ages obtained. Heat-induced alteration of sediments surrounding and under a hearth are commonly observed in preserved combustion features, and have been documented by experimental studies (Aldeias et al., 2016; Dibble et al., 2012; Mentzer, 2014; Röpke and Dietl, 2017).

The sediments underlying the hearth are also bioturbated by micromammal and other microorganisms, which was observed in the field. The sediments are unsorted and include abundant components deriving from biological and anthropogenic waste. Heated and non-heated bone, pottery, charcoal, excrements of different origins, allochthonous and autochtonous rocks show different sizes, shapes, orientations, and alterations, in a

fine matrix of poorly sorted sand and silt with abundant fine phosphates from the decay of organic matter. It is clear these deposits accumulated elsewhere and were dumped in the back of the chamber. Site maintenance activities and floor preparation for the occupation is the most likely explanation. This is consistent with the absolute dates retrieved from a lower depth offered a younger age than the other. Although the radiocarbon dates have a similar age range there are mixed aggregates of previous occupations in the cave. The thick structureless and poorly organized deposit observed in the field, and expressed by the crumby microstructures and spongy pattern observed in sample M4 related to VOJ-GU5 seems to corroborate this assumption. Similar features have been observed in other cave sites (Karkanas and Goldberg, 2018a, p. 111). These micromorphological observations indicate that humans were the most important post-depositional agent.

Phosphatization is clear in samples 521B and M4 of area VOJ by the presence of abundant fine phosphatic material in the matrix and features like phosphatic rinds in coarse components. The abundance of bone and excrements from different sources (omnivores, carnivores and herbivores) present in the stratigraphy of the cave suggests these sources are rather more prevalent that the geogenic phosphates from natural sediments or bedrock.

In area JCF, abundant fine phosphates can be observed in the matrix of samples M7 and M6 but it is not fully understood what is the source. Very few bone fragments were found in these thin sections, which could either indicate the phosphates are from bone material previously existing in the profile similar to the samples 50-1/2, or the phosphates derive from bat guano and other dung. This hypothesis remains to be tested with further microanalytical work.

In addition to water dripping and occasionally puddling across the profile during wet cycles, pedofeatures detected in samples from region JCF are connected to the bioturbation agents that produce biogalleries. These are expressed by the silty and dusty clay coatings, crescents, porostriated and granostriated b-fabrics observed in samples M7 and M6. The patterns observed show there were inherited pedofeatures in the sediments infilling this area of the cave, altered by illuviation. These pedofeatures are very different from those observed in the samples collected in 1950 in which carbonate nodules and matrix cementation are clear. These pedofeatures are similar to those observed in samples from the back of the cave. Evidently the post-excavation exposure of the profile added to the quarrying in the upper hill, produced a disruption in the microenvironment of the cave, air circulation and, possibly even, groundwater flow,

influencing the location and frequency of the dripping water in the cave. Consequently, water saturation of the sediments on the floor is dependent on these cycles, which ultimately vary according to rainfall.

In area DMT, features related to bioturbation were also observed but not extensively. Secondary carbonate and iron-manganese features associated with dripping water over the profile were observed both at the macroscale and microscale causing induration of the deposit as crusts, nodules and general cementation of the more porous micro-units. Cementation of geological units of the inner cave strata at Leba Cave is the result of rainfall/temperature fluctuation between wet and dry periods, with CO2-rich water dripping down the walls and roof.

Similar features were observed on the samples from 1950, coming from from area JCF. They are strongly developed in sample 50-2. However, they are not present in samples M7 and M6 collected in the same area in 2018. Clay pedofeatures, like dusty crescent coatings and infillings following the pore space, relate to illuviation in the profile and translocation of inherited clay present in the aggregates. These are related to localized puddling during heavy rainfall seasons.

7.3. Site formation model

The formation model presented here is based on the combination of the landscape work regarding the geomorphology of the plateau, observations of the cave systems across the Leba Formation, excavation work, assemblage analysis and laboratorial analysis of the micromorphology samples collected inside Leba Cave. In some instances, this model is conjectural, and some of the depositional phases may never be fully understood, due to intrinsic dynamic environment or more recent anthropogenic activity obliterating infills of the Leba karstic system. Ultimately this model highlights a complex history of sedimentation and erosion, followed by human use of the valley and the site since the Pleistocene.

The geomorphology of the site indicates that the cave genesis relates to a phreatic environment (Fig. 58, Stage I). At this stage, residual clays and other fine materials are some of the first infillings to occur through cracks and joint fissures, and conduits connecting with the surface environment. During this phase chambers at subsurficial level can already start be trapping soil materials and other sediments transported by the river.

Progressively, incision of the valley and lowering of the water table formed chimneys and pipes eventually promoting the formation of galleries at subsurficial level and possibly

passages between the subsurficial and phreatic tube. The lowering of the water table and hot conditions likely contributed to the deposition of secondary iron and cementation of the fluvio-karstic sediments. These were eventually eroded (Fig. 58, Stage II). Part of the infill remains attached to the western wall and roof of the phreatic tube suggesting one or more erosional phases and continuous disaggregation. Considering the position of the hanging breccia, and the characteristics of the lithoclasts (siltstone-gothite clays) found throughout the site, it seems the deposit represents the oldest infill of Leba, before the deposition of any artifacts inside the tube. This deposit is continuously being eroded and is a major source of detrital material being introduced and reworked inside the cave.

In some areas of the karst system, we have observed solution chambers that were never exposed until the quarrying in the 1940s as observed not too far from Leba Cave, at Tchaticuca or Cangalonge (view section 2). The solution chambers at Tchaticuca are not infilled with clastic materials, but chemogenic deposits. Secondary carbonates cover the walls and roof with ornaments, drapes, botryoidal and eccentric calcite and aragonite crystal forms. It is possible that chambers such as these were also present in the Leba Cave system and were destroyed by the quarry or eroded.

At Leba Cave, directly on the south margin of the Leba river (currently 1 km away), sediments from surface deposits progressively infill at least in the upper levels of the cave system (Fig. 58 – Schematic site formation model representing the main stages of formation and infillings of Leba Cave approached in this study.Fig. 58, Stage III). Some of the oldest chambers are at 5-6m depth, currently exposed by the quarry and there are fossil remains assigned to Early and Middle Pleistocene by other authors (Pickford et al., 1994).

The top yellow granules unit, probably formed from the disaggregation of the hanging breccia, was found at the base of the sequence investigated in area JCF, but it is not clear how thick this unit is and if others of different nature are buried under, as excavations in this are are still forthcoming. In any case, it is clear the cave was emptied out long before, and the phreatic tube was accessible. The subtriangular handaxe was found on top of the yellow unit (JCF, GU7) and was coated by a yellow cement. The tool is fresh and does not present water wear or patina frequently observed in materials transported by water or in the open-air which would imply the lithics were deposited inside the cave or suffered very little transport before deposited into its current position.

The sharp erosional boundary the basal sequence of JCF (GU6-GU7) suggests a transition from intra-cave infilling (yellow granules-bedrock debris gravel) to a red matrix sand from allochthonous source, deriving from surficial red sediments and soil cover.

The composition of the red sands (JCF, GU3-GU5) indicates a source outside in the river valley. Fe-Mn nodules are typical of Oxisols, Ferralitic and Lateritic horizons of subtropical regions (Kaboré et al., 2021; Ricardo et al., 1980; Stoops and Marcelino, 2018). In the sediments inside the cave, coarse Fe-Mn nodules with internal fabric display sharp boundaries, likely caused by transport. They are typically subrounded with undulating edges, but can also be angular like in DMT-MU2.2d, and consist of relicts of soil horizons present in the environment, possible from terraces or surfaces not observed at present. Inherited soil pedofeatures and bimodal grain sizes suggest that allochthonous sediments can have a variety of lateritic and oxisol features which do not occur in-situ. These characteristics are observed in hand specimens from the valley but also in the control sample (1x), in sample 171C from area DMT, which would imply a relationship between these aggregates. Mass wasting of materials deriving from the surface was occurring in the cave, and it is possible this sediment was introduced by a chimney currently sealed by rockfall from hanging breccia blocks and dripstone. These soil relicts can be trapped in fissures and cracks for a long time, and be transported by gravitational forces or occasional rainfall, when joint widening occurs forming conduits between different galleries. In some caves of currently semi-arid regions, tropical soil relicts have been found trapped in flowstones and interpreted as evidence of past tropical conditions (Sousa et al., 2022).

The sequence described in area DMT (consisting of about 0.90 cm of sediment) has 16 erosional contacts, between cm-thick laminae of intra-cave debris (bedrock-hanging breccia) and allochthonous sediments from the Leba valley, including coarse sands of likely fluvial origin and inherited Fe-Mn nodules from Oxic and Laterite soil horizons. The minimum age of 150 ka was obtained from luminescence measurements on quartz grains (DMT-MU2.3). Further results from the U/Th series on mammal teeth from this sequence will help the criticial assessement of the results.

The thin section analysed from area DMT revelead a series of erosional contacts between microunits with distributions associated with hyperconcentrated flows and post-depositional cementation forming a series of crusts. The rip-up clasts observed across the sequence seem to corroborate this interpretation (Karkanas and Goldberg, 2018a). The structure and composition of the deposit indicates that the intercalation of gravels derived from rockfall and mass wasting, either from the sediments at the surface or from those trapped in cracks and fissures, along with biogenic activity. The rockfall fragments and granules include material derived from the disaggregation of the roof and walls, not only bedrock debris but also lithoclasts of hanging breccia with fluvial-karstic features and coarse fragments of flowstones. The rocks, lithoclasts and aggegates observed

across the column (Samples 171/172) are subrounded with sharp smooth edges suggesting translocation of some distance, although there are no features relating to water transport. It is possible these sediments are at least partially associated with the MSA human occupations, but only a few lithics were found at the top of the sequence (MU2.1a).

The cementation of the DMT deposit was observed following void spaces forming different sizes and mineral shapes. Secondary deposition of $CaCO_3$ is promoted by water percolating through the host rock and transporting minerals in solution, which further dripped on the sediment through the walls and roof. The repetead pattern or alternation of phases of erosion and cementation forming crusts is interpreted as part of the reworking of geogenic material inside the cave followed by diagenesis which relate to alternating seasonal climatic conditions and polyphasic evolution of the cave infill. More samples from the area would be necessary to understand the lateral variation of these structures and if the overall loose pattern in aggregation (generally with crumby and granular microstructures) connect with the sediments of area JCF, and if they are related to a talus debris or a chimney currently not observed. Confirming this hypothesis will be difficult, but may only be resolved with further exploration of the galleries in the upper level.

The thin sections from area JCF show that the red units (JCF-GU3-6) have similar inherited pedofeatures observed in the control sample and in the samples from area DMT. These sediments have also been extremely altered by recent exposure to guano and dripping water causing illuviation and fragmentation of inherited pedofeatures. Sediments have the same characteristics as the components deriving from soil, or transported by the river, but they do not seem to be extensively represented at present which suggests that paleosoil relicts were distributed during the Pleistocene.

The samples collected in 2019 (M6, M7) only differ from the samples from the 1950 excavations because of secondary features. The samples from 1950 (50-1/2) suggest that the MSA layers excavated were indurated and closer resembling the pink breccia. Although sample 50-1 does not have highly developed nodules, red sandy-clayey aggregates with inherited oxic features are clearly visible. The preliminary ages for bovid teeth in the museum collection assigned to the MSA II phase (point-blade technology) was preliminarily dated to 75±5 ka.

The components from the surface in area DMT may be chrono-culturally related to the area JCF, but the scarcity of lithic materials and the abundance of fragments of bone

and coprolites, in the rear the suggests the bone may have been exclusively accumulated by carnivores.

After this phase it is hard to say exactly what happened inside the cave until the deposition of the sequence excavated in area VOJ (Fig. 58, Stage IV).

After a phase of rockfall, resulting in the accumulation of boulders of hanging breccia and bedrock from the roof, the chamber would have been cemented, since dripstone covers rock fall in area JCF.

The rockfall in the center of the cave sealed off the room where JCF and DMT are located. In the front, slope retreat and erosion of Pleistocene infillings in upper levels of the system would have occurred, and sedimentation with guano and aeolian particles would have occurred, although this is only based on the composition of the materials dumped in area VOJ and covering the central roof spall cone.

The samples from the base of square L2 show different coarse components deriving from previous infills (sample 250) mixed with biogenic components mostly derived from anthropogenic activity. This would suggest that previous infills could have been removed by humans, for instance if there were thick guano deposits like those observed in other caves in the surrounding like Malola and Cangalongue, that could have been explored for fertilizers by early farming communities in the region. Many different causes can be associated with the erosion of the infills of area VOJ anterior to 1000 AD. Seasonal flooding events and anthropic action are hypotheses to be tested in future research.

In general, the characteristics of the units investigated in area VOJ relate to a dry environment, and plenty of remnants of human occupation are introduced with other aeolian and trampled materials. No evidence of occupational floors or surfaces was found between VOJ-GU5 and VOJ-GU7, and the disparity of radiocarbon dates between strata confirm these are mixtures of deposits from different ages. Spongy microstructures, with remants of hearths and pottery, dung and guano-derived phosphatic nodules (leucophosphite) suggest these units represent dumped material, probably moved from another gallery, but also extreme diagenesis and carbonate dissolution affecting the entrance area (Goldberg and Sherwood, 2006; Macphail and Goldberg, 2018; Schiegl et al., 2003).

Radiocarbon dates from burnt bone collected in the hearth suggest the combustion feature is very young (1694 years AD). The potsherds are also interesting as they show patterns mixed between Early and Late Iron Age decorations (B. Clist, pers. comm). The lithic assemblage associated shows the presence of Levallois, little to no retouch in

finished pieces, abundance of thick scrapers, and no refinement. Lithic points are not particularly spectacular or much different from those studied in the MSA I and II assemblages (de Matos and Pereira, 2020). The preservation of cattle dung in VOJ-GU3 suggests the cave was used by herders during the last few centuries.

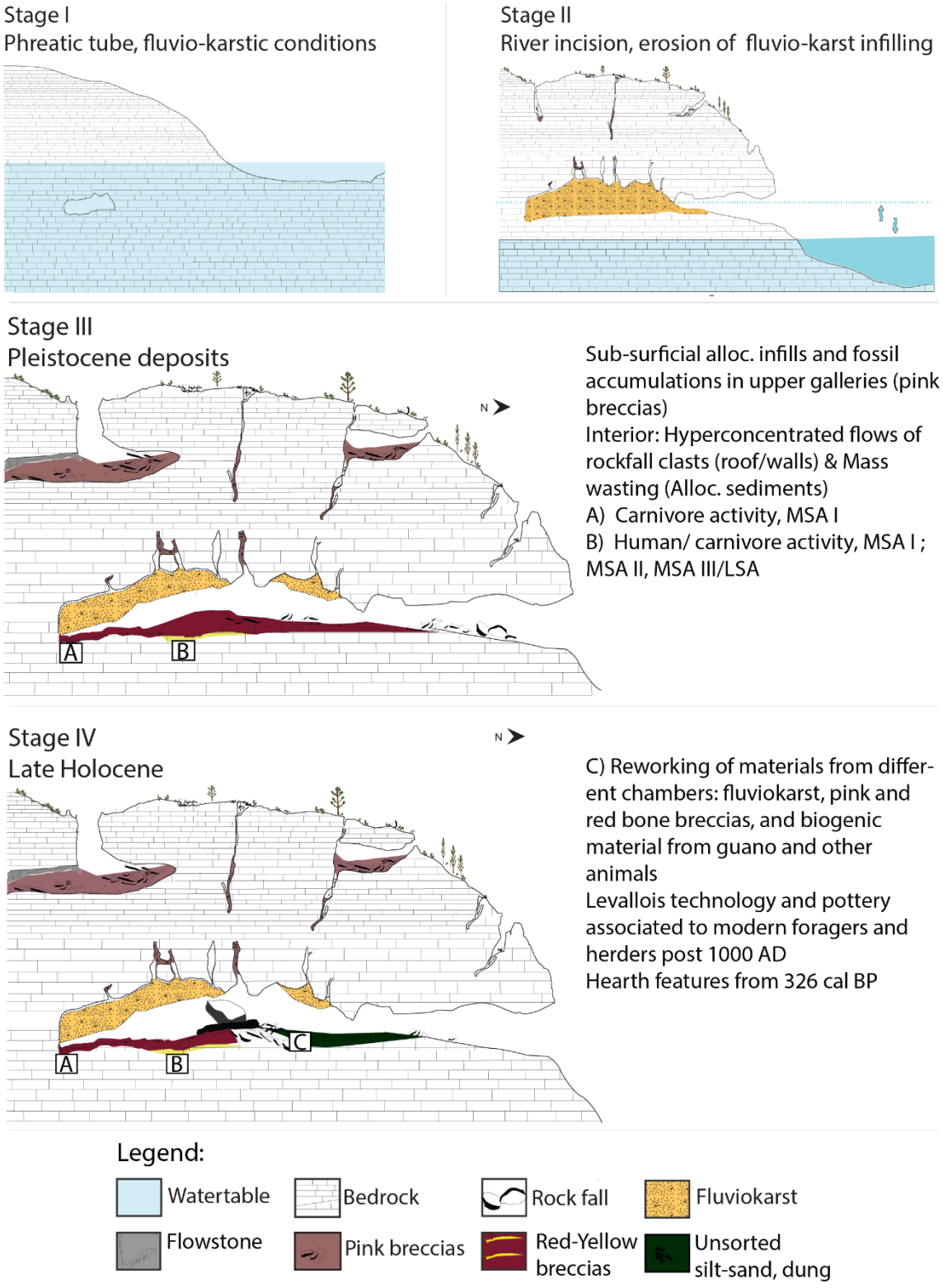

Fig. 58 – Schematic site formation model representing the main stages of formation and infillings of Leba Cave approached in this study.

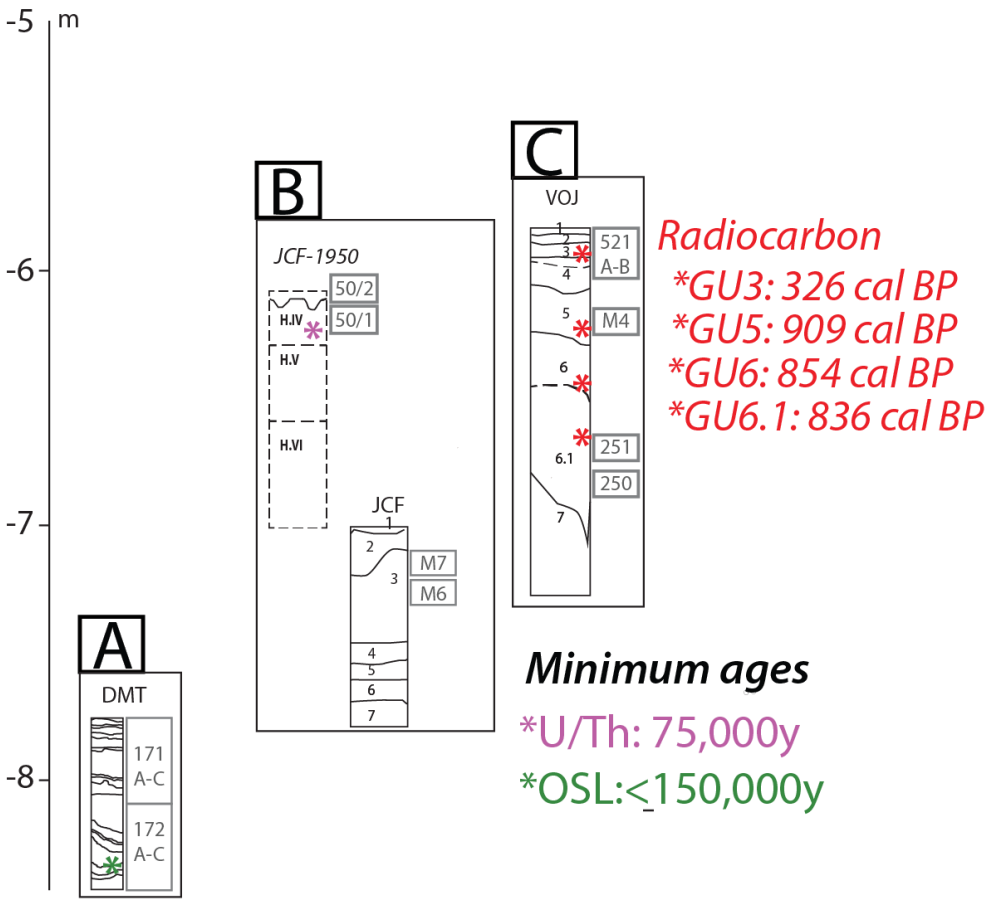

Fig. 59 – Schematic representation of infillings studied and correlating to figure 58.

Sometime between 1947 and 1950 AD, with the construction of the factory and the lime kilns in front of the cave, the upper levels of the karst system were blasted with dynamite. The quarrying caused alterations of the slope and a disruption of the micro-environment inside the cave.

Inside the phreatic tube, a colonial floor constructed of red earth bricks, pottery, limestone fragments from the quarry and other construction debris were dumped over the archaeological layers and covered the deposit. This phase would refer to a stage V

in the site formation model (Fig. 58) already presented in section 2 (

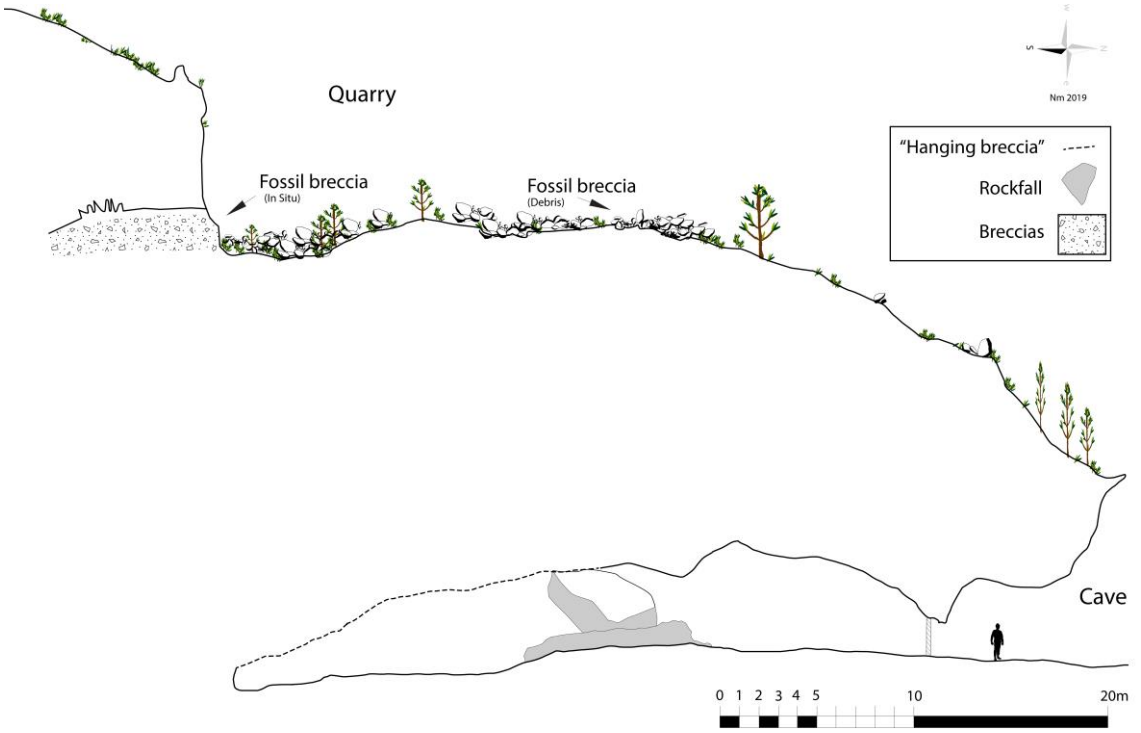

Fig. 7), as the current state of the cave. Further inside the tube, the archaeological excavations by J. Camarate-França in 1950 exposed the profile investigated in area JCF. More intense diagenesis affected area JCF, and seems to be related to incremental dissolution due to the seasonal puddling and the action of bat roosting over the excavation pit. Changes in temperature-air circulation in the recent past could have accelerated dissolution and shrinkage processes usully occurring in guano-rich sediments. It is possible that guano deposits were being removed from the cave by farming communities.

Evidently there is a gap in our knowledge between the sedimentation of the inner chamber and the recent sedimentation of area VOJ, which we are not able to explain completely. The intensity of bio-anthropogenic action in area VOJ and reworking of aggregates from past occupations suggests that anthropogenic action could have been a major factor in the removal of guani beds, but the sediments located in area DMT still preserve original sedimentary structures. This would suggest that despite the quarrying activities, other cemented deposits in the area may also contain similar structures and MSA artifacts.

7.4. Cultural variability and regional comparisons

Reconstructing the formation history of the archaeological site was the starting premise of this study, particularly aiming at the context of the deposit known for the Middle Stone

Age stone-tools and fauna. As a starting point, it was important to look for the location where the museum assemblages of the University of Lisbon were collected.

The first report about Leba Cave described a stratigraphic sequence of about 1.75 m to 2 m with six archaeological horizons, the upper two relating to the Holocene and historical occupations, and horizons III-VI with a sequence of assemblages interpreted as corresponding to the Late and Middle Stone Age. Our previous study of the lithic assemblages housed at the University of Lisbon showed the LSA assemblage was composed of mostly small quartz implements produced using bipolar reduction; while horizon IV was composed of blades and points assigned to a “generic MSA” (de Matos and Pereira, 2020). These lithic tools were associated with abundant faunal remains of bovids and primates attributed to hunting game that was burned and consumed inside the cave, but also to taphonomic agents such as carnivores (Gautier, 1995).

As described in section 2, the analysis of the faunal materials from horizon IV using Uranium/Thorium series suggested a minimum age of 75 ka for the “generic MSA” (de Matos et al., 2014). Furthermore, this would indicate that the basal levels of the 1950 excavation could relate to an early stage of the MSA, even possibly a “transitional” phase between the Early and Middle Stone Age, based on the occurrence of large cutting tools with large blades (de Matos and Pereira, 2020). These materials have been previously classified as "Sangoan” tools (Camarate-França, 1964) also called "MSA of Acheulean tradition" (Ramos, 1982).

Although we did not find preserved structures or primary deposits associated with the human occupation of the cave as described above, we found a handaxe at the base of the test pit. From our interpretation of the site, the handaxe found in area JCF is anterior or contemporaneous to H.VI of the 1950 excavation, which would then corroborate a late Acheulean cultural stage. Our site formation model also suggests that the co-occurrence of Acheulean and MSA artifacts can derive from formation processes and not from human behavior. The formation processes identified in area JCF indicate the intercalation of inner cave infilling (derived from the erosion of the “hanging breccia”) with allochthonous material derived from the surface. Mass wasting processes were observed and led to a new hypothesis that infillings in the inner part of the cave occurred through a connection with the surface through a shaft which is currently covered by flowstone and rubble.

During our fieldwork, we observed the existence of a gallery with pink fossil breccias, partially dismantled by the quarry, and connected to the surface by a vertical fissure. On the profile, we observed mammalian bone fragments *in situ*. We also observed a bovid

calcaneus in the rubble discarded by the quarry, along with other small bone shafts. This area was heavily explored by the quarry but further research may be able to define the chronological relationship with the sediments inside the phreatic tube.

Our study concludes the Pleistocene sediments are found in subsurficial galleries cut by the quarry and the innermost part of the Leba Cave, and these two areas were likely connected in the past. The formation history of the Leba Cave infillings is characterized by repeated erosion and infilling, occurring at least since the late Pliocene. A similar pattern was previously identified in the caves of Malola and Cangalongue, located in the Leba dolomites (Pickford et al., 1994). Following the development of the cave systems, there was a period of sinter deposition, followed by erosion, followed by deposition of coarse breccia, often containing fragments of cave sinter, followed by a period during which finer-grained pink to red breccias accumulated. These were then eroded to their present configurations (Pickford et al., 1992).

In the vicinity of Leba, at the caves Malola, Tchiua, and Ufefua, there are large volumes of pink breccia, some of which contain indications of its near-surface origins. Termite foraging tunnels and root holes were observed at Malola and Tchíua respectively (Pickford et al., 1992). As we saw in the micromorphological analysis, many more indicators can be found at the microscale, for instance, relicts of oxisols and well-rounded iron-impregnated coarse quartz grains of allochthonous origin infilling the cave through mass wasting. The inherited pedofeatures were observed in the samples from area JCF and DMT, and also in the museum samples from the 1950 excavation. Another major conclusion is that the faunal aggregates from the interior of the cave showed indications of movement, which suggests these are not *in situ*. This is true at least for the samples we collected and analyzed.

Nevertheless, the evidence seems to corroborate our previous interpretation that the oldest lithic assemblages from Leba Cave are Acheulean, and likely relate to a late Acheulean or early Middle Stone Age (EMSA). This cultural stage is older than 150 ka, according to the preliminary optically stimulated luminescence results, and not younger than 75 ka. These ages will be validated by electron spin resonance and uranium/thorium series of the teeth collected in area DMT currently in the laboratory.

The available data places the earliest cultural assemblages of Leba Cave in a crucial time for human evolution as it is recognized for the on-set of human cultural diversity and migration of *Homo sapiens* across Africa and beyond (Scerri et al., 2019). Since the Early Stone Age, the coastal zone of Angola has been intensely occupied by human populations. Although the Early Stone Age in Angola is only superficially explored at this

point, the high concentration of stone age sites emphasizes the importance of the region for human subsistence (de Matos et al., 2021b). This was likely due to the rich and diverse food sources from marine and terrestrial fauna. Particularly marine food resources may have played a key role as these were explored at Baía Farta, Benguela, since the Middle Pleistocene (Chazan and Horwitz, 2006; Gutierrez et al., 2010; Gutierrez and Benjamim, 2019).

The fieldwork promoted by the National Archaeology Museum of Benguela since the 1980s detected a total of thirteen locations with lithic materials at Dungo assigned to different cultural periods from the Acheulean to the Late Stone Age (de Matos et al., 2021b; Pais Pinto, 1988). Specifically, at the site Dungo IV, the burial of lithic tools associated with scavenging of stranded whales was estimated between 614.5 ± 9.5 ka and 662.05 ± 10.24 ka (Gutierrez et al., 2001; Gutierrez and Benjamim, 2019; Lebatard et al., 2019 (Gutierrez and Benjamim, 2019; Lebatard et al., 2019).

Numerous open-air sites along the coast from Baía Farta to the Cunene River mouth are known for Acheulean assemblages. Other surface occurrences have been detected incisions further inland the semi-desert plains and hilly country dividing the Namibe and Huíla province frequently exposed by river. For instance, at S. Nicolau/Bentiaba, Lucira, Moçamedes, and Ponta do Giraul assemblages with both ESA-MSA stone tools classified as Upper Acheulean and “Fauresmith” toolkits were reported by numerous authors (Allchin, 1964; Breuil and Almeida, 1964; Clark, 1966; Ervedosa, 1980; Jorge, 1974). Aside from Dungo IV, no other radiometric ages are available for archaeological sites of ESA-MSA in Angola.

While in the Congo and Zambezi zones, north and east of Angola, cultural affinities closely align with the cultures of the tropical rainforest of West and Central Africa (Clark, 1968, 1963; Taylor, 2022, 2016), the south-west presented more varied typologies frequently interpreted as “transitional industries”, or “local traditions” with affinities to the southern African technocomplexes (Ramos, 1982). Similar issues have been raised in lithic studies about neighboring countries (Barham, 2012; Barham et al., 2015; Herries, 2011; Mehlman, 1991; Sheppard and Kleindienst, 1996). Nevertheless, the Stone Age lithic sequence of Southern Africa was revised to include datasets across sub-Saharan Africa, including open-air sites from Namibia, Botswana, Zimbabwe, Eswatini, and Mozambique (eg. Lombard et al., 2022).

The lithic assemblages from southwest Angola also closely align with the southern African sequence, although raw materials are more coarse-grained (Allchin, 1964; Ervedosa, 1980). Particularly with what concerns the convention of technocomplexes

from the late ESA to the Late Stone Age, such as the Acheulean, Fauresmith, EMSA, Still Bay, Smithfield, and Wilton cultures (Ramos, 1982). The late Acheulean, Fauresmith, and EMSA are recognized as stages key to our understanding of cultural and behavioral traits of early modern humans in southern Africa (Chazan, 2022; Kuman et al., 2020; Underhill, 2011; Wilkins and Chazan, 2012). In Angola, the vast majority of archaeological sites reportedly from the Early Stone Age have not been re-approached in recent years except for Dungo (Gutierrez et al., 2010; Gutierrez and Benjamim, 2019; Lebatard et al., 2019; Mesfin et al., 2021).

The “Fauresmith” is a long-debated term for the either late ESA assemblages frequently observed in open-air sites of the interior drylands of southern Africa. It is recognized by the finely retouched bifaces, scrapers, Levallois points, prepared cores, and blades, and includes “Sangoan” tools (Kuman et al., 2020; Lombard et al., 2022; Tryon and McBrearty, 2002; Underhill, 2011).

The oldest dated EMSA tools (co-occurring with Fauresmith) are from Kathu Pan 1 to ca. 511-435 ka (Porat et al., 2010; Wilkins and Chazan, 2012). The Fauresmith technocomplex is estimated to span from 233.7 to 471.5 ka and overlaps the EMSA which is estimated to span from 126.5 to 266.5 ka (eg. Lombard et al., 2022).

For the southwest Atlantic coast, there is one site with absolute ages. The site of Cafema, on the margins of the Cunene River, at the border between Angola and Namibia, is included in the EMSA. Field research at Cafema retrieved a small lithic assemblage that was considered a “generic” MSA dated to 220 ka by Optical Stimulated Luminescence (OSL) – single-aliquot regenerative-dose (SAR) (Nicoll, 2010, 2009). The assemblage is mainly composed of flakes, cores, and Levallois points, similar to the MSA from Leba Cave (de Matos and Pereira, 2020). At Apollo 11 Rock Shelter the oldest assemblages are assigned to the Still Bay dated to around 70 ka (Lombard et al., 2022; Ossendorf, 2017a; Vogelsang et al., 2010). Other dated sites from Namibia present much younger ages ranging from MIS 3 to 1 (Marks, 2015; Mccall et al., 2011; Ossendorf, 2017b; Schmidt et al., 2016; Veldman et al., 2017).

Stone artifacts of Early, Middle, and Later Stone Age complexes are widely present and exposed across the land surface of the Namib desert from Angola to South Africa (Corvinus, 1983; Davies, 1962; Kandel and Conard, 2012; Kinahan, 2011, 2016; Mackay et al., 2014; Ossendorf, 2017a; Ramos, 1982; Schmidt, 2011). These are testimonies of human activity across this landscape for a long time span, but representing a palimpsest record (Binford, 2001; Marks, 2015). Although offering the chance for longer stratified deposits, rock shelters and caves are subject to the same earth surface processes,

depending on factors such as geology, environment, and human activity (Clark, 2002; Goldberg and Sherwood, 2006; Karkanas et al., 2021). The Leba Cave record is no exception to this norm.

From our analysis of the site formation, human activity seems to play a significant role in the reworking (and even removal) of sediments from the cave. Our assessment of the area closer to the entrance shows there were very recent alterations mixing older and younger sediments. The composition of the geological units is very heterogenous. The structure and geometry suggests these horizons result from mixing of aggregates of different ages.

From the extensive analysis of the lithic findings from area VOJ we found reduction sequences relying on prepared core technology and bipolar reduction. Unretouched pieces are dominant. Only a few pieces such as the cleavers and handaxes fall into the category of large cutting tools frequently associated to Mode 2 (Acheulean) technologies but these are also occasional findings in LSA sites (Clark, 1968; Ervedosa, 1980).

The cultural assemblage had a very low frequency of pieces with surface alterations, which would be expected in materials that were buried for longer, as observed in areas DMT and JCF. Neverthless, considering the micromophological assessment it is possible that some of the lithic materials in area VOJ relate to aggregates of Pleistocene or Early Holocene age, but were reworked by human agents after 1000 AD. This stage was assigned to the Ceramic LSA cultures, a term frequently used to describe the atypical industries from Late Holocene hunter and forager populations of southern Africa (Clist et al., 2022).

8. Final remarks

Leba is a very special location for the people of Angola because of the famous road and Miradouro national heritage site, a touristic hotspot on the escarpment over the vast lowlands of the Namib desert stretching to the Atlantic Ocean.

Since the colonial occupation by the Boers and the Portuguese, from the late 17th century to 1974, the area was key as an intermediate point in the communication between the ports and the central plateau of Angola. Slave trade, mining operations, and the agricultural potential of the area were main focuses ot the European settlers that occupied the plateau. The colonization caused not only a complete disruption of the local society but also an unprecedented environmental change derived from intense agricultural activity and quarrying..

When the Europeans arrived many tribes lived in the plateau including hunter-gatherers, semi-nomadic herders and permanent communities with both non- and -Bantu languages. Ethnographic records are abundant and reported on the diversity of populations and cultures, as well as an important oral memory. These records report the Bantu groups arrived in the southwestern plateau after 1000 AD (Estermann, 1981). In local memory, the arrival of the herders pushed the hunter-gatherers to the lowlands. However there is evidence that hunter-gatherers had clientele relationships with Bantu kingdoms, with whom they traded pottery and beads (Estermann, 1976), assemblages that have been found in LSA campsites associated with rock art locations of the ‘Kwisi which have evidence of repeated visits at least over the last 2000 years (eg. Ervedosa, 1980).

The database of archaeological sites identified by the Portuguese colonial missions reports a high frequency and diversity of sites with ESA, MSA and LSA tools. Thousands of artifacts assigned to different chrono-cultural periods kept in museum collections are steadily being cataloged and published (Casanova and Romeiras, 2020; Coelho et al., 2014; de Matos et al., 2021b; de Matos and Pereira, 2020). The vast majority of assemblages from the Ramos legacy (including lithics and sediments) is yet to be published in depth, particularly the excavations at the site of Capangombe-velho, which has several thousands of artifacts assigned to the ESA and MSA (de Matos et al., 2021b). It should be noted that the vast majority of the sites in the database are located along the main roads, which consists of a research bias, and the interior of the escarpment is yet to be surveyed. These are also some of the most remote locations in the Namib desert and where the last few Khoi descendents of Angola are concentrated nowadays (Oliveira et al., 2018). A few San-descendents are also known to live in the

plateau around Lubango city (Ferreira, 2018), but have mostly been absorbed by the Bantu language communities. Many aspects of the cultural evolution of hunter-gatherers in Southern Angola are yet to be explored.

The research developed by the National Archaeology Museum of Angola has been particularly important to provide new data about the early Pleistocene coastal populations of Dungo, Baía Farta, reporting on human use of coastal resources at least since 600 ka (Gutierrez and Benjamim, 2019). But there is little progress on the studies of the MSA, beyond the coastal sites of Luanda, Benfica and Benguela which shows cultural affinities closely associated with LSA populations.

The study started by Ramos in the late 1960s about the transition of the ESA-MSA was supposed to bring forth more data about the Sangoan (Allchin, 1964; Breuil and Almeida, 1964; Janmart, 1953), and if there was a direct relationship between the sequences studied in the Congo (Clark, 1968, 1963). The Sangoan industry was considered evidence for a distinctive intermediate culture between the ESA to MSA and perceived as an adaptation to forested environments, with many sites located around the Congo basin. Progressively, the term “Sangoan” has been abandoned, as there was little to no evidence for ecological conditions matching the presumed functionality of those tools (McBrearty, 1991; Taylor, 2016; Van Peer et al., 2004), although some authors focusing on West Africa continue to use the name (Douze et al., 2021). For the most part, archaeologists in the field are still debating if the Three Age system and conventioned lithic taxonomy is useful to studies about material culture in sub-Saharan Africa (eg. Grove and Blinkhorn, 2021; Mehlman, 1991)

The conventioned chronocultural system for the Stone Age sites of Southwestern Angola outlined by Ramos (1982) proposed a new sequence based on local traditions, although in some sites showing either affinities with technocomplexes from Namibia and Southern Africa, and other sites containing tools with closer relation with Central African sequences. This convention, however, relies mostly on surface materials from open-air sites and poor environmental evidence. Since preservation of organic material is very rare in these latitudes, no absolute ages were proposed for the MSA in Southwestern Angola until now.

Our study about the Leba Cave addressed the site formation processes in order to integrate the MSA assemblages excavated inside the cave in 1950, and during the Paleoleba project from 2018 to 2019. Our current knowledge about the cave sedimentation does not provide a complete picture of what happened in the cave since the MSA. Neverthless, there is evidence for several erosional phases, as well as intense

anthropogenic activity. Moreover the OSL minimim ages suggest the base of the EMSA infillings are older than 150 ka.

Our work also pushed back the preliminary ages obtained for the MSA units excavated in 1950, suggesting a minimum age of 75 ka. It seems the cultural phases reported by the first excavators and further developed with the study of the lithic assemblages are consistent with previous interpretations of an MSA sequence of three phases (de Matos and Pereira, 2020). Even though we could not find preserved archaeological layers that can be assigned to the Late Pleistocene-early Holocene. The heavy erosion and post-depositional processes suggest these sediments were already removed, or are not visible, and there are phases that can never be fully reconstructed. By no means is the site formation model provided in this dissertation a closed model, and it may be improved.

The testing and sampling of exposures inside the cave was key to refine our interpretation of the material used for absolute dating methods. New research can still be pursued in other cave systems and open-air sites and of the Humpata Plateau. The background research and the site formation model developed for Leba cave now provide a better understanding of the nature and character of these sites, how they form and how to approach them in the field and in the laboratory.

Further avenues of research can be pursued towards a better characterization of the surrounding landscape and prehistoric communities of the southwestern plateau of Angola.

The analysis and characterization of the deposits in other caves systems for comparable data for site formation processes, relationships in clastic phases and cementation, and how these affect the preservation of the human record. The approach could also benefit from geophysical work to detect pockets of sediment that are sealed or covered.

Analysis of ecofacts like the faunal assemblages should also be developed towards a better understanding of the ecological diversity of the region and characterization of endemic groups. Taxonomic identification of fragmented material using Proteomics could be a solution to overcome the fragmentation and taxonomical challenges. There is the issue that the materials from the Pleistocene are remineralized and fossil assemblages did not provide sufficient collagen for ^{14}C ages. However there is evidence for organic preservation of aminoacids in other cave sites in the vicinity (David and Pickford, 1999; Pickford et al., 1994). For the site of Leba Cave alone there are several thousand unidentified pieces in the museum collection in Lisbon (Gautier, 1995) which we concluded as prevenient from area JCF. There is wide representation of different

families/taxonomic groups proven by our study and previous studies. These datasets can still provide novel on extinct and extanct faunal groups in the region. This will be key to understand local environmental regimes and characterizing the paleolandscape.

The high frequency and good preservation of mammal teeth from the Leba Cave also offers the chance to explore other terrestrial proxies on the local resource availability, diet and seasonality. The isotopic study of the mammal teeth from Pleistocene and Holocene deposits from Leba Cave are currently ongoing

Landscape work was pursued to understand how these geologic features and biomes may have developed and evolved over time, it is important to investigate modern environmental dynamics. As part of this study, local water bodies on the Humpata Plateau, including cold springs and rivers, were investigated (Robakiewicz et al., 2021). Data were collected on the cations and anions present in the water, the isotopic composition of the water, and the algal communities, with a particular focus on diatoms, a siliceous alga often used as a water quality/pollution proxy. These investigations were used to determine how water moves through the karstic systems and will be used to conduct environmental reconstructions, building on the knowledge of how these cave systems, biomes, and prehistoric communities all interacted. Our fieldwork is also focused on hydrochemistry variability and diatom communities to understand local and regional dynamics and setting the stage for longer term coring in the area. These proxies are key for both past environments but also modern land use, risk management and climate change studies. Ultimately, the multiscalar approach to the landscape will provide contextual information to understand the evolution of Homo sapiens at the coastal escarpment of the south Atlantic since the Pleistocene.

Bibliography

Agabi, C., 1999. Hachereau. Encycl. berbère, 21.

Aitken, J.D., 1967. Classification and environmental significance of cryptalgal limestones and dolomites, with illustrations from the Cambrian and Ordovician of southwestern Alberta. J. Sediment. Res. 37, 1163–1178. https://doi.org/10.1306/74D7185C-2B21-11D7-8648000102C1865D

Aldeias, V., Dibble, H.L., Sandgathe, D., Goldberg, P., McPherron, S.J.P., 2016. How heat alters underlying deposits and implications for archaeological fire features: A controlled experiment. J. Archaeol. Sci. 67, 64–79. https://doi.org/https://doi.org/10.1016/j.jas.2016.01.016

Aldeias, V., Goldberg, P., Dibble, H.L., El-Hajraoui, M., 2014. Deciphering site formation processes through soil micromorphology at Contrebandiers Cave, Morocco. J. Hum. Evol. 69, 8–30. https://doi.org/10.1016/j.jhevol.2013.12.016

Allchin, B., 1964. A Preliminary Survey of the Sites of the Serra-Abaixo, South-West Angola. Memórias da Junta Investig. do Ultramar Estud. sobre pré-história do Ultramar Port. 50, 81–100.

Allsworth-Jones, P., Harvati, K., Stringer, C., 2010. The archaeological context of the Iwo Eleru cranium from Nigeria and preliminary results of new morphometric studies. Bar.

Almeida, A., 1965. Bushmen and other non-Bantu peoples of Angola. Institute for the study of man in Africa, Johannesburg.

Almeida, A., 1964. Prefácio, in: Estudos Sobre a Pré-História Do Ultramar Português. Junta de Investigações do Ultrmar, Lisboa.

Andirkó, A., Moriano, J., Vitriolo, A., Kuhlwilm, M., Testa, G., Boeckx, C., 2022. Temporal mapping of derived high-frequency gene variants supports the mosaic nature of the evolution of Homo sapiens. Sci. Rep. 12, 9937. https://doi.org/10.1038/s41598-022-13589-0

Arambourg, A., Mouta, F., 1952. Les Grottes et Fentes a ossements du sud de l'Angola, in: Actes Du IIème Congrès Panafricain de Préhistoire d'Alger. p. 301.

Backwell, L., d'Errico, F., Wadley, L., 2008. Middle Stone Age bone tools from the Howiesons Poort layers, Sibudu Cave, South Africa. J. Archaeol. Sci. 35, 1566–1580. https://doi.org/10.1016/j.jas.2007.11.006

Barbosa, L.A.G., 1970. Carta Fitogeográfica de Angola. Instituto de Investigação Científica de Angola-Oficinas Gerais de Angola, Luanda.

Barham, L., 2012. Clarifying some fundamental errors in herries' "a chronological perspective on the acheulian and its transition to the middle stone age in southern Africa: the question of the fauresmith" (2011). Int. J. Evol. Biol. 2012, 230156. https://doi.org/10.1155/2012/230156

Barham, L., Mitchell, P.J., 2002. The First Africans: African archaeology from the earliest toolmakers to most recent foragers. Cambridge University Press, Cambridge.

Barham, L., Tooth, S., Duller, G.A.T., Plater, A.J., Turner, S., 2015. Excavations at Site C North, Kalambo Falls, Zambia: New insights into the mode 2/3 transition in South-Central Africa. J. African Archaeol. 13, 187–214. https://doi.org/10.3213/2191-5784-10270

Barnard, A., 1992. Hunters and herders of southern Africa: A comparative ethnography of the Khoisan peoples. Cambridge University Press., Cambridge.

Basell, L.S., 2008. Middle Stone Age (MSA) site distributions in eastern Africa and their relationship to Quaternary environmental change, refugia and the evolution of Homo sapiens. Quat. Sci. Rev. https://doi.org/10.1016/j.quascirev.2008.09.010

Beck, H.E., Zimmermann, N.E., McVicar, T.R., Vergopolan, N., Berg, A., Wood, E.F., 2018. Present and future köppen-geiger climate classification maps at 1-km resolution. Sci. Data 5, 1–12. https://doi.org/10.1038/sdata.2018.214

Beetz, P.F., 1933. Geology of South West Angola between Cunene and Lunda Acis. Trans. Geol. Soc. South Africa 12, 43–50.

Beja, P., Vaz Pinto, P., Veríssimo, L., Bersacola, E., Fabiano, E., Palmeirim, J.M., Monadjem, A., Monterroso, P., Svensson, M.S., Taylor, P.J., 2019. The Mammals of Angola BT - Biodiversity of Angola: Science & Conservation: A Modern Synthesis, in: Huntley, B.J., Russo, V., Lages, F., Ferrand, N. (Eds.), . Springer International Publishing, Cham, pp. 357–443. https://doi.org/10.1007/978-3-030-03083-4_15

Berger, L.R., Hawks, J., Dirks, P.H.G.M., Elliott, M., Roberts, E.M., 2017. Homo naledi and Pleistocene hominin evolution in subequatorial Africa. Elife. https://doi.org/10.7554/eLife.24234

Berger, R., Libby, W.F., 1969. UCLA Radiocarbon Dates IX. Radiocarbon 11, 194–209. https://doi.org/10.1017/S0033822200064547

Bergmann, I., Hublin, J.J., Ben-Ncer, A., Sbihi-Alaoui, F.Z., Gunz, P., Freidline, S.E., 2022. The relevance of late MSA mandibles on the emergence of modern morphology in Northern Africa. Sci. Rep. 12. https://doi.org/10.1038/s41598-022-12607-5

Binford, L.R., 2001. Constructing Frames of Reference: An Analytical Method for Archaeological Theory Building Using Hunter-Gatherer and Environmental Data Sets. University of California Press.

Binford, L.R., 1983. In pursuit of the past: decoding the archaeological record. Thames and Hudson, London& New York.

Blum, W.E.., Schad, P., Nortcliff, S., 2018. Essentials of soil science : soil formation, functions, use and classification (World Reference Base, WRB) /. CSIRO Publishing, Clayton South, Vic.

Boaz, N.T., Ninkovich, D., Rossignol-Strick, M., 1982. Paleoclimatic setting for Homo sapiens neanderthalensis. Naturwissenschaften 69, 29–33. https://doi.org/10.1007/BF00441096

Bordes, F., 1961. La Typologie du Paleolithique Ancien et Moyen. CNRS, Paris.

Borges, F., Mouta, F., 1926. Congrès géologique international: communication de la Mission Géologique de l'Angola. Bol. da Agência Geral das Colónias Ano II, 30–55.

Bosak, T., Mariotti, G., MacDonald, F.A., Perron, J.T., Pruss, S.B., 2013. Microbial Sedimentology of Stromatolites in Neoproterozoic Cap Carbonates. Paleontol. Soc. Pap. 19, 51–76. https://doi.org/10.1017/s1089332600002680

Bouzouggar, A., Barton, N., Vanhaeren, M., D'Errico, F., Collcutt, S., Higham, T., Hodge, E., Parfitt, S., Rhodes, E., Schweninger, J.L., Stringer, C., Turner, E., Ward, S., Moutmir, A., Stambouli, A., 2007. 82,000-Year-old shell beads from North Africa and implications for the origins of modern human behavior. Proc. Natl. Acad. Sci. U. S. A. 104, 9964–9969. https://doi.org/10.1073/pnas.0703877104

Brain, C.K., 1981. The Hunters or the Hunted? An Introduction to African Cave Taphonomy. https://doi.org/10.2307/279840

Brain, C.K., 1974. Some suggested procedures in the analysis of bone accumulations from Southern African Quaternary sites. Transvaal Museum, Pretoria.

Braucher, R., Oslisly, R., Mesfin, I., Ntoutoume, P.P., 2022. In situ -produced 10 Be and 26 Al indirect dating of Elarmékora Earlier Stone Age artefacts: first attempt in a

savannah forest mosaic in the middle Ogooué valley, Gabon . Philos. Trans. R. Soc. B Biol. Sci. 377. https://doi.org/10.1098/rstb.2020.0482

Breuil, H., Almeida, A., 1964. Introdução à Pré-História de Angola. Memórias da Junta Investig. do Ultramar Estud. sobre Pré-história do Ultramar Port. 50, 159–163.

Brochier, J.É., Thinon, M., 2003. Calcite crystals, starch grains aggregates or... POCC? Comment on “calcite crystals inside archaeologial plant tissues.” J. Archaeol. Sci. 30, 1211–1214. https://doi.org/10.1016/S0305-4403(02)00031-6

Brock, F., Wood, R., Higham, T.F.G., Ditchfield, P., Bayliss, A., Ramsey, C.B., 2012. Reliability of Nitrogen Content (%N) and Carbon:Nitrogen Atomic Ratios (C:N) as Indicators of Collagen Preservation Suitable for Radiocarbon Dating. Radiocarbon 54, 879–886. https://doi.org/DOI: 10.1017/S0033822200047524

Bullock, P., 1985. Handbook for soil thin section description. Waine Research Publ., Albrighton.

Burgess, N., D’Amico Hales, J., Underwood, E., Dinerstein, E., Olson, D., Itoua, I., Schipper, J., Ricketts, T.., Newman, K., 2004. Terrestrial eco-regions of africa and Madagascar: A conservation assessment. Island Press, Washington, DC. 1–550.

Butzer, K.W., 1982. Archaeology as Human Ecology: Method and Theory for a Contextual Approach. Cambridge University Press, Cambridge. https://doi.org/DOI: 10.1017/CBO9780511558245

Cain, A., 2017. Water resource management under a changing climate in Angola’s coastal settlements About the author.

Camarate-França, J., 1964. Nota preliminar sobre uma gruta pré-histórica do planalto da Humpata. Memórias da Junta Investig. do Ultramar Estud. sobre Pré-história do Ultramar Port. 60, 59–67.

Camarate-França, J., 1953. As gravuras rupestres do «Tchitundo-Hulo» (deserto de Moçamedes), in: Mensario Administrativo. Luanda, p. 44.

Cañaveras, J.C., Sánchez-Moral, S., Duarte, E., Santos-Delgado, G., Silva, P.G., Cuezva, S., Fernández-Cortés, Á., Lario, J., Muñoz-Cervera, M.C., de la Rasilla, M., 2021. Micromorphological study of site formation processes at el sidrón cave (Asturias, Northern Spain): Encrustations over neanderthal bones. Geosci. 11. https://doi.org/10.3390/geosciences11100413

Cancellieri, E., Bel Hadj Brahim, H., Ben Nasr, J., Ben Fraj, T., Boussoffara, R., Di

Matteo, M., Mercier, N., Marnaoui, M., Monaco, A., Richard, M., Mariani, G.S., Scancarello, O., Zerboni, A., di Lernia, S., 2022. A late Middle Pleistocene Middle Stone Age sequence identified at Wadi Lazalim in southern Tunisia. Sci. Rep. 12, 1–12. https://doi.org/10.1038/s41598-022-07816-x

Carvalho, H., 1983. Notice Explicative Préliminaire sur La Géologie de L'Angola. Garcia Orta 6, 15–30.

Carvalho, S.C.P., Santos, F.D., Pulquério, M., 2017. Climate change scenarios for Angola: an analysis of precipitation and temperature projections using four RCMs. Int. J. Climatol. 37, 3398–3412. https://doi.org/10.1002/joc.4925

Casanova, C., Romeiras, M.M., 2020. Legacy of the scientific collections of the Instituto de Investigação Científica Tropical, University of Lisbon: A critical review and outlook. Conserv. Patrim. 33, 32–43. https://doi.org/10.14568/cp2018040

Cerling, T.E., 1984. The stable isotopic composition of modern soil carbonate and its relationship to climate. Earth Planet. Sci. Lett. https://doi.org/10.1016/0012-821X(84)90089-X

Cerling, T.E., Harris, J.M., Ambrose, S.H., Leakey, M.G., Solounias, N., 1997. Dietary and environmental reconstruction with stable isotope analyses of herbivore tooth enamel from the Miocene locality of Fort Ternan, Kenya. J. Hum. Evol. 33, 635–650. https://doi.org/https://doi.org/10.1006/jhev.1997.0151

Cerling, T.E., Wynn, J.G., Andanje, S.A., Bird, M.I., Korir, D.K., Levin, N.E., MacE, W., MacHaria, A.N., Quade, J., Remien, C.H., 2011. Woody cover and hominin environments in the past 6-million years. Nature 476, 51–56. https://doi.org/10.1038/nature10306

Chazan, M., 2022. The Fauresmith and Cultural Dynamics at the End of the Southern African Earlier Stone Age, in: Oxford Research Encyclopedia of Anthropology. Oxford University Press. https://doi.org/10.1093/acrefore/9780190854584.013.29

Chazan, M., Berna, F., Brink, J., Ecker, M., Holt, S., Porat, N., Thorp, J.L., Horwitz, L.K., 2020. Archeology, Environment, and Chronology of the Early Middle Stone Age Component of Wonderwerk Cave, Journal of Paleolithic Archaeology. Journal of Paleolithic Archaeology. https://doi.org/10.1007/s41982-020-00051-8

Chazan, M., Horwitz, L.K., 2006. Finding the message in intricacy: The association of lithics and fauna on Lower Paleolithic Multiple Carcass Sites. J. Anthropol. Archaeol. 25, 436–447. https://doi.org/10.1016/j.jaa.2006.03.005

Chevrier, B., Lespez, L., Lebrun, B., Garnier, A., Tribolo, C., Rasse, M., Guérin, G., Mercier, N., Camara, A., Ndiaye, M., Huysecom, E., 2020. New data on settlement and environment at the Pleistocene/Holocene boundary in Sudano-Sahelian West Africa: Interdisciplinary investigation at Fatandi V, Eastern Senegal. PLoS One 15, e0243129.

Chevrier, B., Rasse, M., Lespez, L., Tribolo, C., Hajdas, I., Guardiola Fígols, M., Lebrun, B., Leplongeon, A., Camara, A., Huysecom, É., 2016. West African Palaeolithic history: New archaeological and chronostratigraphic data from the Falémé valley, eastern Senegal. Quat. Int. 408, 33–52. https://doi.org/https://doi.org/10.1016/j.quaint.2015.11.060

Clark, J.D., 2002. Human Ecology During Pleistocene and Later Times in Africa South of the Sahara. Curr. Anthropol. 1, 307–324. https://doi.org/10.1086/200115

Clark, J.D., 2001. Ecological and behavioral implications of the siting of Middle Stone Age rockshelter and cave settlements in Africa, in: N.J. Conard (Ed.), Settlement Dynamics of the Middle Paleolithic and Middle Stone Age. Tubingen, pp. 91–98.

Clark, J.D., 1971. Human Behavioral Differences in Southern Africa during the Later Pleistocene. Am. Anthropol. 73, 1211–1236.

Clark, J.D., 1968. Further Paleo-Anthropological Studies in Northern Lunda. Museu do Dundo: Subsídios para a História, Arqueologia e Etnografia dos Povos da Lunda, vol. I/II. Publicações Culturais: 78, Diamang, Lisboa.

Clark, J.D., 1966. The Distribution of Prehistoric Culture in Angola. Museu do Dundo: Subsídios para a História, Arqueologia e Etnografia dos Povos da Lunda, Publicações Culturais. Publicações Culturais: 62, Diamang, Lisboa.

Clark, J.D., 1963. Prehistoric Cultures of Northeast Angola and Their Significance in Tropical Africa. Museu do Dundo: Subsídios para a História, Arqueologia e Etnografia dos Povos da Lunda. Publicações Culturais: 78, Diamang, Lisboa.

Clark, J.L., Plug, I., 2008. Animal exploitation strategies during the South African Middle Stone Age: Howiesons Poort and post-Howiesons Poort fauna from Sibudu Cave. J. Hum. Evol. 54, 886–898. https://doi.org/10.1016/j.jhevol.2007.12.004

Clist, B., Denbow, J., Lanfranchi, R., Mindzie, C.M., Lufu, P.B., Jesus, M. da P. de, 2022. Long-Term Demographic Trends of the last 50,000 years in Central Africa. Azania Archaeol. Res. Africa.

Clist, B., Lanfranchi, R., 1992. Contribution a l'étude de la sedentarisation en République

Populaire d'Angola. LEBA Estud. pré-história e Arqueol. 7, 245–268.

Coelho, A.G., Pinto, I., Casanova, M. da C., 2014. A coleção arqueológica do IICT no novo milénio. Antrope Metodologi, 6–22.

Coelho, V., 2015. A classificação etnográfica dos povos de Angola (1.ª parte)Classification ethnography of the people of Angola (Part I). Mulemba 5, 203–220. https://doi.org/10.4000/mulemba.473

Conard, N.J., Brenner, M., Bretzke, K., Will, M., 2022. What do spatial data from Sibhudu tell us about life in the Middle Stone Age? Archaeol. Anthropol. Sci. 4. https://doi.org/10.1007/s12520-022-01585-4

Cornelissen, E., 2016. The Later Pleistocene in the Northeastern Central African Rainforest BT - Africa from MIS 6-2: Population Dynamics and Paleoenvironments, in: Jones, S.C., Stewart, B.A. (Eds.), . Springer Netherlands, Dordrecht, pp. 301–319. https://doi.org/10.1007/978-94-017-7520-5_16

Correia, H., 1976. O grupo chela e a formação leba como novas unidades litoestratigráficas resultantes da redefinição da «formação da Chela» na região do planalto da Humpata (sudoeste de Angola). Bol. da Soc. Geológica Port. XX XX, 65–130.

Corvinus, G., 1983. The raised beaches of the west coast of South West Africa/Namibia: an interpretation of their archaeological and palaeontological data. Beck, München.

Courty, M.A., Goldberg, P., Macphail, R.I., 1989. Soils and Micromorphology in archaeology. Cambridge University Press, Cambridge.

Cruz, A., Graça, A., Oosterbeek, L., Almeida, F., Delfino, D., 2013. Gruta do Morgado Superior. Um Estudo de Caso Funerário no Alto Ribatejo (Tomar, Portugal). Vinculos Hist. 2, 143–168. https://doi.org/10.18239/vdh.v0i2.62

Cruz, J.R., 1940. Elementos de climatologia: o clima de Angola.

d'Errico, F., Banks, W.E., Warren, D.L., Sgubin, G., van Niekerk, K., Henshilwood, C., Daniau, A.-L., Sánchez Goñi, M.F., 2017. Identifying early modern human ecological niche expansions and associated cultural dynamics in the South African Middle Stone Age. Proc. Natl. Acad. Sci. 114, 7869–7876. https://doi.org/10.1073/pnas.1620752114

Dart, R.A., 1950. A Note on the Limestone Caverns of Leba, near Humpata, Angola. South African Archaeol. Bull. 5, 149. https://doi.org/10.2307/3887137

David, H., Pickford, M., 1999. Composition en acides aminés d ' os de mammifères fossiles de deux sites du Plio-Pléistocène d ' Angola . Comparaison. Geodiversitas 1, 215–227.

Davies, O., 1962. The raised beaches of Angola and South-west Africa., in: Proceedings of the 4th Panafrican Congress on Prehistory (Vol. L). Musee royal de l'Afrique centrale Annales 8, Sciences humaines 40, pp. 289–94.

de Matos, D., Bicho, N., McKinney, C., 2014. New data on the Middle Stone Age of southwest Angola: the sequence of Leba Cave, Huíla, in: 14th Pan African Archaeological Association and 22nd Biennual Meeting of the Society of Africanist Archaeologists. University of Witwatersrand, Johannesburg.

de Matos, D., Francisco, R., Barros, B., Fernandes, J., Robakiewicz, E., 2021a. A paisagem cársica do Sudoeste de Angola: Primeira abordagem ao património subterrâneo da Formação Leba. Rev. Angolana Geociências 2, 127–143.

de Matos, D., Martins, A.C., Senna-Martinez, J.C., Pinto, I., Coelho, A.G., Ferreira, S.S., Oosterbeek, L., 2021b. Review of Archaeological Research in Angola. African Archaeol. Rev. 38, 319–344. https://doi.org/10.1007/s10437-020-09420-8

de Matos, D., Pereira, T., 2020. Middle Stone Age lithic assemblages from Leba Cave (Southwest Angola). J. Archaeol. Sci. Reports 32, 102413. https://doi.org/10.1016/j.jasrep.2020.102413

Debénath, A., Dibble, H.L., 1994. Handbook of Paleolithic Typology. University of Pennsylvania Press. https://doi.org/10.9783/9781934536803

Delson, E., Terranova, C.J., Jungers, W.L., Sargis, E.J., Jablonski, N.G., Dechow, P.C., 2000. Body Mass in Cercopithecidae (Primates, Mammalia): Estimation and Scaling in Extinct and Extant Taxa, 1st ed, Anthropological papers. American Museum of Natural History, New York.

Denbow, J., 2013. The Archaeology and Ethnography of Central Africa. Cambridge University Press, Cambridge. https://doi.org/DOI: 10.1017/CBO9781139629263

Dibble, H.L., Aldeias, V., Alvarez-Fernández, E., Blackwell, B., Hallett-Desguez, E., Jacobs, Z., Goldberg, P., Lin, S.C., Morala, A., Meyer, M.C., Olzsewski, D.I., Reed, K., Reed, D., Rezek, Z., Richter, D., Roberts, R.G., Sandgathe, D., Schurmans, U., Skinner, A., Steele, T., El-Hajraoui, M., 2012. New Excavations at the Site of Contrebandiers Cave, Morocco. PaleoAnthropology 2012, 145–201. https://doi.org/10.4207/PA.2012.ART74

Diniz, A.C., 2006. Caracteristícas Mesológicas de Angola. Lisboa.

Diniz, A.C., 1991. Angola, o meio físico e potencialidades agrárias. Instituto para a Cooperação Económica, Lisboa.

Diniz, A.C., 1973. Características mesológicas de Angola. Missão de Inquéritos Agrícolas de Angola. Lisboa.

do Amaral, I., 1973. Nota sobre o karst ou carso do planalto do Planalto da Humpata (Huíla) no Sudoeste de Angola. Garcia Orta Série de G, 29–36.

Douze, K., Lespez, L., Rasse, M., Tribolo, C., Garnier, A., Lebrun, B., Mercier, N., Ndiaye, M., Chevrier, B., Huysecom, E., 2021. A West African Middle Stone Age site dated to the beginning of MIS 5: Archaeology, chronology, and paleoenvironment of the Ravin Blanc I (eastern Senegal). J. Hum. Evol. 154, 102952. https://doi.org/10.1016/j.jhevol.2021.102952

Ecker, M., Brink, J., Horwitz, L.K., Scott, L., Lee-Thorp, J.A., 2018. A 12,000 year record of changes in herbivore niche separation and palaeoclimate (Wonderwerk Cave, South Africa). Quat. Sci. Rev. 180, 132–144. https://doi.org/10.1016/j.quascirev.2017.11.025

Ervedosa, C., 1980. Arqueologia Angolana, 1st ed. Edições 70, Lisboa.

Estermann, C., 1981. The ethnography of southwestern Angola. The Herero People, Instituto. ed. Africana Publishing Company, New York.

Estermann, C., 1976. The ethnography of Southwestern Angola: The Non-Bantu Peoples and the Ambo Ethnic Group. Africana Pub. Co., New York.

Fagundes, N.J.R., Ray, N., Beaumont, M., Neuenschwander, S., Salzano, F.M., Bonatto, S.L., Excoffier, L., 2007. Statistical evaluation of alternative models of human evolution. Proc. Natl. Acad. Sci. 104, 17614–17619. https://doi.org/10.1073/pnas.0708280104

Feio, M., 1981. O relevo do sudoeste de Angola. Estudo de Geomorfologia. Memórias da Junta de Investigações Científicas do Ultramar. Nº67 (Segunda Série). Lisboa. Deposito legal nº 614/82.

Feio, M., 1964. A evolução da escadaria de aplanações do Sudoeste de Angola. Garcia Orta 12, 323–354.

Fernandes, J.B.C., 2014. As Pinturas Do Abrigo Do Tchitundu-Hulu Mucai. UTAD.

Ferreira, S., 2018. Quotidiano San. Chá de Caxinde, Luanda.

Fisher, J.W., 1995. Bone surface modifications in zooarchaeology. J. Archaeol. Method Theory 2, 7–68. https://doi.org/10.1007/BF02228434

Fu, Q., Li, H., Moorjani, P., Jay, F., Slepchenko, S.M., Bondarev, A.A., Johnson, P.L.F., Aximu-Petri, A., Prüfer, K., De Filippo, C., Meyer, M., Zwyns, N., Salazar-García, D.C., Kuzmin, Y. V., Keates, S.G., Kosintsev, P.A., Razhev, D.I., Richards, M.P., Peristov, N. V., Lachmann, M., Douka, K., Higham, T.F.G., Slatkin, M., Hublin, J.J., Reich, D., Kelso, J., Viola, T.B., Pääbo, S., 2014. Genome sequence of a 45,000-year-old modern human from western Siberia. Nature. https://doi.org/10.1038/nature13810

Fu, Q., Posth, C., Hajdinjak, M., Petr, M., Mallick, S., Fernandes, D., Furtwängler, A., Haak, W., Meyer, M., Mittnik, A., Nickel, B., Peltzer, A., Rohland, N., Slon, V., Talamo, S., Lazaridis, I., Lipson, M., Mathieson, I., Schiffels, S., Skoglund, P., Derevianko, A.P., Drozdov, N., Slavinsky, V., Tsybankov, A., Cremonesi, R.G., Mallegni, F., Gély, B., Vacca, E., Morales, M.R.G., Straus, L.G., Neugebauer-Maresch, C., Teschler-Nicola, M., Constantin, S., Moldovan, O.T., Benazzi, S., Peresani, M., Coppola, D., Lari, M., Ricci, S., Ronchitelli, A., Valentin, F., Thevenet, C., Wehrberger, K., Grigorescu, D., Rougier, H., Crevecoeur, I., Flas, D., Semal, P., Mannino, M.A., Cupillard, C., Bocherens, H., Conard, N.J., Harvati, K., Moiseyev, V., Drucker, D.G., Svoboda, J., Richards, M.P., Caramelli, D., Pinhasi, R., Kelso, J., Patterson, N., Krause, J., Pääbo, S., Reich, D., 2016. The genetic history of Ice Age Europe. Nature. https://doi.org/10.1038/nature17993

Gasparatos, D., Massas, I., Godelitsas, A., 2019. Fe-Mn concretions and nodules formation in redoximorphic soils and their role on soil phosphorus dynamics: Current knowledge and gaps. CATENA 182, 104106. https://doi.org/https://doi.org/10.1016/j.catena.2019.104106

Gasparatos, D., Tarenidis, D., Haidouti, C., Oikonomou, G., 2005. Microscopic structure of soil Fe-Mn nodules: Environmental implication. Environ. Chem. Lett. 2, 175–178. https://doi.org/10.1007/s10311-004-0092-5

Gautier, A., 1995. Restes Animaux Holocènes et du Paléolitique Moyen (MSA) de la Grotte de Leba sur le Plateau de Humpata (Angola). Archaeofauna 4, 131–141.

Gibson, G.D., Yellen, J.E., 1978. A Middle Stone Age Assemblage from the Munhino Mission, Huila District, Angola. South African Archaeol. Bull. 33, 76. https://doi.org/10.2307/3888253

Gilbert, C.C., McGraw, W.S., Delson, E., 2009. Brief communication: Plio-Pleistocene eagle predation on fossil cercopithecids from the Humpata Plateau, southern Angola. Am. J. Phys. Anthropol. 139, 421–429. https://doi.org/10.1002/ajpa.21004

Giresse, P., 2008. Lithic Artefact Dating Environment Context, in: Developments in Quaternary Sciences. pp. 323–338. https://doi.org/10.1016/S1571-0866(08)80025-5

Giresse, P., 2007. Tropical and sub-tropical West Africa - Marine and continental changes during the Late Quaternary, Developmen. ed. Elsevier. https://doi.org/10.1016/S1571-0866(08)80002-4

Goldberg, P., 2000. Micromorphology and site formation at Die Kelders Cave I, South Africa. J. Hum. Evol. 38, 43–90. https://doi.org/10.1006/jhev.1999.0350

Goldberg, P., Macphail, R.I., 2006. Geoarchaeology. https://doi.org/10.1002/gea.20163

Goldberg, P., Sherwood, S.C., 2006. Deciphering human prehistory through the geoarcheological study of cave sediments. Evol. Anthropol. 15, 20–36. https://doi.org/10.1002/evan.20094

Gomes, A.L., Revermann, R., Gonçalves, F.M.P., Lages, F., Aidar, M.P.M., Sanguino Mostajo, G.A., Finckh, M., 2021. Suffrutex grasslands in south-central Angola: Belowground biomass, root structure, soil characteristics and vegetation dynamics of the “underground forests of Africa.” J. Trop. Ecol. 37, 136–146. https://doi.org/10.1017/S0266467421000298

Grove, M., Blinkhorn, J., 2021. Testing the Integrity of the Middle and Later Stone Age Cultural Taxonomic Division in Eastern Africa. J. Paleolit. Archaeol. 4. https://doi.org/10.1007/s41982-021-00087-4

Güldemann, T., Fehn, A.-M. (Eds.), 2014. Beyond “Khoisan,” Current Issues in Linguistic Theory. John Benjamins Publishing Company, Amsterdam. https://doi.org/10.1075/cilt.330

Gutierrez, M., Benjamim, M.H., 2019. Recherches archéologiques à Baia Farta (Benguela-Angola), 1st ed. L’Harmattan, Nanterre, Paris.

Gutierrez, M., Fançony, R., Benjamim, M.H., 2018. Découverte d’un important site archéologique à Baia Farta (Angola). Afrique Archeol. Arts. https://doi.org/10.4000/aaa.1833

Gutierrez, M., Guérin, C., Karlin, C., Jesus, M. da P. de, Benjamim, M.H., Lebatard, A.-

É., Bourlès, D., Braucher, R., Leanni, L., 2010. Recherches archéologiques à Dungo (Angola): Un site de charognage de baleine de plus d'un million d'années. Afrique Archeol. Arts. https://doi.org/10.4000/aaa.694

Gutierrez, M., Guérin, C., Léna, M., Piedade da Jesus, M., 2001. Exploitation d'un grand cétacé au Paléolithique ancien : le site de Dungo V à Baia Farta (Benguela, Angola). Comptes Rendus l'Académie des Sci. - Ser. IIA - Earth Planet. Sci. 332, 357–362. https://doi.org/10.1016/S1251-8050(01)01518-X

Hajdinjak, M., Fu, Q., Hübner, A., Petr, M., Mafessoni, F., Grote, S., Skoglund, P., Narasimham, V., Rougier, H., Crevecoeur, I., Semal, P., Soressi, M., Talamo, S., Hublin, J.J., Gušić, I., Kućan, Z., Rudan, P., Golovanova, L. V., Doronichev, V.B., Posth, C., Krause, J., Korlević, P., Nagel, S., Nickel, B., Slatkin, M., Patterson, N., Reich, D., Prüfer, K., Meyer, M., Pääbo, S., Kelso, J., 2018. Reconstructing the genetic history of late Neanderthals. Nature. https://doi.org/10.1038/nature26151

Hall, B.P., 1960. The faunistic importance of the scarp of Angola. Ibis (Lond. 1859). 102, 420–442.

Harvati, K., Stringer, C., Grü, R., Aubert, M., Allsworth-Jones, P., Folorunso, C.A., 2011. The Later Stone Age Calvaria from Iwo Eleru, Nigeria: Morphology and Chronology. PLoS One 6. https://doi.org/10.1371/journal.pone.0024024

Henshilwood, C.S., Marean, C.W., 2006. Remodeling the Origins of Modern Human Behavior. Prehistory Africa Tracing Lineage Mod. Man 33–46.

Herries, A.I.R., 2011. A Chronological Perspective on the Acheulian and Its Transition to the Middle Stone Age in Southern Africa: The Question of the Fauresmith. Int. J. Evol. Biol. 2011, 1–25. https://doi.org/10.4061/2011/961401

Hill, J.E., Carter, T.D., 1949. The Mammals of Angola. Bull. Am. Museum Nat. Hist. 65, 14–17. https://doi.org/https://digitallibrary.amnh.org/handle/2246/982

Hublin, J.J., Ben-Ncer, A., Bailey, S.E., Freidline, S.E., Neubauer, S., Skinner, M.M., Bergmann, I., Le Cabec, A., Benazzi, S., Harvati, K., Gunz, P., 2017. New fossils from Jebel Irhoud, Morocco and the pan-African origin of Homo sapiens. Nature. https://doi.org/10.1038/nature22336

Huntley, B.J., 2019. Angola in Outline: Physiography, Climate and Patterns of Biodiversity BT - Biodiversity of Angola: Science & Conservation: A Modern Synthesis, in: Huntley, B.J., Russo, V., Lages, F., Ferrand, N. (Eds.), . Springer International Publishing, Cham, pp. 15–42. https://doi.org/10.1007/978-3-030-

03083-4_2

Huntley, B.J., Ferrand, N., 2019. Angolan biodiversity: Towards a modern synthesis, in: Biodiversity of Angola: Science and Conservation: A Modern Synthesis. https://doi.org/10.1007/978-3-030-03083-4_1

Huntley, B.J., Russo, V., Lages, F., Ferrand, N., 2019. Biodiversity of angola: Science & conservation: A modern synthesis, Biodiversity of Angola: Science and Conservation: A Modern Synthesis. https://doi.org/10.1007/978-3-030-03083-4

Inglis, R.H., French, C., Farr, L., Hunt, C.O., Jones, S.C., Reynolds, T., Barker, G., 2018. Sediment micromorphology and site formation processes during the Middle to Later Stone Ages at the Haua Fteah Cave, Cyrenaica, Libya. Geoarchaeology 33, 328–348. https://doi.org/10.1002/gea.21660

Jablonski, N.G., 1994. New fossil cercopithecid remains from the Humpata Plateau, southern Angola. Am. J. Phys. Anthropol. 94, 435–464. https://doi.org/10.1002/ajpa.1330940402

Janmart, J., 1953. The Kalahari Sands of the Lunda (N.E. Angola), their earlier Redistributions and the Sangoan Culture. Museu do Dundo: Subsídios para a História, Arqueologia e Etnografia dos Povos da Lunda. Publicações Culturais: 20, Diamang, Lisboa.

Jessen, O., 1936. Reisen und forschungen in Angola,. D. Reimer, Andrews & Steiner, Berlin.

Jones, D.L., McFadden, P.L., Kröner, A., McWilliams, M.O., 1992. Palaeomagnetic results from the late Precambrian Chela Group of southwest Angola. Precambrian Res. 59, 1–13. https://doi.org/10.1016/0301-9268(92)90048-S

Jorge, V.O., 1977. Alguns elementos para o estudo dos Recintos Muralhados do Planalto da Humpata - Angola. Rev. Guimarães 219–245.

Jorge, V.O., 1975. Novas estações arqueológicas do Sudoeste de Angola. Rev. Guimarães 85.

Jorge, V.O., 1974. Breve Introdução à Pré-História de Angola. Rev. Guimarães 84, 149–170.

Kaboré, F., Zongo, G.H., Dogbey, B.F., Ouattara, K., Millogo, Y., Kaboré, L., Hien, E., Zombré, P.N., 2021. Implications of Non-Carbonate Dolomite Minerals in the Formation of Red Soils in a Paleokarstic Context in the Taoudeni Basin in Burkina

Faso. Open J. Soil Sci. 11, 59–71. https://doi.org/10.4236/ojss.2021.112004

Kandel, A.W., Conard, N.J., 2012. Settlement patterns during the Earlier and Middle Stone Age around Langebaan Lagoon, Western Cape (South Africa). Quat. Int. 270, 15–29. https://doi.org/10.1016/j.quaint.2011.06.038

Karkanas, P., Bar-Yosef, O., Goldberg, P., Weiner, S., 2000. Diagenesis in prehistoric caves: The use of minerals that form in situ to assess the completeness of the archaeological record. J. Archaeol. Sci. 27, 915–929. https://doi.org/10.1006/jasc.1999.0506

Karkanas, P., Brown, K.S., Fisher, E.C., Jacobs, Z., Marean, C.W., 2015. Interpreting human behavior from depositional rates and combustion features through the study of sedimentary microfacies at site Pinnacle Point 5-6, South Africa. J. Hum. Evol. 85, 1–21. https://doi.org/https://doi.org/10.1016/j.jhevol.2015.04.006

Karkanas, P., Goldberg, P., 2018a. Reconstructing Archaeological Sites: Understanding the Geoarchaeological Matrix. John Wiley & Sons Ltd. https://doi.org/10.1002/9781119016427

Karkanas, P., Goldberg, P., 2018b. Chapter 12 - Phosphatic Features, in: Stoops, G., Marcelino, V., Mees, F.B.T.-I. of M.F. of S. and R. (Second E. (Eds.), . Elsevier, pp. 323–346. https://doi.org/https://doi.org/10.1016/B978-0-444-63522-8.00012-7

Karkanas, P., Marean, C., Bar-Matthews, M., Jacobs, Z., Fisher, E., Braun, K., 2021. Cave life histories of non-Anthropogenic sediments help us understand associated archaeological contexts. Quat. Res. (United States) 99, 270–289. https://doi.org/10.1017/qua.2020.72

Kaspar, F., Helmschrot, J., Mhanda, A., Butale, M., de Clercq, W., Kanyanga, J.K., Neto, F.O.S., Kruger, S., Castro Matsheka, M., Muche, G., Hillmann, T., Josenhans, K., Posada, R., Riede, J., Seely, M., Ribeiro, C., Kenabatho, P., Vogt, R., Jürgens, N., 2015. The SASSCAL contribution to climate observation, climate data management and data rescue in Southern Africa. Adv. Sci. Res. 12, 171–177. https://doi.org/10.5194/asr-12-171-2015

Kinahan, J., 2016. Human Responses to Climatic Variation in the Namib Desert During the Last 1,000 Years. African Archaeol. Rev. 33, 183–203. https://doi.org/10.1007/s10437-016-9221-3

Kinahan, J., 2011. From the Beginning: The archaeological evidence, in: Wallace, M., Kinahan, J. (Eds.), From the Beginning: The Archaeological Evidence. A History of

Namibia. from the Beginning to 1990. Columbia University Press, New York, pp. 15–44.

Klein, R.G., 1994. Southern Africa before the Iron Age, in: Corruccini, R.S., Ciochon, R.L. (Eds.), Integrative Paths to the Past: Paleoanthropological Advances in Honor of F. Clark Howell. Prentice Hall, Englewood Cliffs, NJ, pp. 471–519.

Kroner, A., Correia, H., 1980. Continuation of the pan african damara belt into angola: a proposed correlation of the Chela group in southern Angola with the Nosib group in northern Namibia/SWA. Trans. Geol. Soc. South Africa 83, 5–16.

Kröner, A., Stern, R.J., 2005. AFRICA | Pan-African Orogeny. Encycl. Geol. 1, 1–12. https://doi.org/10.1016/b0-12-369396-9/00431-7

Kuman, K., Lotter, M.G., Leader, G.M., 2020. The Fauresmith of South Africa: A new assemblage from Canteen Kopje and significance of the technology in human and cultural evolution. J. Hum. Evol. 148, 102884. https://doi.org/https://doi.org/10.1016/j.jhevol.2020.102884

Lebatard, A.E., Bourlès, D.L., Braucher, R., 2019. Absolute dating of an Early Paleolithic site in Western Africa based on the radioactive decay of in situ-produced 10Be and 26Al. Nucl. Instruments Methods Phys. Res. Sect. B Beam Interact. with Mater. Atoms 1–11. https://doi.org/10.1016/j.nimb.2019.05.052

Lipson, M., Ribot, I., Mallick, S., Rohland, N., Olalde, I., Adamski, N., Broomandkhoshbacht, N., Lawson, A.M., López, S., Oppenheimer, J., Stewardson, K., Asombang, R.N., Bocherens, H., Bradman, N., Culleton, B.J., Cornelissen, E., Crevecoeur, I., de Maret, P., Fomine, F.L.M., Lavachery, P., Mindzie, C.M., Orban, R., Sawchuk, E., Semal, P., Thomas, M.G., Van Neer, W., Veeramah, K.R., Kennett, D.J., Patterson, N., Hellenthal, G., Lalueza-Fox, C., MacEachern, S., Prendergast, M.E., Reich, D., 2020. Ancient West African foragers in the context of African population history. Nature 577, 665–670. https://doi.org/10.1038/s41586-020-1929-1

Liu, H., Prugnolle, F., Manica, A., Balloux, F., 2006. A Geographically Explicit Genetic Model of Worldwide Human-Settlement History. Am. J. Hum. Genet. 79, 230–237. https://doi.org/10.1086/505436

Lombard, M., Bradfield, J., Caruana, M. V., Dusseldorp, G., Kramers, J.D., Wurz, S., 2022. The South African Stone Age Sequence updated (II). South African Archaeol. Bull. 77, 172–212.

Lopes, F.C., Pereira, A.J., Mantas, V.M., Mpengo, H.K., 2016. Morphostructural characterization of the western edge of the Huila Plateau (SW Angola), based on remote sensing techniques. J. African Earth Sci. 117, 114–123. https://doi.org/10.1016/j.jafrearsci.2016.01.007

Lyman, R.L., 1994. Quantitative Units and Terminology in Zooarchaeology. Am. Antiq. 59, 36–71. https://doi.org/10.2307/3085500

Mackay, A., Stewart, B.A., Chase, B.M., 2014. Coalescence and fragmentation in the late Pleistocene archaeology of southernmost Africa. J. Hum. Evol. 72, 26–51. https://doi.org/10.1016/j.jhevol.2014.03.003

Macphail, R.I., 2020. Experimental Geoarchaeology BT - Encyclopedia of Geoarchaeology, in: Gilbert, A.S., Goldberg, P., Mandel, R.D., Aldeias, V. (Eds.), . Springer International Publishing, Cham, pp. 1–11. https://doi.org/10.1007/978-3-030-44600-0_124-1

Macphail, R.I., Goldberg, P., 2018. Chapter 27 - Archaeological Materials, in: Stoops, G., Marcelino, V., Mees, F.B.T.-I. of M.F. of S. and R. (Second E. (Eds.), . Elsevier, pp. 779–819. https://doi.org/https://doi.org/10.1016/B978-0-444-63522-8.00027-9

Mallick, S., Li, H., Lipson, M., Mathieson, I., Gymrek, M., Racimo, F., Zhao, M., Chennagiri, N., Nordenfelt, S., Tandon, A., Skoglund, P., Lazaridis, I., Sankararaman, S., Fu, Q., Rohland, N., Renaud, G., Erlich, Y., Willems, T., Gallo, C., Spence, J.P., Song, Y.S., Poletti, G., Balloux, F., Van Driem, G., De Knijff, P., Romero, I.G., Jha, A.R., Behar, D.M., Bravi, C.M., Capelli, C., Hervig, T., Moreno-Estrada, A., Posukh, O.L., Balanovska, E., Balanovsky, O., Karachanak-Yankova, S., Sahakyan, H., Toncheva, D., Yepiskoposyan, L., Tyler-Smith, C., Xue, Y., Abdullah, M.S., Ruiz-Linares, A., Beall, C.M., Di Rienzo, A., Jeong, C., Starikovskaya, E.B., Metspalu, E., Parik, J., Villems, R., Henn, B.M., Hodoglugil, U., Mahley, R., Sajantila, A., Stamatoyannopoulos, G., Wee, J.T.S., Khusainova, R., Khusnutdinova, E., Litvinov, S., Ayodo, G., Comas, D., Hammer, M.F., Kivisild, T., Klitz, W., Winkler, C.A., Labuda, D., Bamshad, M., Jorde, L.B., Tishkoff, S.A., Watkins, W.S., Metspalu, M., Dryomov, S., Sukernik, R., Singh, L., Thangaraj, K., Pääbo, S., Kelso, J., Patterson, N., Reich, D., 2016. The Simons Genome Diversity Project: 300 genomes from 142 diverse populations. Nature. https://doi.org/10.1038/nature18964

Mallol, C., Mentzer, S.M., 2015. Contacts under the lens: Perspectives on the role of microstratigraphy in archaeological research. Archaeol. Anthropol. Sci.

https://doi.org/10.1007/s12520-015-0288-6

Marcelino, V., Schaefer, C.E.G.R., Stoops, G., 2018. Chapter 23 - Oxic and Related Materials, in: Stoops, G., Marcelino, V., Mees, F.B.T.-I. of M.F. of S. and R. (Second E. (Eds.), . Elsevier, pp. 663–689. https://doi.org/https://doi.org/10.1016/B978-0-444-63522-8.00023-1

Marean, C.W., 2015. An Evolutionary Anthropological Perspective on Modern Human Origins. Annu. Rev. Anthropol. 44, 533–556. https://doi.org/10.1146/annurev-anthro-102313-025954

Marean, C.W., Bar-Matthews, M., Bernatchez, J., Fisher, E., Goldberg, P., Herries, A.I.R., Jacobs, Z., Jerardino, A., Karkanas, P., Minichillo, T., Nilssen, P.J., Thompson, E., Watts, I., Williams, H.M., 2007. Early human use of marine resources and pigment in South Africa during the Middle Pleistocene. Nature 449, 905–908. https://doi.org/10.1038/nature06204

Maret, P.. de, Noten, F.. van, Cahen, D.., 1977. Radiocarbon Dates from West Central Africa: A Synthesis. J. African Hist. 18, 481–505.

Marks, T.P., 2015. Middle and Later Stone Age land use system in the desert environment: Insights from the Namibian surface record. South African Archaeol. Bull. 70, 180–192.

Marks, T.P., McCall, G., 2014. New approaches to the study of surface paleolithic artefacts: a pilot project at Zebra River by Terry Hardaker. Lithic Technol. 39, 200–202.

McBrearty, S., 1991. Recent research in western Kenya and its implications for the status of the Sangoan industry., in: Clark, J.D. (Ed.), Cultural Beginnings: Approaches to Understanding Early Hominid Lifeways in the African Savanna, Monographien 19. Romisch-Germanisches Zentralmuseum, Forschunginstitut fur Vor- und Fruhgeschichte, Bonn, pp. 156–176.

McBrearty, S., 1990. Consider the humble termite: Termites as agents of post-depositional disturbance at african archaeological sites. J. Archaeol. Sci. 17, 111–143. https://doi.org/https://doi.org/10.1016/0305-4403(90)90054-9

Mccall, G.S., Marks, T.P., Thomas, J.T., Eller, M., Horn, S.W.I., Horowitz, R. a., Kettler, K., Taylor-Perryman, R., 2011. Erb Tanks: a Middle and Later Stone Age Rockshelter in the Central Namib Desert, Western Namibia. PaleoAnthropology 398–421. https://doi.org/10.4207/PA.2011.ART67

McPherron, S.P., Dibble, H.L., 2002. Using Computers in Archaeology: a Practical Guide. McGraw Hill, New York.

Mehlman, M., 1991. Context of the emergence of modern man in eastern Africa: some new Tanzanian evidence., in: Cultural Beginnings.

Mendelsohn, J.M., 2019. Landscape Changes in Angola BT - Biodiversity of Angola: Science & Conservation: A Modern Synthesis, in: Huntley, B.J., Russo, V., Lages, F., Ferrand, N. (Eds.), . Springer International Publishing, Cham, pp. 123–137. https://doi.org/10.1007/978-3-030-03083-4_8

Mendelsohn, J.M., Mendelsohn, S., 2018. Sudoeste de Angola, Um retrato da terra e da vida/South West Angola. A portrait of land and life. Raison, Porto.

Meneganzin, A., Pievani, T., Manzi, G., 2022. Pan-Africanism vs. single-origin of Homo sapiens: Putting the debate in the light of evolutionary biology. Evol. Anthropol. Issues, News, Rev. 31, 199–212. https://doi.org/10.1002/evan.21955

Mentzer, S.M., 2014. Microarchaeological Approaches to the Identification and Interpretation of Combustion Features in Prehistoric Archaeological Sites. J. Archaeol. Method Theory 21, 616–668. https://doi.org/10.1007/s10816-012-9163-2

Mesfin, I., Lotter, M.G., Benjamim, M.H., 2021. A new approach to quantifying raw material selectivity in the African Acheulean: Perspectives from Angola and South Africa. J. African Archaeol. 4, 1–30. https://doi.org/10.1163/21915784-20210013

Miller, C.E., 2015. A tale of two Swabian caves: Geoarchaeological investigations at Hohle Fels an Geissenklosterle. Kerns Verlag, Tübingen.

Miller, C.E., 2011. Deposits as Artifacts. TÜVA Mitteilungen 14, 91–107.

Miller, C.E., Conard, N.J., Goldberg, P., Berna, F., 2008. Dumping, Sweeping And Trampling: Experimental Micromothpological Analysis of Anthropogenically Modified Combustion Features.

Miller, C.E., Mentzer, S.M., Berthold, C., Leach, P., Ligouis, B., Tribolo, C., Parkington, J., Porraz, G., 2016. Site-formation processes at Elands Bay Cave, South Africa. South. African Humanit. 29, 69–128.

Mills, M.S.L., Melo, M., 2013. The checklist of the birds of Angola/A Lista das Aves de Angola. Luanda.

Mitchell, P., 2010. Genetics and southern African prehistory: An archaeological view. J. Anthropol. Sci. 88, 73–92.

Mitchell, P.J., 2017. Discontinuities in hunter-gatherer prehistory in southern African drylands. J. Anthropol. Archaeol. 46, 40–52. https://doi.org/10.1016/j.jaa.2016.07.001

Monadjem, A., Taylor, P.J., Denys, C., Cotterill, F.P.D., 2015. Ara Monadjem, Peter J. Taylor, Christiane Denys, Fenton P.D. Cotterill Rodents of Sub-Saharan Africa.

Morley, M.W., Goldberg, P., 2017. Geoarchaeological research in the humid tropics: A global perspective. J. Archaeol. Sci. 77, 1–9. https://doi.org/10.1016/j.jas.2016.11.002

Mouta, F., 1954. Notícia Explicativa do Esboço Geológico de Angola (1:2.000.000). Lisboa.

Mouta, F., 1953. Possibilidade de existência de Pré-Hominideos no sul de Angola (Leba, Humpata). An. Inst. Med. Trop. (Lisb). X, 2906–2911.

Mpengo, H., Lopes, F., Pereira, Alcides, Mantas, V.M., 2011. A detecção remota como suporte à caracterização morfo-estrutural do bordo ocidental do planalto da Huíla (SW de Angola), in: Neves, L., Pereira, A., Gomes, C., Tavares, A.O. (Eds.), Modelação de Sistemas Geológicos: Livro de Homenagem Ao Professor Manuel Maria Godinho. Imprensa da Universidade de Coimbra, Coimbra, pp. 253–265. https://doi.org/10.14195/978-989-26-1009-2_18

Munday, C., Washington, R., 2017. Circulation controls on southern African precipitation in coupled models: The role of the Angola Low. J. Geophys. Res. 122, 861–877. https://doi.org/10.1002/2016JD025736

Nicoll, K., 2010. Geomorphic development and Middle Stone Age archaeology of the Lower Cunene River, Namibia-Angola Border. Quat. Sci. Rev. 29, 1419–1431. https://doi.org/10.1016/j.quascirev.2009.02.026

Nicoll, K., 2009. Evidence of Levallois technique at a Middle Stone Age open air site along the Angola-Namibia border. Antiquity 83, http://antiquity.ac.uk/projgall/nicoll/.

Nicoll, K., Zerboni, A., 2019. Is the past key to the present? Observations of cultural continuity and resilience reconstructed from geoarchaeological records. Quat. Int.

Nicosia, Cristiano, Stoops, G., 2017. Archaeological Soil and Sediment Micromorphology, Archaeological Soil and Sediment Micromorphology. https://doi.org/10.1002/9781118941065

Nicosia, Cristiano., Stoops, G.R., 2017. Archaeological Soil and Sediment

Micromorphology. Wiley, Newark. https://doi.org/10.1002/9781118941065

Noonan, J.P., Coop, G., Kudaravalli, S., Smith, D., Krause, J., Alessi, J., Chen, F., Platt, D., Pääbo, S., Pritchard, J.K., Rubin, E.M., 2006. Sequencing and analysis of Neanderthal genomic DNA. Science (80-.). https://doi.org/10.1126/science.1131412

Oliveira, S., Fehn, A.M., Aço, T., Lages, F., Gayà-Vidal, M., Pakendorf, B., Stoneking, M., Rocha, J., 2018. Matriclans shape populations: Insights from the Angolan Namib Desert into the maternal genetic history of southern Africa. Am. J. Phys. Anthropol. 165, 518–535. https://doi.org/10.1002/ajpa.23378

Oliveira, S., Hübner, A., Fehn, A.M., Aço, T., Lages, F., Pakendorf, B., Stoneking, M., Rocha, J., 2019. The role of matrilineality in shaping patterns of Y chromosome and mtDNA sequence variation in southwestern Angola. Eur. J. Hum. Genet. 27, 475–483. https://doi.org/10.1038/s41431-018-0304-2

Olson, D.M., Dinerstein, E., Wikramanayake, E.D., Burgess, N.D., Powell, G.V.N., Underwood, E.C., D'amico, J.A., Itoua, I., Strand, H.E., Morrison, J.C., Loucks, C.J., Allnutt, T.F., Ricketts, T.H., Kura, Y., Lamoreux, J.F., Wettengel, W.W., Hedao, P., Kassem, K.R., 2001. Terrestrial Ecoregions of the World: A New Map of Life on Earth: A new global map of terrestrial ecoregions provides an innovative tool for conserving biodiversity. Bioscience 51, 933–938. https://doi.org/10.1641/0006-3568(2001)051[0933:TEOTWA]2.0.CO;2

Onac, B.P., Forti, P., 2011. Minerogenetic mechanisms occurring in the cave environment: An overview. Int. J. Speleol. 40, 79–98. https://doi.org/10.5038/1827-806X.40.2.1

Ossendorf, G., 2017a. Technological analyses of late pleistocene later stone age lithic assemblages from apollo 11 rock shelter, ||karas region, southwestern Namibia. South African Archaeol. Bull. 72, 17–37.

Ossendorf, G., 2017b. Two Holocene Later Stone Age stratigraphies from the Sesfontein area, northwestern Namibia. Azania 52, 233–266. https://doi.org/10.1080/0067270X.2017.1296626

Pais Pinto, L., 1988. Le Museé National d'Archaeologie de Benguela (Angola): Bilan des Premiers Travaux: 1979-1987.

Patania, I., Porter, S.T., Keegan, W.F., Dihogo, R., Frank, S., Lewis, J., Mashaka, H., Ogutu, J., Skosey-Lalonde, E., Tryon, C.A., Niespolo, E.M., Colarossi, D., Ranhorn,

K.L., 2022. Geoarchaeology and Heritage Management: Identifying and Quantifying Multi-Scalar Erosional Processes at Kisese II Rockshelter, Tanzania. Front. Earth Sci. 9, 1–20. https://doi.org/10.3389/feart.2021.665193

Pereira, E., Tassinari, C.C.G.., Rodrigues, J.F., Van-Dúnem, M. V., 2011. New data on the deposition age of the volcano-sedimentary Chela Group and its Eburnean basement: implications to post-Eburnean crustal evolution of the SW of Angola. Comun. Geol. t. 98 98, 29–40.

Pereira, E., 1977. Serra da Neve (Angola) - Nota sobre a geomorfologia da região e idade das aplanações. Bol. da Soc. Geológica Port. XX XX, 277–282.

Pickford, M., Fernandes, T., Aço, S., 1990. Nouvelles découvertes de remplissages de fissures à primates dans le Planalto da Humpata, Huíla, Sud de l'Angola. C. R. Acad. Sc. Paris 310, 843–848.

Pickford, M., Mein, P., Senut, B., 1994. Fossiliferous Neogene karst fillings in Angola, Botswana and Namibia. S. Afr. J. Sci. 90, 227–230.

Pickford, M., Mein, P., Senut, B., 1992. Primate bearing Plio-Pleistocene cave deposits of Humpata, Southern Angola. Hum. Evol. 7, 17–33. https://doi.org/10.1007/BF02437475

Pickford, M., Senut, B., 2010. Karst Geology and Palaeobiology of Northern Namibia, Geology. Geological Survey of Angola, Ministry of Mines and Energy of Namibia, Windhoek.

Pineda, A., Saladié, P., 2022. Beyond the Problem of Bone Surface Preservation in Taphonomic Studies of Early and Middle Pleistocene Open-Air Sites, Journal of Archaeological Method and Theory. Springer US. https://doi.org/10.1007/s10816-022-09550-0

Pombo, S., Proença de Oliveira, R., Mendes, A., 2017. Comparative performance analysis of climate re-analysis approaches in Angola. Hydrol. Sci. J. 62, 698–714. https://doi.org/10.1080/02626667.2016.1257856

Porat, N., Chazan, M., Grün, R., Aubert, M., Eisenmann, V., Horwitz, L.K., 2010. New radiometric ages for the Fauresmith industry from Kathu Pan, southern Africa: Implications for the Earlier to Middle Stone Age transition. J. Archaeol. Sci. 37, 269–283. https://doi.org/10.1016/j.jas.2009.09.038

Porraz, G., Val, A., Tribolo, C., Mercier, N., De La Peña, P., Haaland, M.M., Igreja, M., Miller, C.E., Schmid, V.C., 2018. The MIS5 pietersburg at 28' bushman rock Shelter,

Limpopo Province, South Africa, PLoS ONE. https://doi.org/10.1371/journal.pone.0202853

Prüfer, K., Racimo, F., Patterson, N., Jay, F., Sankararaman, S., Sawyer, S., Heinze, A., Renaud, G., Sudmant, P.H., De Filippo, C., Li, H., Mallick, S., Dannemann, M., Fu, Q., Kircher, M., Kuhlwilm, M., Lachmann, M., Meyer, M., Ongyerth, M., Siebauer, M., Theunert, C., Tandon, A., Moorjani, P., Pickrell, J., Mullikin, J.C., Vohr, S.H., Green, R.E., Hellmann, I., Johnson, P.L.F., Blanche, H., Cann, H., Kitzman, J.O., Shendure, J., Eichler, E.E., Lein, E.S., Bakken, T.E., Golovanova, L. V., Doronichev, V.B., Shunkov, M. V., Derevianko, A.P., Viola, B., Slatkin, M., Reich, D., Kelso, J., Pääbo, S., 2014. The complete genome sequence of a Neanderthal from the Altai Mountains. Nature. https://doi.org/10.1038/nature12886

Ramos, M., 1982. Le Paléolitique du Sud-Ouest de l'Angola - Vue d'ensemble. LEBA Estud. pré-história e Arqueol. 5, 43–52.

Ramos, M., 1981. As escavações de Capangombe e o problema da M.S.A. no SW de Angola. LEBA Estud. pré-história e Arqueol. 4, 29–35.

Ramos, M., 1970. Algumas descobertas recentes no Sudoeste de Angola (nota prévia), in: Actas Das I Jornadas Arqueológicas, Lisboa, 1969, Vol. I.

Redinha, J., 1975. Etnias e Culturas de Angola. Instituto de Investigação Científica de Angola, Luanda.

Rhodes, S.E., Goldberg, P., Ecker, M., Horwitz, L.K., Boaretto, E., Chazan, M., 2022. Exploring the Later Stone Age at a micro-scale: New high-resolution excavations at Wonderwerk Cave. Quat. Int. 614, 126–145. https://doi.org/10.1016/j.quaint.2021.10.004

Ricardo, R.P., Marques, M.M., Ramos, M.F., 1980. Nota sobre o processo de formação dos solos ferralíticos da região do Hoque (província da Huíla - Angola). Bol. da Soc. Geológica Port. XXII XXII, 337–347.

Richter, D., Grün, R., Joannes-Boyau, R., Steele, T.E., Amani, F., Rué, M., Fernandes, P., Raynal, J.P., Geraads, D., Ben-Ncer, A., Hublin, J.J., McPherron, S.P., 2017. The age of the hominin fossils from Jebel Irhoud, Morocco, and the origins of the Middle Stone Age. Nature. https://doi.org/10.1038/nature22335

Robakiewicz, E., de Matos, D., Stone, J.R., Junginger, A., 2021. Hydrochemistry and Diatom Assemblages on the Humpata Plateau , Southwestern Angola. Geosciences 11, 1–21.

Röpke, A., Dietl, C., 2017. Burnt Soils and Sediments, in: Archaeological Soil and Sediment Micromorphology. pp. 173–180. https://doi.org/https://doi.org/10.1002/9781118941065.ch21

Rots, V., Peer, P., 2006. Early evidence of complexity in lithic economy: core-axe production, hafting and use at Late Middle Pleistocene site 8-B-11, Sai Island (Sudan). J. Archaeol. Sci. 33, 360–371. https://doi.org/10.1016/j.jas.2005.08.002

Russell, T., Steele, J., 2009. A geo-referenced radiocarbon database for Early Iron Age sites in sub-Saharan Africa: Initial analysis. South. African Humanit. 21, 327–344.

Sadr, K., Sampson, G., 2006. Through Thick and Thin: Early Pottery in Southern Africa. J. African Archaeol. https://doi.org/10.3213/1612-1651-10074

Saladié, P., Rodríguez-Hidalgo, A., Díez, C., Martín-Rodríguez, P., Carbonell, E., 2013. Range of bone modifications by human chewing. J. Archaeol. Sci. 40, 380–397. https://doi.org/https://doi.org/10.1016/j.jas.2012.08.002

Scerri, E.M.L., 2017. The North African Middle Stone Age and its place in recent human evolution. Evol. Anthropol. Issues, News, Rev. 26, 119–135. https://doi.org/10.1002/evan.21527

Scerri, E.M.L., Blinkhorn, J., Groucutt, H.S., Niang, K., 2016. The Middle Stone Age archaeology of the Senegal River Valley. Quat. Int. 408, 16–32. https://doi.org/https://doi.org/10.1016/j.quaint.2015.09.025

Scerri, E.M.L., Chikhi, L., Thomas, M.G., 2019. Beyond multiregional and simple out-of-Africa models of human evolution. Nat. Ecol. Evol. 2019 310 3, 1370–1372. https://doi.org/10.1038/s41559-019-0992-1

Scerri, E.M.L., Thomas, M.G., Manica, A., Gunz, P., Stock, J.T., Stringer, C., Grove, M., Groucutt, H.S., Timmermann, A., Rightmire, G.P., d'Errico, F., Tryon, C.A., Drake, N.A., Brooks, A.S., Dennell, R.W., Durbin, R., Henn, B.M., Lee-Thorp, J., deMenocal, P., Petraglia, M.D., Thompson, J.C., Scally, A., Chikhi, L., 2018. Did Our Species Evolve in Subdivided Populations across Africa, and Why Does It Matter? Trends Ecol. Evol. https://doi.org/10.1016/j.tree.2018.05.005

Schiegl, S., Goldberg, P., Pfretzschner, H.-U., Conard, N.J., 2003. Paleolithic burnt bone horizons from the Swabian Jura: Distinguishing between in situ fireplaces and dumping areas. Geoarchaeology 18, 541–565. https://doi.org/https://doi.org/10.1002/gea.10080

Schiffer, M.B., 1987. Formation processes of the archaeological record.

Schlebusch, C.M., Loog, L., Groucutt, H.S., King, T., Rutherford, A., Barbieri, C., Barbujani, G., Chikhi, L., Stringer, C., Jakobsson, M., Eriksson, A., Manica, A., Tishkoff, S.A., Scerri, E.M., Scally, A., Brierley, C., Thomas, M.G., 2021. Human origins in Southern African palaeo-wetlands? Strong claims from weak evidence. J. Archaeol. Sci. 130, 0–5. https://doi.org/10.1016/j.jas.2021.105374

Schlebusch, C.M., Malmström, H., Günther, T., Sjödin, P., Coutinho, A., Edlund, H., Munters, A.R., Vicente, M., Steyn, M., Soodyall, H., Lombard, M., Jakobsson, M., 2017. Southern African ancient genomes estimate modern human divergence to 350,000 to 260,000 years ago. Science (80-.). 358, 652–655. https://doi.org/10.1126/science.aao6266

Schmidt, I., 2011. A Middle Stone Age Assemblage with Discoid Lithic Technology from Etemba 14, Erongo Mountains, Northern Namibia. J. African Archaeol. 9, 85–100. https://doi.org/10.3213/1612-1651-10183

Schmidt, I., Hensel, E., Bubenzer, O., Eichhorn, B., Gessert, L., Gwasira, G., Henselowsky, F., Imalwa, E., Kehl, M., Rethemeyer, J., Astrid, R., 2016. New investigations at the Middle Stone Age site of Pockenbank Rockshelter , 1–6. https://doi.org/10.15184/aqy.2016.165

Sen, S., Pickford, M., 2022. Red Rock Hares (Leporidae, Lagomorpha) past and present in southern Africa and a new species of Pronolagus from the early Pleistocene of Angola. Commun. Geol. Surv. Namibia 24, 67–97.

Sessa, E., Rellini, I., Traverso, A., Molinari, I., Montinari, G., Rossi, G., Firpo, M., 2019. Microstratigraphic records as tools for the detection of climatic changes in tana di badalucco cave(Liguria, NW Italy). Geosci. 9. https://doi.org/10.3390/geosciences9060276

Shahack-Gross, R., 2017. Archaeological formation theory and geoarchaeology: State-of-the-art in 2016. J. Archaeol. Sci. 79, 36–43. https://doi.org/10.1016/j.jas.2017.01.004

Sheppard, P.J., Kleindienst, M.R., 1996. Technological change in the earlier and middle stone Age of Kalambo Falls (Zambia). African Archaeol. Rev. 13, 171–196. https://doi.org/10.1007/BF01963510

Shipton, C., Roberts, P., Archer, W., Armitage, S.J., Bita, C., Blinkhorn, J., Courtney-Mustaphi, C., Crowther, A., Curtis, R., Errico, F.D., Douka, K., Faulkner, P., Groucutt, H.S., Helm, R., Herries, A.I.R., Jembe, S., Kourampas, N., Lee-Thorp, J.,

Marchant, R., Mercader, J., Marti, A.P., Prendergast, M.E., Rowson, B., Tengeza, A., Tibesasa, R., White, T.S., Petraglia, M.D., Boivin, N., 2018. 78,000-year-old record of Middle and Later stone age innovation in an East African tropical forest. Nat. Commun. 9, 1–8. https://doi.org/10.1038/s41467-018-04057-3

Slon, V., Hopfe, C., Weiß, C.L., Mafessoni, F., De La Rasilla, M., Lalueza-Fox, C., Rosas, A., Soressi, M., Knul, M. V., Miller, R., Stewart, J.R., Derevianko, A.P., Jacobs, Z., Li, B., Roberts, R.G., Shunkov, M. V., De Lumley, H., Perrenoud, C., Gušić, I., Kućan, Ž., Rudan, P., Aximu-Petri, A., Essel, E., Nagel, S., Nickel, B., Schmidt, A., Prüfer, K., Kelso, J., Burbano, H.A., Pääbo, S., Meyer, M., 2017. Neandertal and Denisovan DNA from Pleistocene sediments. Science (80-.). 356, 605–608. https://doi.org/10.1126/science.aam9695

Soriano, S., Villa, P., Delagnes, A., Degano, I., Pollarolo, L., Lucejko, J.J., Henshilwood, C., Wadley, L., 2015. The Still Bay and Howiesons Poort at Sibudu and Blombos: Understanding Middle Stone Age Technologies. PLoS One 10, e0131127–e0131127. https://doi.org/10.1371/journal.pone.0131127

Sousa, D., Spinola, D., Santos, J., Tatumi, S., 2022. Relict Soil Features in Cave Sediments Record Periods of Wet Climate and Dense Vegetation Over the Last 100 Kyr in a Present-Day Semiarid Region of Northeast Brazil. SSNR.

Stein, J.K., 2001. A Review of Site Formation Processes and Their Relevance to Geoarchaeology. Earth Sci. Archaeol. 37–51. https://doi.org/10.1007/978-1-4615-1183-0_2

Stiner, M.C., Kuhn, S.L., Surovell, T.A., Goldberg, P., Meignen, L., Weiner, S., Bar-Yosef, O., 2001. Bone preservation in Hayonim Cave (Israel): A macroscopic and mineralogical study. J. Archaeol. Sci. 28, 643–659. https://doi.org/10.1006/jasc.2000.0634

Stiner, M.C., Kuhn, S.L., Weiner, S., Bar-Yosef, O., 1995. Differential Burning, Recrystallization, and Fragmentation of Archaeological Bone. J. Archaeol. Sci. 22, 223–237. https://doi.org/10.1006/jasc.1995.0024

Stoops, G., 2020. Guidelines for Analysis and Description of Soil and Regolith Thin Sections, 2nd editio. ed. Wiley.

Stoops, G., 2003. Guidelines for Analysis and Description of soil regolith thin sections. Soil Science Society of America, Madison, USA.

Stoops, G., Marcelino, V., 2018. Chapter 24 - Lateritic and Bauxitic Materials, in: Stoops,

G., Marcelino, V., Mees, F.B.T.-I. of M.F. of S. and R. (Second E. (Eds.), . Elsevier, pp. 691–720. https://doi.org/https://doi.org/10.1016/B978-0-444-63522-8.00024-3

Stoops, G., Marcelino, V., Mees, F., 2018. Interpretation of micromorphological features of soils and regoliths.

Stoops, G., Marcelino, V., Mees, F., 2010. Interpretation of Micromorphological Features of soils and regoliths, 1st ed. Elsevier.

Tavares, A.O., Henriques, M.H., Domingos, A., Bala, A., 2015. Community involvement in geoconservation: A conceptual approach based on the geoheritage of South Angola. Sustain. 7, 4893–4918. https://doi.org/10.3390/su7054893

Taylor, N., 2022. Riddles wrapped inside an enigma. Lupemban MSA technology as a rainforest adaptation: revisiting the lanceolate point. Philos. Trans. R. Soc. B 377. https://doi.org/10.1098/RSTB.2020.0484

Taylor, N., 2016. Across Rainforests and Woodlands: A Systematic Reappraisal of the Lupemban Middle Stone Age in Central Africa, in: Jones, S.C., Stewart, B.A. (Eds.), Africa from MIS 6-2: Population Dynamics and Paleoenvironments. Springer, pp. 273–299. https://doi.org/10.1007/978-94-017-7520-5_15

Thompson, J.C., Wright, D.K., Ivory, S.J., Choi, J.H., Nightingale, S., Mackay, A., Schilt, F., Otárola-Castillo, E., Mercader, J., Forman, S.L., Pietsch, T., Cohen, A.S., Arrowsmith, J.R., Welling, M., Davis, J., Schiery, B., Kaliba, P., Malijani, O., Blome, M.W., O'Driscoll, C.A., Mentzer, S.M., Miller, C., Heo, S., Choi, J., Tembo, J., Mapemba, F., Simengwa, D., Gomani-Chindebvu, E., 2021. Early human impacts and ecosystem reorganization in southern-central Africa. Sci. Adv. 7. https://doi.org/10.1126/sciadv.abf9776

Tixier, J., 1956. Le hachereau dans l'Acheuléen nord-africain. Notes typologiques, in: Congr. Préhist, de France, XVe Session, Poitiers. pp. 914–923.

Tribolo, C., Mercier, N., Douville, E., Joron, J.L., Reyss, J.L., Rufer, D., Cantin, N., Lefrais, Y., Miller, C.E., Porraz, G., Parkington, J., Rigaud, J.P., Texier, P.J., 2013. OSL and TL dating of the Middle Stone Age sequence at Diepkloof Rock Shelter (South Africa): A clarification. J. Archaeol. Sci. 40, 3401–3411. https://doi.org/10.1016/j.jas.2012.12.001

Tribolo, C., Mercier, N., Valladas, H., 2005. Chronologie des technofaciès Howieson's Poort et Still Bay (Middle Stone Age, Afrique du Sud): Bilan et nouvelles données de la luminescence. Bull. la Soc. Prehist. Fr.

https://doi.org/10.3406/bspf.2005.13187

Tribolo, C., Mercier, N., Valladas, H., Lefrais, Y., Miller, C.E., Parkington, J., Porraz, G., 2016. Chronology of the Pleistocene deposits at Elands Bay Cave (South Africa) based on charcoals, burnt lithics, and sedimentary quartz and feldspar grains. South. African Humanit. 29, 129–52.

Tryon, C.A., McBrearty, S., 2002. Tephrostratigraphy and the Acheulian to Middle Stone Age transition in the Kapthurin Formation, Kenya. J. Hum. Evol. 42, 211–235. https://doi.org/10.1006/jhev.2001.0513

Tryon, C.A., Potts, R., 2011. Approaches for understanding flake production in the African Acheulean. Paleoanthropology 376–389. https://doi.org/10.4207/PA.2011.ART65

Underhill, D., 2011. The study of the Fauresmith: A review. South African Archaeol. Bull. 66, 15–26.

Van Peer, P., Fullagar, R., Stokes, S., Bailey, R.M., Moeyersons, J., Steenhoudt, F., Geerts, A., Vanderbeken, T., De Dapper, M., Geus, F., 2003. The Early to Middle Stone Age Transition and the emergence of modern human behaviour at site 8-B-11 Sai Island, Sudan. J. Hum. Evol. 45, 187–193. https://doi.org/10.1016/S0047-2484(03)00103-9

Van Peer, P., Rots, V., Vroomans, J.-M., 2004. A story of colourful diggers and grinders: the Sangoan and Lupemban at site 8-B-11, Sai Island, Northern Sudan. Before Farming 1 3, 1–28. https://doi.org/10.3828/bfarm.2004.3.1

Veldman, A., Parsons, I., Lombard, M., 2017. Kuidas spring 1, Namibia: First impressions of a later stone age site complex. South African Archaeol. Bull. 72, 60–70.

Veress, M., 2020. Karst types and their karstification. J. Earth Sci. 31, 621–634.

Vogelsang, R., Richter, J., Jacobs, Z., Eichhorn, B., Linseele, V., Roberts, R.G., 2010. New excavations of Middle Stone Age deposits at Apollo 11 rockshelter, Namibia: Stratigraphy, archaeology, chronology and past environments. J. African Archaeol. 8, 185–218. https://doi.org/10.3213/1612-1651-10170

Wilkins, J., Chazan, M., 2012. Blade production ~500 thousand years ago at Kathu Pan 1, South Africa: Support for a multiple origins hypothesis for early Middle Pleistocene blade technologies. J. Archaeol. Sci. 39, 1883–1900. https://doi.org/10.1016/j.jas.2012.01.031

Will, M., Kandel, A.W., Conard, N.J., 2019. Midden or Molehill: The Role of Coastal Adaptations in Human Evolution and Dispersal, Journal of World Prehistory. Springer US. https://doi.org/10.1007/s10963-018-09127-4

Will, M., Parkington, J.E., Kandel, A.W., Conard, N.J., 2013. Coastal adaptations and the Middle Stone Age lithic assemblages from Hoedjiespunt 1 in the Western Cape, South Africa. J. Hum. Evol. 64, 518–537. https://doi.org/10.1016/j.jhevol.2013.02.012

Willoughby, P.R., 2020. Modern Human Behavior. https://doi.org/10.1093/acrefore/9780190854584.013.46

Wright, D.K., Thompson, J.C., Schilt, F., Cohen, A.S., Choi, J.H., Mercader, J., Nightingale, S., Miller, C.E., Mentzer, S.M., Walde, D., Welling, M., Gomani-Chindebvu, E., 2017. Approaches to Middle Stone Age landscape archaeology in tropical Africa. J. Archaeol. Sci. https://doi.org/10.1016/j.jas.2016.01.014

Wurz, S., 2013a. Technological Trends in the Middle Stone Age of South Africa between MIS 7 and MIS 3. Curr. Anthropol. 54, S305–S319. https://doi.org/10.1086/673283

Wurz, S., 2013b. Technological trends in the middle stone age of South Africa between MIS 7 and MIS 3. Curr. Anthropol. https://doi.org/10.1086/673283

Wurz, S., Pickering, R., Mentzer, S.M., 2022. U-Th dating, taphonomy, and taxonomy of shell middens at Klasies River main site indicate stable and systematic coastal exploitation by MIS 5c-d. Front. Earth Sci. 10, 1–25. https://doi.org/10.3389/feart.2022.1001370

Ziegler, M., Simon, M.H., Hall, I.R., Barker, S., Stringer, C., Zahn, R., 2013. Development of Middle Stone Age innovation linked to rapid climate change. Nat. Commun. 4, 1905–1909. https://doi.org/10.1038/ncomms2897

Appendix 1 – Faunal analysis

Area VOJ

Macromammals	1		2		3		4		5		6		7		Total	
Taxon	NISP	%	NISP	%	NISP	%	NISP	%	NISP	%	NISP	%	NISP	%	NISP	%
Bovids																
Bov I/ II	1	2	-	-	-	-	1	2.5	-	-	-	-	-	-	**2**	1.4
Bov II	4	7.8	3	50	2	12.5	2	5	1	4.2	-	-	-	-	**12**	8.2
Springbuck (*Antidorcas marsupialis*)	-	-	-	-	-	-	3	7.5	-	-	-	-	-	-	**3**	2.1
Bov II/ III	2	3.9	-	-	1	6.3	8	20	3	12.5	1	14.3	-	-	**15**	10.3
Bov III	3	5.9	-	-	-	-	2	5	-	-	-	-	-	-	**5**	3.4
Bov III/IV	4	7.8	1	16.7	-	-	1	2.5	-	-	-	-	-	-	**6**	4.1
Bov IV	1	2	-	-	-	-	-	-	-	-	-	-	-	-	**1**	0.7
Indet. Bov.	2	3.9	-	-	-	-	9	22.5	2	8.3	-	-	1	50	**13**	8.9
Other ungulates																
Zebra (*Equus* cf. *quagga*)	-	-	-	-	-	-	2	5	-	-	-	-	-	-	**2**	1.4
Pig/ warthog (Cf. *Phacochoerus*/*Potamochoerus*)	1	2	-	-	-	-	-	-	-	-	-	-	-	-	**1**	0.7
Rodents																
Porcupine (*Hystrix africaeaustralis*)	3	5.9	-	-	-	-	-	-	-	-	1	14.3	-	-	**4**	2.7
Indet. mammals																
Indet. medium mammals	26	51	2	33.3	13	81.3	12	30	17	70.8	5	71.4	1	50	**75**	51.4
Indet. small/ medium mammals	3	5.9	-	-	-	-	-	-	1	4.2	-	-	-	-	**4**	2.7
Indet. small mammals	1	2	-	-	-	-	-	-	-	-	-	-	-	-	**1**	0.7
Total	**51**	**100**	**6**	**100**	**16**	**100**	**40**	**100**	**24**	**100**	**7**	**100**	**2**	**100**	**146**	**100**

Micromammals	1			2			3			4			5			6			7			Total		
Taxon	NISP	%	MNI	NISP	%	MNI	NISP	%	MNI	NISP	%	MNI	NISP	%	MNI	NISP	%	MNI	NISP	%	MNI	NISP	MNI	%
Rodentia																								
Muridae	39	26.5	7	82	15.3	19	16	4	10	3	15	1				3	3.6	2	9	11.8	3	152	42	15.3
Murinae	1	0.7	1	66	12.3	13	88	22.1	23	2	10	1	20	46.5	3	8	9.5	3	9	11.8	2	194	46	16.8
Aethomys namaquensis	4	100	1	5	0.9	1	5	1.3	1	4	20	1				5	6	1				23	5	1.8
Aethomys sp.				44	8.2	9	5	1.3	1													49	10	3.6
Cryptomys sp.							5	1.3	2													5	2	0.7
Dasymys incomtus																			5	6.6	1	5	1	0.4
Hylomyscus sp.							9	2.3	2													9	2	0.7
Lemniscomys sp.	3	2	1	3	0.6	1	5	1.3	1	3	15	1										14	4	1.5
Mastomys natalensis							8	2	2	4	20	1										12	3	1.1
Mastomys sp.				8	1.5	1	21	5.3	6										11	14.5	3	32	10	3.6
Mus sp.	12	8.2	2	74	13.8	10	30	7.5	2				7	16.3	1	19	22.6	3				142	18	6.6
Oeonomys hypoxantos	3	2	1																			3	1	0.4
Otomys sp.	43	29.3	6	95	17.7	11	80	20.1	17				4	9.3	1	12	14.3	3	18	23.7	2	252	40	14.6
Otomys cuanzensis	5	3.4	1																			5	1	0.4
Praomys tullbergi							3	0.8	1													3	1	0.4
Praomys sp.				3	0.6	1	4	1	1							3	3.6	1				10	3	1.1
Rhabdomys pumilio	7	4.8	2	4	0.7	1	4	1	1													15	4	1.5
Saccostomus camprestris	4	2.7	1				5	1.3	1				2	4.6	1							11	3	1.1
Steatomys sp.													4	9.3	1							4	1	0.4
Thallomys nigricauda				6	1.1	1	12	3	3													18	4	1.5
Thallomys sp.				3	0.6	1	2	0.5	2													5	3	1.1
Zelotomys sp.				4	0.7	2																4	2	0.7

Micromammals (cont.)	1			2			3			4			5			6			7			Total		
Taxon	NISP	%	MNI	NISP	%	MNI	NISP	%	MNI	NISP	%	MNI	NISP	%	MNI	NISP	%	MNI	NISP	%	MNI	NISP	MNI	%
Gerbillidae				11	2	4	3	0.75	1										5	6.6	1	19	4	1.5
Gerbilliscus sp.				14	2.6	4	7	1.8	1	4	20	1	2	4.7	1	8	9.5	1	3	3.9	1	38	9	3.3
Desmodillus auricularis	4	2.7	1	5	0.9	1													6	7.9	2	14	4	1.5
Desmodillus sp.				1	0.2	1													1	1.3	1	2	2	0.7
Gerbillurus paeba				3	0.6	1	2	0.5	1													5	2	0.7
Tatera leucogaster				11	2	1	8	2	2													19	3	1.1
Tatera sp.				7	1.3	1																7	1	0.4
Insectivora																								
Macroscilidae				1	0.2	1																1	1	0.4
Atelerix sp.				1	0.2	1																1	1	0.4
Crocidura sp.	7	4.8	1	14	2.6	2	29	7.3	3							12	14.3	2				62	8	2.9
Elephantulus sp.	18	12.2	2	37	6.9	7	37	9.3	8				4	9.3	1	9	10.7	3	3	3.9	1	108	22	8
Suncus lixus				26	4.8	4	7	1.8	1							5	6	1	1	1.3	1	39	7	2.5
Sylvisorex megalura				9	1.7	1																9	1	0.4
Lagomorpha																								
Leporidae	1	0.7	1																			1	1	0.4
Sciuridae																								
Heliosciurus gambianus							4	1	1										5	6.6	1	9	2	0.7
Grand total	151	100	28	537	100	100	399	100	94	20	100	6	43	100	9	84	100	20	76	100	19	1301	274	100

Birds	1		2		3		4		5		6		7		Total	
Sizes	**NISP**	**%**	**NISP**	**%**	**NISP**	**%**	**NISP**	**%**	**NISP**	**%**	**NISP**	**%**	**NISP**	**%**	**NISP**	**%**
Small passerines	17	45.9	40	43	12	24.5			**3**	60	**6**	42.9			**75**	36.4
Medium passerines	12	32.4	19	20.4	14	28.6	**2**	40			**4**	28.6	**2**	66.7	**53**	25.7
Non passerines (small)			10	10.8	4	8.2	**1**	20							**15**	7.3
Non passerines (medium)	4	10.8	9	9.7	5	10.2			**1**	20	**1**	7.1	**1**	33.3	**20**	9.7
Non passerines (large)					1	2									**1**	0.5
Non-identifiable material	4	10.8	15	16.1	13	26.5	**2**	40	**1**	20	**3**	21.4			**37**	18
Total	**37**	**100**	**93**	100	**49**	100	**5**	**100**	**5**	**100**	**14**	**100**	**3**	**100**	**206**	100

Area DMT

Macromammals	**1**		**2.1**		**2.2**		**Total**	
Taxon	NISP	%	NISP	%	NISP	%	NISP	%
Bovids								
Bov I					1	1.1	1	0.7
Klipspringer (Oreotragus oreotragus)			1	2.3			1	0.7
Bov I/ II			2	4.7	1	1.1	3	2.1
Bov II			6	14	9	9.5	15	10.6
Bov II/ III	1	33	3	7	6	6.3	10	7.1
Bov III			1	2.3	8	8.4	9	6.4
Bov III/IV					3	3.2	3	2.1
Bov IV								
Indet. Bov.			6	14	12	13	18	12.8
Other ungulates								
Zebra (*Equus* cf. *quagga*)					1	1.1	1	0.7
Pig/ warthog (Cf. Phacochoerus/ Potamochoerus)			5	11.6	2	2.1	7	5
Carnivores								
Indet. small carnivore					1	1.1	1	0.7
Rodents								
Porcupine (Hystrix africaeaustralis)					1	1.1	1	0.7
Indeterminate								
Indet. medium mammals	2	67	19	44.2	50	53	71	50.4
Total	3	100	43	100	95	100	141	100

Appendix 2 – Lithic analysis

Acronyms: F- flake; P-point; B-blade; Bt – bladelet

Cortex type and quantity

Cortex	F	%	P	%	B	%	Bt	%	Total	%
Thick	*73*	*7.4*	*-*	*-*	*2*	*0.2*	*-*	*-*	*75*	*7.6*
<25	34	3.4	-	-	-	-	-	-	34	3.4
25-50	21	2.1	-	-	1	0.1	-	-	22	2.2
50-75	9	0.9	-	-	1	0.1	-	-	10	1.0
>75	2	0.2	-	-	-	-	-	-	2	0.2
100	7	0.7	-		-	-	-	-	7	0.7
Water worn	*111*	*11.2*	*3*	*0.3*	*1*	*0.1*	*-*	*-*	*115*	*11.6*
<25	55	5.5	2	0.2	1	0.1	-	-	58	5.8
25-50	36	3.6	1	0.1	-	-	-	-	37	3.7
50-75	20	2.0	-	-	-	-	-	-	20	2.0
None	*736*	*74.2*	*28*	*2.8*	*35*	*3.5*	*3*	*0.3*	*802*	*80.8*
Total	**920**	**92.7**	**31**	**3.1**	**38**	**3.8**	**3**	**0.3**	**992**	**100**

Fragmentation

Fraction	F	%	P	%	B	%	Bt	%	Total	%
Complete	495	49.9	23	2.3	20	2.0	1	0.1	539	54.3
Almost complete	60	6.0	3	0.3	2	0.2	-	-	65	6.6
Proximal	91	9.2	4	0.4	3	0.3	1	0.1	99	10.0
Distal	101	10.2	1	0.1	5	0.5	-	-	107	10.8
Lateral	67	6.8	-	-	1	0.1	-	-	68	6.9
Mesial	106	10.7	-	-	7	0.7	1	0.1	114	11.5
Total	**920**	**92.7**	**31**	**3.1**	**38**	**3.8**	**3**	**0.3**	**992**	100

Platform types

Butt	F	%	P	%	B	%	Bt	%	Total	%
Flat	412	41.5	17	1.7	14	1.4	1	0.1	444	44.8
Burinated	6	0.6	-	-	-	-	-	-	6	0.6
Cortical	91	9.2	1	0.1	3	0.3	-	-	95	9.6
Dihedral	60	6.0	3	0.3	3	0.3	1	0.1	67	6.8

Faceted	32	3.2	7	0.7	-	-	-	-	39	3.9
Punctiform	27	2.7	-	-	2	0.2	-	-	29	2.9
Removed	33	3.3	1	0.1	-	-	-	-	34	3.4
Retouched	1	0.1	-	-	-	-	-	-	1	0.1
Smashed	28	2.8	1	0.1	1	0.1	-	-	30	3.0
NA	230	23.2	1	0.1	15	1.5	1	0.1	247	24.9
Total	**920**	**92.7**	**31**	**3.1**	**38**	**3.8**	**3**	**0.3**	**992**	**100**

Platform preparation

Butt preparation	**F**	**%**	**P**	**%**	**B**	**%**	**Bt**	**%**	**Total**	**%**
Chipping	9	1.3	-	-	1	0.1	-	-	10	1.4
Frontal retouches	17	2.4	1	0.1	-	-	-	-	18	2.6
Lateral notches	21	3.0	-	-	-	-	-	-	21	3.0
Not observed	607	86.3	21	3.0	24	3.4	2	0.3	654	93.0
Total	654	93.0	22	3.1	25	3.6	2	0.3	703	100

Section

Section	**F**	**%**	**P**	**%**	**B**	**%**	**Bt**	**%**	**Total**	**%**
Trapezoidal	272	27.4	11	1.1	22	2.2	1	0.1	306	30.8
Triangular	280	28.2	14	1.4	8	0.8	1	0.1	303	30.5
Other	27	2.7%	-	-	-	-	-	-	27	2.7
NA	341	34.4	6	0.6	8	0.8	1	0.1	356	35.9
Total	**920**	**92.7**	**31**	**3.1**	**38**	**3.8**	**3**	**0.3**	**992**	**100**

Profile

Profile	**F**	**%**	**P**	**%**	**B**	**%**	**Bt**	**%**	**Total**	**%**
Straight	460	46.4	18	1.8	25	2.5	2	0.2	505	50.9
Arched	65	6.6	-	-	5	0.5	-	-	70	7.1

Other	8	0.8	-	-	-	-	-	-	8	0.8
Twisted	22	2.2	2	0.2	-	-	-	-	24	2.4
NA	365	36.8	11	1.1	8	0.8	1	0.1	385	38.8
Total	920	92.7	31	3.1	38	3.8	3	0.3%	992	100

Edge morphology

Edge type	F	%	P	%	B	%	Bt	%	Total	%
Biconvex	53	5.3	-	-	-	-	-	-	53	5.3
Circular	18	1.8	2	0.2	-	-	-	-	20	2.0
Convergent	48	4.8	21	2.1	-	-	-	-	69	7.0
Convex-concave	26	2.6	1	0.1	2	0.2	-	-	29	2.9
Divergent	134	13.5	-	-	2	0.2	-	-	136	13.7
Irregular	81	8.2	-	-	1	0.1	-	-	82	8.3
Parallel	74	7.5	-	-	21	2.1	1	0.1	96	9.7
NA	486	49.0	7	0.7	12	1.2	2	0.2	507	51.1
Total	920	92.7	31	3.1	38	3.8	3	0.3	992	100

Tip pattern

Tip	F	%	P	%	B	%	Bt	%	Total	%
Burinated	2	0.2	-	-	-	-	-	-	2	0.2
Cleavage	1	0.1	-	-	-	-	-	-	1	0.1
Feathered	122	12.3	2	0.2	2	0.2	-	-	126	12.7
Fractured	75	7.6	5	0.5	7	0.7	-	-	87	8.8
Overpassed	13	1.3	-	-	-	-	-	-	13	1.3
Pointed	70	7.1	17	1.7	5	0.5	1	0.1	93	9.4
Retouched	10	1.0	-	-	-	-	-	-	10	1.0

Thick	183	18.4	-	-	13	1.3	-	-	196	19.8
NA	444	44.8	7	0.7	11	1.1	2	0.2	464	46.8
Total	**920**	**92.7**	**31**	**3.1**	**38**	**3.8**	**3**	**0.3**	**992**	**100**

Dorsal pattern

Dorsal pattern	F	%	P	%	B	%	Bt	%	Total	%
Radial/Centripetal	205	20.7	6	0.6	4	0.4	-	-	215	21.7
Unidirect-indt	50	5.0	-	-	2	0.2	-	-	52	5.2
Unidirect-parallel	54	5.4	1	0.1	17	1.7	1	0.1	73	7.4
Unidirect-convergent	61	6.1	19	1.9	2	0.2	1	0.1	83	8.4
Unidirect-opposed-fracture	4	0.4	-	-	1	0.1	-	-	5	0.5
Cortical	32	3.2	-	-	1	0.1	-	-	33	3.3
Alternate	2	0.2	-	-	-	-	-	-	2	0.2
Bulb (Kombewa)	1	0.1	-	-	-	-	-	-	1	0.1
Crossed	4	0.4	-	-	-	-	-	-	4	0.4
Multidirectional	12	1.2	-	-	-	-	-	-	12	1.2
Opposed-parallel	3	0.3	-	-	-	-	-	-	3	0.3
None (fracture)	12	1.2	-	-	-	-	-	-	12	1.2
Indeterminate	10	1.0	-	-	-	-	-	-	10	1.0
NA	470	47.4	5	0.5	11	1.1	1	0.1	487	49.1
Total	**920**	**92.7**	**31**	**3.1**	**38**	**3.8**	**3**	**0.3**	**992**	**100**